AFFDL-TR-67-89

PARAMETRIC FATIGUE ANALYSIS OF USAF AIRCRAFT

GEORGE J. [illegible]
JOHN P. [illegible]
JAMES C. SULLIVAN

AFFDL-TR-67-89

PARAMETRIC FATIGUE ANALYSIS OF USAF AIRCRAFT

GEORGE J. ROTH
JOHN P. RYAN
JAMES C. SLIEMERS

UNIVERSITY OF DAYTON
RESEARCH INSTITUTE

TECHNICAL REPORT AFFDL-TR-67-89

1967

AIR FORCE FLIGHT DYNAMICS LABORATORY
DIRECTORATE OF LABORATORIES
AIR FORCE SYSTEMS COMMAND
WRIGHT-PATTERSON AIR FORCE BASE, OHIO 45433

NOTICE

When Government drawings, specifications, or other data are used for any purpose other than in connection with a definitely related Government procurement operation, the United States Government thereby incurs no responsibility nor any obligation whatsoever; and the fact that the Government may have formulated, furnished, or in any way supplied the said drawings, specifications, or other data, is not to be regarded by implication or otherwise as in any manner licensing the holder or any other person or corporation, or conveying any rights or permission to manufacture, use, or sell any patented invention that may in any way be related thereto.

Copies of this report should not be returned unless return is required by security considerations, contractual obligations, or notice on a specific document.

400 - August 1967 - CO455 - 5-108

PARAMETRIC FATIGUE ANALYSIS OF USAF AIRCRAFT

GEORGE J. ROTH
JOHN P. RYAN
JAMES C. SLIEMERS

FOREWORD

This report was prepared by the University of Dayton Research Institute, Dayton, Ohio, under Air Force Contract AF 33(615)-3812, BPSN 6(61146704-62405334). The contract was initiated under Project No. 1467, Task No. 146704. The program was administered by the Air Force Flight Dynamics Laboratory, Air Force Systems Command, Wright-Patterson Air Force Base, Ohio, Mr. Robert Engle (FDTR), Project Engineer.

The research effort was conducted from 1 May 1966 to 1 May 1967. The report was submitted by the authors in June 1967.

This program was conducted under the general direction of Mr. Dale H. Whitford, Supervisor of Aerospace Mechanics Research.

The authors gratefully acknowledge the cooperation and assistance of Mr. B. J. Nasal of the Systems Engineering Group, and of Mr. Vincent Kearney of the Structures Division, Air Force Flight Dyamics Laboratory.

This technical report has been reviewed and is approved.

Francis J. Janik, Jr.
Chief, Theoretical Mechanics
Branch
Structures Division

ABSTRACT

This report contains the result of an effort to optimize the format and procedures for conducting a parametric fatigue analysis of Air Force aircraft on a flight-by-flight basis. Parameters which affect the environmental loads and those which affect the resulting stresses are discussed. It is suggested that flights be divided into mission segments of taxi, ascent, cruise, descent, landing, etc., to take advantage of the standard operational procedures of the Air Force. Methods of calculating and presenting the parametric damage charts for each segment are presented for both heavy bomber and cargo aircraft and for fighter aircraft. It is suggested that to obtain a resonable accuracy, a statistical counting accelerometer with a pilot-controlled print-out be installed in all fighter aircraft. Results indicated that tabular formats are preferred to graphical formats for manual solution of large volumes of flights. It is concluded that a parametric analysis can be used to calculate the fatigue damage on a flight-by-flight basis and that the required pilot log information is now available. This abstract is subject to special export controls and each transmittal to foreign governments or foreign nationals may be made only with prior approval of the Air Force Flight Dynamics Laboratory (AFSC), Wright-Patterson Air Force Base, Ohio 45433, ATTN: FDTR.

TABLE OF CONTENTS

ILLUSTRATIONS

ILLUSTRATIONS, continued

ILLUSTRATIONS, continued

TABLES

SYMBOLS

$\bar{A}$	Airplane response parameter relating root-mean-square input and output values
b	Composite root-mean-square gust velocity
b_1, b_2	Composite root-mean-square gust velocity in nonstorm and storm type turbulence
C_L	Lift coefficient
C_{L_α}	Lift curve slope
C_N	Normal load coefficient
$C_{N_{max}}$	Maximum normal load coefficient
cg	Center of gravity of aircraft
d	Flight distance in turbulence of given intensities
G_o	Average number of zero crossings per unit distance with positive slope for vertical gust velocity
G(w)	Number of exceedances of input gust velocity level (w)
KEAS	Knots equivalent air speed
KT	Notch sensitivity factor
L	Scale of turbulence
M	Mach number
MAC	Mean aerodynamic chord
n/N	Cycle ratio
N	Life cycles
N_o	Average number of zero crossings per unit distance with positive slopes for response
N(y)	Number of exceedances of y response level per unit distance

n_z	Normal load factor
n_{z_d}	Design limit load for the configuration
n_{z_i}	Instantaneous normal load factor
PDLL	Percent design limit load
P_1, P_2	Probability of being in nonstorm and storm type turbulence
$p(\sigma)$	Probability density function
p_n	Proportion of distance in the nth patch
T	Time
q	Dynamic pressure
S	Reference area
$T_y(\Omega)$	Frequency response function as a function of reduced frequency
$T_y(\omega)$	Frequency response function as a function of circular frequency
U_{de}	Derived gust velocity
V	Airplane speed
w	True vertical gust velocity
W_d	Design weight for the configuration
W_i	Instantaneous gross weight
W/S	Ratio of aircraft weight to wing area
$w(s)$	Vertical gust intensity as a function of distance flown
y	General response quantity
Δy	Incremental response from mean condition
μ	Mass ratio

σ	Root-mean-square value
σ_n	Complete root-mean-square value for given patches of turbulence
σ_w	Complete root-mean-square gust value
σ_y	Complete root-mean-square response value
$\Phi(\omega)$	Power spectral density as a function of circular frequency
$\Phi(\Omega)$	Power spectral density as a function of reduced frequency
$\Phi_{wy}(\omega)$	Cross spectrum
χ^2	Chi squared test
ω	Angular or circular frequency
Ω	Reduced frequency

SECTION I

INTRODUCTION

This effort is part of the Air Force Fatigue Certification Program, which has the overall objectives: a) to provide the Air Force with aircraft which have specified life capabilities; b) to provide the Air Force with a rational means of scheduling aircraft for required structural modifications so that the required life can be achieved with minimum downtime and loss of combat capability; and c) to provide the Air Force with a means to assess the life trade-off requirements for various mission mixes and subsequent long range planning for aircraft replacement.

To achieve these objectives, much time and money have been invested in refining fatigue analysis procedures, conducting multi-load level full-scale fatigue tests, and developing flight load recorders. Some recorders are now being installed on individual aircraft deployed throughout the various fleets. However, cost for recorders and data reduction precludes recording data on 100% of the fleet. A sufficient number (approximately 20%) of the aircraft are being instrumented to provide a statistical description of the operational load experience. However, the actual mission mix flown by the majority of the aircraft in the fleet will not be monitored by a recorder. Therefore, some other means for economically determining the fatigue damage for individual aircraft must be devised.

The life expended by individual aircraft can be represented as a function of two main variables. One of these is the spectrum of input loads, i.e., the spectrum of gust and maneuver loads actually encountered per mission segment; and the other is the utilization of the aircraft, or the mission mix of mission segments actually flown and the response of the aircraft to the input loads. These response parameters, which allow one to convert gust velocities or maneuver load factors to stresses, are a function of velocity, altitude, gross weight, and aircraft configuration. Until recently no attempt was made to account for the mission mix flown by individual aircraft. Aircraft are currently programmed for modification on the basis of total flight hours accumulated, regardless of the specific utilization of the individual aircraft. It is possible to monitor these uninstrumented aircraft by logging the mission mix actually flown in sufficient detail (recording gross weight, configuration, velocity, altitude, etc.), and by using the fatigue analysis computer programs and the recorded loads spectra to calculate the life expended per individual aircraft. However, this procedure would be much more time-consuming and expensive than a procedure which involved a parametric fatigue analysis study.

A parametric fatigue analysis study should result in an orderly and systematic presentation of fatigue damage versus the various parameters within the mission profile of the aircraft under study. The structural components which were discovered to be fatigue critical after the completion of the component and full-scale fatigue tests would be the subjects of re-calculation of fatigue damage for varying values of gross weight, velocity, altitude, configuration, etc., for the input spectrum of each mission segment. These damage curves presented for various mission segments such as climb, cruise, refueling, low level penetration, descent, landing, taxi, etc., could be entered with selected values of the parameters, thus yielding a damage prediction for a mission mix of the user's own choosing. Instead of using flight hours as a basis for modification and inspection schedules, a detailed pilot's log and the results of a parametric fatigue analysis could be used to compute fatigue damage for each flight. Then, damage rather than hours could be used as the criteria for modification and inspection.

The magnitude of the error which can be realized by basing aircraft life on flight-hour criteria rather than on cumulative damage basis was recently demonstrated during a study of the B-58 fleet usage during operational Strategic Air Command missions. By means of a parametric analysis, the damage experienced at a number of fatigue-critical locations on each aircraft was computed for each flight of each aircraft. Thus, the total accumulated damage for a number of fatigue critical locations (control points) and the corresponding total number of flight hours was tabulated for each aircraft. These damage vs flight-hour data for the most fatigue-critical point on the B-58 are presented in the following bi-variate frequency distribution. This table indicates the number of aircraft that can be grouped within specified class intervals of fatigue damage and flight hours. For example, four aircraft had expended between 44% and 46% of their life in an interval of from 1450 to 1550 flight hours.

Bi-Variate Distribution % of Life vs. Flight Hours
B-58 Fleet, Bathtub Fitting, Control Point 10

Hundred of Flight Hours	Accumulated Damage - % of Life																								
	29	31	33	35	37	39	41	43	45	47	49	51	53	55	57	59	61	63	65	67	69	71	73	75	77
21																						1		1	
20																									
19														1											
18			1								1														
17							1						1	1	1	1									
16									1	2	3	2	3		1										
15						2		2	4	4	1	2	1	1											1
14						2		2	3	4	1		2		1										
13						2	2	1	2	3	1														
12			2	2		2	1	3		1															
11					1	2		2																	
10	1		1							1	1														

From this table, one can readily see that there is no correlation between flight hours and fatigue damage. There is a spread of from about 1500 flight hours to about 2100 flight hours between two aircraft having used nearly 75% of their total life. Also, within the 1450-hour to 1550-hour interval, the damage scatter varies from about 39% to 77%. Thus, it is evident that if inspections or modifications were scheduled on a flight-hour basis, two possible errors would be realized: some aircraft would receive unnecessary modifications and inspections, and some aircraft could actually experience failure before they accumulated the specified number of flight hours.

It is believed that the above example shows a scatter that is smaller than that of most aircraft fleets because: (1) the B-58 aircraft is used on relatively few different types of mission; and (2) the effects of environmental variation (gust and maneuver spectra) on a flight by flight basis were not included in the damage calculations represented in the bi-variate table.

Therefore, it is concluded that damage accumulation, rather than flight hours, is a much more rational method for evaluating the age of an airframe. In addition, continued use of the pilot's log and the parametric fatigue analysis would result in a superior basis for the retirement and replacement of individual aircraft. Another advantage of this procedure is that it would yield damage vs mission data that could be used for scheduling mission mixes that would minimize structural damage. Further, logistics problems related to structural maintenance for combat and noncombat situations could be worked out in advance, and specific recommendations for time between inspections could be given.

There are several feasible means of accomplishing a parametric fatigue analysis study, and the results can be arranged in many different formats. The specific approach employed and the relative importance of the pertinent parameters are likely to change with different types of aircraft and with the various locations of the fatigue critical components. Since many calculations are involved, a parametric analysis study must be based on a computerized fatigue analysis program. However, the parametric charts which result from the study can have great utility without being automated.

The first edition of the parametric fatigue analysis study for a particular aircraft would be prepared after the full-scale fatigue tests have identified the critical components. A fatigue analysis program would be used to calculate the damage for these critical components for the various parameters, using the best input load spectrum available at that time. Subsequently, the fleet aircraft which are instrumented will yield data more closely defining the load experience of the fleet and may also yield additional

breakdowns of the loading spectra. That is, the loads data from the instrumented aircraft may show a significantly different spectrum of gust or maneuver loadings for different geographical locations, or the landing or taxi damage may be significantly different for various air bases. Using the improved measured load spectrum, the fatigue analysis program would generate revised damage calculations. Therefore, it is important to find a convenient means of changing the parametric fatigue analysis study to include the revised damage calculations.

A parametric fatigue analysis study in the form of a report (collection of charts) can be used manually to predict the life expended per aircraft. A detailed pilot's log would be interpreted in terms of the defining parameters and the damage due to this particular mix of mission segments; parameters can be read from the various charts and summed to yield the life expended for that particular flight. However, it would be more advantageous to automate the parametric fatigue analysis study and thus achieve greater accuracy with fewer man-hours.

The primary objective of the present study is to provide the optimum format for the parametric fatigue analysis study for each general class of aircraft. This optimization will be based on a study of those parameters which must be considered to calculate the damage within acceptable accuracy for each general class of aircraft, mission segment, and critical component. The optimization is generally in the presentation of the charts, so that by manual means a person can conveniently and quickly calculate the damage on a tail number basis. Also, certain assumptions are suggested that will result in a minimum amount of data being required on the pilot's log. The two secondary objectives are: first, to suggest a design of the pilot's log sheet that will contain the required data to permit the damage calculations; and second, to suggest a design of a semiautomatic pilot's log recorder for the fighter or fighter-bomber aircraft type.

SECTION II

FATIGUE DAMAGE PARAMETERS

1. INPUT PARAMETERS

In this report, input parameters are defined as those parameters which cause an alternating load to be induced into the aircraft structure. These parameters may be gust velocity, maneuver load factor, sinking speed at touchdown, runway roughness, turning radius and velocity during taxi, maintenance procedures, store release or ejection loads, special environments or events such as thermal stresses, cabin pressurization, drag chute loads, nuclear weapon delivery, etc. Each of these input parameters will be discussed in relation to the remote parameters which affect its frequency of occurrence or magnitude.

a. Gust *

The history of gust analysis originated with a discrete-gust approach (U_{d_e}) involving the concept of a rigid airplane and a ramp-type gust with a gradient distance of 10 chords and a specified maximum vertical velocity. A somewhat arbitrary alleviation curve was used to attempt to adjust for differences in such factors as wing chord and pitching effects. This alleviation curve was expressed in terms of the design parameter W/S, the wing loading. This curve, when applied to the gust load formula, gave results which were, in effect, the same as if the airplane had encountered a step-type gust of less magnitude than the maximum design velocity used in the ramp gust; hence, the concept of "sharp-edge gust encounters" was frequently mentioned. Later, the design procedure was changed so that the alleviation curve was expressed in terms of the more fundamental parameter μ, the mass ratio. It was also decided to define the discrete gust shape as a (1-cosine) type with a gradient distance of 12.5 chords. The discrete gust is, in principle, a convenient and simple way of relating the vertical accelerations experienced by one airplane to those likely to be experienced by another aircraft. This concept is acceptable as long as the aircraft in question have essentially the same response characteristics or if both aircraft can be assumed rigid bodies and are used in the same manner. Later work has increased the accuracy of the U_{d_e} approach by using actual lift curve slopes (C_{L_α}) of the aircraft (References 1 and 2). Some work was performed to include aeroelastic effects on a U_{d_e} basis (Reference 3).

With the advent of aircraft with higher speeds and altitude operation, greater airplane flexibility, and the wing sweep angle,

* Details of gust analysis have been taken from reference 4.

a more general approach was needed. The power spectral techniques of generalized harmonic analysis were introduced by Press, Clementson, Wiener, Rice, Tukey (References 4, 5, 6 and 7). At present, design philosophy makes use of both the discrete gust and the spectral approach. Many times they are used as checks against each other; in fact, the discrete gust concept normally constitutes the nucleus of the design approach, with the power spectral portion used to bring out dynamic-response effects more rationally, or possibly to uncover unusual response effects.

The spectral approach takes into account the number of exceedances of load levels, variation of severity of turbulence with altitude, and proportion of time spent in moderate and severe turbulence at each altitude.

To illustrate the concept of the spectral approach, consider a model made up of discrete patches of disturbances of different mean square intensity where each patch is Gaussian and stationary in character (Figure 1). This model is then replaced in a limiting-process by a model which has a continuously variable distribution of root mean square (rms) gust velocity (Figure 2). It should be understood that the patches are encountered in random fashion, not necessarily in the succession shown in Figure 1.

Several features must be pointed out before this pseudo representation is continued. The vertical gust data in Figure 1 represent many flight samples at the same altitude, weight, and airspeed, and include what is considered a representative storm operation. Also, Figure 1 shows an accumulation of the distance traveled in non-turbulence (d_o) which was obtained from all runs. Figures 2 and 3 show the density distribution of the rms gust velocities in discrete and continuous form for the segments shown, plus a breakdown in smooth air, nonstorm, and storm turbulence. A composite (rms) value σ_c of vertical velocity of the discrete model would be

$$\sigma_c^2 = \frac{1}{d}\left[\int_{s_0}^{s_1} W_0^2(s)\,ds + \int_{s_1}^{s_2} W_1^2(s)\,ds + \int_{s_2}^{s_3} W_2^2(s)\,ds + \ldots\right] \quad (1)$$

where: W(s) is the vertical gust intensity as a function of distance and s is the distance flown.

After integration of Equation 1 the result in terms of the distances shown in Figure 1 is

$$\sigma_c^2 = \frac{1}{d}\left[d_0\sigma_0^2 + d_1\sigma_1^2 + d_2\sigma_2^2 \ldots\ldots d_n\sigma_n^2\right] \quad (2)$$

but d_n/d is the percentage of distance in each patch, therefore

$$\sigma_c^2 = p_1\sigma_1^2 + p_2\sigma_2^2 + \ldots + p_n\sigma_n^2 \ldots\ldots \quad (3)$$

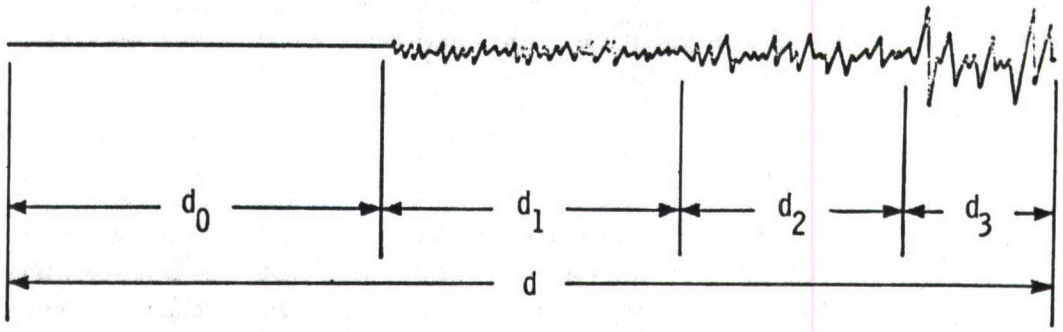

Figure 1. Discrete-Gust Patches

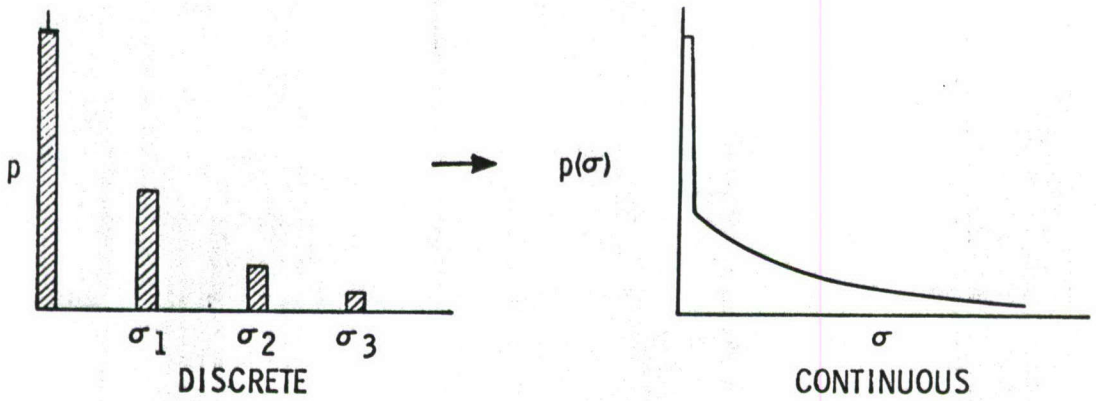

Figure 2. Combined Nonstorm and Storm Operation

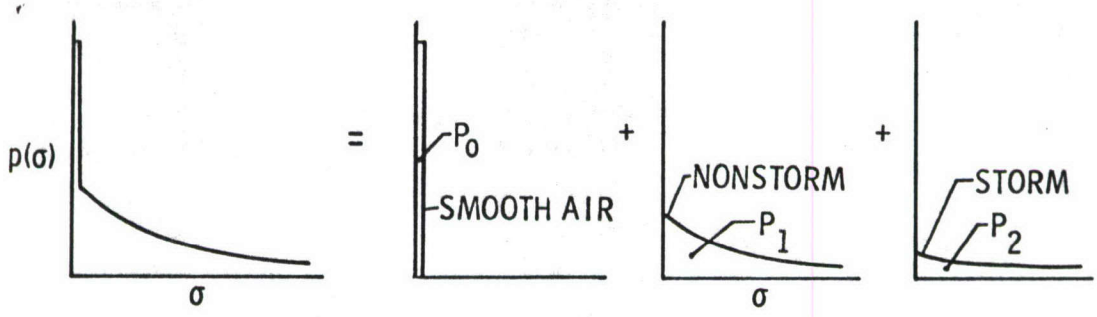

Figure 3. Continuous Probability Distributions

NOTE: $\int_0^\infty p\sigma\, d\sigma = 1$ thus $P_0 + P_1 + P_2 = 1$

where: p_n represents the proportion of distance in the n^{th} patch and σ_n the associated rms gust velocity of the n^{th} patch. For the limiting case in which the turbulence model is represented by a continuous variation in rms gust velocity, Equation 3 above becomes

$$\sigma_c^2 = \int_0^\infty \sigma^2 \, p(\sigma) \, d(\sigma) \tag{4}$$

In order to build up the model of Figure 1 the proper proportion of storm and nonstorm turbulence and of smooth air would have to be included in the model for the same altitude and speed. In addition to these restrictions, a proper proportion of terrain levels, wind levels, geographical areas, and time of day should be included.

Two equations have been used to represent the power spectral density (PSD) of the gust velocity;

$$\phi_w(\Omega) = \frac{\sigma_w^2 L}{\pi} \left[\frac{1 + 3L^2 \Omega^2}{(1 + \Omega^2 L^2)^2} \right] \tag{5}$$

and

$$\phi_w(\Omega) = \frac{\sigma_w^2 L}{\pi} \left[\frac{1 + 8/3 \, (1.339 \, L \, \Omega)^2}{\left[1 + (1.339 \, L \, \Omega)^2\right]^{11/6}} \right] \tag{6}$$

where: σ_w^2 is the mean square value of the vertical gust
Ω is the reduced frequency
and L is the scale of turbulence.

It is debatable which of the above expressions is the most appropriate for expressing the power spectral density in terms of the reduced frequency of the sinusoidal components which make up the gust disturbance. The choice of either Equation 5 or 6 and the value for L must be based on the best fit for the various combinations of patches, i.e.,various power spectral density curves of individual flight segments at the same altitude.

For a complete model an equation for approximating the average number of vertical gust peaks which exceed a given level of rms velocity (σ) is

$$G(w) = G_o \int_o^\infty p(\sigma) e^{-w^2/2\sigma^2} \, d\sigma \tag{7}$$

where: $p(\sigma)$ is the probability density distribution of $\sigma(w)$ for a given altitude
and G_o is the average number of times per unit distance that the gust velocity goes through the zero value with positive slope.

Based on airplane operational data, $p(\sigma)$ may be approximated with good accuracy by

$$p(\sigma) = \frac{1}{b}\sqrt{\frac{2}{\pi}}\ e^{-\sigma^2/2b^2} \tag{8}$$

By substituting Equation 8 into Equation 4 it can be shown that the composite rms gust velocity σ_c is equal to b. Also by substituting the expression for $p(\sigma)$ into Equation 7 and integrating the resultant expression, G(w) becomes

$$G(w) = G_o\, e^{-w/b} \ . \tag{9}$$

If one were to apply Equation 9 to a discrete patch representation such as Figure 1, a value of b would exist for each patch. Thus the total spectrum would be the sum of the various patches,

$$G(w) = G_o P_1 e^{-w/b_1} + G_o P_2 e^{-w/b_2} \ldots . G_o P_n e^{-w/b_n} \ . \tag{10}$$

Equation 10 will yield the number of times that a given gust velocity (w) is equaled or exceeded per unit distance.

The complete turbulence model for a given altitude band has usually been divided into two parts: nonstorm and storm, with P_1 being the percent of time in nonstorm turbulence and P_2 the percent of time in storm turbulence.

At the present time for design considerations it is generally assumed that the values of p and b for a given altitude apply worldwide. For increased accuracy of damage calculations on a flight-by-flight basis, it was felt that the effect of geographical and seasonal variations on the p and b values should be investigated. Comparison of V-G-H (i. e., velocity, vertical load factor, and altitude) flight loads data were made on the basis of U_{d_e}. These comparisons are presented in the Appendix. The Appendix also presents an outline of a method for determining the p and b values from conventional V-G-H data. As shown by the graphs in the Appendix, there is a considerable variation in the frequency of occurrence of U_{d_e} levels for different geographic locations and seasons, particularly for low altitudes. In looking at V-G-H data it was observed that if one takes data from all geographical areas in the United States over a period of one or two years and compares the data by seasons, he may not see any variation by season. However, when the data are divided into both seasonal and geographic areas there is an obvious variation. The reason for this is that some parts of the United States have more turbulence during the spring and summer, but other parts have more turbulence during the fall and winter.

It has generally been accepted that atmospheric turbulence is isotropic and therefore very little difference is expected between the input spectrum for lateral gust velocities and that for vertical gust velocities.

b. Maneuver

The maneuver load input spectrum used herein is defined as the rate of occurrences or exceedances of specified cyclic load levels within the segment environment. Exceedances are defined as the number of times that a given load level is equaled or exceeded per unit time or distance.

Take for example, a symmetric maneuver input spectrum expressed in terms of exceedances per 1000 hours vs. positive center of gravity (cg) vertical load factor (n_z) for a flight segment.

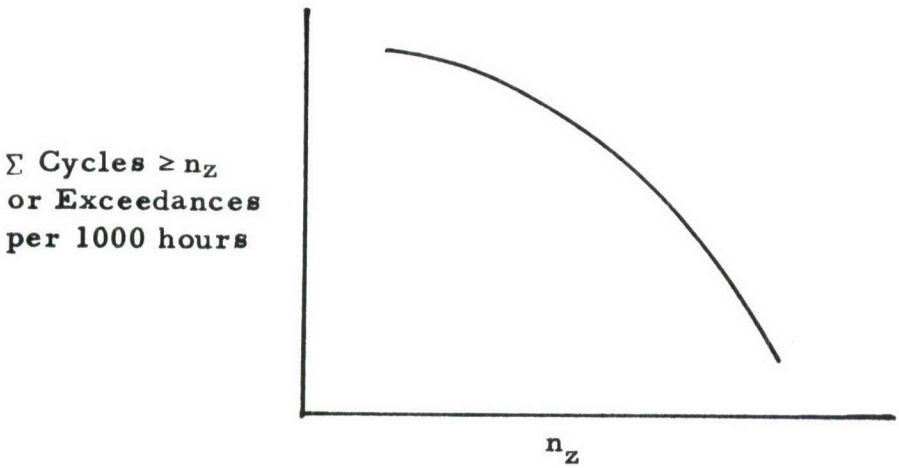

Figure 4. Maneuver Load Exceedance Curve

This input spectrum can be obtained directly from operational V-G-H data. Because maneuvers are usually nondynamic in nature, only the aeroelastic effects need be considered in the cg-structural element relationships (i.e., a dynamic magnification (DMF) is not involved).

The major concern is to determine the effect of varying parameters on the spectrum of Figure 4. This exceedance curve is highly dependent on the mission segment and possibly type of mission, i.e., pilot training, combat, autopilot, etc.; on the type of aircraft; on the gross weight of the aircraft; and possibly on the external stores arrangement.

It was determined that the mission segment parameter with various configuration and flight regime subdivisions as listed below would have the most effect on the input spectrum:

Mission Segment (including pilot capability and/or operational conditions) with subbreakdowns of,

(a) Stores Arrangement (if necessary) and Wing Sweep Setting

(b) Speed Categories (subsonic, supersonic).

The effect of gross weight (and possibly external stores arrangement) on the input spectra may be considered by changing the abscissa of Figure 4 to percent design limit load (PDLL) where

$$PDLL = \frac{n_{z_i} \cdot W_i}{n_{z_d} \cdot W_d} \cdot 100, \qquad (11)$$

and

n_{z_d} = design limit load for the configuration involved.

W_d = design weight for the configuration involved.

W_i = instantaneous weight at the load factor encountered.

n_{z_i} = load factor encountered.

NOTE: $n_{z_d} \cdot W_d$ = Constant (for each stores arrangement).

To formulate the symmetric maneuver load input spectrum, it is essential that design weights and design limit loads be specified for each possible external configuration type. In addition to this, a method must be devised to correlate the recorded n_{z_i} values with the gross weight (W_i). With these changes a representative maneuver input spectrum might be shown as Figure 5.

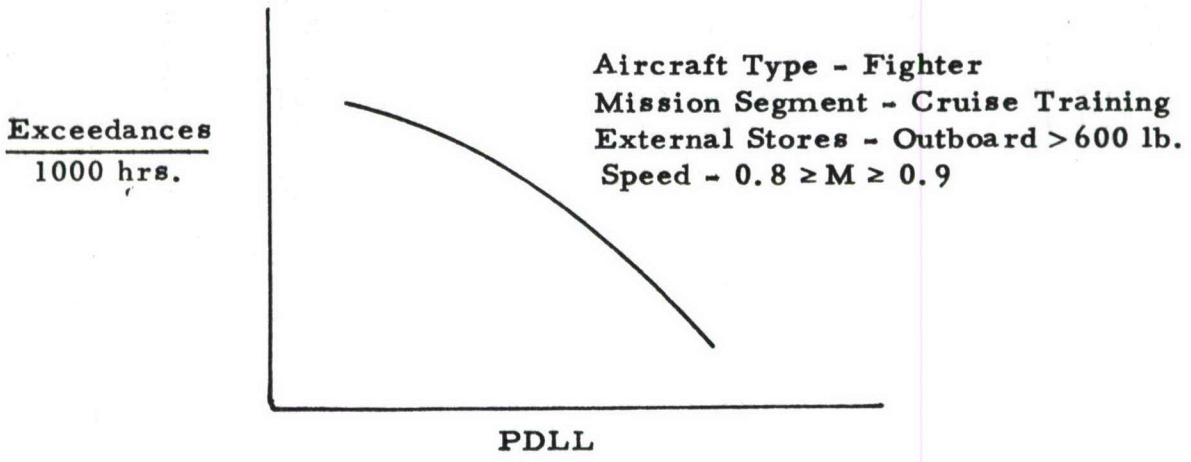

Figure 5. Percent Design Limit Load Exceedance Curve

Some typical exceedance curves based on this approach are shown in Figures 6 through 9. The data were obtained from Reference 8, which deals entirely with the F-5A aircraft. These curves show that there is a

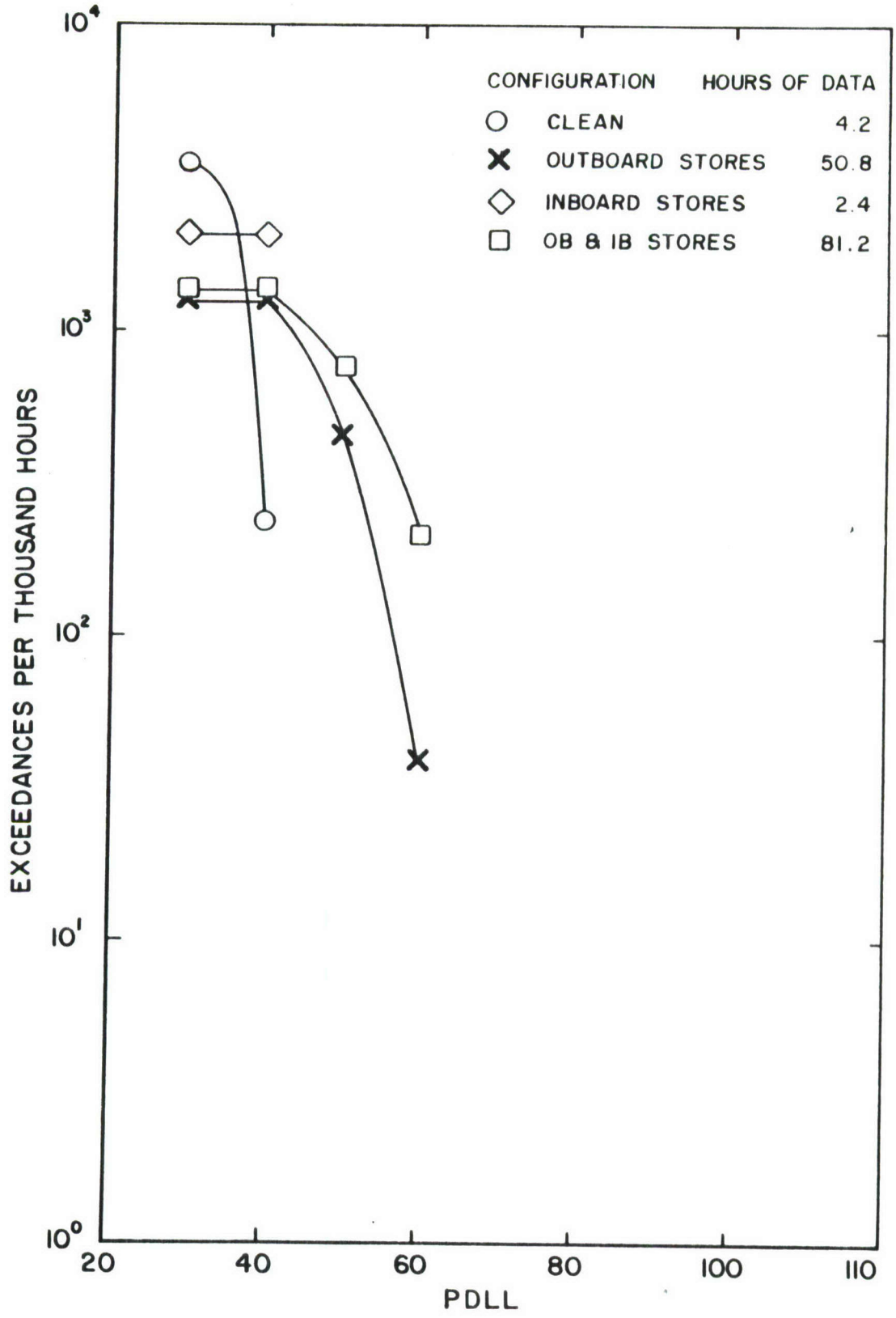

Figure 6 Exceedance Curves vs. Percent Design Limit Load for Various Ascent Configurations of the F-5A

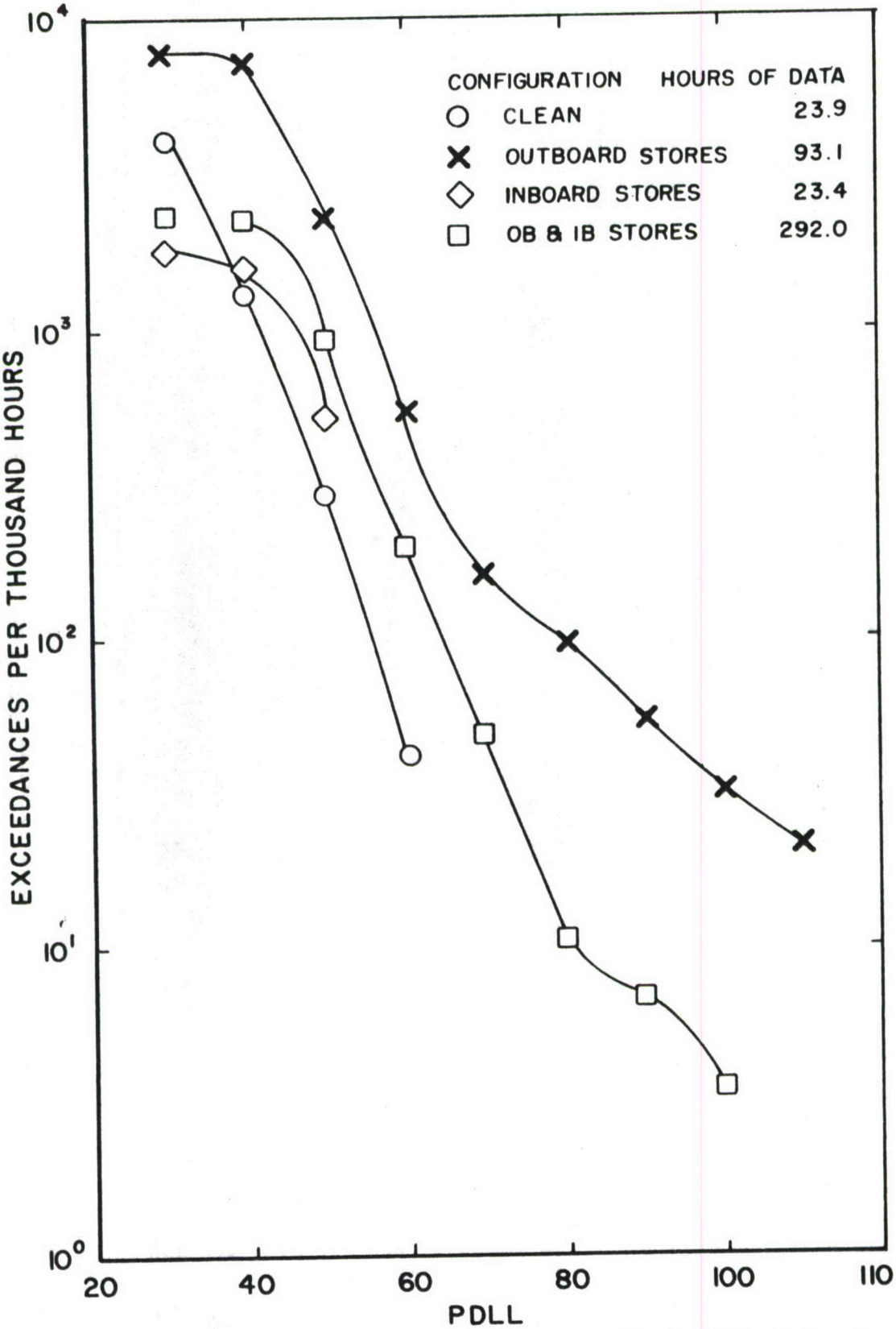

Figure 7 Exceedance Curves vs. Percent Design Limit Load for Various Cruise-Out Configurations of the F-5A

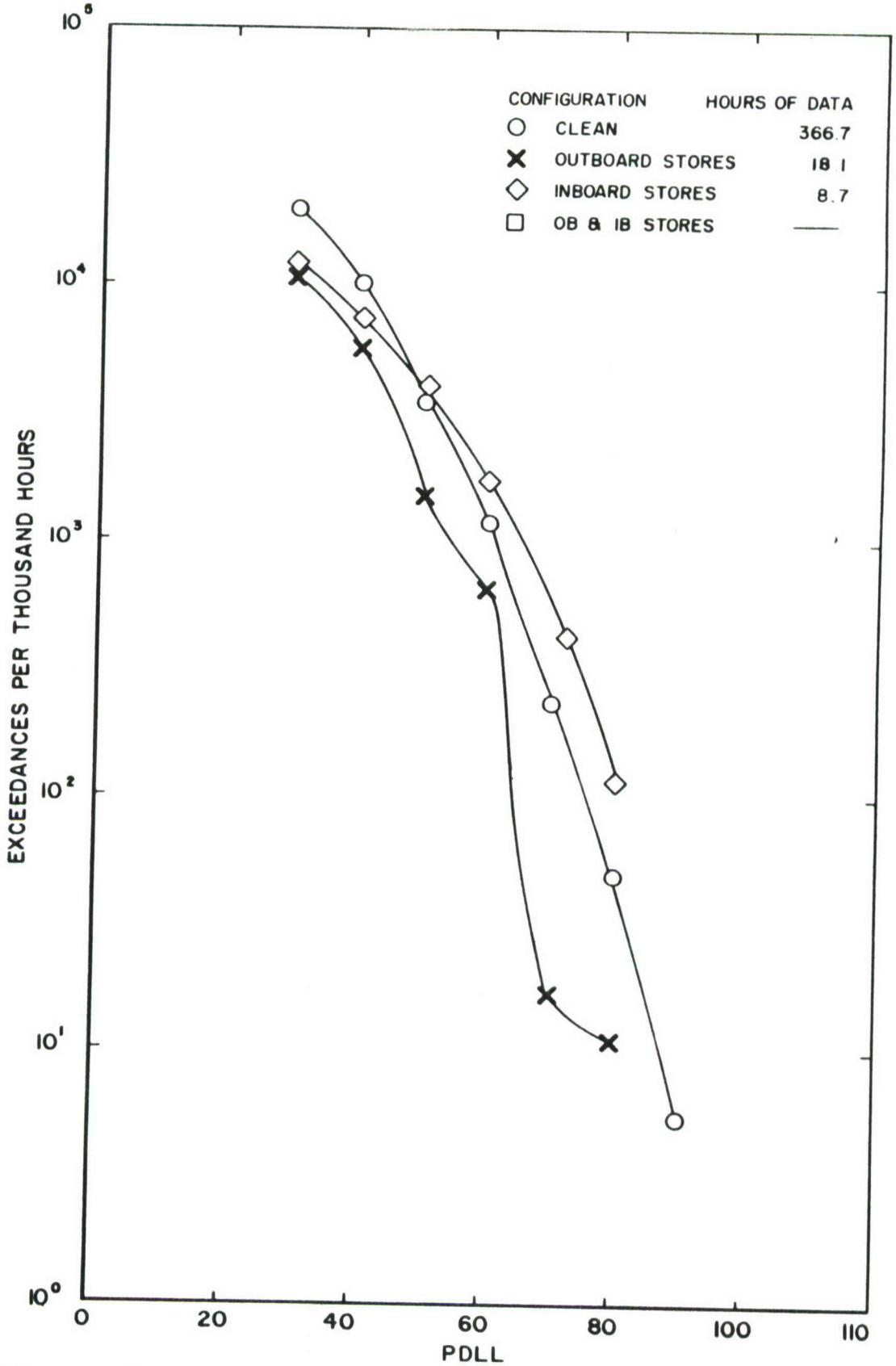

Figure 8 Exceedance Curves vs. Percent Design Limit Load for Various Cruise-Back Configurations of the F-5A

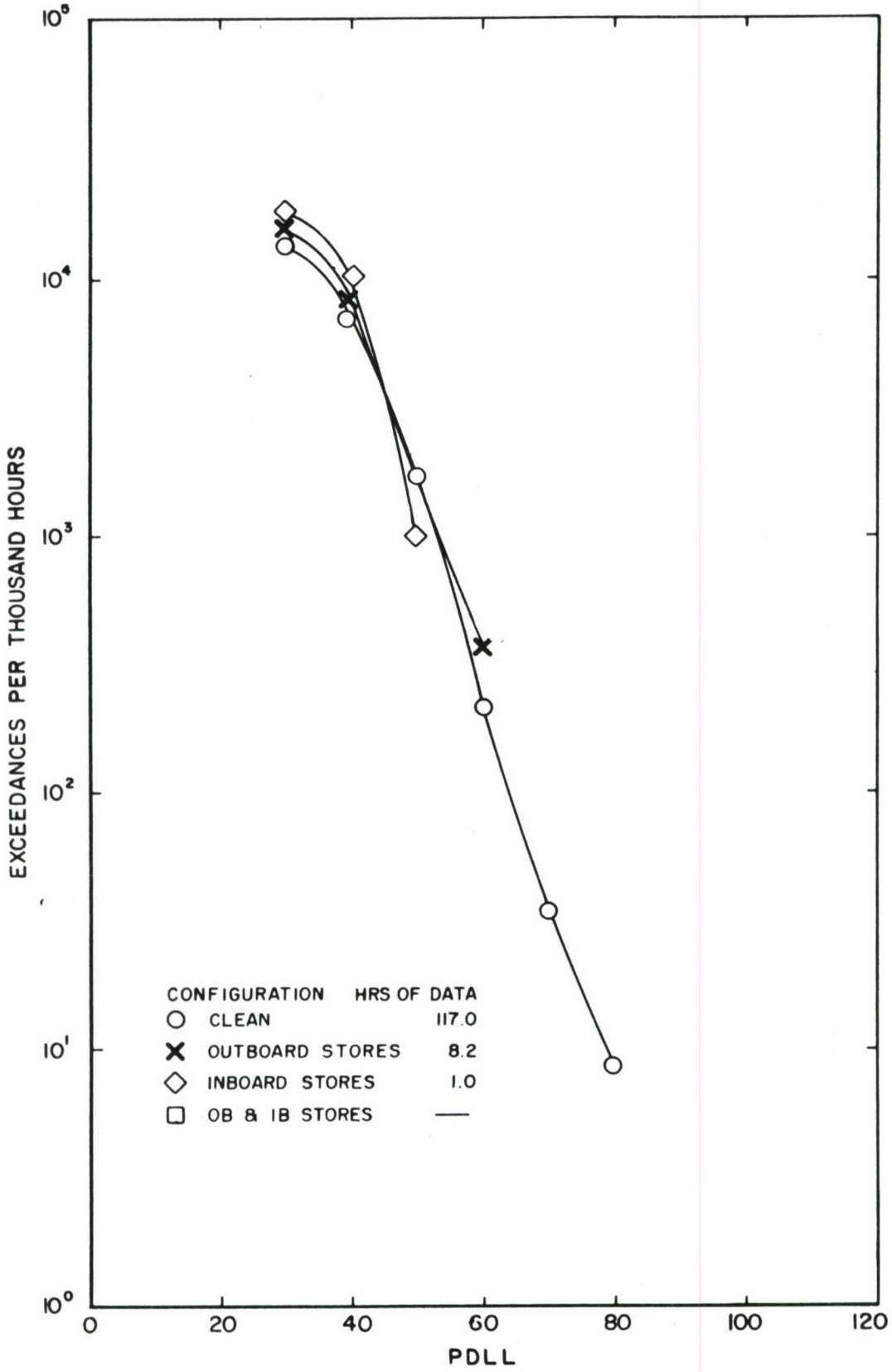

Figure 9 Exceedance Curves vs. Percent Design Limit Load for Various Descent Configurations of the F-5A

difference in input spectra due to external configuration; however, in many instances the number of hours recorded is quite small.

An additional restriction which must be imposed on Figure 5 is the lift capability of the aircraft. As an extreme example, a fighter aircraft at M 0.5 and 35,000 feet altitude cannot pull 7 g's. According to Equation 11, the product (n_{z_i}) (W_i) is equal to the normal loading on the aircraft. Thus it is possible to plot constant (qS) lines as a function of Mach number and altitude (Figure 10) where

q = dynamic pressure
S = reference area used in calculating C_N or C_L

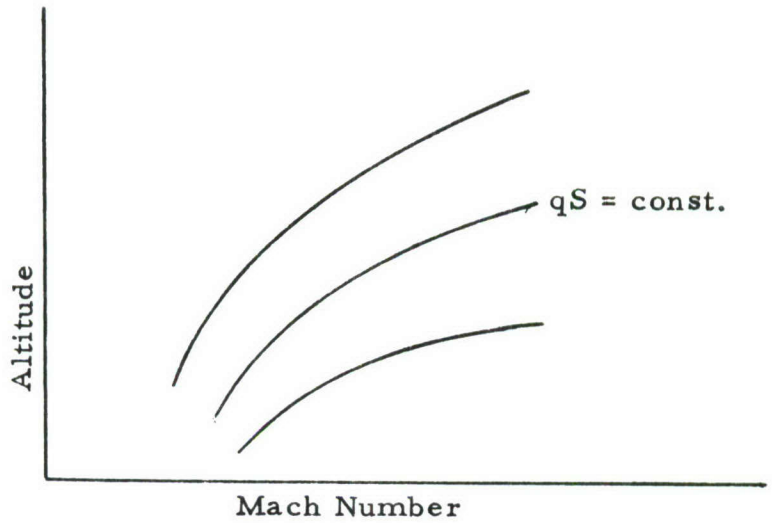

Figure 10. Constant (qS) Lines as a function of (Mach No., Alt.)

Since $C_{N_{max}}$ may be expressed as a function of Mach number for the vehicle and configuration involved, one can plot constant normal load capability also as a function of Mach number and altitude (Figure 11).

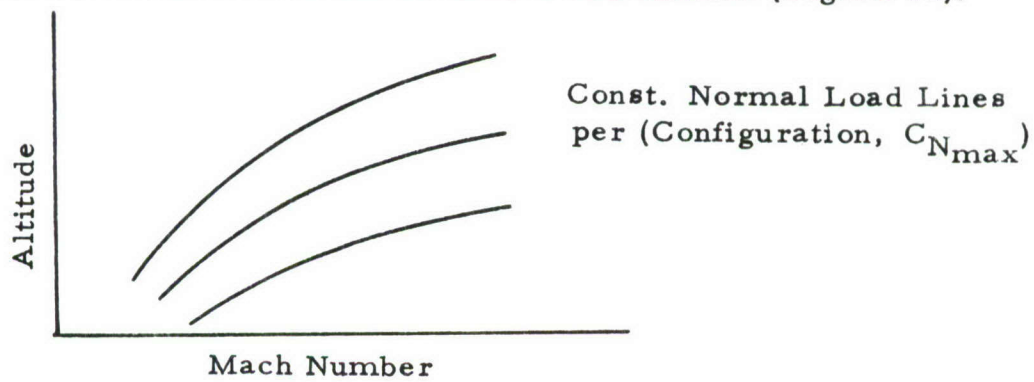

Figure 11. Constant Normal Load Lines as a function of ($C_{N_{max}}$, Config., Mach No., Alt.)

It is therefore possible to determine a table of PDLL max as a function of Mach number, altitude, and configuration so that an upper limit on Figure 5 is defined for each combination of the foregoing parameters. This feature is represented by Figure 12.

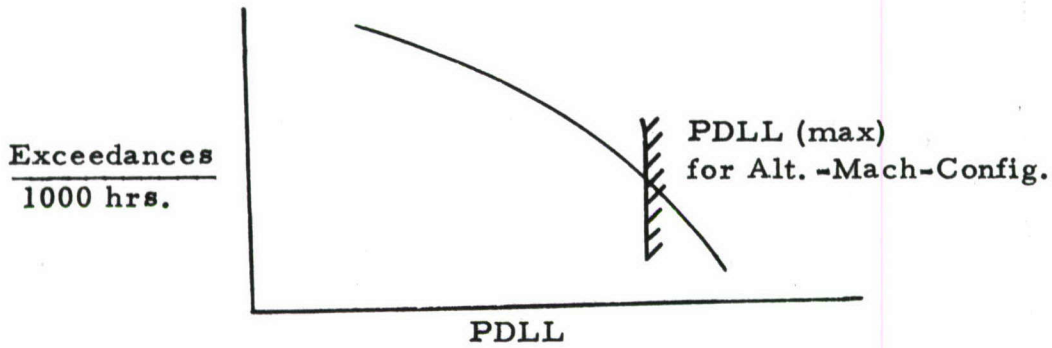

Figure 12. Upper Limit for Percent Design Limit Load

Another parameter which should be discussed is the pilot input. The same pilot could record a segment of V-G-H data under the same environmental conditions for two different days, yet because of a change in his disposition have two recognizably different spectra. This situation is compounded by the fact that "hot rodders" and "overly conservative" pilots exist. The only solution to this is to rotate the pilots and to obtain sufficient data, so that stabilized parent distributions can be found.

The mission segment is a most important parameter for maneuver input spectra. As a consequence, each mission segment must have a different spectrum. It is most likely that additional breakdown will be necessary according to type of mission, such as instruments or autopilot, training flights, peacetime operational flights, and wartime operational flights. The mission segment exceedance curves are usually dependent on time or distance; thus it is essential that some uniform ground rules be made and adhered to when defining and extracting data from each time period involved (i.e., each type of mission segment) from the V-G-H flight history. It is also necessary, on noninstrumented aircraft, that the pilot log utilize the same ground rules as those used in formulating the spectrum. Studies of the pilot's log and V-G-H data for the same flight has shown that fairly large discrepancies exist in defining mission segments and time spent in these segments. For example, Figure 13 shows a histogram of the percent difference between the time used to determine the low level environmental spectrum and the time which the pilot recorded on AFTO-70 forms for this same low level segment. Figure 14 shows a typical flight history and various methods which could be used to define the low level segment. Figure 15 is a bar graph showing the increments of time recorded for low level flight for various flights and is used as an intermediate step for determining Figure 13. Figure 16 is a histogram of number of flights vs. percent deviation in time for refueling segments.

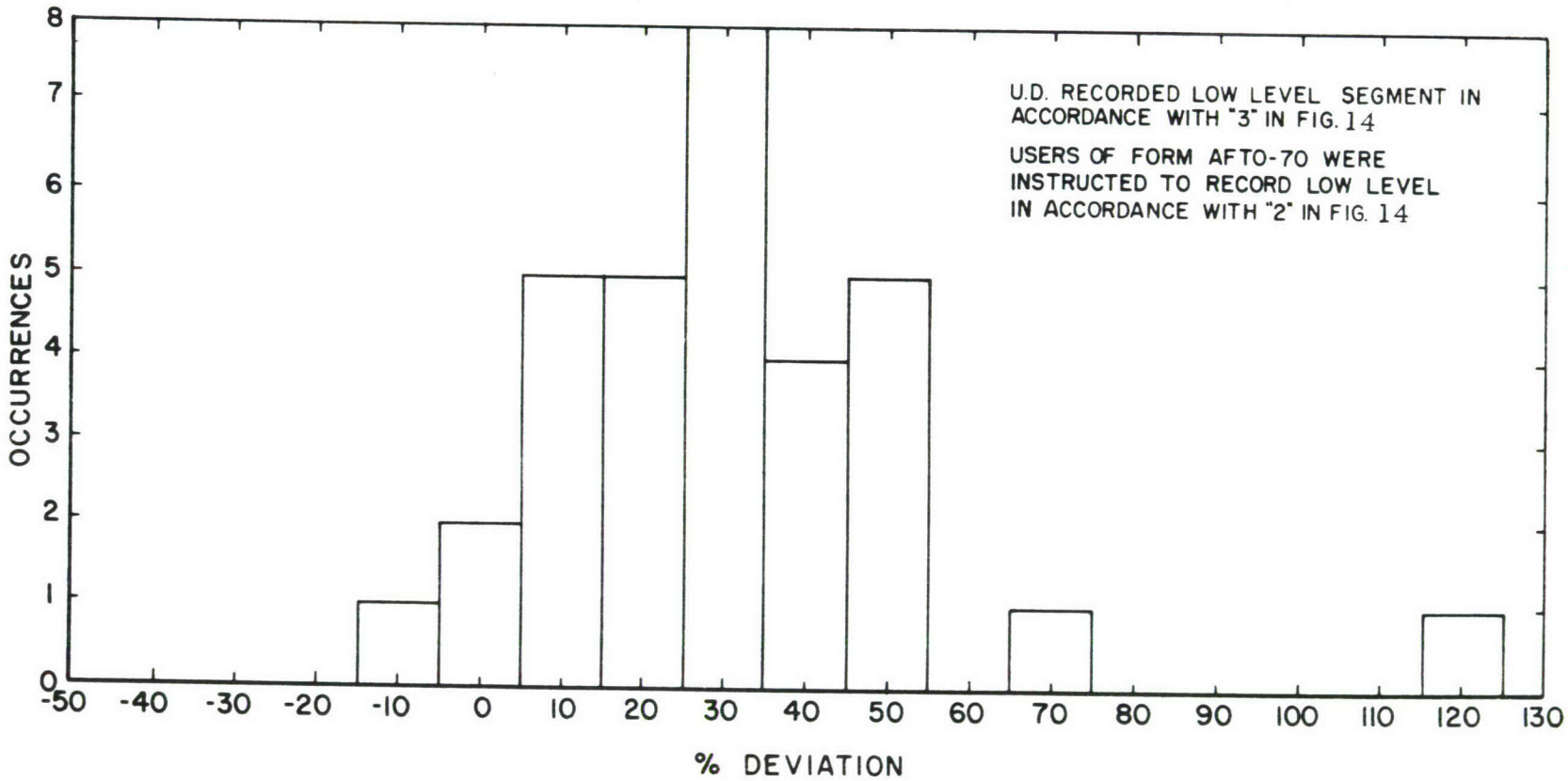

Figure 13. Percent Deviation Between the Time Used by University of Dayton in Determining the Low Level Environmental Spectrum and that Recorded on the Pilot Log AFTO-70 for B-58

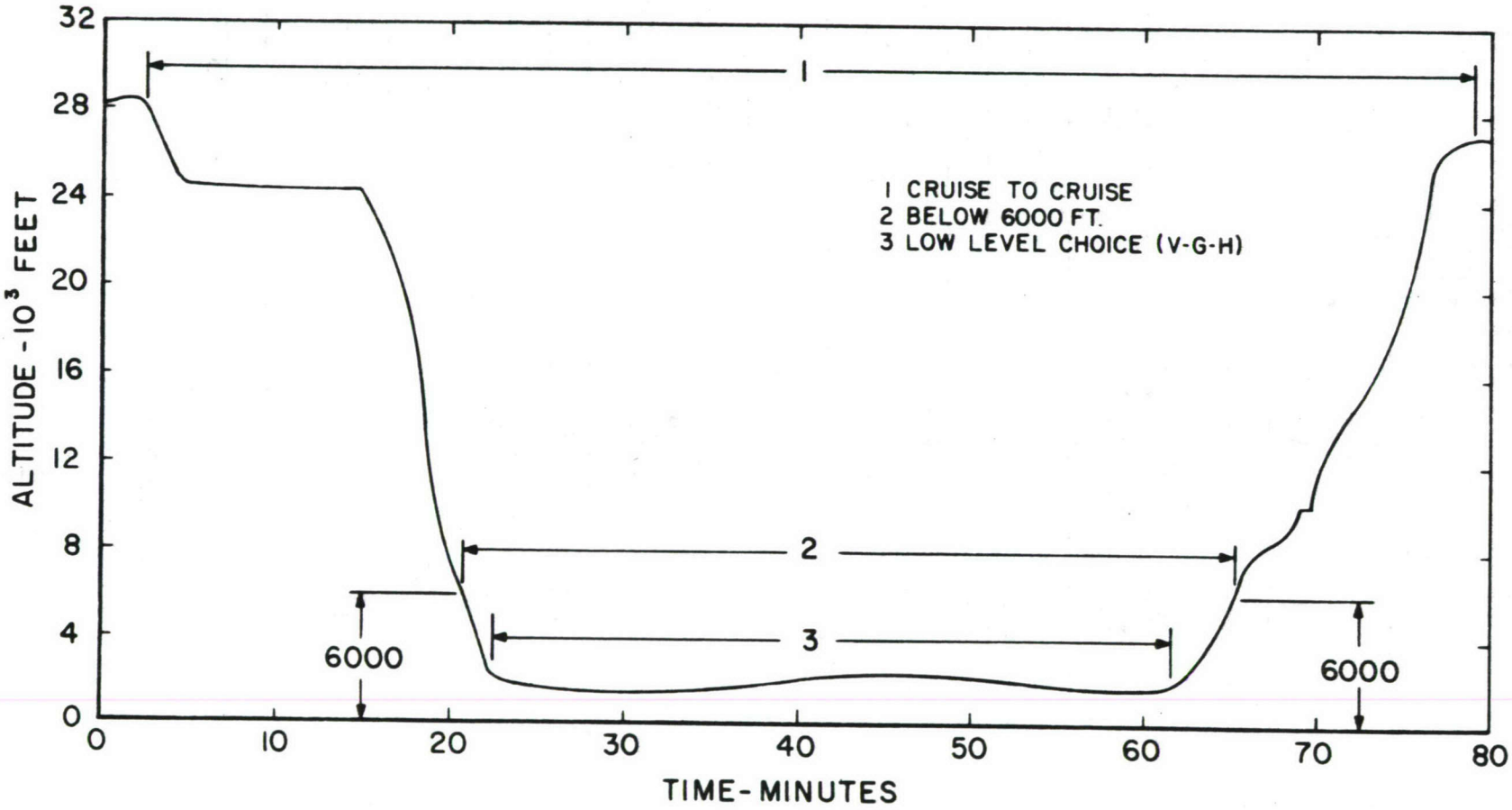

Figure 14 Possible Methods of Determining Low Level Flight from Typical B-58 Flight Profile

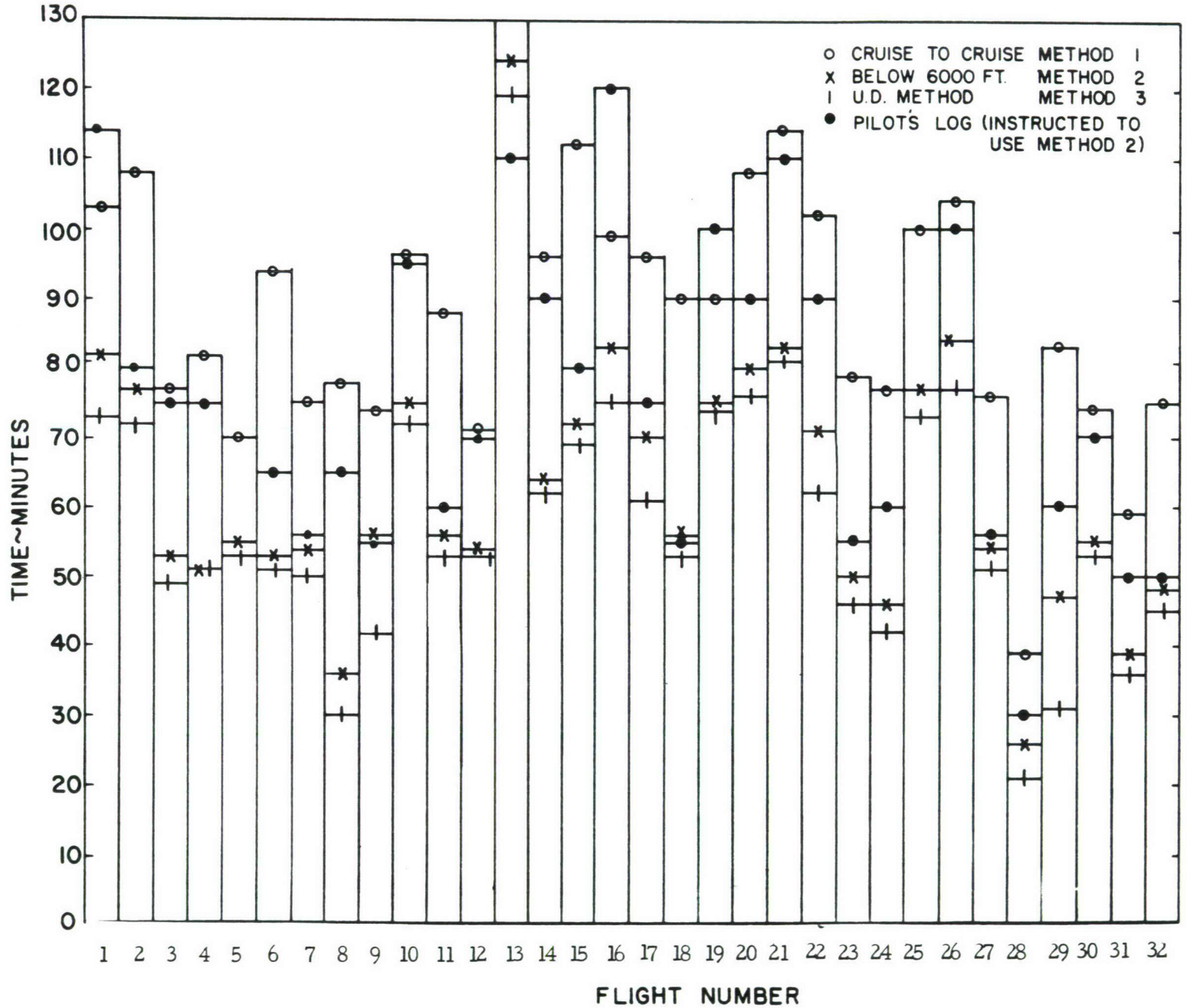

Figure 15 Bar Graph by Flight Number of Time Spent in Low Level Environment by Methods of Figure 14 for Thirty-two B-58 Flights

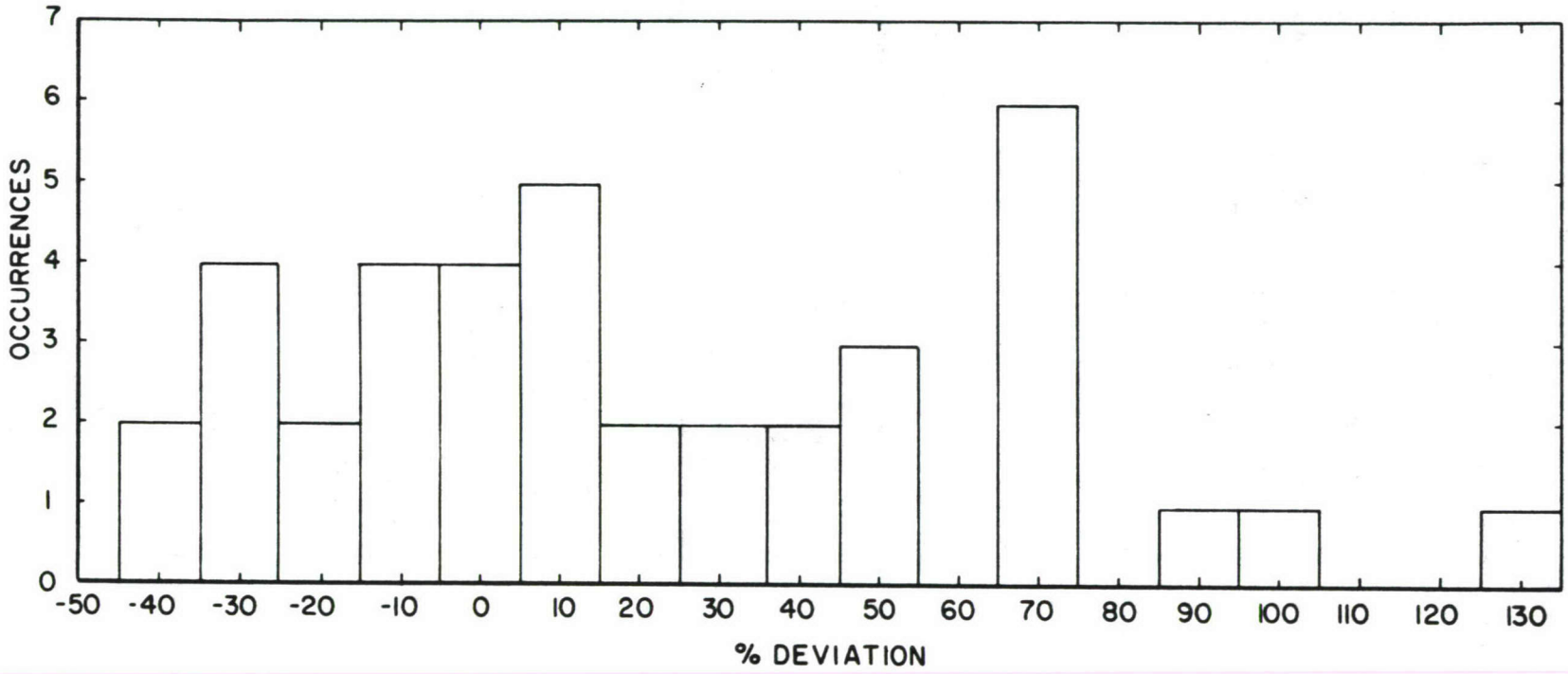

Figure 16 Percent Deviation Between the Time Used by University of Dayton in Determining Refuel Environmental Spectrum and that Recorded on the Pilot Log AFTO-70 Form for the B-58

In the following paragraphs the various in-flight mission segments will be discussed in greater detail. In using the segmented mission approach, note that for fighter aircraft very little data is available in report form by this method. Table I and Figure 17 have been reproduced from Reference 9. These input spectra are for total missions (i.e., they include ascent, cruise, descent, etc.). The questions that arise from this approach are:

(1) These spectra reflect a specific mix or usage for the aircraft. What happens if this usage changes?

(2) What should be done when a mission involved a combination of special maneuvers (e.g., low angle bombing, air to ground gunnery and on the cruise back segment, air tactics)?

Figures 18 through 23 give representative input spectra based on the mission segment approach. These figures will be referred to in the applicable paragraphs.

(1) Ascent

In addition to making the previously mentioned breakdowns for maneuver input spectra representation, it is advisable to investigate the difference between nominal and full power climb input spectra. There is a possibility that the two input spectra may plot as parallel lines on semi-log paper. This situation would indicate that the occurrence rate of one spectrum was a constant multiple of the other.

Several maneuver climb input spectra are presented to show the various formats and to show relative comparison for the various vehicle classes.

Nominal Climb

Fighters - Figure 18 (F-105D)
Bombers - Figure 19 (B-58)
Tankers and Transports - Figures 20-22 (C-135 A/B)

Full Power Climb

No data available.

(2) Cruise

In addition to the proposed general breakdown of input spectra, two or three optimum cruise conditions (i.e., Mach number and altitude) should sufficiently define representative input spectra. The choice of these conditions will be a function of the aircraft design requirements. In addition to the optimum cruise conditions, representative spectra for low

Table I

Fighter, Trainer, and Small Bomber Maneuver Data
Mission Breakdown

No.	Mission	Fighters	Time-Hrs.	(1) Trainers Time-Hrs.	(2) Small Bombers Time-Hrs.
1	Air to Air Gunnery	F-100, 104	1412.8	121.1	- - -
2	Air Tactics	F-100, 105	2308.3	993.5	- - -
3	Special Weapons Delivery	F-100, 105	565.0	- - -	85.3
4	High Angle Bombing with Rockets	F-100	206.9	38.4	64.1
5	Low Angle Bombing and Strafing	F-100, 104	641.1	55.3	
6	Conventional Bombing	F-101, 105	178.1	- - -	- - -
7	Air to Ground Gunnery	F-104	101.5	- - -	- - -
1-7			5413.7	1208.3	149.4
8	Intercept	F-102, 106	2483.5	- - -	- - -
9	Transition	F-100, 105 RF-101	2056.3	626.9	1172.2
10	Navigation and Instrumentation	F-101, RF 101	630.6	- - -	- - -
11	Reconnaissance	RF-101	1658.4	- - -	- - -
8-11			6828.8	626.9	1172.2

(1) T-33, T-37
(2) B-57

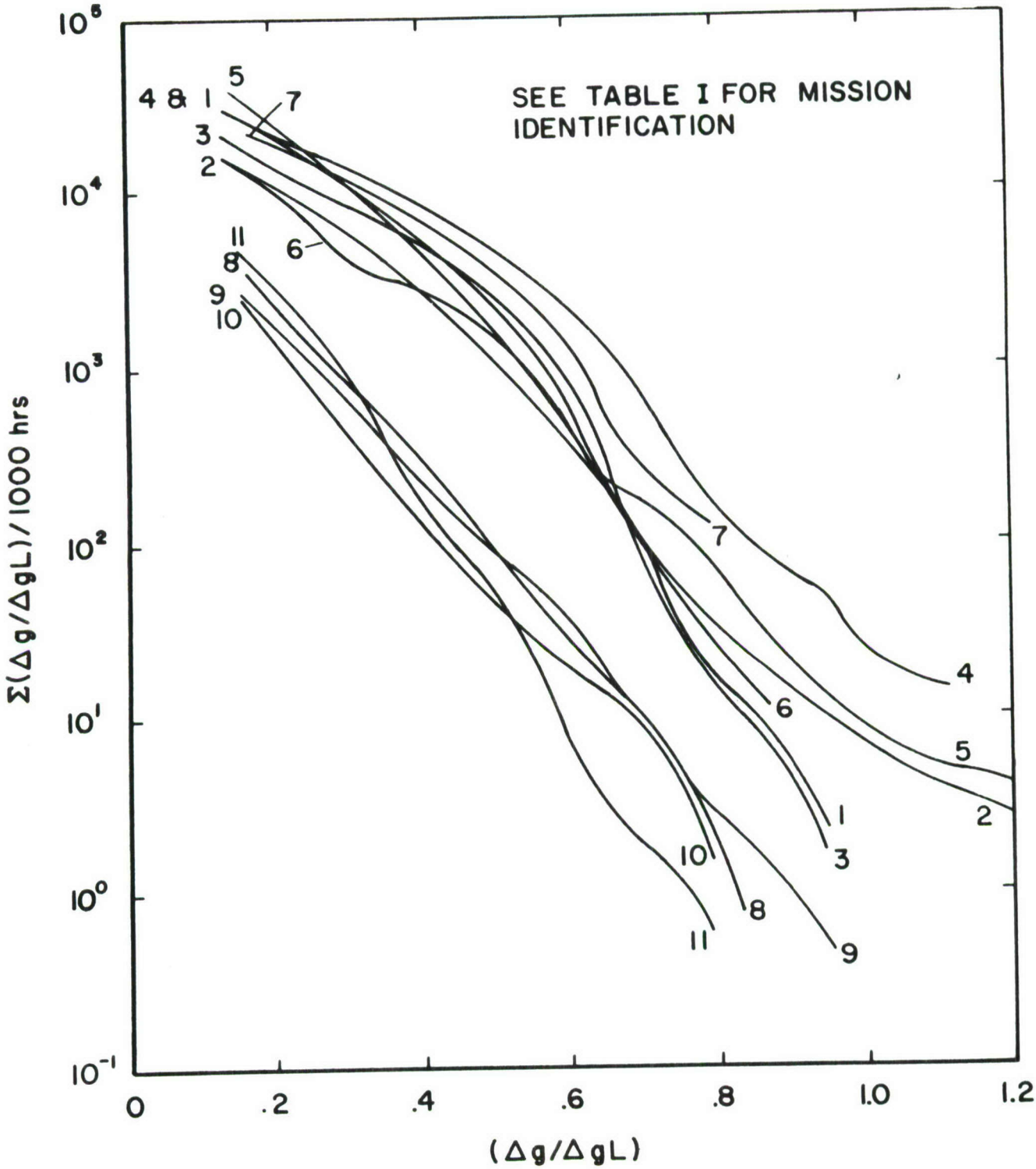

Figure 17 Fighter Maneuver Spectra for Different Missions

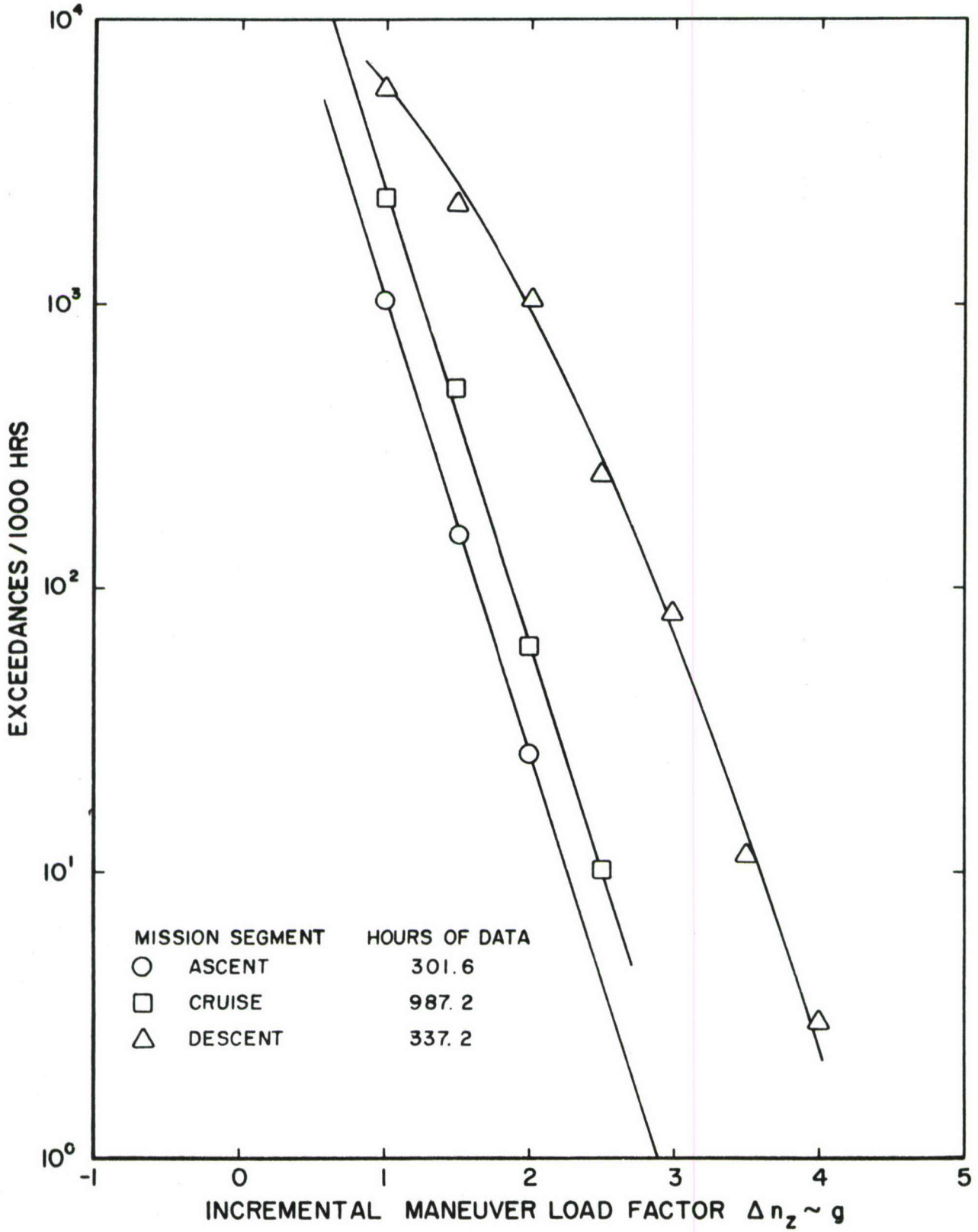

Figure 18 Incremental Maneuver Load Factor Exceedance Curves by Conventional Mission Segment for the F-105D

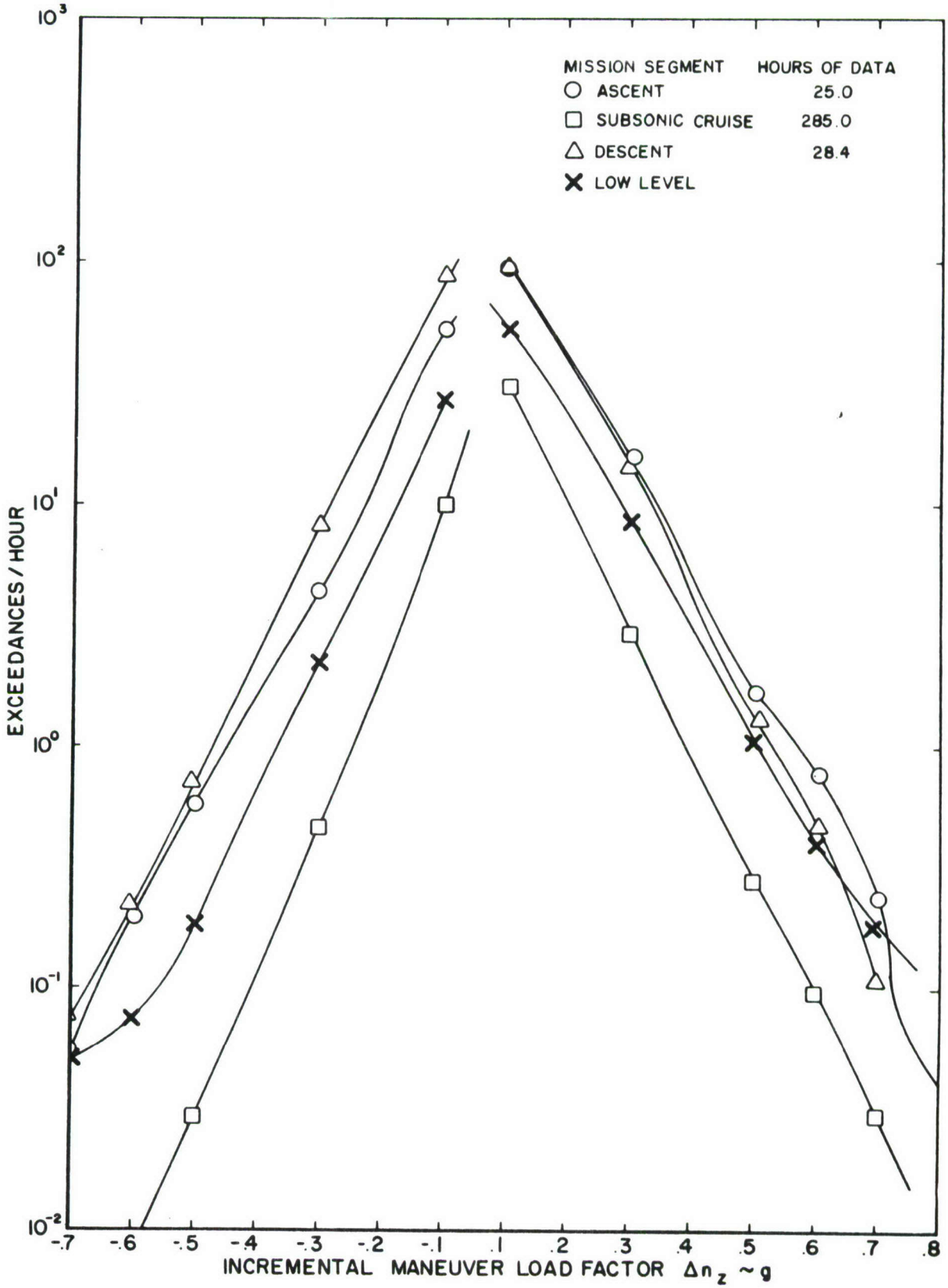

Figure 19 Incremental Maneuver Load Factor Exceedance Curves for Mission Segments for the B-58

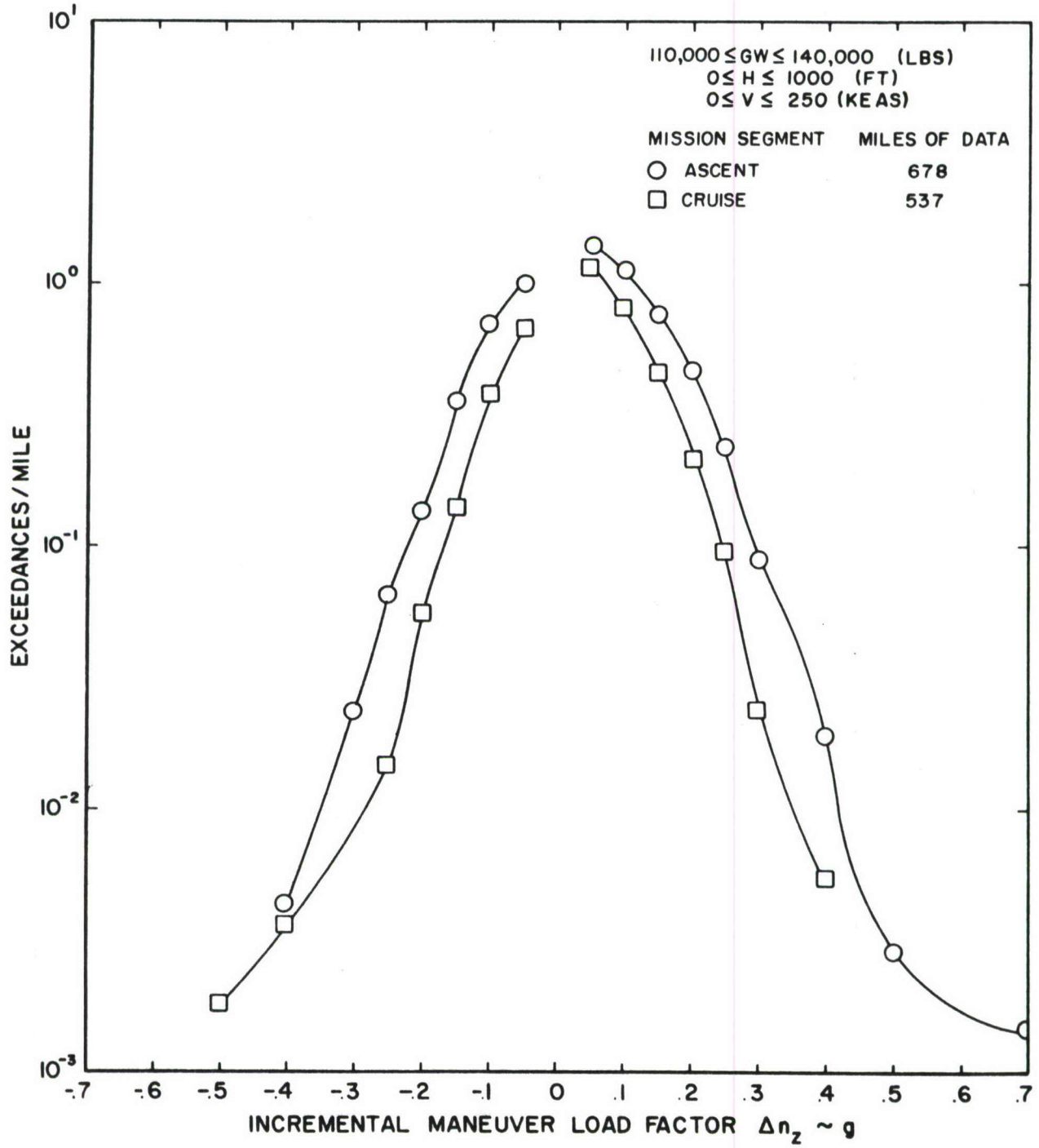

Figure 20 Incremental Maneuver Load Factor Exceedance Curves for the C-135 A/B Aircraft by Gross Weight, Altitude, Airspeed Blocks

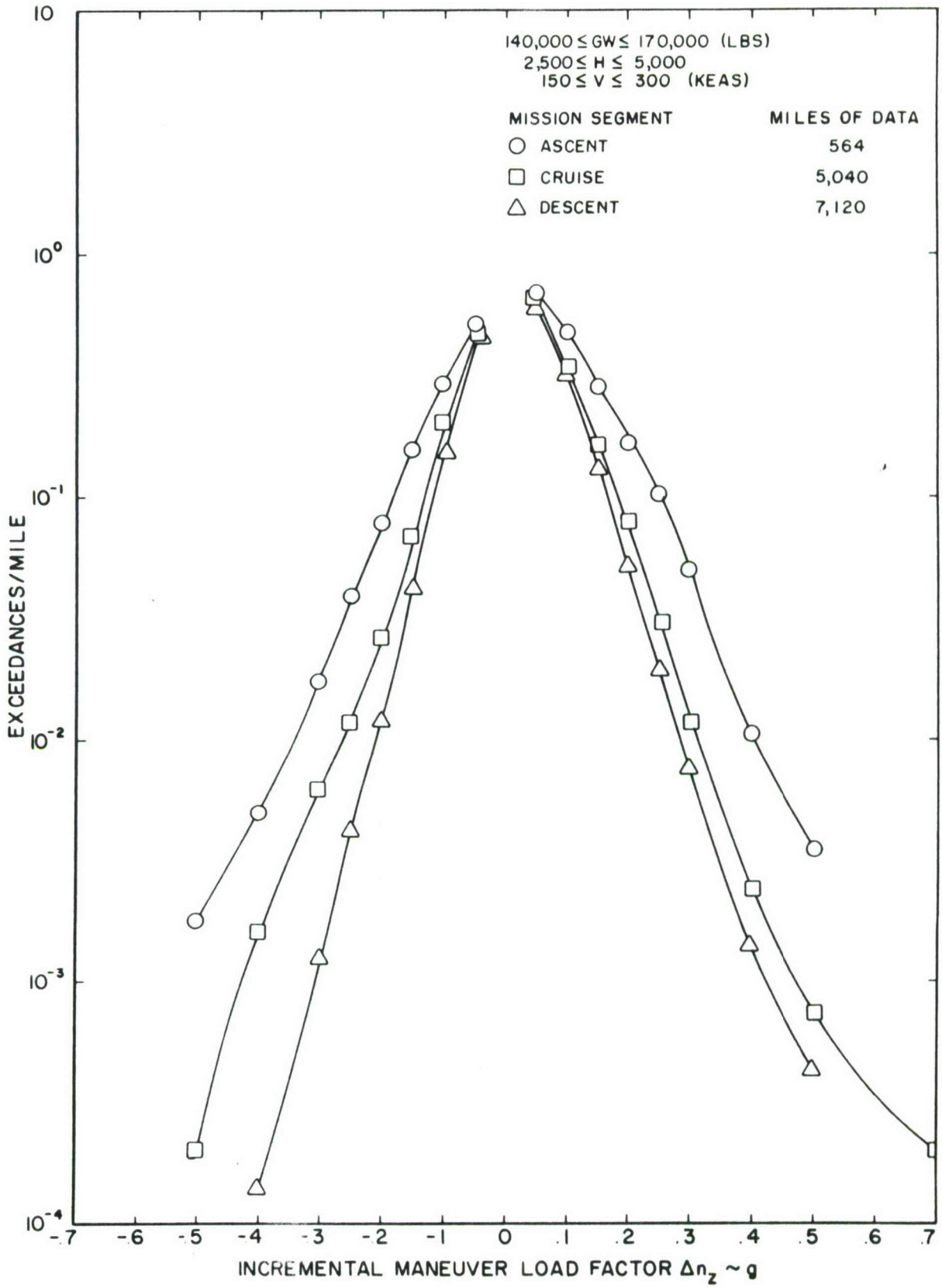

Figure 21 Incremental Maneuver Load Factor Exceedance Curves for the C-135 A/B Aircraft by Gross Weight, Altitude, Airspeed Blocks

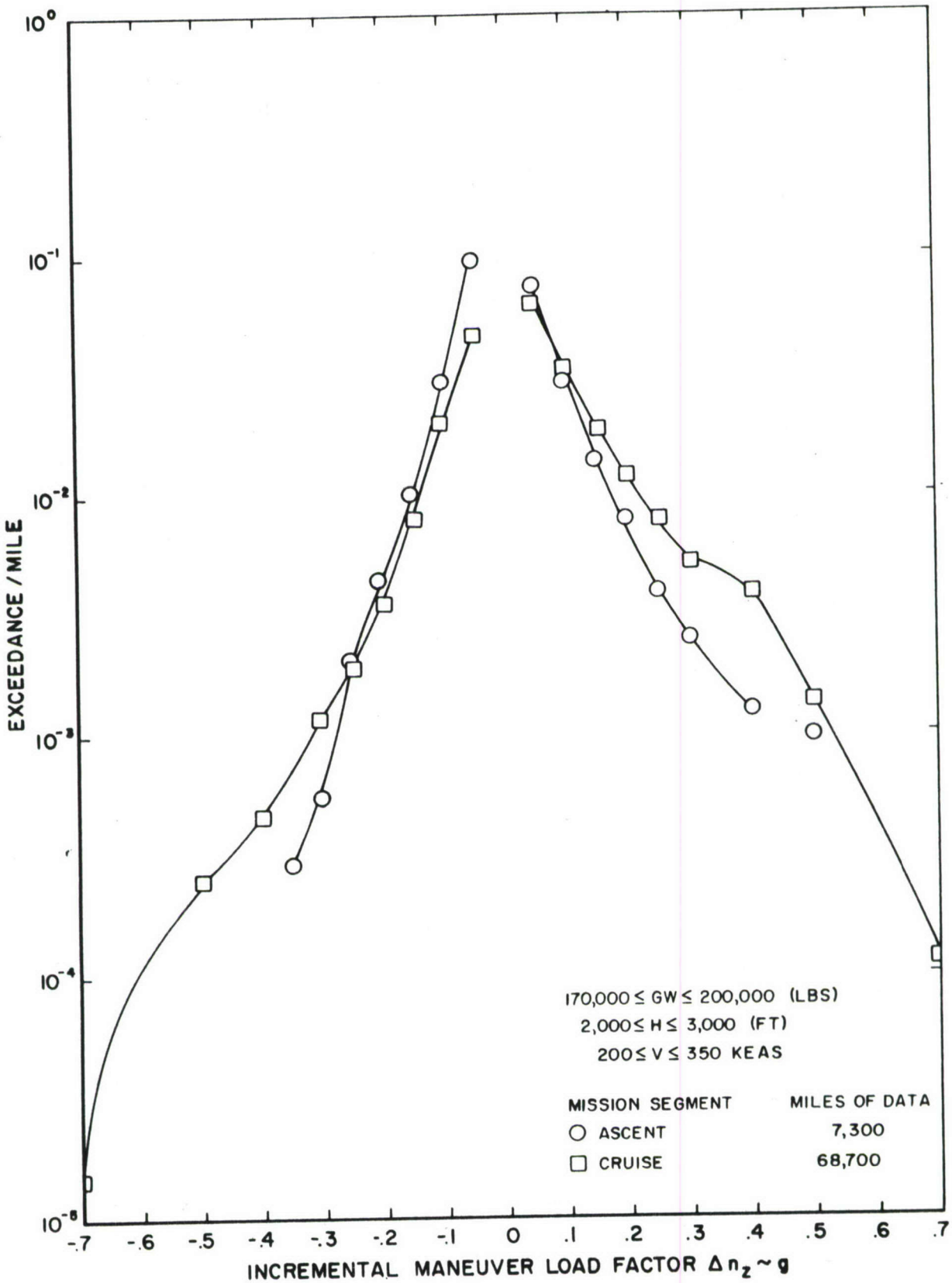

Figure 22 Incremental Maneuver Load Factor Exceedance Curves for the C-135 A/B Aircraft by Gross Weight, Altitude, Airspeed Blocks

level penetration runs should also be included. In all, there will be the following additional breakdowns:

Supersonic	1 Optimum Mach-Alt Combination
Subsonic	1 or 2 Optimum Mach-Alt Combination(s)
Low Level Penetration	
Terrain Clearance	Mach-Alt Conditions as required
Terrain Following	Mach-Alt Conditions as required

Representative cruise maneuver input spectra are shown for:

Fighters - Figure 18 (F-105D)
Bombers - Figure 19 (B-58)
Tankers and Transports - Figures 20-22 (C-135 A/B)

(3) Descent

Descent maneuver spectra will have a breakdown similar to the ascent spectra. Two breakdowns should be made so that nominal descent and full-powered dive are considered.

Typical descent maneuver spectra are presented for:

Fighters - Figure 18 (F-105D)
Bombers - Figure 19 (B-58)
Tankers and Transports - Figure 21 (C-135 A/B)

(4) Refueling

The environmental conditions under which refueling will occur will be a function of the flight characteristics of the tanker and the aircraft being refueled. A fixed Mach number and altitude condition can be assigned, according to the aircraft combination involved. The capability and experience of both pilots, plus the downwash effects, will be the most important parameters for this input spectrum (the possibility of tanker autopilot must be considered). On many occasions experienced pilots accomplished a refueling segment for fighter aircraft with no recorded g's above the 2-g threshold (References 9 and 10). However, for large bomber aircraft the refueling mission segment can be one of the most severe flight conditions.

(5) Special Maneuver Segments

There are special maneuver segments which must be considered for fighter and in certain instances for all aircraft. The breakdown of anticipated special segments is as follows:

Air to Ground

- Bombing
  - Low Angle
  - High Angle
- Ground Gunnery
- Rocket Launch
- Photography and Reconnaissance
- Special Weapons Delivery
- Cargo Drop
- Other

Air to Air

- Air Tactics
- Air to Air Gunnery
- Missile Launch
- Other

Other Operational Segments

- Loiter
- Practice Landing

In order to achieve as fine a breakdown of maneuver input spectra as that shown above, more data than V-G-H will be required. For instance, for input spectra which are expressed as a function of time, some method must be devised to define accurately the entry and exit times and the type of segment involved. To acquire these data, a considerable amount of pilot assistance and/or instrumentation will be required. This is especially true when it is realized that the external configuration and gross weight change abruptly when stores or munitions are dropped or fired. It has been found that input spectra for conventional bombing, ground gunnery, and air-to-ground rocket launch might better be expressed as a function of the number of drops or passes, rather than as a time rate.

Very little data is presently available by segments for flights which have special maneuvers, primarily because in the past V-G-H data were accumulated for a mission type and the resulting input spectrum represented the total mission. The fallacy of this approach has been pointed out. In addition to the need for input spectra for these special segments, it is also very important to show the environmental conditions of Mach number and altitude under which these spectra should be applied.

A considerable amount of effort was expended to define input spectra for various mission segments in Reference 10; however, the environmental data is obliterated by presenting it for total mission types. A sample case (Refrence 10, Volume I) concerns air-to-air gunnery. Although 71.7 hours of recorded data for air-to-air gunnery are shown, the listing of environmental relationships reveals that 18.7 hours of ascent data, 26.7 hours of cruise data, 0.1 hour of refueling data, and 17.1 hours of descent data have also been included. Figure 23 shows special maneuver input spectra obtained on a time rate basis for the F-105D aircraft.

c. Landing Spectra

The problem of specifying aircraft input loads under landing conditions requires a complete knowledge of the initial contact conditions. The major parameters are sinking speed, forward speed, aircraft attitude and/or attitude rates, and the wind speed. The problem is to determine a proper distribution of combinations of these parameters. Most analyses that were found considered only the sinking speed with arbitrary choices made on combinations of attitude at impact. One source (Reference 15, paragraph 3.2) does define an elliptical envelope utilizing most of the parameters mentioned; however, different coefficients would have to be developed for land-based aircraft.

If fatigue damage due to landing impact loads is determined to be negligible for the most critical locations in comparison to damage from other loadings, excessive refinements in specifying the input spectrum as it pertains to each parameter may be unwarranted. However, experience has shown that landing causes severe fatigue damage on some types of aircraft. A rational combination of values for these parameters might be decided mutually by the contractor and the Government agency, utilizing sink speed data from Table IV of Reference 7 and/or other representative statistical data, such as that in Reference 2.

d. Taxi and Runway Spectra

The spectra involved encompass the cyclic loads resulting from runway-taxiway roughness during pre- and post-flight taxiing, takeoff run and landing rollout. The major parameters involved are landing gear characteristics, airplane flexibility, gross weight, taxiway and runway roughness, taxi or runway speed, and taxi or runway time or distance. Two approaches are possible; however, they are not necessarily independent:

(1) Use power spectral density methods.

(2) Formulate input spectra from operational V-G-H data.

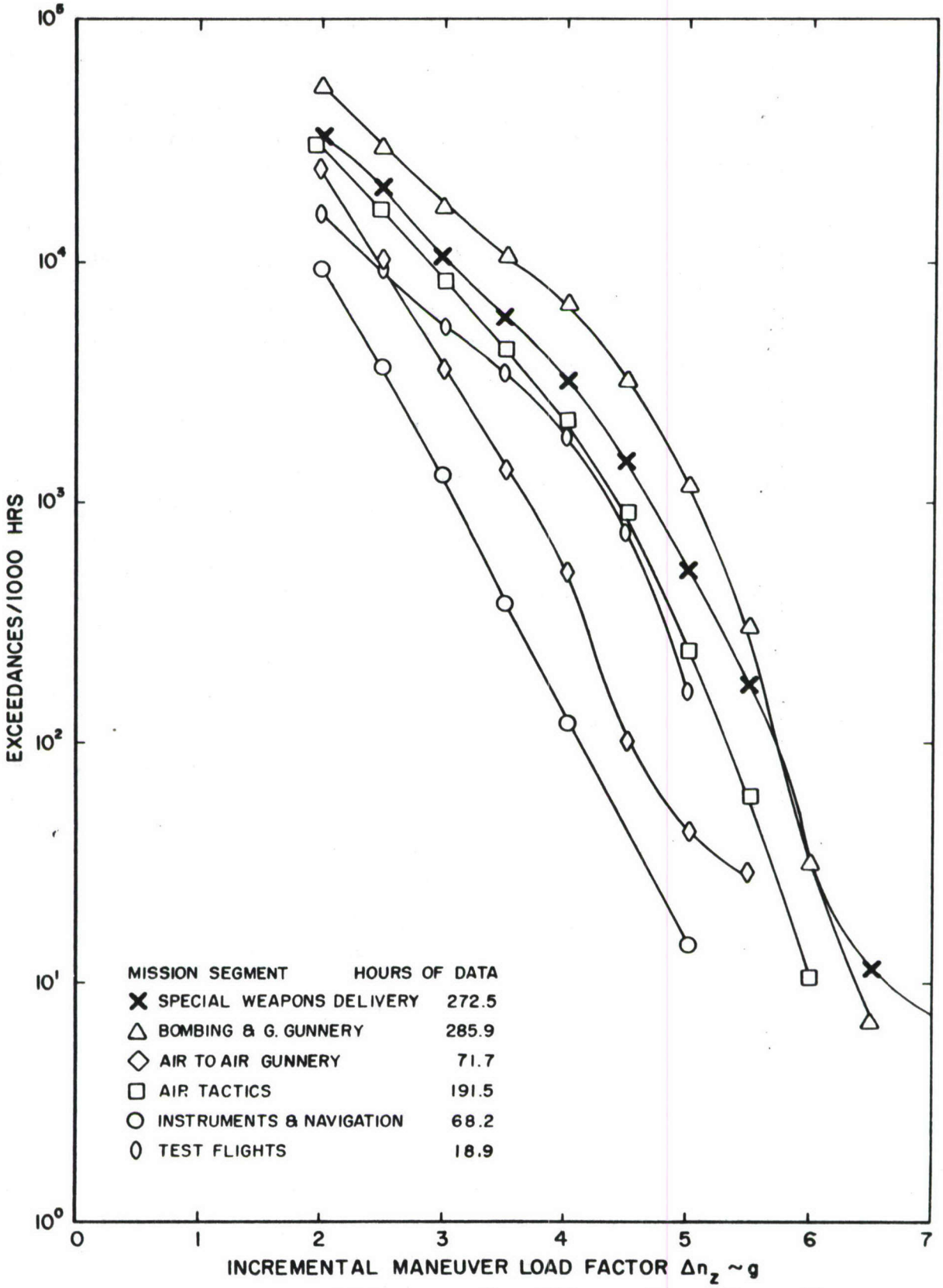

Figure 23 Incremental Maneuver Load Factor Exceedance Curves for Special Mission Segments for the F-105D

A considerable amount of work has been done concerning taxiway roughness properties (Reference 1). Various runways have been classified as rough, medium, or smooth, and plots are shown of the power spectral density of many runways based on elevation measurements. Methods are shown by which equations may be fitted to the spectral density curves based on smoothing of discrete masses. The environmental loads resulting from taxi takeoff or rollout depend not only on the surface conditions, but also on taxi velocity. The nonlinear characteristics of modern aircraft landing gear are serious obstacles to the direct application of surface roughness spectra in analysis. These nonlinear characteristics are chiefly manifest in the oleo damping and friction forces. One approach to this problem would be to linearize these forces, thus facilitating the usual spectral analysis through frequency response techniques. One investigation (Reference 12) indicated that this was not a promising avenue of approach since the results proved to be too sensitive to the linearization techniques employed. In the study of Reference 12, it was considered to be feasible to obtain analog solutions to the nonlinear gear and elastic airplane equations of motion in response to stationary random inputs having the spectral characteristics of the runway population. Reference 2 extended and refined the techniques of Reference 12 and applied them to taxiing spectra for two aircraft (the DC-7C and the C-133) for three field roughness intensities and four taxi speeds. A condensed version of the steps follow:

(1) Collect and classify as to roughness intensity, taxi, and runway power spectral densities.

(2) Review each spectrum to verify that grade effects have been removed. In effect, a linear trend in elevation data appears as zero frequency power in the spectral density. This distortion is particularly serious because of the insensitivity of aircraft to runway grade (Reference 2).

(3) The root-mean-square runway height, σ, was used as a convenient measure of roughness intensity.

$$\sigma = \left[\int_{\Omega_1}^{\Omega_2} \phi\ (\Omega)\ d\ \Omega \right]^{1/2} \tag{12}$$

Typical values for σ are given for smooth, average, or rough runways (Reference 2).

(4) A regression analysis was performed on the data to arrive at a mean spectrum

$$\phi\ (\Omega) = C\ \Omega^{-n} \qquad \frac{\pi}{80} \leq \Omega \leq \frac{\pi}{2} \tag{13}$$

where $\Omega = \omega/V$

and the constants found for the data used were

$C = 0.577 \times 10^{-5}$, and
$n = 2.576$.

(5) For analog purposes, the mean spectrum equation (see item 4) required a rational function approximation, since a realizable shaping filter was necessary to generate noise with a desired spectral density. The fitted curve $\phi_0(\Omega)$ approximated the mean spectrum quite well in the interval $.08 \leq \Omega \leq .75$ where

$$\phi_0(\Omega) = \frac{0.01593\,\sigma^2\,\Omega^2\,0.1884 + \Omega^2)}{(0.0004 + \Omega^2)(0.0001 + \Omega^2)(0.04216 + \Omega^2)\,(2 + \Omega^2)} \qquad (14)$$

(6) The dynamic characteristics were calculated for the aircraft involved in the form of mode shapes, frequencies, mass and inertia data and gear equations. In addition to this, the equations of motion were developed and placed in proper analog format.

(7) The primary noise source of the input to the mechanized system of equations was a random telegraph wave, i.e., a square wave with zero crossings controlled by emissions of particles from a radioactive source and hence having a Poisson distribution (Reference 2).

A parametric study (Reference 2) was performed, using the two aircraft with two weight configurations, four taxi velocities and three classes of runway roughness. In this power spectral analysis study, the output was the number of vertical g's that the aircraft center of gravity experiences. In this study it was found that a cycle is best represented by a $\pm\Delta g$ from the 1-g mean load level. These g-loadings must be converted to stress levels for each critical fatigue point which is a function of the environmental condition. In regard to the taxi input spectra, it was found that the effect of taxi velocity on the input spectrum was as pronounced as the roughness intensity of the taxiway. It was also found that taxi velocity as a random variable would not be independent of roughness intensity; i.e., it is likely that a pilot, on finding himself exposed to large roughness intensities, would decrease taxi speed to reduce response levels. This feature obviously does not apply to take-off or rollout.

In summary, an analog computer method has been developed to determine taxi input spectra as a function of runway roughness, taxi speed, landing gear characteristics, gross weight, and, to a minor extent, other aircraft characteristics. A considerable amount of additional work will be necessary to consider speeds greater than 70 miles per hour. In certain

instances, linearization of the gear nonlinearities may be feasible (Reference 13).

Operational taxi and runway data are essential, if only to determine the period of time or distance within the environment. If sufficient data are collected, it might also be possible to ascertain the effects of

(1) flaps or spoilers in takeoff,
(2) different bases having comparable roughness intensity.

If sufficient V-G-H data are collected, the spectrum would account for field roughness and speeds, insofar as the usage is representative. Because the spectrum is also a function of gear characteristics and airplane flexibility, considerable care must be taken before using spectra developed from one model aircraft on another model.

e. Braking, Turning, and Pivoting Spectra

The input spectra for braking, turning, and pivoting for use as design requirements are defined as follows (Reference 7, paragraph 3.6):

Braking

Type	Load Level	Cycles/1000 Landings
Hard	Max. Braking function of Gross Weight	2000
Medium	1/2 Maximum Braking	5000

Turning

Left	0.4 (GW)	Any combination with
Right	0.4 (GW)	total of 5000 turns

Pivoting

Pivoting	1/2 Limit Torque	100

It is not known whether these data have been obtained from statistical data. However, in order to determine damage calculations by aircraft tail number, operational data should be taken to substantiate the spectra selected. Additional data on the vertical loading and representative friction coefficients are shown in Reference 14:

Braking, paragraph 3.3.1
Turning, paragraph 3.3.2
Pivoting, paragraph 3.3.3

Dynamic response and methods of combined loading interaction are also discussed in this specification. If an aircraft designer can provide other rational methods, based on theory or experimental data, the method will be acceptable, subject to approval by the procuring activity.

f. Handling and Maintenance Cycles

The spectra involved in this paragraph should be based to a varying extent on operational procedures at a given base or for the particular type aircraft involved. The mix of loading cycles sometimes seems to be based on rational decisions but sometimes on arbitrary decisions.

(1) Towing Loads Spectra

Towing conditions and the respective loadings are considered in paragraph 3.4.1, in Table III, and in Figure 1, of Reference 14. However, the expected number of applications under each condition is not shown. Some rational approach should be made to determine a proper mix of towing loads per 1000 flights and verified by recorded data. The following is a typical breakdown for symmetric and asymmetric towing conditions.

Symmetric Towing:

Load Levels	Number of Cycles/1000 flights	
function (GW, DMF)	Forward	Aft

Asymmetric:

Select Towing Angle(s)

Load Levels	Number of Cycles/1000 flights			
	Left		Right	
function (GW, DMF, Towing angle)	Fwd.	Aft	Fwd.	Aft

(2) Testing Actuating Mechanisms

Each aircraft and base may have unique standard check-out procedures, such as operation of flaps, rudder, elevators, ailerons, bomb bay doors, etc. In addition to these cycles, it is likely that servicing, cleaning, ground refueling, etc., may also incur fatigue loading cycles which may be harmful to a given control point. Some method of rationally assessing input load levels as well as frequency of occurrence should be made. If it can be shown that the representative load levels have an insignificant effect on the lifetime of the control points involved, the corresponding input spectra may be ignored.

(3) Special Ground Loading

In addition to input spectra previously mentioned, it is considered appropriate to investigate the frequency of occurrence and load cycles

anticipated in:

(1) dry run tests of pylon loading of stores and munitions,
(2) engine rev-up.

In addition to these types of loadings it is advisable to investigate the load levels for:

(1) jacking,
(2) hoisting,
(3) other handling procedures.

The frequency of occurrence of these later loadings will be quite obvious on a tail number basis, provided that the maintenance crew properly records this information.

g. Store Release and Ejection Loads

Consider an aircraft in horizontal flight and at a steady state condition at the time a store is released. The release of the store (not considering the change in aerodynamics), will give an incremental vertical load factor on the center of gravity of

$$\Delta n_z = \frac{\Delta W}{(W-\Delta W)} = \frac{\dfrac{\Delta W}{W}}{1-\dfrac{\Delta W}{W}} \qquad (15)$$

where ΔW is the weight of stores released, and
W is the initial aircraft weight prior to store release.

The vertical load factor is therefore a function of the ratio of stores weight to aircraft weight prior to release. If the stores are attached to wing pylons, a dynamic loading condition occurs because of the sudden change in mass distribution. In this case, aircraft flexibility and aerodynamic damping must be considered. The problem is compounded when the stores, drag, and longitudinal inertia effects are included. Changes in value of these parameters will cause a sudden change in the wing chordwise bending and torque loading. Using the steady state condition in horizontal flight was primarily for illustrative purposes; however, use of D'Alembert's principle and the equations of motion will account for any flight path angle, angle of attack, and initial dynamic condition. In most instances an impulse loading is given to the stores in order to eject them out of the slipstream of the aircraft. The impulse reaction force on the aircraft can be determined by theory and confirmed by test. In most instances, this ejection force will have a greater effect than the change in configuration.

The fatigue damage at several wing control points due to wingtip stores ejection > 600 lb on the F-5A was rather minor. Thi s aircraft was quite

small (14,000 lb); however, because it was a fighter, it was also relatively stiff. If fatigue damage due to stores release or ejection cyclic loading is verified to be insignificant, this damage may be ignored.

h. Special Environmental Cycles

Some input cycles are entirely dependent on the aircraft capabilities and usage. With the increased speeds, higher altitude capabilities, and greater landing speed requirements, it is necessary to investigate thermal stress cycles, cabin pressurization cycles and landing drag chute or arresting gear loads.

(1) Thermal Stresses

Thermal stresses occur in a rigid composite structure when differential expansions exist. The differential expansion is caused by temperature differentials or different material coefficients of expansion. The temperature differentials are caused by the heating rate input and the existence of heat sinks (heavier structural members and/or liquid storage tanks). The input heating rate is a function of such parameters as the Mach number, altitude, aircraft contour, Reynolds number and/or boundary layer thickness, the material and/or coating thermal properties (i.e., conductivity and emissivity).

The temperature variation over applicable structural members and panels can be expressed as a function of time and displacement from a reference coordinate axis for a designated flight history. Thermal stresses can be calculated for any structural section if this temperature variation and the restraints involved are known. It would be difficult to consider thermal stress cycles without pre-determining an environmental pattern. Once a soaking temperature has been reached, thermal stresses will probably be reduced except possibly in regions of liquid storage tanks or where there are different materials in the structure. In addition to the skin friction heating source, other localized heating sources exist, such as the aircraft engines, avionics equipment, and other equipment distributed throughout the aircraft. In a sense, thermal stresses at a given fatigue point may be considered on a cycle per flight basis. The cycles attributed only to thermal stress change might best be determined from a history of a representative mission for the aircraft involved with consideration given to secondary cycles.

(2) Cabin Pressurization Cycles

The cabin pressurization cycles will be a function of the altitude environment in a mission, selected cabin altitude environment, and the operation of the relief valve.

In many instances the pilot has the opportunity of selecting an equivalent altitude cabin environment, and this selected cabin pressure will be held until the difference between ambient pressure and cabin pressure (ΔP) tends to become greater than the relief valve setting. The relief valve will not allow ΔP to exceed the design specification, no matter what the altitude.

The differential pressure environment in a flight will affect the fatigue damage by changing the mean stress level of an applicable control point, and hence it will affect the ground-air-ground cycle. Previous studies have not shown that secondary pressurization cycles are essential in fatigue studies of large aircraft.

(3) Special Weapons Delivery

This environmental mission segment was introduced in the maneuver input discussion; however, because it is a special case it will be discussed in greater detail here. Because of the vulnerability of the aircraft to the explosion and the requirement of an accurate drop, the altitude, Mach number, and maneuver can be predicted with a considerable degree of confidence for each type of aircraft. If more than one operational procedure is used in a delivery, these, too, may be predetermined as to altitude, Mach number, and type of maneuver. Therefore, V-G-H data can be used to accumulate a reliable statistical data on normal load factor or PDLL exceedances per 1000 drops under each operational procedure.

i. Special Events

Certain fatigue points have special input spectra because of their proximity to actuating systems. These include such things as flight flap cycles, landing gear extension and retraction, wing sweep settings, bomb bay door cycles, engine thrust cycles, and any other loading cycle of this type. To arrive at a representative number of cycles and the environmental conditions under which they occur, rational assumptions must be made.

2. RESPONSE PARAMETERS

Response factors are those factors or functions which relate the change in stress at a fatigue critical location to the input parameter. These are terms such as incremental stress per unit gust velocity, stress as a function of load factor, incremental stress per ft/sec sinking speed, incremental stress per lateral unit acceleration, incremental stress per unit braking load, etc. Since the magnitude of the alternating stress is generally measured from the 1-g trim stress reference level, the parameters which affect the 1-g trim stress will also be presented in this section.

a. One-g Trim Stress Levels

The calculation of fatigue damage always involves the determination of a change in stress level which results from some input load. Therefore, one of the important parameters is the starting point for this change in stress. For most fatigue cycles the starting point for the stress level is the stress that exists in the structure when the aircraft is in an equilibrium condition at straight and level flight. These stresses will be referred to as the 1-g trim stresses in this report.

(1) Loading Condition

The first condition which affects the 1-g trim stress is the aircraft loading condition; that is, whether the aircraft is on the ground or airborne. Obviously, the stresses in the structure differ greatly depending on whether the weight of the aircraft is being supported by the landing gear or by aerodynamic lifting forces. Of particular importance are the upper and lower wing surfaces outboard of the main landing gear, since these areas have a reversal in the type of stress (i.e., tension to compression or compression to tension). The same may be true of fuselage section near the main gear or between the main gear and the nose gear.

(2) Altitude Effects

Altitude affects the 1-g trim stress levels, since for a constant airspeed, greater angles of attack are required to develop the required lift at higher altitudes. The higher angle of attack will change the center of pressure on the wings and will also change the tail loads as well as the aerodynamic forces on the fuselage. The drag forces for different altitudes will vary greatly for a constant velocity, and therefore affect the thrust and chordwise bending moments.

(3) Airspeed Effects

Airspeed affects the 1-g trim stresses in that for a constant altitude the drag and thrust forces vary greatly with velocity; also the center of pressure will be affected, which in turn will change the angle of attack and the tail and fuselage airloads.

(4) Gross Weight Effects

The gross weight of the aircraft has a direct effect on the 1-g trim stresses because the net lift forces must be equal to the gross weight. Therefore, to develop the required lift, the angle of attack and other aerodynamic loads will change greatly with gross weight. Involved directly with the gross weight is the weight distribution and the resulting center of pressure and center of gravity. As the gross weight is changed, there is usually also a change in the weight distribution in either or both the wing and fuselage sections. These changes will have a more pronounced

effect according to the various locations on the aircraft. Changes in the gross weight due to changes in weight of the fuel in the wings, for example, will have a large effect on the stresses within the wing but may have little effect on the tail or fuselage stresses. Changes in gross weight usually affect the center of gravity position and therefore will require a change in the trim of the aircraft, resulting in a change in the tail loads.

(5) Control Surface Position

The position of control surfaces such as flaps, spoilers, leading edge slats, etc., will cause a change in the 1-g trim stresses.

(6) Wing Sweep Setting

For some of the newer aircraft which have variable sweep wings, the wing sweep angle will have a pronounced effect on the 1-g trim stresses. Because of the large change in the center of pressure position, this may require a shift in ballast weight or a redistribution of fuel; otherwise the tail loads may become excessively large or change direction.

(7) Thermal Effects

The newer supersonic aircraft, which have longer periods of supersonic flight, may have thermal stresses of significant magnitude because of aerodynamic heating. These thermal stresses will, at certain locations, change the 1-g trim stress levels.

(8) External Configuration

The existance of external stores, either weapons or fuel pods, will affect the 1-g trim stresses. Whereas these are really considered to be a part of the gross weight and weight distribution, they should be handled as a separate parameter, since the drag forces on these stores are functions of both velocity and altitude, and the stores themselves are subject to change as new weapons or missions are designed.

b. Gust Load Cyclic Stress

The cyclic stress at a particular location on the structure resulting from a gust disturbance is dependent on the flight condition and the dynamic response of the aircraft. In the analysis of damage resulting from gust disturbances it is generally assumed that a stress cycle is composed of a positive gust peak followed immediately by an equal magnitude negative peak; therefore, the mean stress used with the S-N curves is the 1-g trim stress and the alternating stress is the change in stress due to the positive gust peak. Two methods have been widely used for determining the stress level resulting from a gust disturbance. The older and no longer popular method was to calculate a dynamic magnification factor (DMF), which was the ratio

obtained by dividing the stress at a given point on the structure caused by a dynamically applied center of gravity load factor by the stress at the same point on the structure resulting from a statically applied center of gravity load factor of constant magnitude equal to the peak of the dynamic acceleration. In this method, the magnitude of the center of gravity load factor is a function of the gross weight, airspeed, and altitude. The DMF is a function of the aircraft stiffness and weight distribution. The more popular method used today is the power spectral density approach. In this latter method, the gust disturbance is described as the power in a unit magnitude gust wave as a function of frequency, and the response of the aircraft is determined for a unit sinusoidal disturbance of varying frequencies for a multiple degree of freedom system. The response of the aircraft is then shown by the following equation:

$$\bar{A} = \left[\frac{1}{\sigma_W^2} \int_0^\infty \phi_W(\omega) \mid T_y(\omega) \mid^2 d\omega \right]^{1/2}, \qquad (16)$$

where $\bar{A}$ is the rms stress at a control point for a unit rms gust input. The resulting stress for a unit gust is a function of the input power spectral density, $\phi_W(\omega)$, and the transfer function, $T_y(\omega)$,. This technique is described more fully in the Appendix.

(1) Altitude Effects

The altitude will affect the $\bar{A}$ values because the wave shape of the gust, and therefore its PSD, will vary with altitude, and because the transfer functions will change because of the effect of aerodynamic damping and aeroelastic effects.

(2) Airspeed Effects

Airspeed will have a great effect on the $\bar{A}$ value, since the wave shape of the gust as seen by the aircraft will be expanded or compressed timewise, depending on the velocity with which the aircraft flies through the gust. The change in the time required for the aircraft to traverse a gust will cause a shift in the apparent frequency (reduced frequency) of the gust components and will therefore cause a shift of the power spectrum toward a higher or lower frequency. The transfer function will also be affected by velocity because of aeroelastic effects.

(3) Gross Weight Effects

The gross weight of the aircraft and the distribution of weight both in the fuselage and the wing will have a pronounced effect on the $\bar{A}$ values. The gross weight will affect the alleviation factor for the gust. The weight distribution will affect the transfer function to a degree that depends on the location within a given structure and the degrees of freedom considered for the response analysis.

(4) CG Effect

The center of gravity position will affect the $\bar{A}$ value because it will have an effect on the pitching of the aircraft, which, in turn, will change the angle of attack and cause a change in the lift vector.

(5) Control Surface Position

The control surface positions will affect the $\bar{A}$ values, because of a change in the stress distribution, and also because of a change in the aerodynamic load distribution.

(6) Wing Sweep Setting

For variable-sweep wing aircraft, the angle of sweep will have a multitude of effects. These effects are a result of changes in center of pressure, center of gravity, natural frequencies of higher modes, stress distributions, local stress at the wing root fittings, etc.

(7) Thermal Effects

The temperature of the structure may have an effect on the $\bar{A}$ values, because of the change in stiffness of the structure, which results in changes in the frequency response to a gust spectrum.

(8) External Configuration

The weight and location of external stores will have a pronounced effect on the $\bar{A}$ values at certain locations. The changes will be due primarily to the localized masses, which will change the frequency response and modal shapes of the wing when loaded by a gust disturbance.

c. Maneuver Load Cyclic Stress

Maneuver loads are those load factors which result from a control surface motion. These may be deliberate or reflex actions of the pilot, or they may be initiated by the control system. In actually determining the maneuver load spectrum for heavy aircraft from V-G-H data, a maneuver load is defined as a center of gravity acceleration which deviates from the one-g value for two seconds or more, and during which time the airspeed recording is smooth (i.e., the airspeed transducer output does not indicate a turbulent atmosphere). While this definition attempts to separate the gust loads from the maneuver loads, it also has the advantage of automatically dividing the loads into two groups, those which are of short duration and rapid rise time and require a dynamic analysis of the response, and those of long duration and slower rise time that permit a steady state analysis.

(1) Altitude Effects

For a given load factor, the altitude will affect the resulting change in stress because of the control surface deflection and the greater angle of attack at the higher altitudes.

(2) Airspeed Effects

The airspeed will affect the incremental stress for a given load factor because smaller control surface deflections and smaller changes in the angle of attack will be required at higher speeds.

(3) Gross Weight Effects

The gross weight will have a large effect on the cyclic stresses due to maneuver loads, simply because more lift will be required for a given load factor. The gross weight effect will be different for each of the fatigue sensitive locations, because, for instance, high gross weights resulting from heavy cargo stores in the fuselage will cause greater increase in wing bending moments than if the heavier gross weight were a result of heavy loads in the wing, due either to stores or fuel (see weight distribution effects).

(4) CG Effects

The center of gravity will also have an effect on the cyclic maneuver stresses. These effects are primarily due to changes in the tail loads, but also affect the wing loading.

(5) Weight Distribution Effects

Although the gross weight, center of gravity position, and weight distribution are all interrelated, it will sometimes be advantageous to analyze their effects separately, as this may simplify the parametric charts or the data required from the pilot's log. Therefore, the effect of weight distribution should be analyzed for its effect on the cyclic stress. These effects will be a result of the inertia loading of the various parts of the aircraft.

(6) Control Surface Position

Control surface position, such as flaps or spoilers, will affect the maneuver stresses.

(7) Wing Sweep Setting

For variable sweep wing aircraft, the wing sweep angle will have a pronounced effect on the center of pressure and center of gravity, and therefore will greatly affect the tail loads. In turn, the tail loads will affect the magnitude of the stresses at almost all fatigue sensitive locations.

(8) Thermal Effects

The temperature of the structure may have a significant effect on the cyclic stresses resulting from maneuver loads on redundant structures, because of the variation in the modulus of elasticity.

(9) External Configuration

The existence of external stores, particularly when they are on pylons, will affect the cyclic stress levels. This could be a result of the local bending moment introduced at the pylon attachment, particularly for high pitch angles and asymmetric maneuvers.

d. Landing Impact Stresses

The cyclic stresses in the structure resulting from the touch-down operation will be of great importance for certain fatigue critical locations. This operation involves a transfer of load from the wings to the landing gear, and therefore is of rather large magnitude. The vertical load on the gear will be a function of the vertical touch-down velocity (sinking speed). The horizontal force will be a function of the horizontal velocity, because it affects the spin up forces. The dynamics of the gear will also have a great effect on the forces in the gear and supporting structure and also on all other parts of the structure. The weight distribution both in the wing and fuselage will have an effect on the stresses at certain control points. Braking action will also cause cyclic stresses in both the gear and its supporting structures, as well as in other parts of the structure. The braking forces are primarily spectral in nature and controlled by the pilot; however, when anti-skid mechanisms are active, the maximum braking load is controlled by the coefficient of friction between the runway and the tire and also by the vertical load on the gear. Another consideration in analyzing the landing impact operation is the fact that load inputs at touchdown are distributed initially through the main gear and then, after rotation, through the main and nose gear. When the main gear touches down, several cycles of loading may be large enough to cause fatigue damage, and when the nose gear impacts there may be several more cycles large enough to cause fatigue damage. The forces on the nose gear may be rather large, depending on the center of gravity location and the weight distribution. The initial rollout should be considered in two parts, beginning with a main gear support (two wheel roll) and then changing to a main and nose gear support (three wheel roll). This may be particularly important for rough field landings.

e. Taxi

Fatigue damage during taxi is primarily due to taxiway roughness, turning, and braking. The variation in damage from one taxi to another will depend on the gross weight, center of gravity location, weight distribution

both in the fuselage and the wing, and velocity, since most of the input from taxiway roughness will require a dynamic analysis of the structural response. Also, since the radius of turns and the velocity determine the lateral load factors, velocity and radius must be considered for turning.

f. Takeoff Run

The fatigue damage during the takeoff run will be caused primarily by runway roughness. The cyclic stresses resulting from the runway roughness are functions of the roughness, gear dynamics, gross weight, center of gravity location, weight distribution, and the ground speed.

g. Ground-Air-Ground

The concept of the ground-air-ground cycle is an attempt to account for the damage caused by the variation of the mean stress during flight. Since the largest change in the mean stress is usually between the stress on the ground and the stress in flight, the cycle has been named the ground-air-ground.

The definition of the magnitude of the stresses to use in the calculation of ground-air-ground damage has varied widely. Some organizations define the cycle to include the minimum preflight mean stress and the maximum inflight, 1-g trim stress; other groups use the minimum ground stress resulting from taxi or other ground operation and the maximum in-flight stress caused by gust or maneuver which will occur one time per mission. Another popular definition is to use the minimum stress, which on the average occurs 1000 times in 1000 identical flights, and a maximum stress, which on the average occurs 1000 times in 1000 identical flights. Although several different definitions have been used, verification can be made only by a correlation of laboratory fatigue tests with an accumulative damage method. One such study is reported in Reference 16. The data presented in Reference 16 were reanalyzed in Reference 17 and an additional definition was added in an attempt to obtain better correlation.

Most definitions involve the maximum and minimum stress, either on a flight-by-flight basis, or on the stress that is exceeded on the average of once per flight in all flights of identical profiles. Thus conducting a parametric study requires a prior knowledge of the flight profiles. This is not to be confused with mission mix, which is handled by mission segments in the parametric study. Typical mission profiles for the ground-air-ground cycle would be: a 5-hour cargo mission without in-flight refueling, a 10-hour airborne alert with 1 in-flight refueling, or a training flight with refueling and a low level penetration segment, etc. The ground-air-ground damage will be discussed in detail in Section III.

The magnitude of the minimum ground environment stress will be most affected by the gross weight, weight distribution, store configuration,

runway roughness, engine thrust, and velocity. The maximum in-flight stress will be affected by the gross weight, weight distribution, store configuration, velocity, altitude, duration of flight, which controls the probability of incurring a large value gust or maneuver cycle, and the mission profile.

SECTION III

PARAMETRIC ANALYSIS

1. SELECTIVE CHOICE OF PARAMETERS

One of the primary objectives of this study is to optimize the parametric formats so that damage on a "tail number basis" per flight can be quickly and conveniently made by manual means. Another objective is to minimize the amount of pilot log information required. To accomplish these objectives it is necessary to keep the number of charts and parameters on the charts to a minimum consistent with the required accuracy of the overall parametric study.

For certain cargo type aircraft which fly an airway route between cities (for example, from Dover or Charleston to Travis, or Travis to Hickham), damage could be presented as a function of takeoff gross weight for each leg of a mission, provided the fuel sequence, velocity, altitude, and cargo configuration were consistent. For other aircraft which do not fly a consistent route, the flight should be divided into segments of taxi, takeoff, ascent, cruise, refueling, descent, landing, ground-air-ground, etc. Since the damaging inputs for most airborne segments (gust and maneuver loading) are time dependent, the damage for airborne segments should be a function of time, or have an implied time. Some damages will also depend on the fact that an event either did or did not occur.

2. CARGO-BOMBER PARAMETER OPTIMIZATION (CONSISTENCY)

In an attempt to minimize the number of charts and pilot log information required, studies were made to determine the consistency of various response and input parameters from one flight to another for a given model aircraft.

a. Taxi

No data was found on the consistency of taxi patterns. The taxi distance, speed, and number of turns may be affected by the runway used, but for many aircraft the damage during taxi is a very small percentage of the total damage, and therefore a constant pattern could be used for a given air base or even a group of air bases. Table II lists the percent of damage due to taxi for three aircraft. Only the B-58 data makes a definite distinction between taxi damage and takeoff or landing damage.

Table II. Percent of Total Fatigue Damage Resulting from Taxi

B-58A Data from 65 Actual Flights

Control Point	% Damage due to taxi	
Aft Inboard Wheel Well Corner	0.0%	
Fuselage Longeron at Bulkhead 9	1.0	Data from
Inboard Nacelle Pylon Rail	0.0	Reference 18
Fuselage Longeron at Bulkhead 5	0.0	

C-135B

Control Point	% Damage due to taxi	% Damage due to taxi, takeoff, landing	
Body Station 820	0.0%	26.0%	
Horizontal Stabilizer Sta. 47.55	0.0	8.6	
Vertical Fin, Fuselage Sta. 111.65	0.0	0.0	Data from
Wing Station 360	0.0	1.2	Reference 19
Wing Station 336	0.0	1.1	
Wing Station W3 BBLO	0.0	0.0	
Wing Station W4 BBL 70.5	0.0	0.0	

F-106

Control Point	% Damage due to taxi, takeoff, landing	
Wing Spar 4 B.L. 34.69	0.0%	
Wing Spar 4 B.L. 55.34	2.0	Data from
Wing Spar 5 B.L. 55.34	0.0	Reference 20
Fuselage Upper Longeron Sta. 308.5	0.1	

The data from Reference 19 for the C-135 is listed in Table II as zero percent for taxi. This is not completely exact, but it is so stated in that reference (page 13.9). The damage due to taxi was found to be small or negligible, and was therefore not listed separately in the reference; rather it was combined in a total ground operation damage. Also shown in Table II is the percent of damage resulting from the sum of taxi, takeoff run, landing impact, and rollout. For most fatigue-critical areas this

damage is still a small part of the total, the taxi damage being only a small portion of that total. At body station 820 of the C-135B the ground operation is a large part of the total damage, but the reference states (page 10.25) that damage at this location due to taxi was negligible. The data for the F-106 did not have a breakdown of damage for taxi, takeoff, and landing. However, the sum of these was a very small percent of the total, as can be seen in Table II.

All of this leads to the conclusion that even though there is a difference from one flight to another in the taxi operation, the damage expected on paved runways would be a small percent of the total; and therefore an average value per flight, calculated from instrumented aircraft, could be used for most control points. The percent damage would be greater for control points which are located on the landing gear or its supporting structure. These control points may require a parametric presentation using gross weight, distance, and number of left and right turns. However, most of the damage at these locations is due to landing impact and the ground-air-ground cycle. The use of an average taxi speed, distance, and number of turns should not adversely affect the accuracy of the damage calculations on a flight-by-flight basis. Very little data is available on rough field taxi loads; the area must be considered as a separate parameter and evaluated after operational data is obtained for a particular aircraft.

b. Takeoff Run

The damage during the takeoff run is primarily a result of the runway roughness and varies with gross weight and velocity. The fatigue analysis should consider the aircraft as starting at the end of the runway with zero velocity and then accelerating down the runway with increasing velocity, decreasing weight, and increasing lift. The distance required for liftoff and velocity versus distance or time can be calculated from the performance of the aircraft and its initial weight. The gross weight variation can be predetermined, since power settings are usually fixed for takeoff. This makes all the parameters a function of only the gross weight at the end of the runway (for a given configuration of fuel and stores). Using the spectrum of the runway roughness and the response functions which are a function of weight and speed, the fatigue damage for each control point can be calculated in increments as the aircraft proceeds down the runway for various initial gross weights and weight configurations. This will permit the presentation of takeoff damage as a function of only the initial gross weight for various aircraft configurations. It may also be necessary to present additional breakdown or correction factors to account for the aircraft performance as a function of runway elevation and air temperature, since the distance required for lift-off varies greatly with these parameters. The situation is complicated by flap position and the use of water injection. If the fatigue damage due to the takeoff run is a significant percent of the

total, and if the takeoff distance is greatly affected by water injection and flaps, then additional parameters of elevation and temperature could be included in the breakdown of the parametric charts. The number of entries or charts could be minimized by using statistical averages of the temperature for different times of day and seasons of the year. The total percent of damage due to takeoff should not be the only criterion used in deciding whether additional breakdown is necessary, because the damage during takeoff may not be a strong function of the distance traveled, but is due to some event like nose wheel lift-off when the load is transferred from the nose wheel to the main gear at rotation velocity. For example, on the B-58 fuselage longeron at bulkhead 9, fuselage station 689.5, Reference 18 indicated that 33.7% of the damage is due to the takeoff run. However, an examination of the flight recordings shows that this damage is due primarily to the rotation or hitting a bump after nose wheel lift-off but before the wings have picked up the load, so that for many of the flights there are only 1, 2, or 3 cycles which cause damage during the takeoff run.

c. Ascent

The damage during ascent is a result of gust and maneuver loadings. Since statistical averages per time or distance are used to determine the frequency of occurrence of the loading magnitude, time becomes the primary parameter in calculating the damage. Most of the gust and maneuver loads data taken from V-G-H recordings are blocked into altitude bands (such as 0-1000 feet, 1000 to 2500 feet, 2500 to 5000 feet, 5000 to 10,000 feet, etc.). The damage for a given aircraft with a given weight, configuration and velocity is really a function of the time spent in each of these altitude bands. The situation again exists, particularly for bomber and cargo type aircraft, that for the ascent segment of a flight the engine power is controlled in a predetermined manner, and the climb rate is controlled so that a predetermined fixed airspeed is maintained. The fixing of the thrust and airspeed or Mach number histories results in the climb rate being a function of only gross weight and altitude for a given aircraft configuration. Ideally, then, every flight of a given gross weight would spend an equal amount of time in a given altitude band. In actual practice this does not occur, and there are significant differences between the times spent in a given altitude band. In Table III is listed the total time required for the B-52 with different takeoff weights to climb from 2,500 to 20,000 feet. These times are taken from actual flight recordings.

The data shown in Table III could be requested on the pilot's log and a correction factor equal to the ratio of the actual time to the time used for the construction of the parametric chart could be applied to the damage shown on the chart. This method of correction does not insure that the corrected damage is the actual damage experienced, because it is the time

Table III

Time Required to Climb from 2,500 to 20,000 Feet
for B-52 B-F

Takeoff Gross Weight in Thousands of Pounds				
340-360	360-380	380-400	400-420	420-440
Minutes	Minutes	Minutes	Minutes	Minutes
10.3	9.9	8.9	9.1	9.4
11.0	10.2	8.9	10.7	10.6
	11.0	9.3	11.5	10.7
	11.8	9.4	11.6	14.2
	13.0	9.9	11.8	15.6
	14.1	10.0	12.1	16.1
		10.1	12.1	18.3
		10.4	12.2	18.4
		10.9	12.7	
		11.0	12.8	
		11.2	14.3	
		11.4	14.4	
		11.4	15.3	
		11.8		
		11.9		
		12.0		
		12.4		
		12.9		
		13.1		
		13.7		
		17.5		
Average	Average	Average	Average	Average
10.7	11.7	11.3	12.3	14.1

spent in each altitude band used to define the gust and maneuver spectrum which is important. Of two flights which take the same time to climb to 20,000 feet, for example, one flight could spend more time at the lower altitudes and less at the higher altitudes, whereas the second could spend less time at the lower altitudes and more at the higher altitudes. The first flight would have a higher damage due to the more severe gust spectrum at the lower altitude, even though both had the same average climb rate. To make an accurate accounting of climb rates would require that the pilot record the time spent in each altitude band that corresponded to the altitude bands of the input spectrum. This method would require an additional burden on the flight crew and would also add appreciably to the time required to manually calculate the damage on a flight by flight basis.

When using a standard time interval from actual flight experience as a function of gross weight for each altitude band, it is logical to expect that some flights will have more and some less damage; however, after many flights the average calculated damage should equal the actual damage. Table IV is a listing of the percent errors on a flight by flight basis for 14 flights of the C-135A. The comparison is made between the calculated damages from Reference 19 where a standardized ascent profile was used, and the calculated damage when the actual profile was used. Some of these errors are very large; however, when the total damage for a typical 8-hour flight is compared, the errors in the ascent segment cause only a small error in the total damage. At the bottom of the table is the percent error in the ascent segment for the sum of the 14 flights. Although these errors are 9.3 and 8.1% for the two control points, it must be recognized that 14 flights is a rather small number. If by adding data the trend continued to show the error to be positive, the standardized spectrum should be changed to represent more nearly an average profile. What is actually gained in making the correction must also be considered; for if a statistical average is used for the gust and maneuver spectrum, it is assumed that these disturbances occur at a fixed frequency, when in reality they occur sporadically. Therefore it is conceivable that a flight which took a longer time to reach cruise altitude could have fewer disturbances than one which took less time to reach the same altitude. Table V shows the damage incurred during the ascent segment for the inboard wheel well corner on the B-58. These damages were calculated from strain gage recordings on operational aircraft and are therefore representative of actual usage. The data show that for these 26 flights zero damage was recorded for 6 flights, and damage less than 1×10^{-7} was recorded for six more flights. For these 12 flights it would be meaningless to make a correction for climb rate. The remaining 14 flights show a variation in damage from 1.69×10^{-7} to 1.29×10^{-4} which is a very large variation when compared to the variation in the climb rate or the time required to reach cruise altitude. In conclusion, for the sake of economy, for minimizing pilot log information, and for the convenience of using the parametric charts, a standardized ascent profile

TABLE IV

Comparison of Actual Damage and Damage Parametric Chart
for Ascent Mission Segment

Horizontal Stabilizer on C-135A

Flight No.	Takeoff Gross Weight	Damage From Chart	Actual Damage	% Error Ascent	% Error 8 Hour Flight
C-55	218,000	0.9	0.687	31	3.5
C-59	274,000	2.95	2.05	44	6
F-83	241,000	1.5	1.52	-1	-.2
G-39	212,000	0.75	0.456	64	5.7
C-40	234,000	1.1	0.75	47	4.1
C-43	238,000	1.4	1.43	-2	-.4
E-48	244,000	1.6	1.71	-6	-1.2
G-55	224,000	0.9	0.87	3	.4
N-72	251,000	1.88	1.54	22	3.4
B-53	168,000	0.28	0.286	-2	*
D-44	228,000	1.12	1.08	2	.5
D-63	185,000	0.4	0.822	-51	*
K-40	196,000	0.43	0.541	-21	*
M-70	200,000	0.48	0.613	-22	*
Total		15.69	14.355	9.3%	

* Too light of takeoff weight for an 8-hour flight.

TABLE IV -- continued

Wing Item 1 on C-135A

Flight No.	Takeoff Gross Weight	Damage From Chart	Actual Damage	% Error Ascent	% Error 8 Hour Flight
C-55	218,000	0.31	0.226	35	4.8
C-59	274,000	0.71	0.488	45	3.1
F-83	241,000	0.44	0.467	6	-2
G-39	212,000	0.29	0.166	75	9
C-40	234,000	0.37	0.25	48	2.2
C-43	238,000	0.41	0.415	-1	0
E-48	244,000	0.457	0.53	13	3.7
G-55	224,000	0.32	0.303	6	1
N-72	251,000	0.51	0.38	34	6.2
B-53	168,000	0.13	0.145	-10	*
D-44	228,000	0.35	0.364	-5	-.8
D-63	185,000	0.180	0.286	-37	*
K-40	196,000	0.205	0.242	-17	*
M-70	200,000	0.22	0.27	-19	*
Total		4.903	4.532	8.1%	

* Too light of takeoff weight for an 8-hour flight.

Table V Fatigue Damage During Ascent for Control Point One on B-58 (Wheel Well Corner)

Flight No.	Gross Weight lbs.	Time To Altitude	Altitude ft.	Gust Damage *	Maneuver Damage *	Total Damage *
01A	145,194	12.1	26,052	1.45×10^{-5}	7.70×10^{-5}	9.15×10^{-5}
83A	146,148	11.9	26,160	0	0	0
39A	146,154	3.9	23,427	0	9.71×10^{-5}	9.71×10^{-5}
85A	146,194	11.6	25,681	9.71×10^{-10}	0	9.71×10^{-10}
56A	146,404	13.1	27,902	0	2.19×10^{-8}	2.19×10^{-8}
47A	146,444	13.5	27,995	0	4.43×10^{-5}	4.43×10^{-5}
11A	147,194	9.2	25,308	0	6.04×10^{-7}	6.04×10^{-7}
54A	147,345	12.7	27,958	0	2.62×10^{-5}	2.62×10^{-5}
45A	147,916	12.0	26,896	0	0	0
62A	147,987	13.8	27,283	8.67×10^{-9}	2.43×10^{-5}	2.43×10^{-5}
04A	148,450	13.2	25,673	0	8.54×10^{-10}	8.54×10^{-10}
61A	148,471	13.2	26,245	1.88×10^{-9}	7.26×10^{-9}	9.14×10^{-9}
06A	148,472	12.9	27,127	0	0	0
30A	149,075	14.6	28,182	2.99×10^{-8}	0	2.99×10^{-8}
60A	149,558	14.2	28.878	0	0	0
67A	149,587	12.6	28,230	1.29×10^{-7}	1.37×10^{-5}	1.38×10^{-5}
22A	149,653	19.1	28,535	0	0	0
72A	149,815	14.2	27,321	0	2.48×10^{-9}	2.48×10^{-9}
53A	149,927	12.2	28,713	0	1.69×10^{-7}	1.69×10^{-7}
26A	150,078	14.4	28,029	0	0	0
20A	150,447	18.8	27,076	2.99×10^{-6}	7.23×10^{-5}	7.53×10^{-5}
40A	150,630	12.9	27,269	4.69×10^{-5}	3.21×10^{-5}	7.90×10^{-5}
38A	150,939	15.1	28,834	5.38×10^{-8}	2.07×10^{-5}	2.07×10^{-5}
78A	151,590	9.0	28,960	6.10×10^{-5}	6.81×10^{-5}	1.29×10^{-4}
31A	151,822	14.9	29,119	5.26×10^{-8}	5.15×10^{-5}	5.16×10^{-5}
23A	154,100	15.7	28,420	2.02×10^{-9}	0	2.02×10^{-9}

* Damages have been multiplied by a scatter factor of 4. Damages less than 10^{-7} are from extrapolated S-N data.

of velocity and altitude vs. time as a function of gross weight can be used for transports and bombers without a loss in accuracy of the calculated damages.

d. Cruise

The fatigue damage during the cruise segment of the flight is a result of gusts and maneuvers. As stated in Section II, 1 and 2, the frequencies of the gust and maneuver inputs are functions of velocity, altitude, gross weight, and perhaps seasons and geographic areas. Since most aircraft have optimum combinations of altitude and Mach numbers for maximum range or minimum flight time, it is reasonable to assume that most of the cruise segment will be at one of these optimum conditions. Therefore, a damage rate for an optimum condition based on maximum range or any other optimized parameter could be calculated as a function of gross weight for various configurations and the parametric chart simply be a table of damage per minute vs. gross weight. From the pilot log one could obtain the time in cruise, excluding low level penetration, and multiply the damage rate to obtain the accumulated damage. However, the user must divide the cruise segment into small sections, determine the average gross weight for each section, and then perform the multiplication for each section and sum the damages. This procedure would work well for computer solutions but is not the most convenient for manual solutions. For manual solutions of a large number of flights the most convenient method is to calculate the cumulative damage as a function of time, starting with the aircraft at its maximum gross weight and continuing to the minimum gross weight. This curve would be constructed by assuming that the cruise segment began at time zero and at maximum gross weight. The aircraft would then fly at constant altitude and velocity but with a decrease in gross weight resulting from the fuel flow rate required for level flight for that particular altitude, velocity, and instantaneous weight. This assumption would define a gross-weight vs. time curve. The damage during cruise is then the difference between the damage read from the chart for the initial and ending gross weights. Figure 24 is an illustration of the proposed format. It is more accurate to use the duration of the cruise to find point 4 than to use the gross weight, since gross weight effects are of second order and gross weight histories are not as accurate as time. Accurate times should be easy to obtain from the pilot's log. It is not necessary to draw a curve of the gross weight, but it should be superimposed on the damage curve in order to give the proper starting point. For aircraft which have only a few configurations and one or two set fuel sequences, the center of gravity and weight distribution parameters could be included as time functions on the charts. In effect, for a given configuration, the center of gravity location and the weight distribution would be only a function of the gross weight and would automatically be taken care of in the calculations of the damage. However, some aircraft allow more freedom in the selection of the fuel sequence; therefore, the center of gravity location is not just a function of gross weight. Also, some aircraft have fuel or ballast

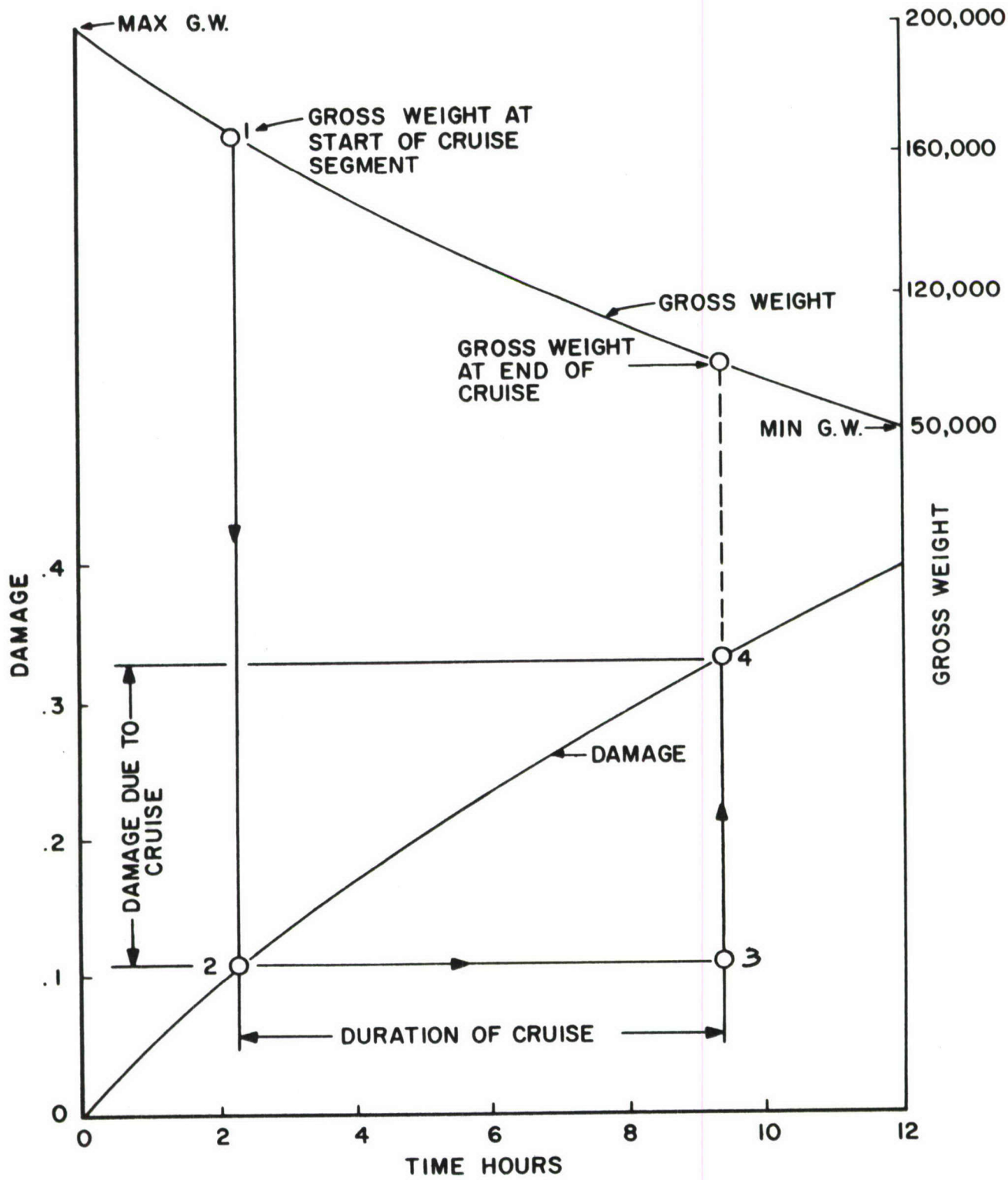

Figure 24 Format for Cruise

transfer which could occur at any time during the flight when the center of gravity moves outside given limits.

There are several methods of accounting for the fuel distribution and center of gravity location. As an example, consider Figures 25 and 26, which show weights of fuel in the aft and forward fuel tanks vs. gross weight for the B-58. These data were taken from actual pilot log data on operational flights. While the data show the same general trend, there is rather a large range of gross weights for a given fuel weight. If the fatigue damage at a particular fatigue critical location is highly sensitive to the fuel in a given tank, then perhaps damage should be plotted vs. time for a family of fuel weights in that tank. Figure 27 is an example of this type of presentation. To construct the chart assume a constant fuel weight in the aft tank (for example, 35,000 lb). Then, using a predetermined gross weight vs. time function, calculate the damage vs. time. This procedure is repeated for 25,000-lb and 15,000-lb fuel weights. The user would then enter the chart at the gross weight at the beginning of the cruise and an average aft body fuel, e.g., 35,000 pounds; then from the pilot's log determine at what time increment the aft fuel had decreased to 30,000 pounds. He would then add that time to the time at point 1. This would locate point 2. Point 3 on the 35,000 pound line is located at the same time as point 2. The damage during this portion of the cruise segment is the damage at point 3 minus the damage at point 1. The user (now with 30,000 pounds in the aft tank) enters the chart a second time at the correct gross weight but with an average of 25,000 pounds of fuel in the tank (point 4), then from the pilot's log it is determined at what time increment the fuel had decreased to 20,000 pounds. Adding this time to the time at point 4 locates point 5, then point 6 is located on the 25,000 pound of fuel line at the same time as point 5. The damage during this portion of the cruise segment is then the damage at point 6 minus the damage at point 4. Suppose at this time, fuel is transferred so that the weight of fuel in the aft tank goes up to 40,000 pounds. The user then enters the chart at the proper gross weight, but on the 35,000 pound line, and repeats the first step. The number of average fuel weight curves would depend on the sensitivity of the damage to the fuel weight. While this method is not exact, it does provide a method of accounting for any fuel weight at any gross weight and at the same time provides a method that is easy to construct and use. The magnitude of error would depend on the number of fuel weight curves.

Suppose another fatigue critical location is sensitive to the location of the center of gravity. Figure 28 is an illustration of how the cg location can vary with gross weight for the same configuration. This situation is similar to the fuel distribution, and can be handled in the same manner. The charts would be constructed similar to Figure 27 but with the cg

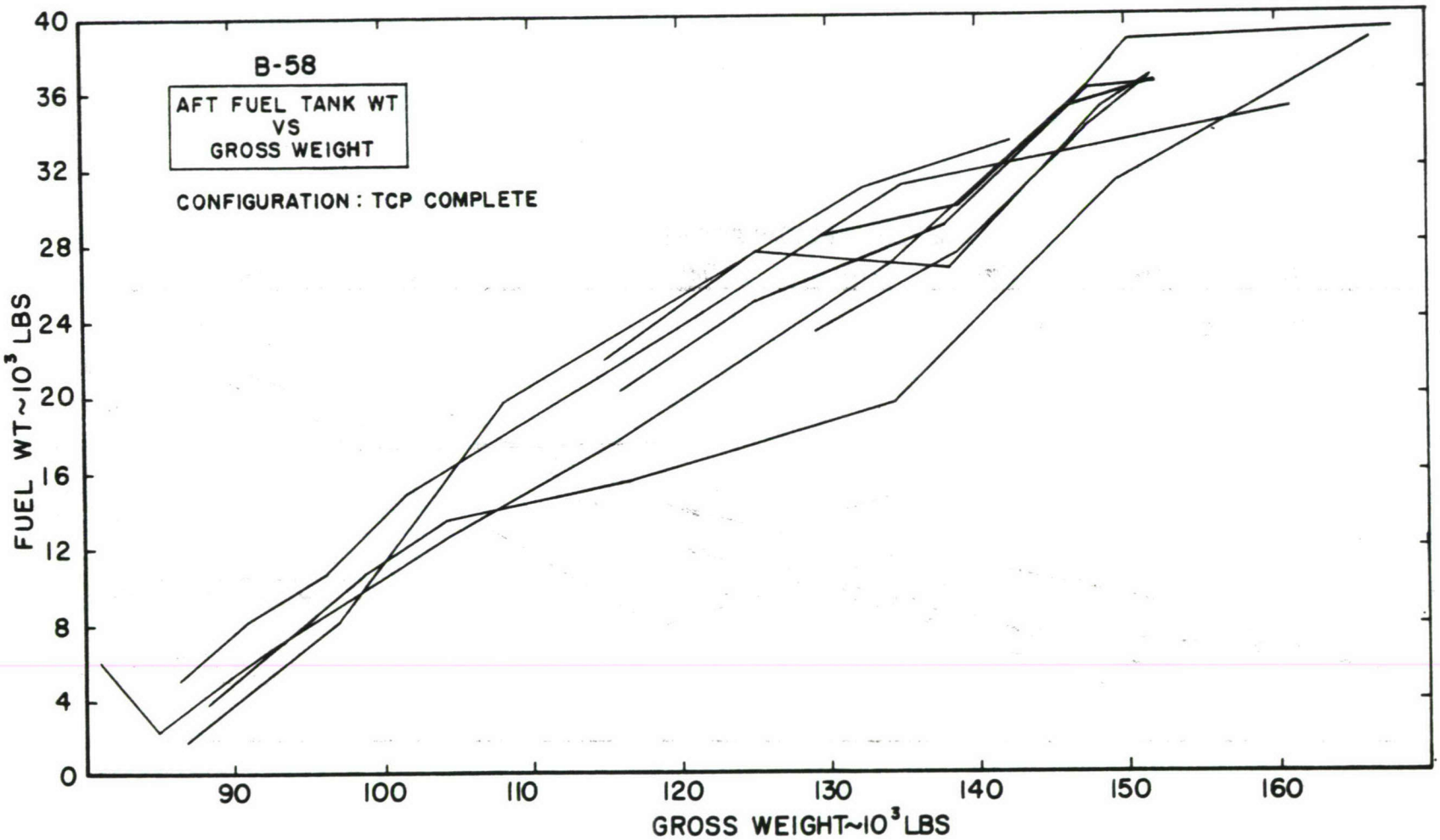

Figure 25 Aft Fuel Tank Weight vs. Gross Weight for the B-58

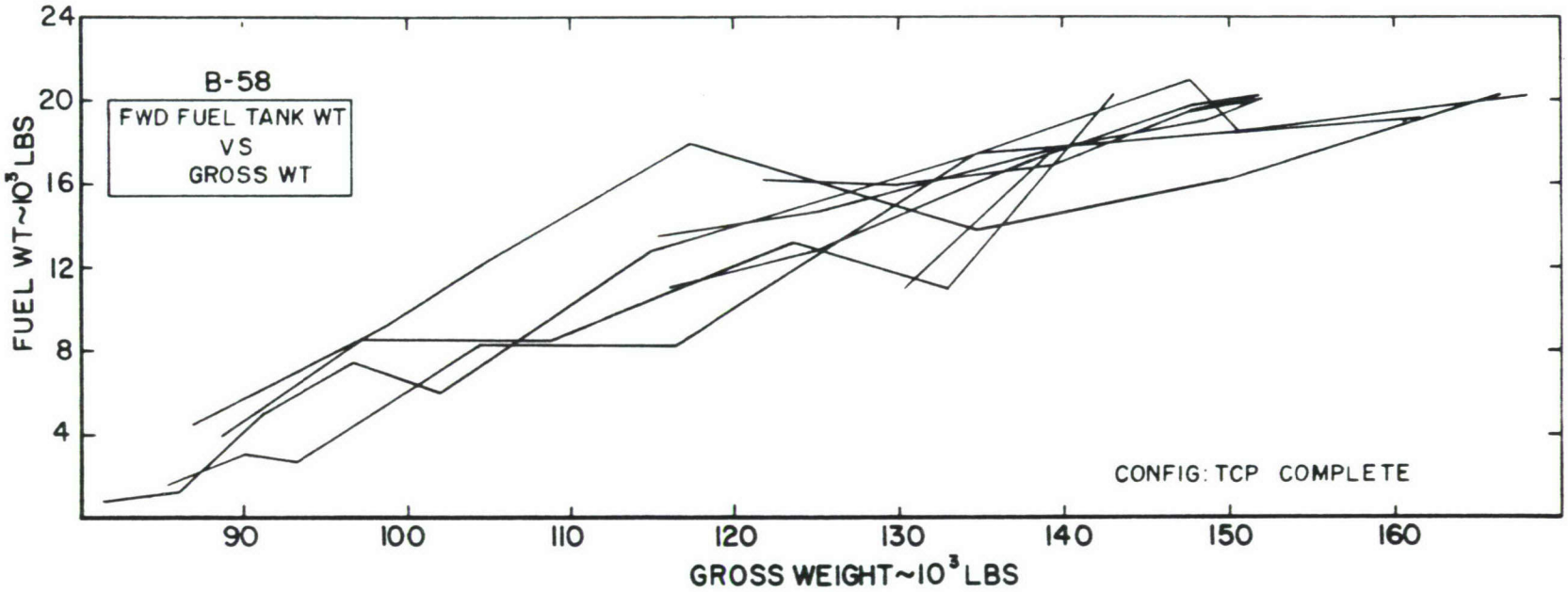

Figure 26 Forward Fuel Tank Weight vs. Gross Weight for the B-58

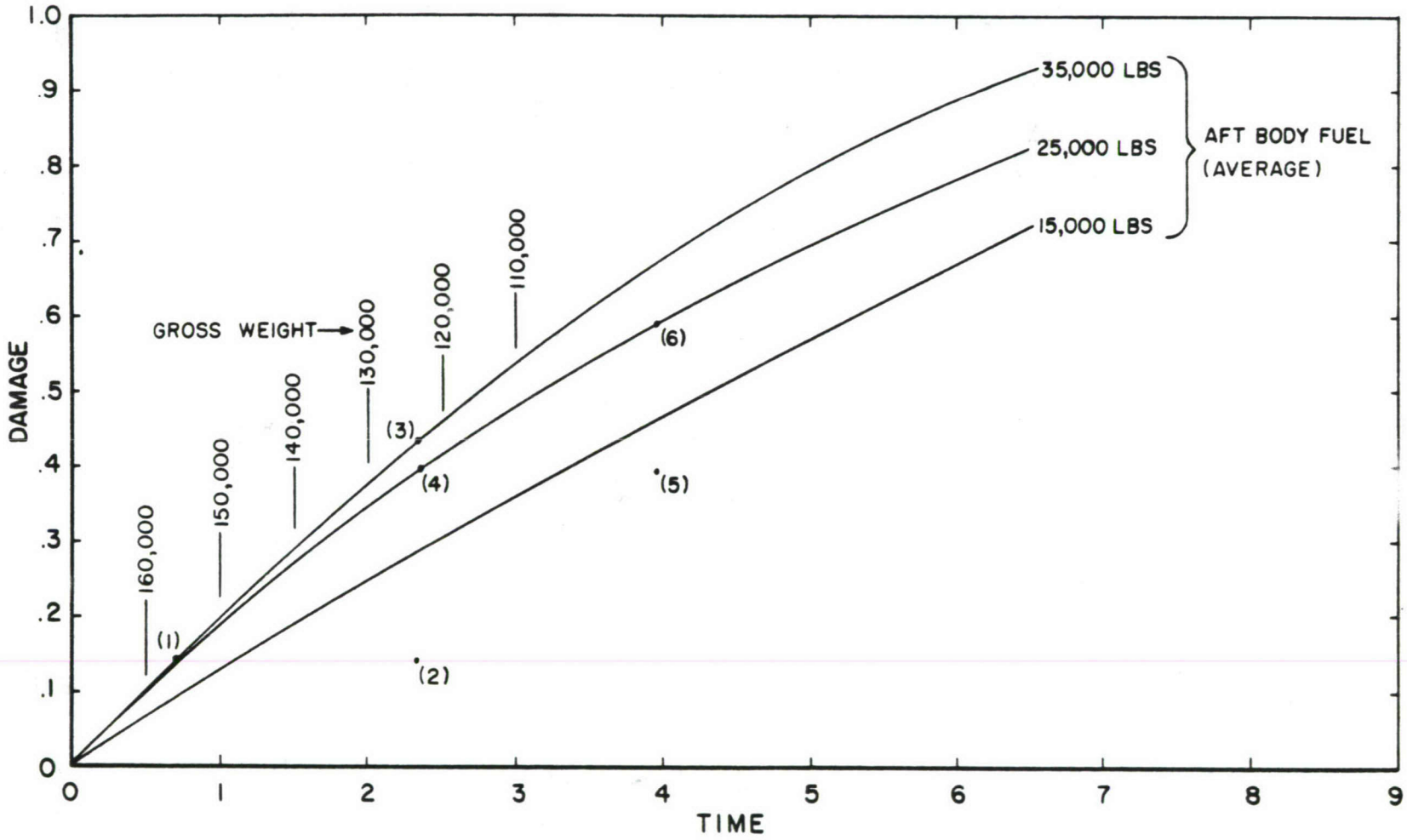

Figure 27 Example of Parametric Damage Chart for Cruise When the Fuel Distribution Is a Significant Parameter

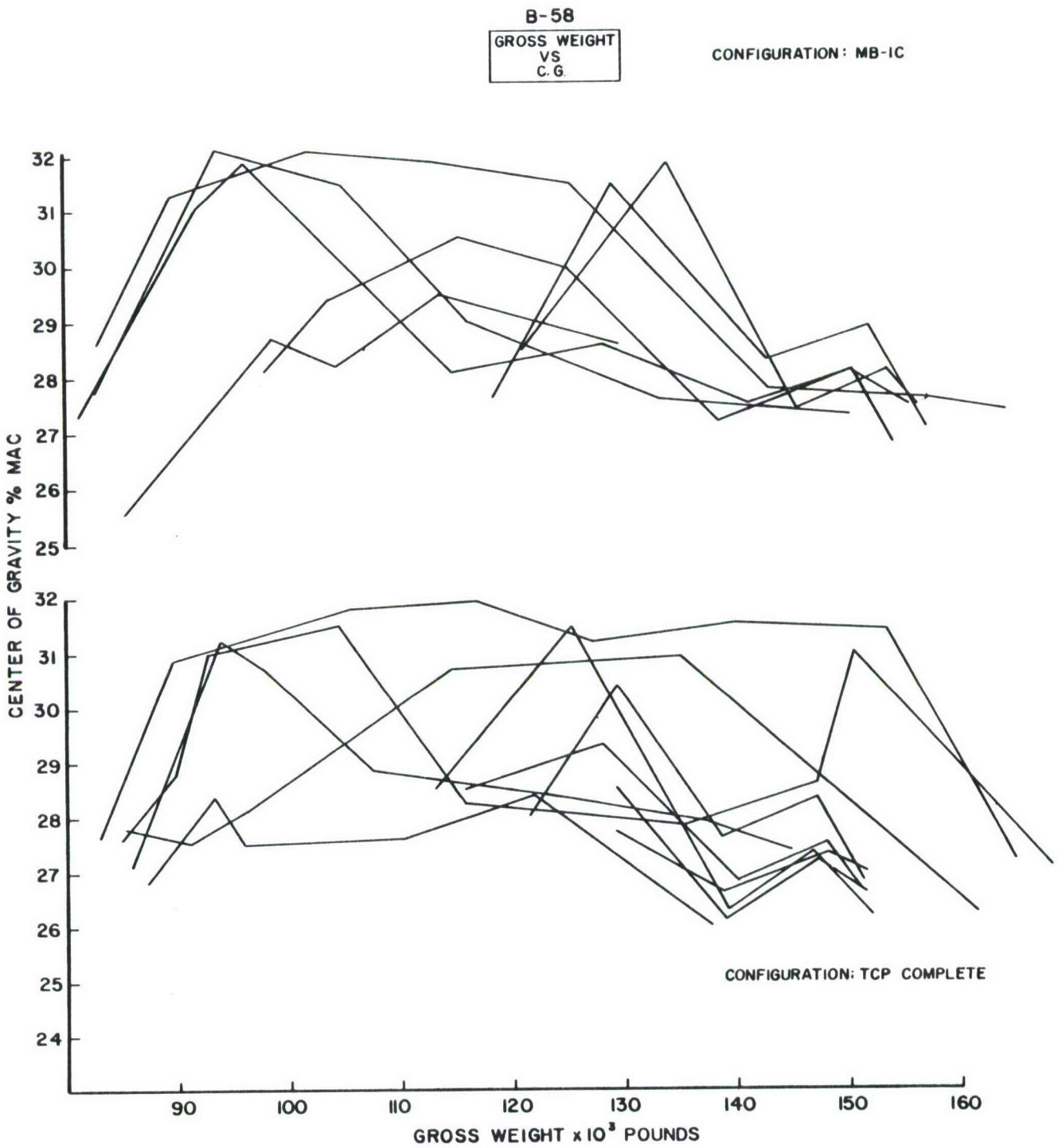

Figure 28 Center of Gravity vs. Gross Weight for Two Weapon Configurations of the B-58

location in % mean aerodynamic chord as the parameter of the family of curves instead of fuel weight in a particular tank. The user would then, from the pilot's log, determine the time interval during which a particular average center of gravity location was applicable and use the time increment to locate points 2 or 5.

To make the study truly parametric, there should be a chart for a number of velocity-altitudes combinations and configurations.

For cargo aircraft, which usually have a large number of combinations of cargo weight and weight distributions, the selection of the parameters for the charts will depend on the location of the fatigue-critical point. For example, a point on the wing is sensitive to the center of gravity location, gross weight, and total fuselage weight, but not particularly sensitive to the distribution of weight in the fuselage. A point on the wing could be presented as damage vs. time for a family of cargo weights, with the gross weight being an implied function of time. The fuel weight and its distribution would cause the magnitude of the damage to vary and is therefore also a parameter; this can be handled by additional charts. For most normal operations the wing tanks are filled first, then the body tanks. The wing tanks are used for taxi, takeoff and ascent because of better fuel flow during these critical parts of the flight. The fuel in the body tanks is used during the first part of the cruise; that in the wing tanks is used later. This somewhat standardized procedure reduces the complexity of analyzing the cruise segment for a wing item, because if the gross weight, cargo weight, weight of fuel used from the wing tanks in reaching the cruise altitude, and center of gravity position are known, the stresses in the wing can be calculated. For the cruise segment there are only four independent variables: cargo weight, center of gravity location, fuel used from the wing tanks, and time. To calculate the parametric chart, assume a cargo weight, fuel used from the wing tanks, and center of gravity position; then using the maximum gross weight and a predetermined fuel flow rate, calculate the cumulative damage vs. time at a constant altitude and Mach number. Figure 29 is an example of how this chart would be presented. The user would enter the chart at the gross weight and cg location at the beginning of the cruise, read the time, add the time during which a constant cg location, obtained from the pilot's log, could be used and then read the incremented damage during this time from the same cg line. The chart is entered again at the new gross weight and cg position and the procedure repeated. The shape of these curves will dictate the number of them that can be presented on one graph.

For body items such as the fuselage crown, the weight and the weight distributions aft of the critical location will have great influence on the amount of damage. If the weight distribution is always the same for a given cargo weight, then the problem is simplified and only the cargo weight need be considered. However, if the distribution can vary, perhaps a more

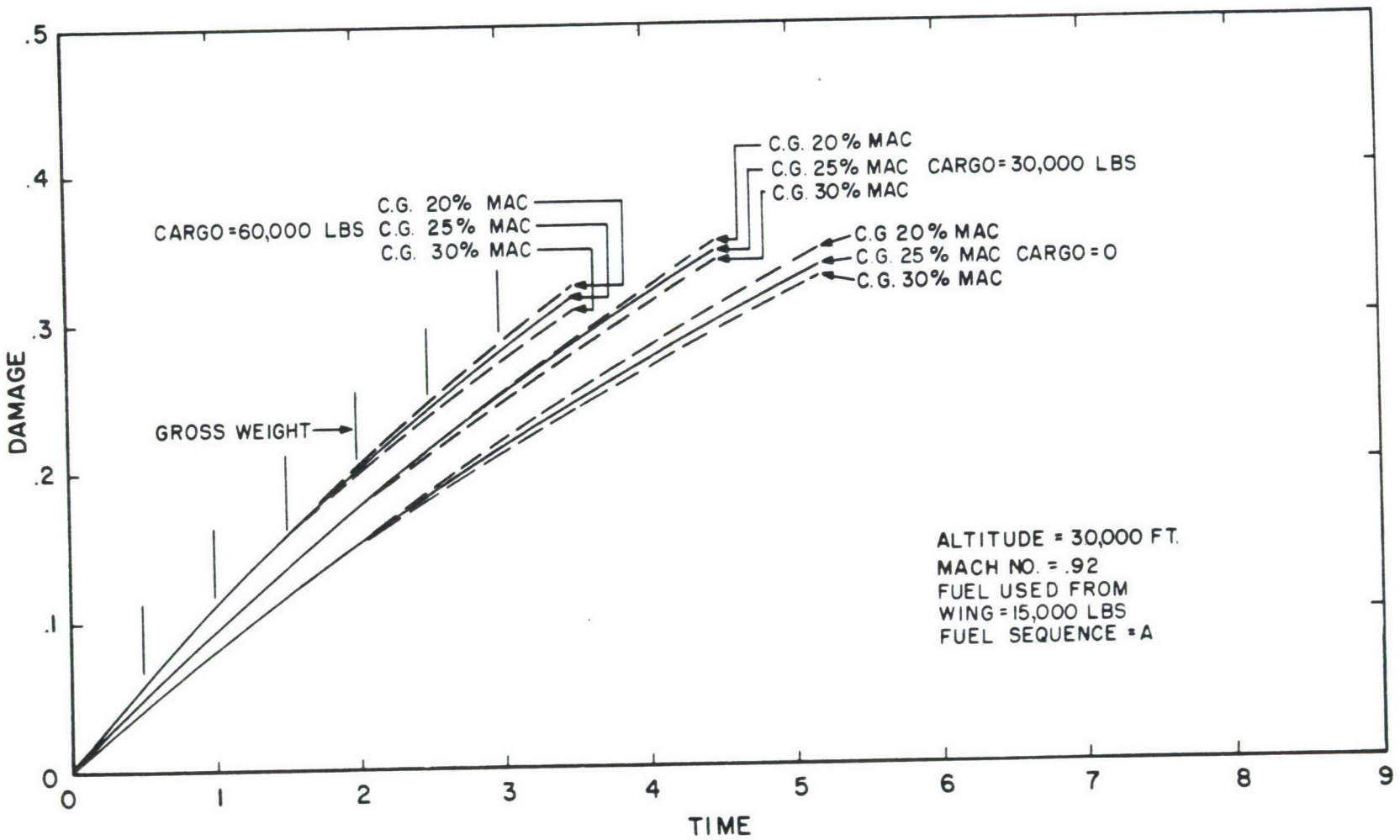

Figure 49 Example of Parametric Damage Chart for Cruise When the CG Location Is a Significant Parameter

useful parameter would be the bending moment due to the aft cargo. Consider a fuselage section aft of the cg. The bending moment at this section is the sum of the moments due to tail loads (a function of the cg position), the empty weight of the aft structure (a constant), and the cg of the aft cargo. Since the weight of the aft structure is a constant, only the overall cg position and the moment due to aft cargo need be presented in parametric form. The damage chart would therefore be similar to Figure 29, except that the bending moment of the cargo aft of the section under investigation would replace the cargo weight. The bending moment could not be obtained from the pilot's log, but this could be calculated from the load master's log (weight and balance sheet) since it lists the weight of cargo between various fuselage stations.

The above discussion is presented as a guideline for possible methods of calculating and presenting the damage for fatigue critical points which are sensitive to parameters that can vary in a somewhat random manner. These procedures, if necessary, will add significantly to the time required to calculate the damage. Although it appears to be a case of "the tail wagging the dog", the cost of constructing the parametric charts and their utilization could be reduced if a greater effort were made to use a standard fuel sequence and to control the center of gravity position in a standardized manner. Standardized cargo weight distribution, although not as practical, would be equally advantageous.

e. In-Flight Refueling

The fatigue damage during the in-flight refueling is also a result of gust and maneuver loadings. Since a spectrum will be used for these disturbances, the duration of the refueling becomes the most important independent parameter in defining the input. The altitude, velocity, gross weight, weight distribution, configuration, and control surface position will also affect the input spectrum and the response functions. Since refueling can occur at any time during the flight it is not possible to predict the gross weight at the time of refueling. The amount of fuel transferred is also unpredictable. Therefore the most workable parametric presentation appears to be a plot of damage rate vs. gross weight for a given altitude, velocity, and configuration. Figure 30 is an example of the proposed presentation. Let us suppose that an aircraft started refueling at a gross weight of 140,000 pounds with the center of gravity at 30% MAC. and ended the refueling at 200,000 pounds with the center of gravity at 25% MAC., and also that the receiving aircraft was in the wake of the tanker for 20 minutes. The user would locate points (1) and (2) on Figure 30, determine the average damage rate between points (1) and (2) and multiply the average damage rate by 20 minutes to obtain the damage during refueling. Now suppose that on a training flight the hookup is made at 140,000 pounds and the c.g. at 30% MAC., but no fuel is transferred for the first 20 minutes but during the next 10 minutes fuel is transferred so that at the end of the transfer the aircraft

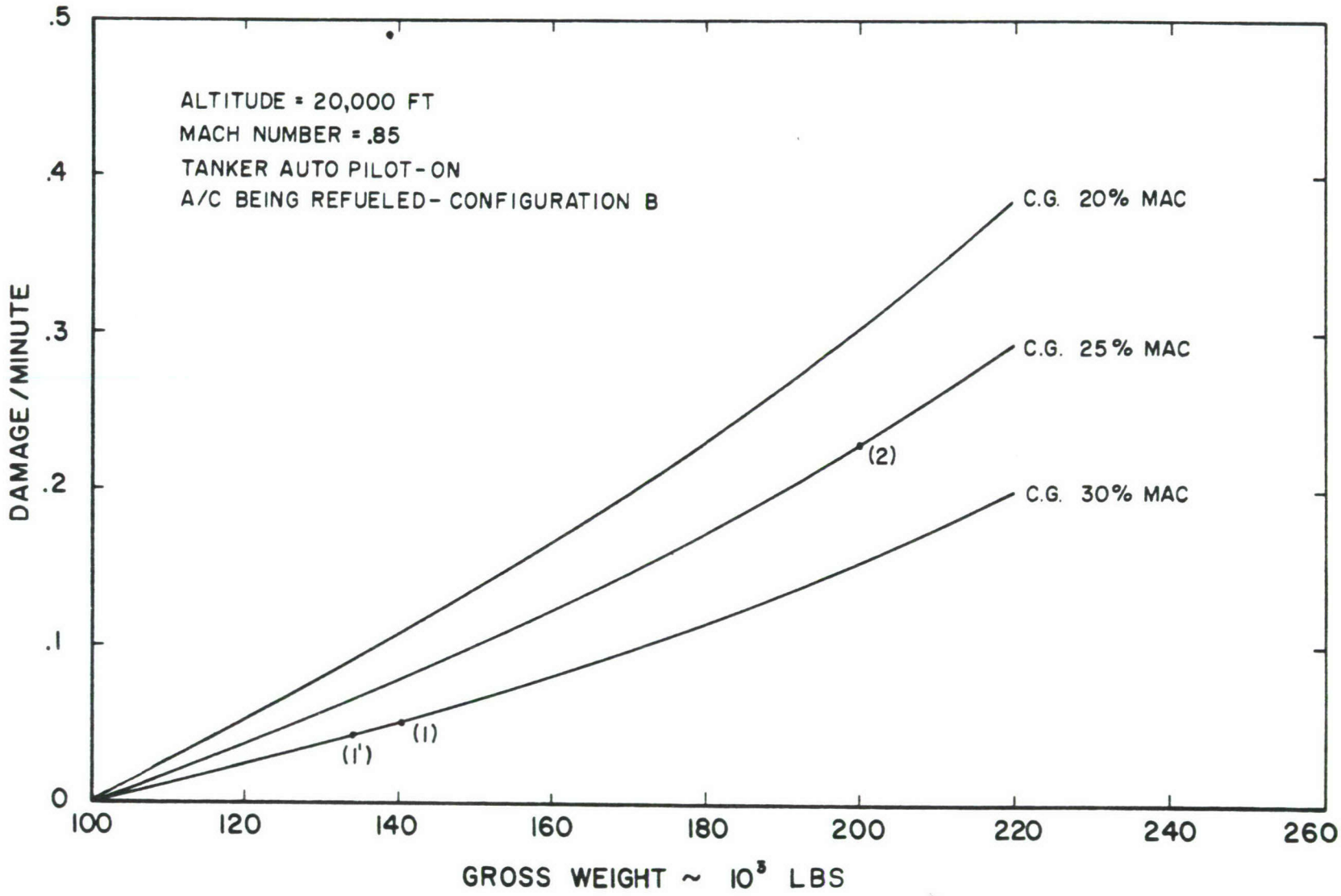

Figure 30 Example of Parametric Damage Chart for In-Flight Refueling

has a gross weight of 200,000 pounds and the cg is at 25% MAC. The user would then locate points (1) and (1'), find the average damage rate between points (1) and (1'), multiply by 20 minutes and add the product of the average between points (1') and (2), times 10 minutes.

This method assumes a linear relationship between damage rate and gross weight when using the charts, but does not assume this for their construction.

Figure 30 is presented as an example, and the damage is shown as a function of gross weight and center of gravity location. However, other parameters may be used instead of cg location. In fact for certain control points, cargo weight or fuel weight in a particular tank, or bending moment, will be more useful and accurate.

f. Airdrop

For cargo or bomber type aircraft, which have airdrop capabilities, the flight segment can be considered as two cruise segments, one segment before the drop and one after the drop, with an instantaneous weight change between the two. The parametric damage calculation would then be the same as for cruise, using the proper input spectra and aircraft configurations for the drop altitude and velocity. The presentation and utilization would be the same as Figure 29, using one set of cargo or configuration curves before the drop and another set after the drop.

When there is significant damage due to the drop operation itself, caused by such things as flying with flaps extended or cargo doors open during the short period of time when the drop is actually made, or due to ejection loads or the instantaneous weight change, this should be handled by a separate chart. No actual statistical flight data was reviewed to determine the consistency of the drop mode; however, it is expected that the damage during the drop should be small compared to the total damage during the flight. It is also expected that the time duration of doors open or flaps extended should be fairly consistent. These assumptions should be checked for the aircraft under investigation; if valid, then a damage per drop as a function of gross weight, cg location, and configuration could be calculated.

If the damage is significant and is not a constant per airdrop, it will be necessary to present damage rate as a function of gross weight and configuration.

g. Low Level Penetration

Low altitude flight, whether for a cargo or bomber type aircraft, can be handled in the same manner as a cruise segment, using the proper

input spectra for the velocity and altitude being presented. As stated in Section II, 1. a. and b., there are two types of low level flight: terrain clearance and terrain following. These would require separate presentations. Geographic location should also be considered as a parameter and a separate chart may be required for each geographic location.

h. Loiter

Loiter can be presented in the same manner as cruise, but at the loiter altitude. A special gust and maneuver spectrum would be used for the loiter segment.

i. Descent

A study of 150 flights of cargo and bomber aircraft indicated that the descent profile of altitude vs. time was not as consistent as the ascent profiles. This is true when the average descent rate from the start of descent to about 2500 feet is examined. However, additional examination of the profiles indicates that the variation is due primarily to short cruise segments during the descent. If these short cruise segments are subtracted from the descent time, the descent rates become somewhat consistent. Table VI lists the descent time by altitude bands for three aircraft types. The data show a considerable variation in both the initial descent rate and in the time required to pass through the two altitude bands. As with ascent, the damage is not a function of the total time required for the descent but is directly proportional to the time spent in each altitude band that has a different input spectrum. As was stated in Section III, 2c, to expect the flight crew to give an accurate accounting of the time when the aircraft passed from one altitude zone to another would be an unreasonable burden; furthermore, parametric study which attempted to account for the variations in time would add substantially to the time required to use the parametric charts. More important, little is gained in overall accuracy by making a correction to the descent segment. Table VII lists the percent of total damage accrued during descent for 65 flights of the B-58 and two typical missions of the C-135B. The data presented for the B-58 indicate that if the descent rate varied by ±50%, the maximum error in the total damage calculation for a particular flight would be about ±4%. For the wing items and the fuselage item on the C-135B, the overall error introduced by a ±50% variation in descent rates would be about 1.5%; however, for the horizontal stabilizer and vertical fin, the overall error could be as much as ±15%. A comparison of the relative damage between the empennage items and the wing items on the C-135B indicated that the wing items accrue damage about 8 times as fast as the empennage items; therefore, parametric studies would probably not be performed on the C-135B empennage. Also one would expect that over a long period of time the descent rates should average out to the standard.

Table VI Time of Descent by Altitude Bands
Aircraft Type C-135A

Initial Altitude	Rate of Descent Between Initial Altitude and 20,000 Feet ft/min	Time of Descent From 20,000 feet to 10,000 feet	Time of Descent From 10,000 feet to 2500 feet	Base
34,800	1947	3.0		McGuire
34,600	1217	6.8	5.9	McGuire
34,200	947	5.2	5.1	McGuire
34,000	1522	6.0	6.5	McGuire
34,000	2258	2.4	3.2	McGuire
33,000	1313	5.9		McGuire
31,800	1686	4.4		McGuire
31,700	1554	9.6		McGuire
30,800	*1421	4.0		McGuire
29,800	1531	7.0		McGuire
29,000	1667	*6.2		McGuire
26,500	722	5.9		McGuire
26,000	3158	3.3	5.2	McGuire
24,800	1171	12.9		McGuire
20,400	1333	7.9		McGuire

* There was a short cruise segment during this segment. The time of the cruise was subtracted from the time of descent.

Table VI -- continued

Aircraft Type C-135B

Initial Altitude	Rate of Descent Between Initial Altitude and 20,000 Feet ft / min	Time of Descent From 20,000 feet to 10,000 feet	Time of Descent From 10,000 feet to 2500 feet	Base
38,800	6714	1.3		McGuire
37,000	2537	2.6		McGuire
35,900	1916	6.7	* 7.7	Travis
35,800	1795	12.4		McGuire
35,500	1649	6.7	10.7	Travis
35,100	1841	8.0		McGuire
34,800	1410	* 9.1		McGuire
33,500	1250	4.9	* 6.4	McGuire
33,200	1320	6.7		McGuire
33,200	1158	3.5	2.9	McGuire
32,200	1743	6.6	14.9	Travis
31,500	2212	6.2	9.6	Travis
30,500	1346	5.2	8.0	Travis
29,900	1523	5.9		McGuire
29,500	* 1250	6.0	5.1	McGuire
29,200	1643	2.9	3.1	McGuire
28,900	1483	7.1		Travis
28,800	1630	6.4	6.6	Travis
28,500	977	4.7	4.6	Travis
28,300	1694	4.5		Travis
27,700	2852	2.5	2.3	McGuire
26,500	2955	4.9		Travis
26,300	2423	4.0		Travis
26,200	2000	4.1	* 3.9	Travis
26,000	* 1667	2.7	3.8	Travis
25,900	1341	9.2		Travis
25,800	1568	4.4	1.9	McGuire
24,700	1958	4.8		Travis
24,500	938	13.2	* 4.0	McGuire
20,500	5000	2.2	4.1	McGuire

* There was a short cruise segment during this segment. The time of the cruise was subtracted from the time of descent.

Table VI -- continued

Aircraft Type B-52B

Initial Altitude	Rate of Descent Between Initial Altitude and 20,000 Feet ft / min	Time of Descent From 20,000 feet to 10,000 feet	Time of Descent From 10,000 feet to 2500 feet	Base
41,200	* 2753	2.5		Castle
36,500	* 2750	4.4	2.4	Castle
36,200	4263	* 2.4		Biggs
35,200	* 3040	2.5		Castle
33,500	1985	* 3.7		Biggs
33,000	903	2.6		Castle
31,000	* 1803	2.3		Biggs
24,800	2000	* 3.0		Biggs
21,600	4000	3.4	3.2	Castle
20,400	4000	3.1		Biggs

Aircraft Type B-52D

46,000	2540	2.0		Fairchild
40,200	3311	* 2.9	* 5.2	Fairchild
39,200	* 3918	2.6		Fairchild
38,000	4286	2.9		Fairchild
36,000	2712	3.4		Fairchild
34,000	3043	2.5	* 7.2	Fairchild
32,500	3289	* 2.5	* 7.5	Fairchild
31,300	3324	2.5		Fairchild
30,000	2041	6.8	* 6.1	Fairchild
20,200	2000	3.1		Fairchild

* There was a short cruise segment during this segment. The time of the cruise was subtracted from the time of descent.

Table VI -- continued
Aircraft Type B-52E

Initial Altitude	Rate of descent Between Initial Altitude and 20,000 Feet ft/min	Time of descent from 20,000 feet to 10,000 feet	Time of descent From 10,000 feet to 2500 feet	Base
40,200	2349	5.6		Clinton-Sherman
35,800	3038	* 2.9	* 3.9	Clinton-Sherman
35,000	* 1786	* 2.6	2.2	Altus
34,300	1521	4.3		Altus
33,600	2720	2.3		Clinton-Sherman
33,400	3190	2.5		Altus
33,000	2500	* 2.9		Altus
32,300	1662	* 5.1		Altus
32,000	2222	* 2.6		Clinton-Sherman
31,200	* 2196	4.1	2.3	Altus
28,300	1122	5.6		Altus
24,500	1667	* 2.8		Altus
22,700	794	5.7	2.1	Altus
22,500	1923	3.4		Altus
20,000	0	2.6	4.6	Clinton-Sherman

* There was a short cruise segment during this segment. The time of the cruise was subtracted from the time of descent.

Table VI -- continued
Aircraft Type B-52F

Initial Altitude	Rate of Descent Between Initial Altitude and 20,000 Feet	Time of Descent From 20,000 feet to 10,000 feet	Time of Descent From 10,000 feet to 2500 feet	Base
48,900	2558	3.5	5.4	Carswell
47,300	*3456	3.0		Barksdale
41,300	2536	5.7	3.0	Carswell
40,000	*3279	3.8		Barksdale
36,500	1460	6.5		Barksdale
35,300	2429	9.0		Barksdale
33,300	3410	* 3.8		Barksdale
32,800	*2098	2.6		Barksdale
32,000	* 2000	* 3.1		Barksdale
31,700	1560	3.1		Barksdale
27,900	3160	2.9	2.9	Barksdale
27,700	1750	5.4		Barksdale
27,000	2121	3.2	1.7	Carswell
25,800	967	2.8	2.8	Carswell

* There was a short cruise segment during this segment. The time of the cruise was subtracted from the time of descent.

Table VI -- continued
Aircraft Type C-141A

Initial Altitude	Rate of Descent Between Initial Altitude and 20,000 Feet	Time of Descent From 20,000 feet to 10,000 feet	Time of Descent From 10,000 feet to 2500 feet	Base
44,800	5167	2.1	2.3	Dover
43,000	1716	7.1	7.3	Charleston
42,700	1645	3.3		Charleston
42,500	2027	5.2		Dover
42,100	2210	4.3		Dover
42,000	7586	1.6		Travis
41,000	1842	7.9	9.5	Dover
40,000	1481	1.9		Charleston
40,000	2532	5.5		Travis
39,200	2259	2.2		Charleston
38,000	1385	6.8		Travis
37,500	1535	* 6.0		Dover
37,500	2612	* 2.6		Dover
37,100	2111	5.5		Dover
36,700	1796	4.7	* 5.0	Dover
36,500	2063	4.3	10.9	Travis
36,100	1643	5.0	7.2	Tinker
36,000	2667	4.9		Travis
35,600	2108	5.6		Tinker
35,100	2359	5.3		Tinker
35,000	2381	5.4	* 8.0	Dover
34,800	1663	4.3		Travis
34,500	1959	7.5		Travis
33,600	* 1046	4.7		Dover
33,500	1227	3.2		Tinker
32,800	2612	6.3		Travis
32,400	1192	4.7	3.7	Tinker
31,900	1608	5.9	5.5	Travis
31,500	9583	2.8	* 3.5	Tinker
30,800	1662	5.2	9.9	Travis
30,500	1909	* 8.9	5.6	Travis
30,200	1097	4.3		Tinker
30,000	1515	2.7		Travis

* There was a short cruise segment during this segment. The time of the cruise was subtracted from the time of descent.

Table VI -- concluded
Aircraft Type C-141A, concluded

Initial Altitude	Rate of Descent Between Initial Altitude and 20,000 Feet ft / min	Time of Descent From 20,000 feet to 10,000 feet	Time of Descent From 10,000 feet to 2500 feet	Base
29,600	1846	7.1	10.5	Tinker
29,300	1860	5.2	* 6.5	Travis
29,300	1148	6.9		Tinker
29,100	583	* 6.8		Travis
29,000	1406	* 6.2		Tinker
28,700	3955	* 5.5		Tinker
27,000	1842	6.0	* 7.3	Travis
27,000	2800	5.5	* 5.5	Travis
26,600	1886	* 6.3	* 5.3	Charleston
26,100	2179	6.1		Travis
25,600	2333	5.4		Tinker
23,200	2133	5.1	* 4.2	Travis
22,800	2545	3.4		Travis
22,000	2000	6.3		Tinker
19,200	-	-		Tinker
18,400	-	-	5.3	Travis
18,100	-	-	6.4	Tinker

* There was a short cruise segment during this segment. The time of the cruise was subtracted from the time of descent.

Table VII Percent of Damage Due to Descent Segment

B-58A Data from 65 Actual Flights

Control Point	% damage due to descent = $\frac{\text{damage during descent}}{\text{total flight damage}}$
Aft inboard wheel well corner	7.7
Fuselage longeron at Bulkhead 9	0.0
Fuselage longeron at Bulkhead 5	1.8
Inboard nacelle pylon rail	6.6

C-135B

Control Point	% damage due to descent = $\frac{\text{damage during descent}}{\text{total flight damage}}$	
	Typical 10 hour mission	Typical 8 hour mission
Body Station 820	0.0%	0.1%
Horizontal Stabilizer Sta. 47.55	15.1	24.4
Vertical Fin Fuselage Sta. 111.65	27.5	27.0
Wing Station 360	2.9	3.7
Wing Station 336	2.9	3.5
Wing Station BBLO	2.2	3.7
Wing Station BBL 70.5	1.0	1.3

It is therefore concluded that a standard descent profile could be used for the descent parametric charts without a significant loss of accuracy. The calculations and parametric presentation would be the same as for ascent, except that the gross weight could be considered a constant for any one descent.

j. Landing

The landing impact and rollout can be a major cause of fatigue damage for many fatigue-sensitive locations, particularly for fuselage and landing gear items. The landing operation should be considered in three segments: 1) the landing impact, 2) the two wheel roll, and 3) the three wheel roll. There are also three types of landing to be considered: 1) full stop at the end of a mission, 2) touch-and-go practice landings, and 3) full-stop-with-taxi-back practice landings.

For the landing impact, the magnitude of stress at a control point is a function of the sinking speed, gross weight, and aircraft dynamics. The sinking speed at touchdown is very difficult to obtain, even on a fully instrumented aircraft, and would be impossible to obtain from a pilot's log. Therefore, a statistical spectrum of the sinking speeds must be used for the parametric study. The landing gross weight can be obtained from the pilot's log and the aircraft dynamics are fixed by the gross weight, weight distribution and configuration. Landing impact damage would then be presented as a function of only gross weight, fuel or cargo distribution, and configuration. For certain control points where the damage is sensitive to cargo weight or fuel weight, the damage could be presented as a function of bending moment at the critical station instead of gross weight. The damage during two wheel rollout and three wheel rollout is a function of the aircraft response to runway roughness at the velocity and weight during the rollout. The horizontal velocity at touchdown will control the spin up forces and is therefore a parameter in determining the damage to the landing gear and its supporting structure. Braking action will also affect the loading on the gear and its supporting structure. The horizontal landing speed should be a function of gross weight; therefore, the spin up forces would be a function of gross weight. The braking action is pilot-controlled, but the frequency and magnitude cannot be obtained from the pilot's log and would have to be taken as a statistical average.

(1) Full Stop at End of Mission

After analyzing the data (available from the pilot's log), it is suggested that only three parameters be used to present the parametric charts for the landing operation, i.e., gross weight, weight distribution and configuration. Since the damage due to the landing impact and two and three wheel rollout is a function of the same three parameters, the three damages can be summed and presented as a single damage chart for each

configuration. Each air base or group of bases may have a separate chart. Rough field landings would also require an additional chart.

(2) Touch-and-Go Practice Landings

Touch-and-go practice landings are normally performed in a specified manner and the flight pattern from one go-around to another will be consistent with respect to velocity and altitude. Due to this high degree of consistency, the total damage for a practice landing can be summed into a single value as a function of gross weight and configuration. This damage would be the sum of the takeoff damage, gust and maneuver damage during the go-around, landing impact damage, rollout damage, and a ground-air-ground cycle.

(3) Full-Stop-Taxi-Back Practice Landings

For full stop practice landings the damage calculations and the parametric presentation would be the same as for a touch-and-go landing, except that the rollout would be to a full stop and a taxi-back segment would be added.

Special attention should be given to the ground-air-ground cycle for both the touch-and-go and the full stop practice landing.

k. Ground-Air-Ground

The calculation and presentation of ground-air-ground damage in parametric form requires an agreement on the definition of the cyclic stresses. The approach to the calculations is to define a typical flight from parked condition before flight to parked condition after the flight. This typical flight would be completely defined as to time histories of gross weight, altitude, velocity, and configurations. Knowing the time histories and the environmental spectrum, the minimum ground stresses and maximum in flight stresses are calculated for a selected initial gross weight and a repeated number of flights. Only integer number of cycles of the stress is used, but the environmental spectrum may not indicate a complete cycle of the higher load levels for a flight segment. Therefore, the time of each flight segment is multiplied by the number of identical flights being used before entering the environmental input spectra. The number of times that a particular maximum or minimum stress occurs is recorded. This will yield two spectra, one of maximum and one of minimum stresses. It now becomes a question of the definition of the stresses to be used for the calculation of the ground-air-ground damage. It has been proposed in Reference 17 that the largest maximum be combined with the smallest minimum, then the second largest maximum be combined with the second smallest minimum, and so forth, until a number of cycles equal to the number of repeated flights is obtained. If there is an unequal

number of the largest maximums and smallest minimums, then a number of cycles equal to the smaller of the two numbers is formed and the remaining number of cycles combined with the second largest or smallest. Using example data from Reference 17, the spectrum of maximum in flight stresses and minimum ground stresses would be as follows:

Maximum Flight Stress		Minimum Ground Stress	
Stress psi	Occurrences/100 flights	Stress psi	Occurrences/100 flights
19,000	2,900	-16,000	1,500
21,000	1,000	-17,000	400
23,000	400	-18,000	80
25,000	129	-19,000	15
27,000	48	-20,000	4
29,000	15	-21,000	1
31,000	5		
33,000	2		
35,000	1		

One hundred cycles of ground-air-ground stresses would then be formed by combining one cycle of 35,000 psi with -21,000 psi; then two cycles of 33,000 psi with two cycles of -20,000 psi; two cycles of -20,000 psi with two cycles of 31,000 psi; the remaining three cycles of 31,000 psi with three cycles of -19,000 psi, etc. The spectrum of ground-air-ground cycles would then be as shown below:

Maximum Stress psi	Minimum Stress psi	Number of Occurrences
35,000	-21,000	1
33,000	-20,000	2
31,000	-20,000	2
31,000	-19,000	3
29,000	-19,000	12
29,000	-18,000	3
27,000	-18,000	48
25,000	-18,000	29
	Σ of occurrences =	100

These cycles are used to determine the ground-air-ground damage for the 100 identical flights. Dividing the sum by 100 yields the average ground-air-ground damage for that particular takeoff gross weight and type of typical mission. The procedure would be repeated for a range of takeoff gross weights and then for a number of typical missions.

Another popular definition is to use the maximum and minimum stress which, on the average, is equaled or exceeded once in all flights. Using the same stress data as above, the ground-air-ground cycle would then be equal to a maximum stress of 25,000 psi and a minimum stress of -18,000 psi. The damage is then calculated for this combination of stresses and is used as the average damage per flight for that particular gross weight and type of mission. The procedure is repeated for a number of takeoff gross weights and typical mission profiles.

Since the actual missions will not duplicate the selected typical missions, an analysis of the mission segments that make up the typical missions will be required. This analysis should show that the 100 or 1000 largest stresses occur in specific mission segments. For example, consider a flight that begins at a particular weight and flies a mission without refueling and without a low level penetration segment. Since stress is usually a function of gross weight, all of the largest stresses would be expected to occur during the early portion of the flight. For another flight where the aircraft refuels to a greater gross weight than at takeoff, most of the largest stresses would be expected to occur shortly after refueling. In a third flight where a low altitude penetration segment was flown at a high gross weight, the majority of the largest stresses would be expected to occur during the low level mission segment. After analyzing the various mission segments, which make up the typical missions and which are used to calculate the ground-air-ground damage, it is expected that what happened before or after the segment which had the majority of high stresses would not affect the damage calculations. The parametric charts would then be presented with a parameter of the events or mission segments composing the flight.

The parametric presentation would be similar to that shown in Figure 31. The user would locate the chart that corresponded to the correct aircraft configuration and then read the ground-air-ground damage from the curve that matched the mission segment and/or event parameter.

1. Summary of Damage by Mission Segments

Table VIII is a presentation of the distribution of the fatigue damage by mission segments for the present operation of the B-58 for 4 fatigue critical locations. Tables IX and X are presentations of the distribution of fatigue damage for two typical flights of the C-135. The B-58 data was obtained from strain gage recordings on 65 actual flights and therefore is representative of the present mission mix and environment. The C-135 data are taken from Reference 19 and are for typical flights using an average spectrum for the various flight segments.

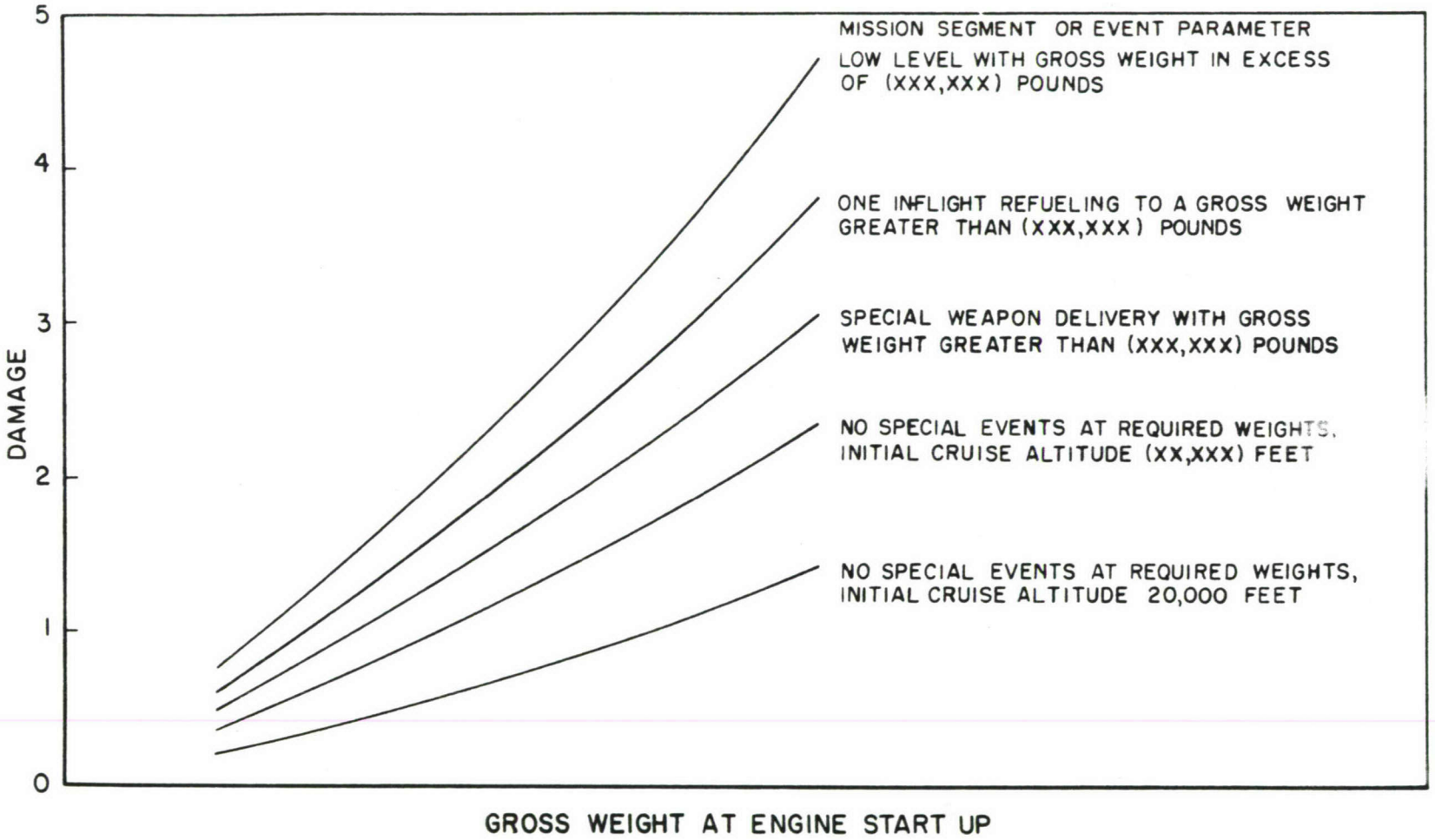

Figure 31 Example of Parametric Damage Chart for Ground-Air-Ground Cycle

Table VIII Distribution of Damage by Mission Segments for the B-58

Mission Segment	% of Total Damage			
	Control Point			
	1	4	5	6
Ground-Air-Ground	40.2	82.2	19.8	26.1
Ground Operations	0.0	0.0	1.0	0.0
Take-Off Run	0.0	3.6	33.7	0.2
Ascent	18.0	0.0	3.7	0.0
Subsonic Cruise	21.1	0.1	2.0	0.1
Supersonic Dash	0.5	0.0	0.6	0.0
Descent	7.7	0.0	1.8	6.6
Low-Level	10.1	0.0	2.0	0.8
Landing Impact	0.0	13.1	26.2	59.3
Two Wheel Roll	0.0	1.2	5.6	5.6
Three Wheel Roll	0.0	0.0	1.6	1.2
Refueling	2.4	0.0	0.2	0.0

Control Point	Description
1	Aft Inboard Wheel Well Corner (Wing Lower Surface) 7075-T6 KT = 4
4	Fuselage Longeron at Bulkhead 5, Fuselage Station 477.90 7075-T6 KT = 6
5	Fuselage Longeron at Bulkhead 9, Fuselage Station 689.5 7075-T6 KT = 6
6	Inboard Nacelle Pylon Rail 2024 KT = 3

Table IX Distribution of Damage by Mission Segments for the C-135B 10-Hour Cargo Mission. Takeoff G.W. = 276,500 pounds

Mission Segment	% of Total Damage						
	Control Point						
	1	2	3	4	5	6	7
Climb	2.1	38.7	41.6	13.1	12.1	10.4	5.2
Cruise	12.3	17.5	30.8	59.6	49.8	47.5	21.5
Descent	0.0	15.1	27.6	2.9	2.9	2.2	1.0
Ground-Air-Ground	59.5	20.0	0	23.2	34.1	39.9	72.3
Ground Damage	26.1	8.7	0	1.2	1.1	0	0

Control Point	Description
1	Body Station 820
2	Horizontal Stabilizer S.S. 47.55
3	Vertical Fin Fin Station 111.65
4	Wing Station 360 Stiffener 8
5	Wing Station 336 Skin at Stiffener 10
6	BBL 0 Skin at Stiffener 8
7	BBL 70.5 Joint, Stiffener 7

Table X Distribution of Damage by Mission Segments for the C-135B 8-Hour Cargo Mission. Takeoff C.W. = 247,200 pounds

Mission Segment	% of Total Damage						
	Control Point						
	1	2	3	4	5	6	7
Climb	0.8	34.1	40.4	9.0	7.9	6.5	3.1
Cruise	12.5	16.7	28.0	60.3	49.4	48.5	20.9
Descent	0.1	17.3	31.6	3.7	3.5	2.8	1.3
Ground-Air-Ground	49.6	21.8	0	25.5	37.5	42.2	74.7
Ground Damage	37.0	10.1	0	1.6	1.4	0	0

Control Point	Description
1	Body Station 820
2	Horizontal Stabilizer S.S. 47.55
3	Vertical Fin Fin Station 111.65
4	Wing Station 360 Stiffener 8
5	Wing Station 336 Skin at Stiffener 10
6	BBL 0 Skin at Stiffener 8
7	BBL 70.5 Joint, Stiffener 7

3. FIGHTER AIRCRAFT PARAMETER OPTIMIZATION (CONSISTENCY)

A parametric fatigue analysis of fighter aircraft presents a different problem from that for large bombers or cargo type aircraft. The analysis becomes more difficult because of the great number of missions flown by fighter aircraft and because of pilot's freedom during the combat phase of these missions. It is further complicated by the large number of combinations of external stores, whether weapons or fuel pods, that can be used. The fact that most fighter aircraft are designed for a limit load factor of 7.33, makes most of them immune to damage from atmospheric gust loading and therefore generally reduces the loadings to maneuver and ground loads.

Since the stresses in the structure and the resulting fatigue damage are functions of the gross weight, altitude, velocity, store configuration, and the load level, all of these should be parameters of the parametric study. However, during combat the altitude and velocity change so rapidly that it would be impossible to obtain these parameters from a manual log. Consequently, either these parameters must be eliminated from the parametric charts, or an automatic recorder must be installed in the aircraft. The cost of time history recorders and the follow-up data processing does not make this approach feasible for a flight by flight tail number analysis.

Studies were undertaken to determine the pilot log information required and the anticipated accuracy of the predicted fatigue damage by using each set of log information.

In order to make comparisons of the accuracy of various methods, the true value must be determined. Computer tabs of 123 flights of the F-105D operating in live combat were obtained. These tabs list for each occurrence of an n_z greater than two: the time after takeoff, velocity, altitude, gross weight, mission segment, and store configuration. Stress relationships were extracted from Reference 21 for the transfer spar at fuselage station 442 and the top cover skin at the access door at fuselage station 509. From this data the fatigue damage for a single occurrence of each n_z level from 2 to 7.5 g's in steps of 0.5 g's was determined for the combinations of Mach, altitude, gross weight, and store configurations shown in Table XI. These calculations yielded the damage per occurrence of each n_z level for 180 combinations of Mach-altitude-gross weight and configuration. Figure 32 and Figure 33 are typical plots showing the variation of damage for a number of Mach-altitude conditions. As shown by these two figures, the Mach-altitude combination has a great influence on the amount of damage. However, the variation in damage is not as great for variations in Mach-altitude as it is for variations in the maneuver load factor; therefore, one could allow a greater variation in the Mach-altitude spectrum than he could in the n_z spectrum for the same accuracy.

Table XI Conditions for Which Unit Damages Were Calculated

Mach	Alt	Gross Weight 31,000	33,000	35,000	37,000	40,000	44,000
0.65	7000	ABCD	ABCD	ABCD	ABCD	CD	CD
0.65	20,000	ABCD	ABCD	ABCD	ABCD	CD	CD
0.85	1,000	ABCD	ABCD	ABCD	ABCD	CD	CD
0.85	7,000	ABCD	ABCD	ABCD	ABCD	CD	CD
0.85	20,000	ABCD	ABCD	ABCD	ABCD	CD	CD
0.92	1,000	ABCD	ABCD	ABCD	ABCD	CD	CD
0.92	7,000	ABCD	ABCD	ABCD	ABCD	CD	CD
0.92	20,000	ABCD	ABCD	ABCD	ABCD	CD	CD
1.2	20,000	ABCD	ABCD	ABCD	ABCD	CD	CD

Configuration	Stores
A	Clean External
	390 Gallon tank in Bomb Bay
B	MA-2 on Wing Outboard
	390 Gallon Tank in Bomb Bay
C	650 Gallon Tank on Centerline Pylon
	2-450 Gallon Tanks on Wing Inboard
	390 Gallon Tank in Bomb Bay
D	650 Gallon Tank on Centerline Pylon
	2-450 Gallon Tanks on Wings Inboard
	390 Gallon Tank in Bomb Bay
	MA-2 on Wing Outboard

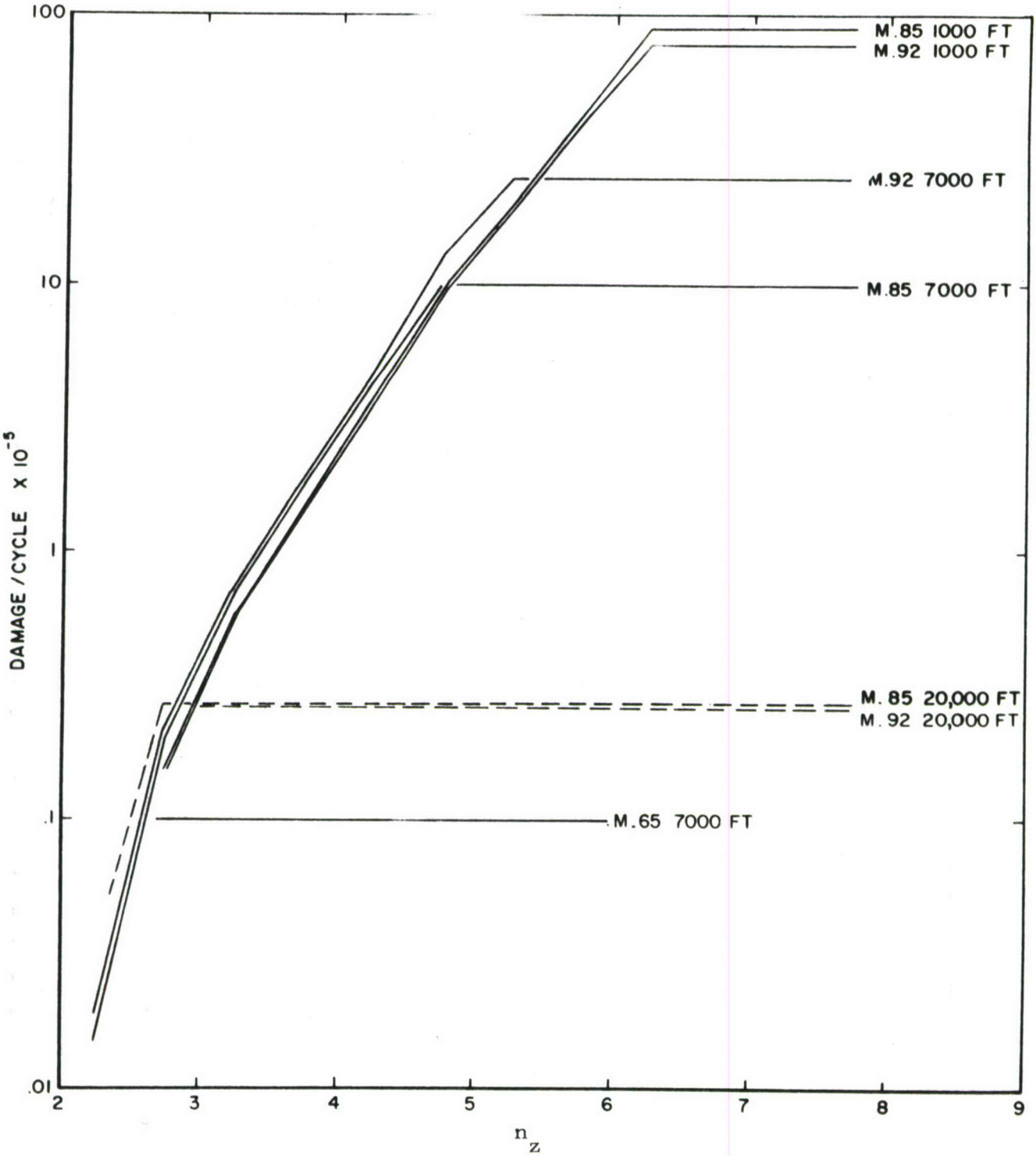

Figure 32 Damage per Cycle vs. n_z for F-105. Transfer Spar at Fuselage Station 442, Gross Weight 40,000 pounds, Store Configuration C

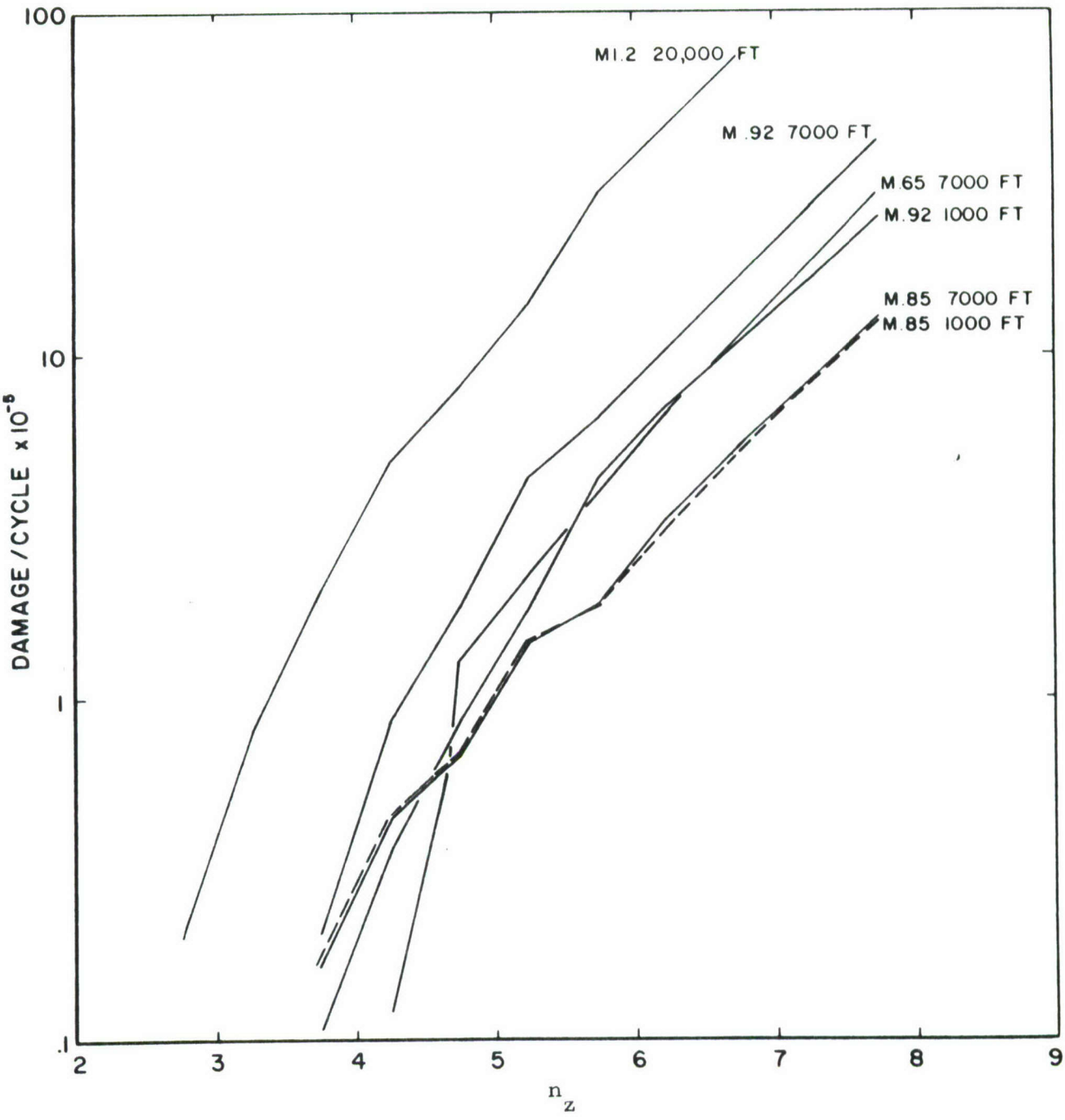

Figure 33 Damage per Cycle vs. n_z for F-105. Top Cover Skin at Fuselage Station 509, Gross Weight 40,000 Pounds, Store Configuration C

Each occurrence of an n_z level from the combat data was then assigned to one of these 180 conditions which most nearly matched the environmental and aircraft conditions. The damage for each occurrence of an actual n_z was then listed and summed by mission phase for the first 51 bomb drops. Three mission phases were used to break down the damage. These were 1) the damage done during the pass over the target when the weapon was dropped, 2) the damage done during other maneuvering in the target area, and 3) the damage done during the remainder of the flight which included ascent, cruise, refueling, and descent.

In an attempt to show the consistency of the flights, they were analyzed in groups of 17 bomb drops. The percentage of the total damage, exclusive of the ground-air-ground cycle, for each mission phase was determined for fuselage station 509, and is listed below. Flights were taken in the order that they were reported. Some flights had two weapon passes per flight and some flights did not have a combat phase. Therefore, the number of drops and flights are different for the mission phases.

First 17 drops:

% of damage during the pass on which the weapon was dropped	$= \frac{.000311710}{.000462125}$	= 67.5%	17 drops
% of damage during other maneuvers in target area	$= \frac{.000148096}{.000462125}$	= 32.0%	12 flights
% of damage due to all other flight segments	$= \frac{.000002319}{.000462125}$	= 0.5%	13 flights

Second 17 drops:

% damage during the pass on which the weapon was dropped	$= \frac{.000770022}{.000849784}$	= 90.7%	17 drops
% damage during other maneuvers in the target area	$= \frac{.000075924}{.000849784}$	= 8.9%	15 flights
% of damage due to all other flight segments	$= \frac{.000003838}{.000849784}$	= 0.4%	20 flights

Third 17 drops:

% of damage during the pass on which the weapon was dropped	$= \frac{.000278118}{.000388469}$	= 71.7%	17 drops
% of damage during other maneuvers in the target area	$= \frac{.000101062}{.000388469}$	= 26.0%	15 flights
% of damage due to all other flight segments	$= \frac{.000009289}{.000388469}$	= 2.3%	16 flights

Total for first 51 drops:

% of damage during the pass on which the weapon was dropped	$= \frac{.001359840}{.001700378}$	= 80%	51 drops
% of damage during other maneuvers in the target area	$= \frac{.000325082}{.001700378}$	= 19%	42 flights
% of damage due to all other flight segments	$= \frac{.000015446}{.001700378}$	= 1%	49 flights

The same analysis was performed for the transfer spar attachment at fuselage station 442. The results are shown below:

First 17 drops:

% damage during the pass on which the weapon was dropped	$= \frac{.002363277}{.003755217}$	= 63%	17 drops
% damage during other maneuvering in the target area	$= \frac{.001381617}{.003755217}$	= 37%	12 flights
% damage due to all other flight segments	$= \frac{.000010323}{.003755217}$	= 0%	13 flights

Second 17 drops:

% damage during the pass on which the weapon was dropped	$= \frac{.002216215}{.003346390}$	= 66.0%	17 drops
% damage during other maneuvers in the target area	$= \frac{.001121231}{.003346390}$	= 33.5%	15 flights
% damage due to all other flight segments	$= \frac{.000008944}{.003346390}$	= 0.5%	20 flights

Third 17 drops:

% damage during the pass on which the weapon was dropped	$= \frac{.002399989}{.003213958}$	= 74.8%	17 drops
% damage during other maneuvers in the target area	$= \frac{.000805183}{.003213958}$	= 25.0%	15 flights
% damage due to all other flight segments	$= \frac{.000008786}{.003213958}$	= 0.2%	16 flights

Total for first 51 drops:

% damage during the pass on which the weapon was dropped	$= \frac{.006979481}{.010315565}$	= 68%	51 drops
% damage during other maneuvers in the target area	$= \frac{.003308031}{.010315565}$	= 32%	42 flights
% damage due to all other flight segments	$= \frac{.000028053}{.010315565}$	= 0%	49 flights

This study shows that for these two control points, one sensitive to wing loadings and one sensitive to aft fuselage loadings, the fatigue damage during ascent, cruise, refueling, and descent is negligible.

A similar study using the maneuver load data from Reference 10 (page 21) for the F-105D, which is a composite of 1934 flights representing 2551 flight hours of training, was attempted. This data was not broken down by Mach-altitude-gross weight-configuration; therefore, to determine the proportioning of damage due to each mission phase it was assumed that all of the n_z occurrences were at Mach number .85, altitude 1000 feet, configuration C, and a gross weight of 40,000 pounds. Using these assumptions it was determined that ascent, cruise, refueling, and descent caused 1.65% of the total fatigue damage at the transfer spar, exclusive of the ground-air-ground cycle. The same study was performed for 1638 live combat flights of the F-5A. The n_z loadings were taken from Reference 8 (page 60). The damages at each n_z level were taken from Reference 22 (pages 7 and 10) for subsonic speeds, clean wings with SUU-20 on the centerline. Using these conditions and loads the ascent, cruise and descent caused 2.3% of the fatigue damage at wing station 27, 41.5% chord.

a. Combat Mission Phase

As a result of these studies it was decided that the most important mission segment was the combat mission phase; and, if the damage during this phase could be accurately calculated, the other phases would be insignificant. Therefore, a detailed parametric study of the combat segment was performed in order to determine which parameters were most significant, and also what would be the expected variation of these parameters. In the calculation of the actual damage for the F-105D, 60% to 80% of the fatigue damage resulted from the pull-up after weapon release. From these calculations the average damage per weapon release was determined for each instrumented aircraft. This was an attempt to evaluate the consistency of the weapon drops. The following table lists the average damage per bomb drop by aircraft number.

Average Damage per Bomb Drop

A/C Tail No.	Station 509	Station 442	Number of Bomb Drops
069	.00006830	.00022970	8
132	.00001413	.00013810	13
160	.00002880	.00014250	17
205	.00001905	.00012150	10
352	.00001604	.00012160	4
367	.00003161	.00013590	13
378	.00003888	.00021770	18
469	.00002799	.00011279	15
732	.00002044	.00015446	21

The data indicate that for this small number of drops there is not enough consistency from one aircraft to another to assume an average damage per weapon drop.

It was next attempted to correlate the damage for each weapon drop by assuming that all drops were at the most probable Mach number-altitude and gross weight but using the actual peak n_z that occurred on the pass when the weapon was dropped. Using the recorded n_z level with the most probable Mach number of .875 and a most probable altitude of 5,000 feet and a gross weight of 39,000 pounds, the calculated damage was .003365 for 116 weapon drops, compared to an actual damage of .003817 for fuselage station 509.

In an attempt to improve on the prediction, a distribution of Mach-altitude conditions was used with the recorded n_z and actual gross weight. The distribution of Mach number and altitude was determined for

each n_z level since both the F-5A and the F-105D data indicated a dependence between n_z and Mach number. These probabilities of Mach-altitude for each n_z level are shown in Table XII.

Weighted damages per occurrence of each n_z level for different gross weights were then determined for the Mach-altitude probabilities shown in Table XII. Figure 34 is a plot of these weighted damages for the F-105D fuselage station 509. Using the damages from Figure 34 and the recorded n_z values with the actual gross weight, a comparison was made between the actual damage and the predicted damage. Table XIII is a listing of the comparison. As one would expect, the total predicted damage after 102 drops is very close to the actual damage. This is true because the 102 flights were included in the 116 flights used to determine the Mach-altitude probabilities. However, it is presented as a possible method for the parametric study. The accuracy of the method would depend on the repeatability of the Mach-altitude conditions. The probabilities shown in Table XII give some indication of the dependency of the n_z level on Mach number. Figure 35, taken from Reference 8, shows the dependence of n_z on the average airspeed for the F-5A. This data is presented to show that a different probability of Mach-altitude should be used for each n_z level.

Figure 36, taken from Reference 8, shows the high degree of consistency and the narrow altitude range for the n_z peak following the weapon release for the F-5A.

Figures 37 and 38 show the distribution of Mach number and altitude by weapon type at the time the pull-up peak load occurred for the F-105D. The figures show that, even for the small number of weapon releases used in the study, there is a pattern to the Mach number and altitude at the time of peak n_z that is dependent on the type of weapon.

Figures 36 through 38 show that the probability of a Mach-altitude combination should be a function of the type weapon that was released.

It is concluded that a spectral distribution be used for the Mach number and altitude that exists at the time of the peak n_z during pull-up after weapon release and that this spectrum be dependent on the type of weapon released and the magnitude of n_z.

Table XIV lists the number of occurrences of each n_z level during the pull-up following weapon release. As can be observed by studying the table, there is a variation in the distribution of the number of occurrences of 4.5, 5 and 5.5 g's for each of the 17 drops; however, there is a greater variation in the number of occurrences of low and high load factors among the groupings. Damages by aircraft serial number were also calculated by

Table XII Probability of Mach-Altitude as a Function of N_z for F-105D for the Pull-Up After the Weapon Drop

	ALTITUDE							
	0-4000 feet				4000-12000 feet			
	Mach Number				Mach Number			
n_z	.6-.7	.7-.8	.8-.9	>.9	.6-.7	.7-.8	.8-.9	>.9
2.0								
2.5		.500	.500					
3.0				.250		.500	.250	
3.5	.143	.143	.286		.143		.286	
4.0		.286				.286	.286	.143
4.5	.043		.130	.043	.043	.087	.565	.087
5.0		.050	.200	.050		.050	.400	.250
5.5		.040	.160	.040		.040	.400	.320
6.0			.083				.250	.667
6.5				.166			.330	.500
7.0								1.000
7.5							.330	.660

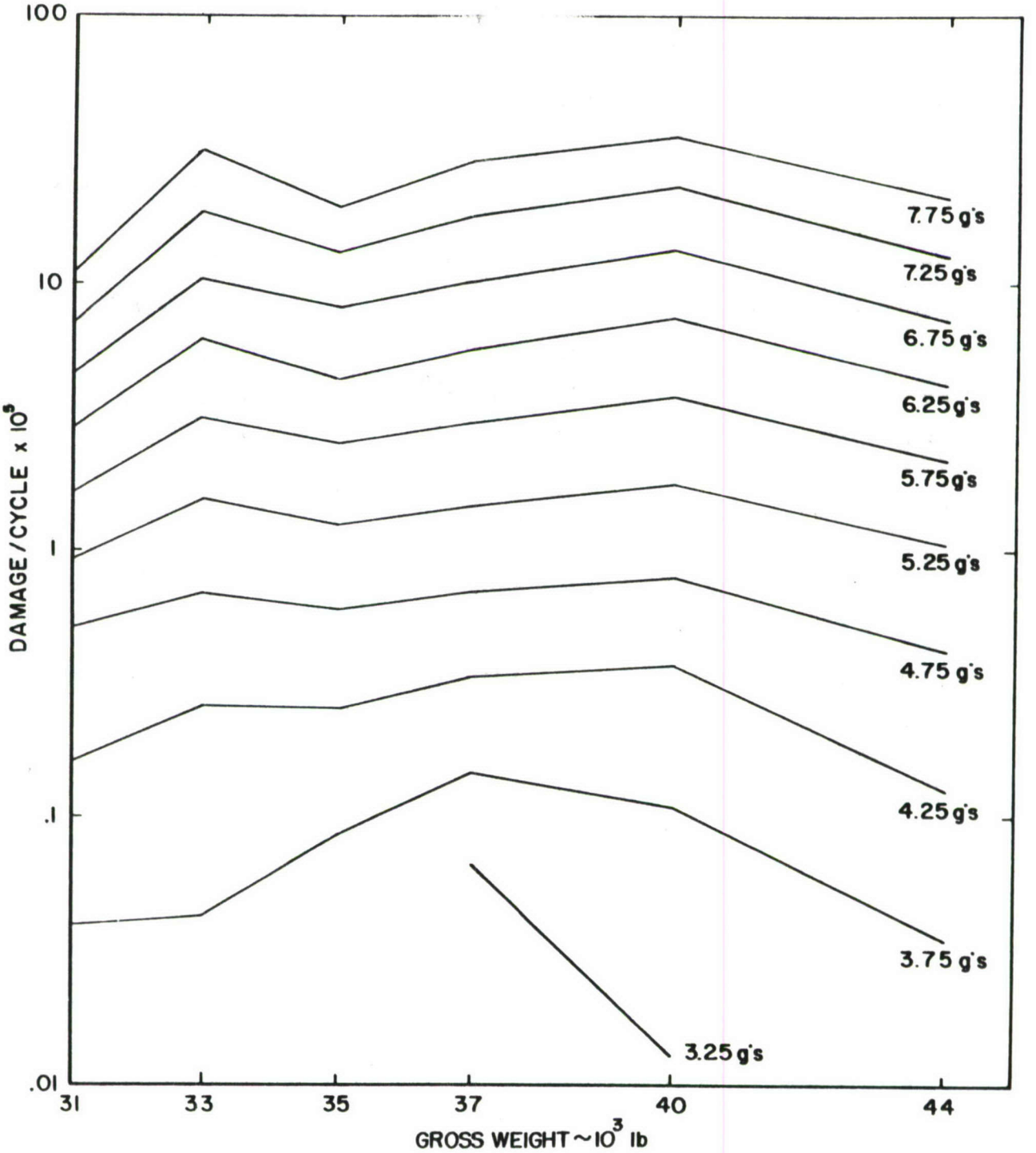

Figure 34 Weighted Damage vs. Gross Weight as a Function of n_z Level for the Mach-Altitude Probabilities Shown in Table XII, Fuselage Station 509, Configuration C

Table XIII Comparison of Actual Damage and Predicted Damage Using Probability of Mach Number and Altitude Conditions for F105D, Fuselage Station 509

Damages are for the pull-up after weapon release

	Actual Damage	Predicted Damage
First 17 Drops	23.01×10^{-5}	24.55×10^{-5}
Second 17 Drops	61.56×10^{-5}	62.87×10^{-5}
Third 17 Drops	27.35×10^{-5}	35.06×10^{-5}
Fourth 17 Drops	65.97×10^{-5}	74.70×10^{-5}
Fifth 17 Drops	51.14×10^{-5}	48.21×10^{-5}
Sixth 17 Drops	88.09×10^{-5}	76.22×10^{-5}
Total 102 Drops	317.12×10^{-5}	321.61×10^{-5}

$$\text{Error after 102 weapon drops} = \frac{4.49}{321.61} = 1.4\%$$

Only flights that had the same configuration after the weapon drop were used.

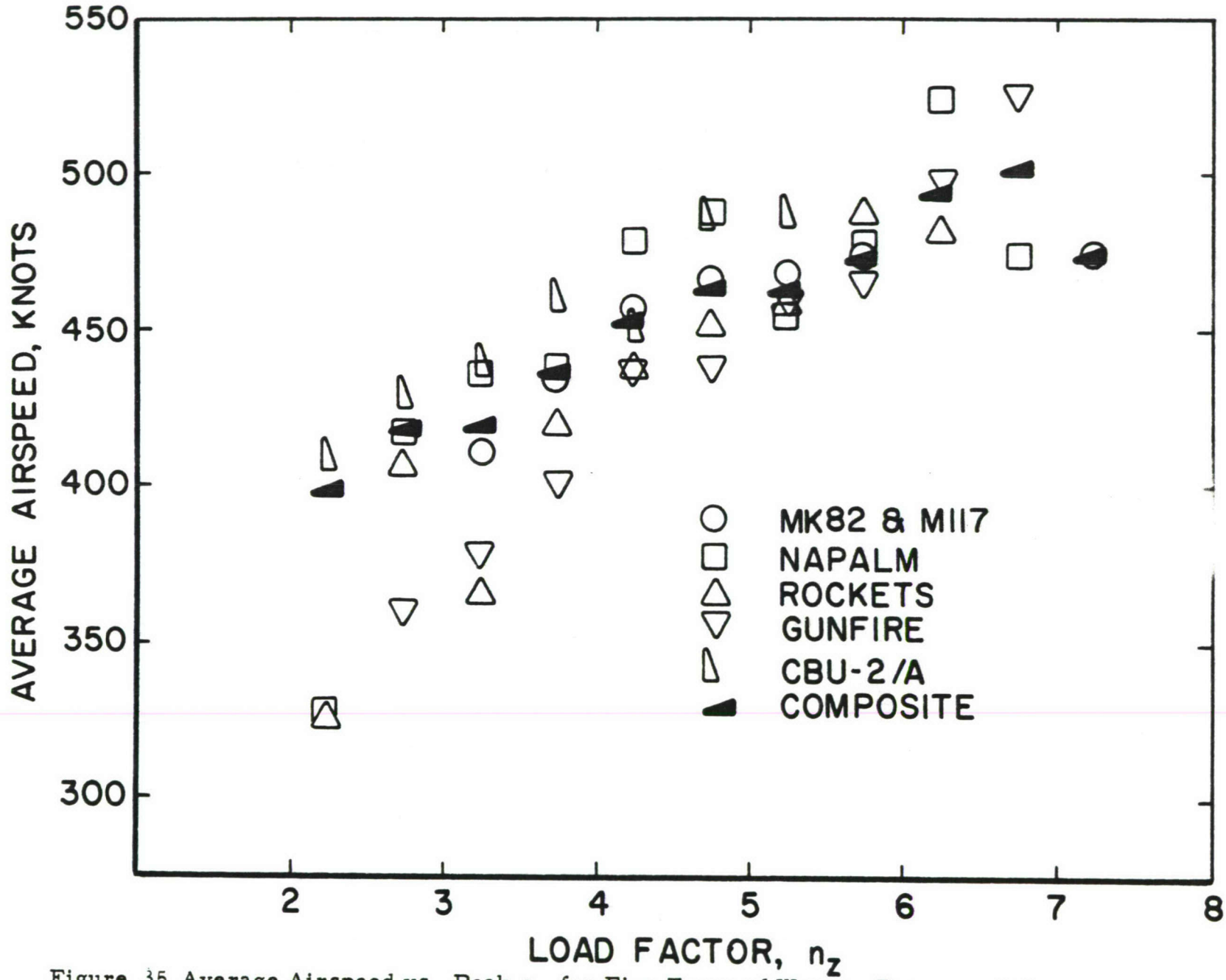

Figure 35 Average Airspeed vs. Peak n_z for Five Types of Weapon Passes and the Composite Average. Live Combat Data for 1551 Flight Hours of the F-5A

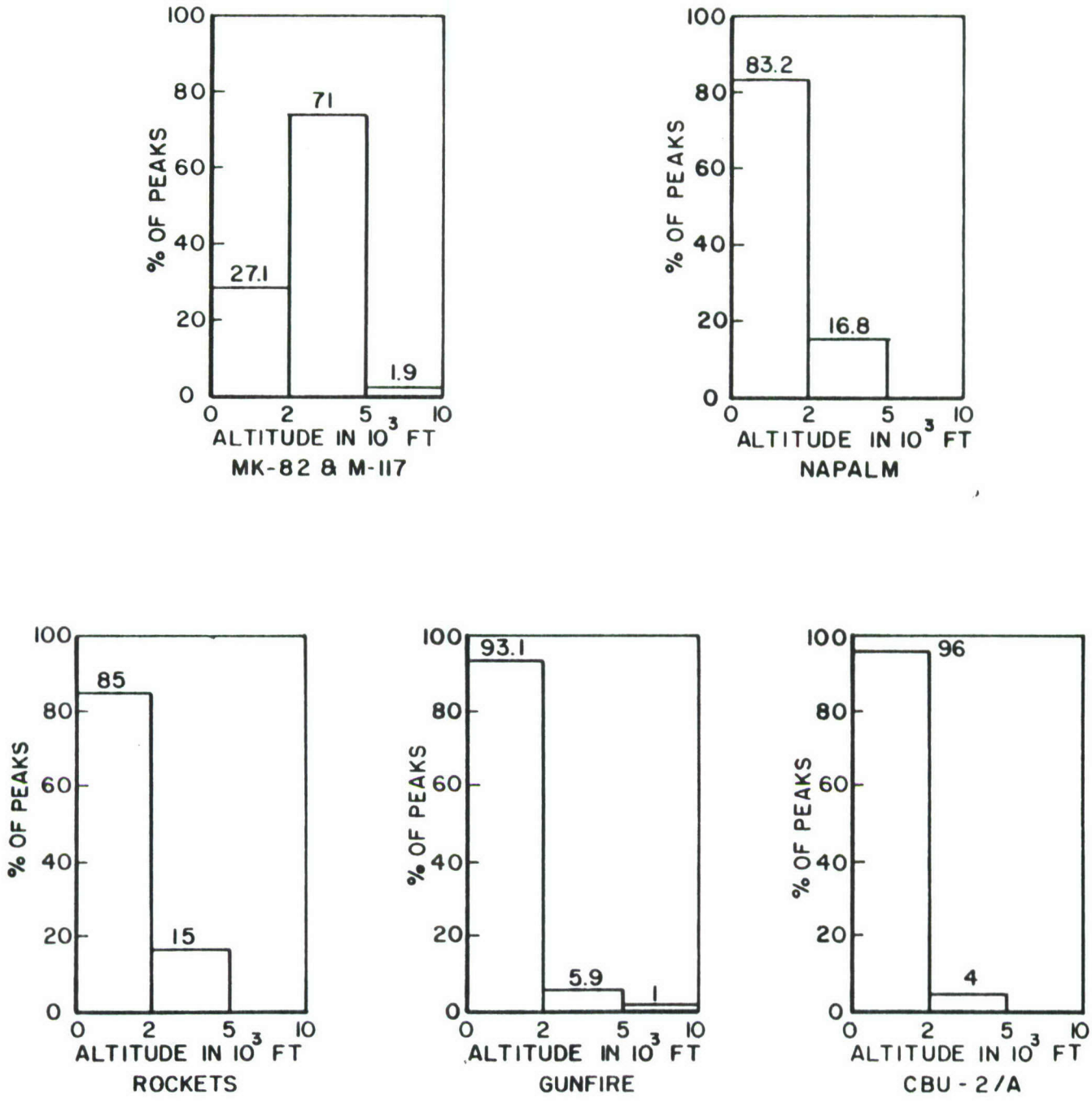

Figure 36 Percentage of n_z Peaks in Altitude Ranges for Five Types of Weapon Passes, F-5A Aircraft, 1551 Flight Hours

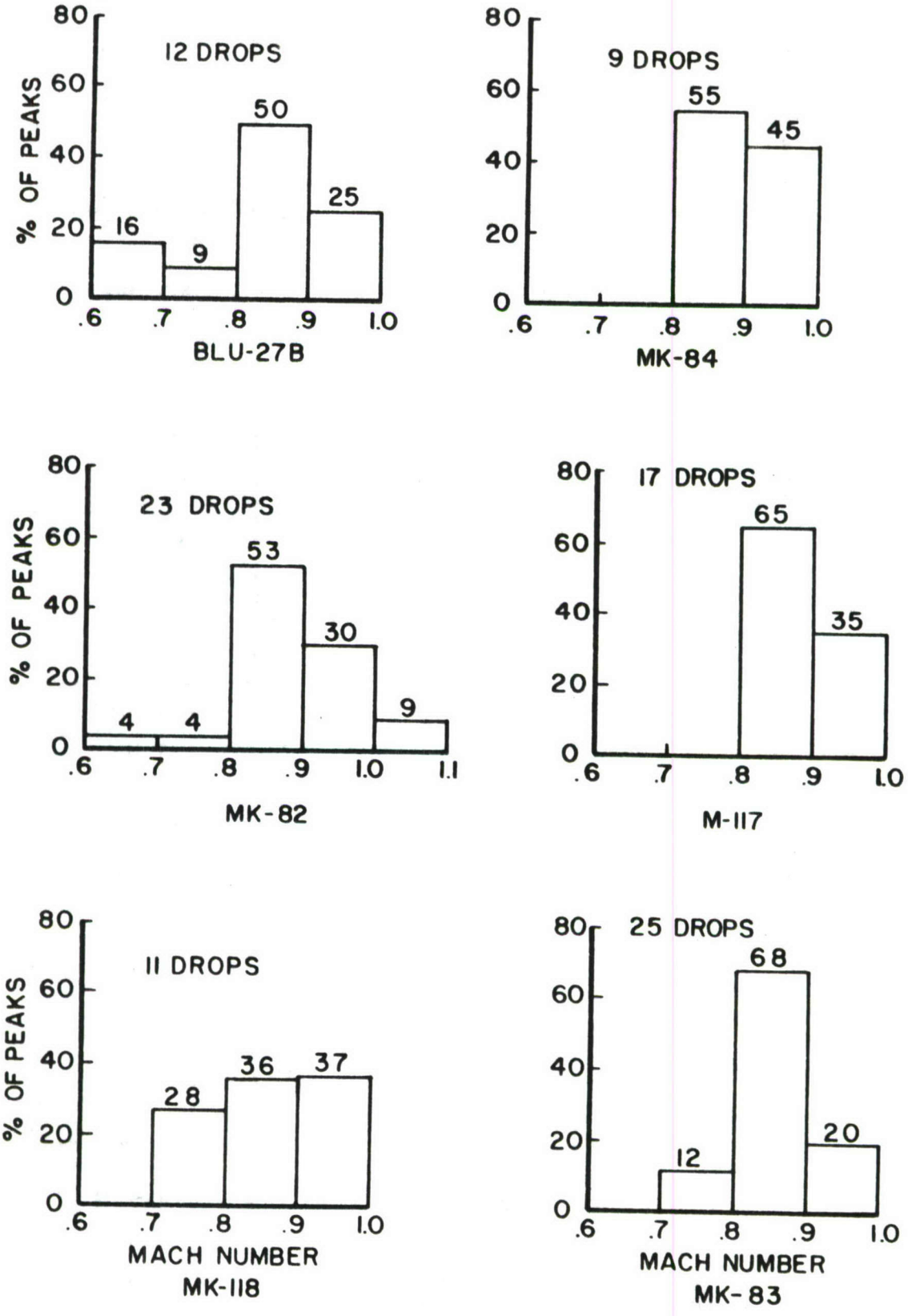

Figure 37 Percentage of n_z Peaks in Mach Number Ranges for Six Types of Weapon Passes, F-105 Aircraft

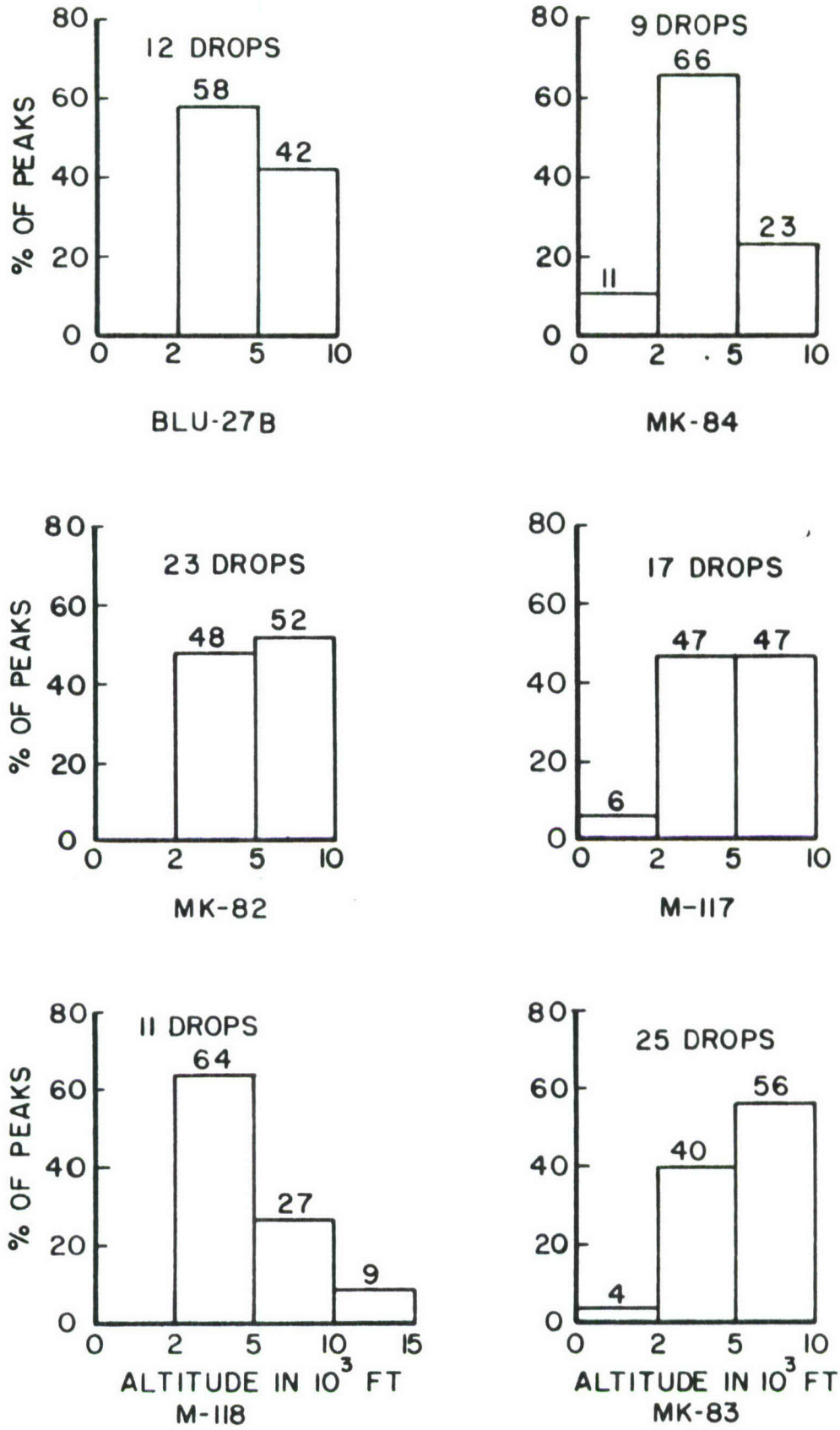

Figure 38 Percentage of n_z Peaks in Altitude Ranges for Six Types of Weapon Passes, F-105 Aircraft

Table XIV Number of Occurrences of an n_z Level During 17 Bomb Drops for the F-105D

n_z	2	2	2.5	3	3.5	4	4.5	5	5.5	6	6.5	7	7.5
First 17		1	1		1	1	3	4	3	3			
Second 17			1		1	1	4	2	3	3		1	1
Third 17		1			3	1	3	4	4		1		
Fourth 17					1	1	2	3	6	3			1
Fifth 17	1				1	3	2	3	4	1	2		
Sixth 17	1			2	1		4	3	1	2	2		1
Remaining 14				1	1		6	1	4		1		
Total 116	2	2	2	3	9	7	24	20	25	12	6	1	3

using an average spectrum of n_z occurrences (the totals shown in Table XIV). These were calculated for the average spectrum of n_z using the Mach-altitude probabilities shown in Table XII but with the actual gross weight at the time of the maneuver load occurrence. These damages are shown in Table XV and are listed as "Damage C", The damage listed in column B is based on Mach-altitude probability and gross weight. The data show that either method will predict the damage to the total fleet; however, the use of a statistical spectrum of load factors (Method C) does not give the proper distribution to each individual aircraft.

The previous discussion of fighter aircraft has dealt primarily with the maneuver load that occurs during the pull-up after weapon release or air-to-ground gunnery. For the F-105D this was shown to account for 60 to 80% of the fatigue damage exclusive of the ground-air-ground cycle. The remaining 20 to 40% of the fatigue damage was found to be a result of maneuvering in the target area between the time the aircraft descended from cruise altitude until it returned to cruise altitude. This maneuvering may be due to low altitude penetration, escape, or loitering while looking for a target or being assigned a target.

The other maneuvering in the target area was also analyzed for consistency of altitude, Mach number, and frequency of load level occurrence. Figures 39 and 40 show the number of times that the F-105D was within a given altitude band and Mach number band when the load factor had a peak greater than 2 g. The two figures show that while the correlation among the three groupings of flights during which 17 weapon drops were made is not perfect, there is a sufficient degree of consistency to believe that with a larger number of flights the distribution of both altitude and Mach number would stabilize. In fact, for the first and third groupings the Mach number distributions are almost the same, and for the second and third groupings the altitude distributions are almost the same. Table XVI lists the frequency of occurrence of each n_z band for the maneuvering in the target area exclusive of the pull-up after weapon release. These frequencies are listed by aircraft serial number in an attempt to show that an average spectrum of maneuvering loadings could be used to calculate the damage during this phase of the mission. The data indicate that there is a considerable variation in the frequency of occurrence at all n_z levels from one aircraft to another. Because these loads are pilot-controlled and are also affected by the type and location of the target as well as by any enemy activity, there is little reason to believe that with more data the variation from one aircraft to another would be greatly reduced.

Since a) the magnitude of the load level is controlled by the pilot and to some extent by the target, b) the amount of maneuvering in the target area has such a wide variation from one flight to another, and c) the amount of damage can vary by two orders of magnitude if the maneuver load level is changed from 4 to 7 g's, it is suggested that an average spectrum of n_z

Table XV Comparison of Damage Due to Pull-Up G's When Calculated by Three Methods (Only Flights with Configuration "C" are Included)

Aircraft Serial No.	Number of Bomb Drops	Damage A $\times 10^{-5}$	Damage B $\times 10^{-5}$	Damage C $\times 10^{-5}$
069	7	39.34	44.33	23.04
132	11	15.44	15.71	38.66
160	13	42.72	56.61	42.60
205	10	19.05	16.64	33.64
352	4	46.42	38.70	13.54
367	9	33.87	22.47	30.29
378	17	68.74	76.14	56.27
469	12	29.77	31.12	41.46
732	16	36.98	36.26	51.88
Total	101	332.08	337.98	331.38

Damage A — Actual damage, calculated by using the actual Mach number, altitude, gross weight, and load level.

Damage B — Estimated damage, calculated by using a spectrum for Mach number and altitude, but using actual gross weight and load level.

Damage C — Estimated damage, calculated by using the same spectrum for Mach number and altitude as Damage B, but also using an average spectrum of load levels with the actual gross weight.

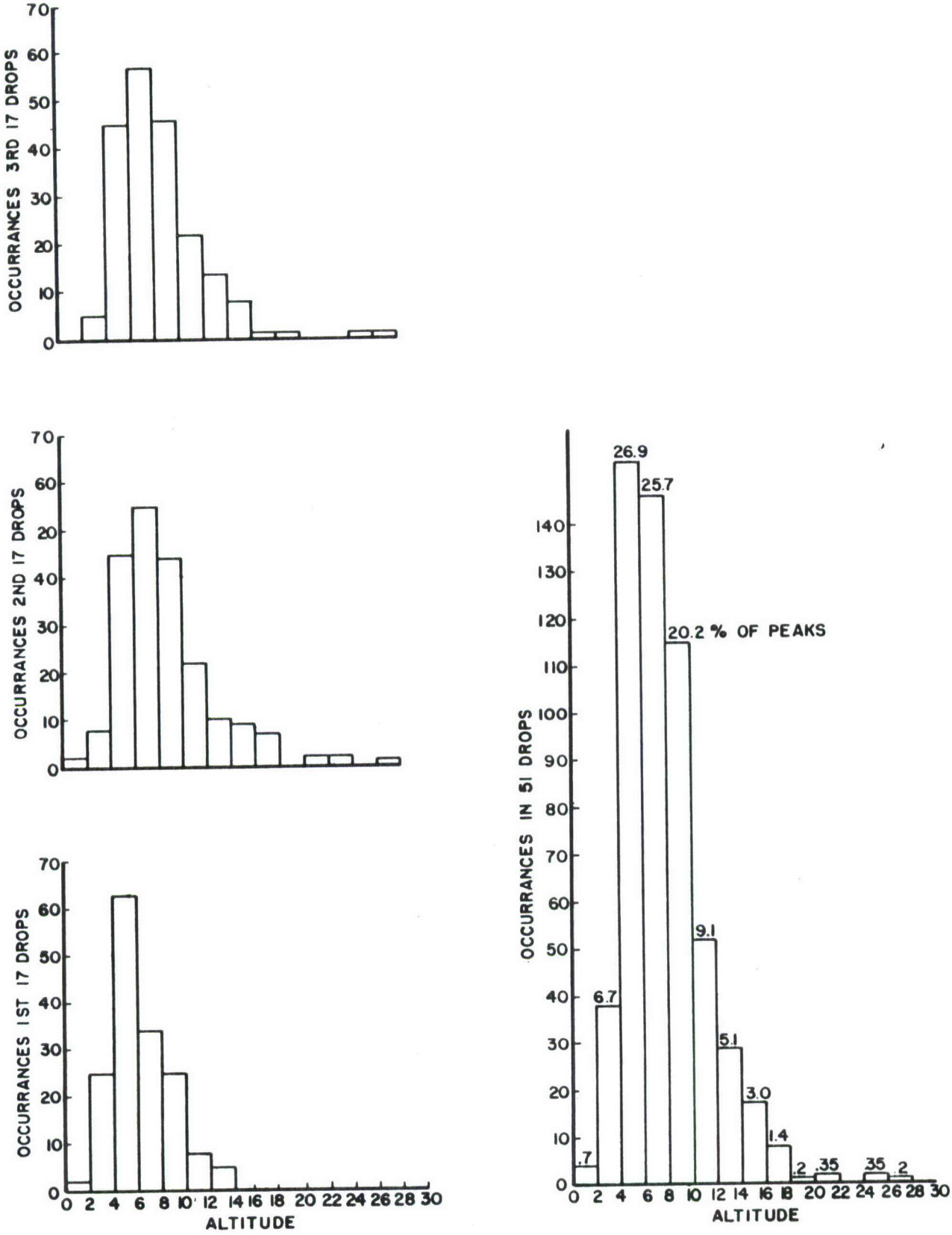

Figure 39 Distribution of Altitude at the Time When n_z Peak Exceeded 2 g for Maneuvering in the Target Area, F-105D

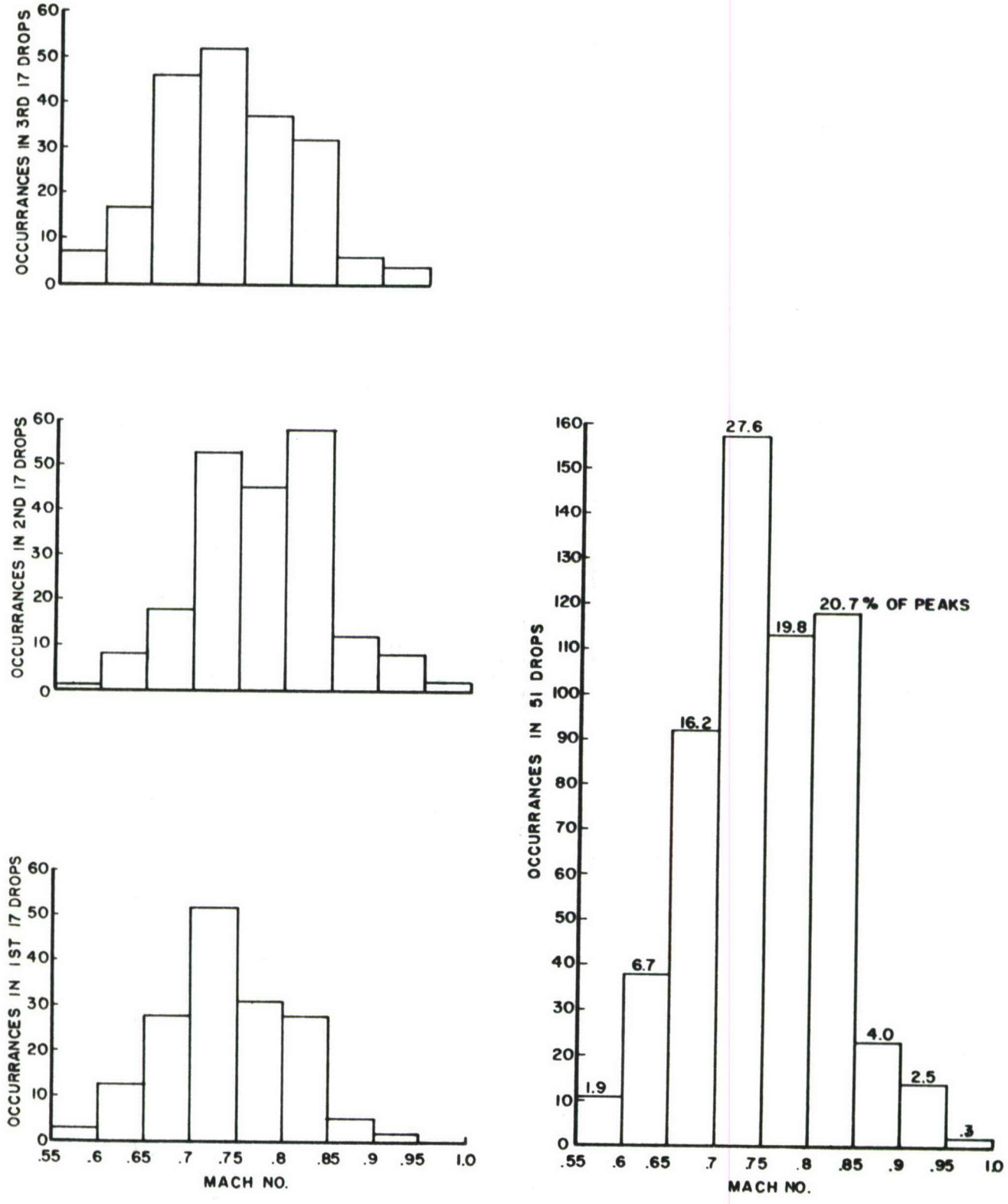

Figure 40 Distribution of Mach Number at the Time When n_z Peak Exceeded 2 g for Maneuvering in the Target Area, F-105D

Table XVI Frequency of Occurrence of an n_z Level by Aircraft Serial Number for the Combat Phase of a Mission (The Pull-Up n_z After Weapon Release Has Been Extracted)

A/C	Time (min)	No. of Flights	Occurrences/minute Load Factor						
			3.0	3.5	4.0	4.5	5.0	5.5	6.0
069	228.5	8	.048	.039	.031	0	0	0	0
132	299.6	9	.073	.033	.013	.003	.003	0	0
160	299.0	12	.061	.057	.033	.003	.003	0	.003
205	260.5	8	.054	.031	.008	.008	.004	0	0
352	176.9	4	.102	.062	.028	.011	0	0	.011
367	274.5	8	.069	.025	.011	.004	.004	0	0
378	450.5	13	.087	.035	.017	.013	0	0	0
732	395.0	12	.094	.023	.013	0	.002	0	.005
Average	2384.5	74	.087	.037	.019	.008	.002	0	.002

levels per weapon drop, or unit time, not be used to determine the load level, but rather that a counting accelerometer be installed on each fighter type aircraft. This counting accelerometer would have windows at each integer n_z level or perhaps one-half g levels. Because of the effects that gross weight and configuration have on the amount of damage, the counts on the accelerometer would have to be read for each change in configuration and periodically for weight changes. It is suggested that the accelerometer be placed at the approximate center of gravity and that it be a series of electrical switches which close when a given n_z level is equalled or exceeded. These switches would be wired to an indexing register that would be in the form of printing wheels. The register could be located in any conveniently accessible place. The register would accumulate the exceedances. The pilot would activate the printer by a convenient switch whenever there was a change in the mission segment or configuration. This would include changes in wing sweep angle on swing wing aircraft. Time after takeoff could also be printed each time the printer was activated. This would allow one to calculate the gross weight. Figure 41 is a schematic of the system. The logic relay box would be required so that the counts at a particular load level would reflect only those peaks which resulted from a change in load level from some threshold to the maximum. In other words, an acceleration history that went from 1 g to 4 g to 6 g to 5 g to 6 g to 1 g would be recorded as only one 6 g count instead of two 6 g counts. The acceleration history would have to pass through the threshold between peaks before a second count would be added. The system depicted in the figure is primarily a mechanical one; however, with modern technology solid state devices and integrated circuits could be used for the logic and accumulating registers. The printer would most probably be one of the new thermal printers which do not use ink. It is roughly estimated that the accelerometer, logic circuitry, registers, and printer should be obtainable in large quantities for approximately $2500.00. The mission could be divided into three logical segments: 1) before weapon release, 2) during weapon release, 3) after weapon release, since most of the damaging cycles occur either shortly before weapon release, during weapon release, or shortly after weapon release. If more than one pass was made at the target, a printing could be made between passes so that one could account for the different weapon configuration. In fact, the weapon release switch with a time delay could also be used to activate the print mechanism. The segment print wheel could be used by the pilot to identify the aircraft configuration during the time the accelerations were being accumulated. Another print wheel could be added to identify which pylon still had stores, using the armament relay box. This would be an aid to the pilot in completing his post-flight comments. The output of the printer would be simply a listing of the exceedances at each n_z level and the time into the flight. A typical print-out would be similar to that depicted in Figure 42.

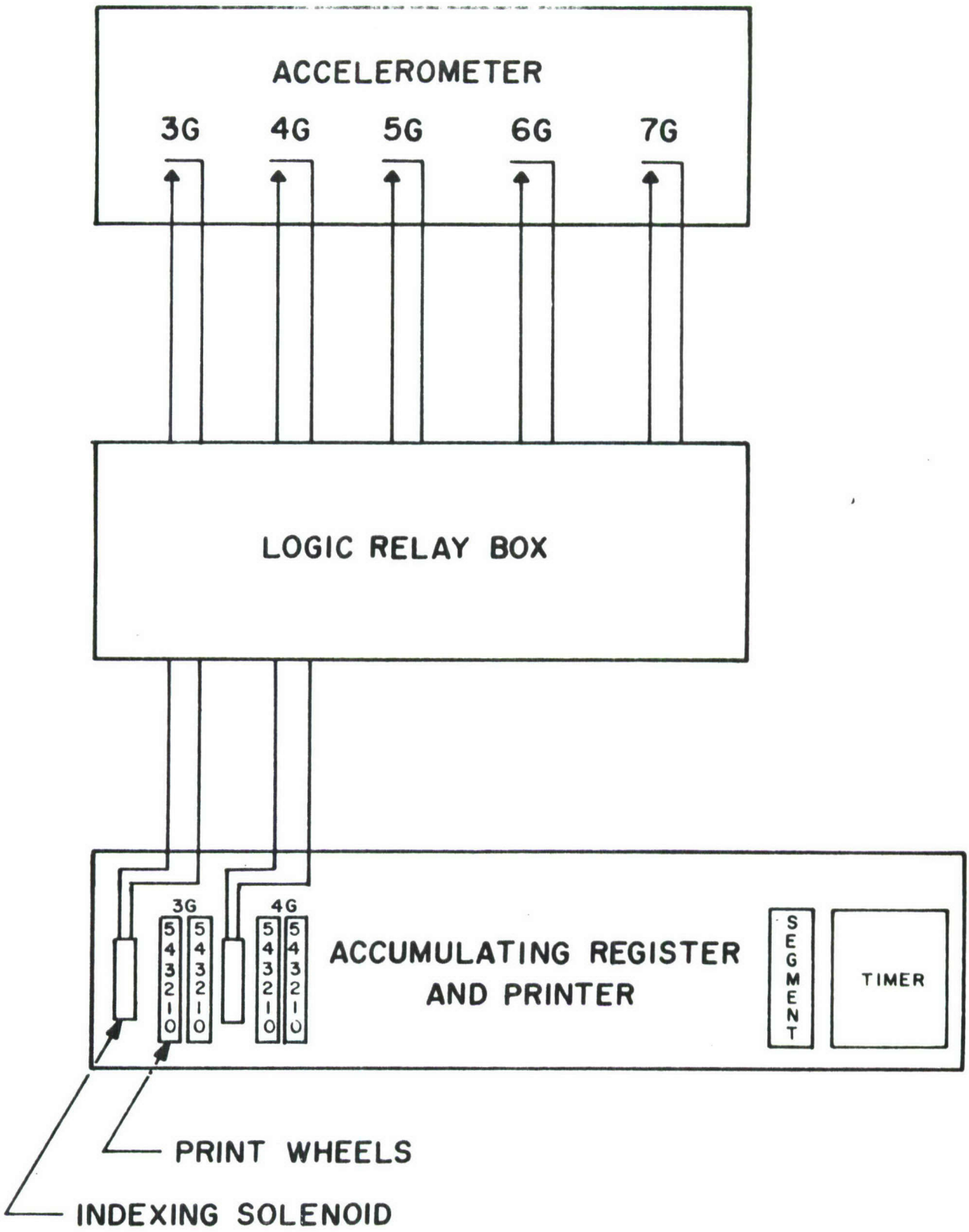

Figure 41 Schema of Recording Accelerometer

3G	4G	5G	6G	7G	Segment	Time	Pilot Comment (added after flight)
08	03	02	01	00	1	130	Beginning of Weapon run
10	04	03	02	00	2	131	After drop of 3000 lbs. from C. L. store
13	05	04	02	00	3	133	After drop of 1400 lbs. from O. B. store
23	06	04	02	00	4	145	Begin cruise back

Figure 42. Typical Print-Out of Accumulation Registers

To calculate the damage, the user of the parametric charts would select a graph similar to Figure 34 that matched the configuration and the mission segment (which fixes the Mach-altitude distribution). The user then finds the occurrences at each n_z level by subtracting the reading at the higher n_z level from the lower. For the data in Figure 42 he would obtain 5 occurrences of 3 g; 1 occurrence of 4 g; 1 occurrence of 5 g; and 1 occurrence of 6 g for the mission segment prior to weapon drop. From the time after takeoff, 1 hour and 30 minutes, he would calculate the gross weight. He would then enter the parametric chart at the proper gross weight and read the damage per occurrence of a particular n_z level and multiply by the number of occurrences at that level. Summing the damages for all n_z levels would then yield the damage during that mission segment. Next, the user would select the parametric chart that corresponded to the mission segment and configuration for a second line in Figure 42 and repeat the process, taking into account the reduction in weight due to stores released. However, this time he would have to subtract the exceedances of the first line from the second line before he could find the occurrences for the second configuration. Therefore, the exceedances for the second configuration would be: 2 at 3 g; 1 at 4 g; 1 at 5 g; and 1 at 6 g. The occurrences would then be: 1 occurrence at 3 g; 0 occurrence at 4 g; 0 occurrences at 5 g; and 1 occurrence at 6 g. This procedure could be simplified somewhat if the accumulation registers were returned to zero after each printing. The pilot's log would then contain only the takeoff gross weight and store configuration, the time and amount of fuel received for any in-flight refueling, the weight and location of stores released between print-outs.

b. Noncombat Mission Phases

Since it was determined for two fighter aircraft having high limit load factors that the ascent, cruise, descent, and refueling flight segments do negligible damage, these segments were not analyzed for consistency. However, if future data should show that a significant amount of damage

occurs during these segments, they could be handled the same as for bomber or cargo aircraft. It seems necessary to know the load levels actually experienced by each aircraft during the combat phase to perform a meaningful accounting of damage by aircraft serial number. Therefore, a printout of the counting accelerometer at the end of ascent, cruise, refueling, and descent could be used to calculate the damage for these segments.

The ground damage would be calculated and presented in the same manner as for the bomber or cargo aircraft.

c. Ground-Air-Ground

If a counting accelerometer is installed on each aircraft, the ground-air-ground damage should be calculated for each flight. The damage would be a function of the takeoff gross weight and configuration, the maximum load factor during flight, and the configuration and gross weight at the time of maximum load factor.

The parametric charts for manual usage would be a plot of damage vs. takeoff gross weight, with a family of curves for maximum load level. One chart would be required for each takeoff configuration combined with each airborne configuration and a number of weight ranges for the time of the maximum load factor.

If one uses the definition of the ground-air-ground cycle that states that the cycle is from the minimum ground stress to the maximum flight stress that occurred in that particular flight, the ground-air-ground damage would be about equal to the damage due to the pull-up after weapon release, since the maximum load factor usually occurs during pull-up. Using this definition the ground-air-ground damage at fuselage station 509 for the F-105D live combat data would then be about 44% of the total flight damage, with the pull-up after weapon release another 44%, and the other maneuvering in the target area the remaining 12%. If one used the definition of the maximum stress which is equalled or exceeded on the average of once per flight, then the maximum stress would be a result of a load factor of 4.5 for the F-105 combat data. Using the data in Figure 34 as an approximate value of the damage, the ground-air-ground damage would be 0.77×10^{-5} for a typical gross weight of 39,000 pounds. Adding this damage to that for fuselage station 509 on the F-105D for the first 51 weapon drops which involved 49 flights, the total damage for these 49 flights would be $0.001700378 + 49(0.77 \times 10^{-5})$ equalling 0.0020776. The ground-air-ground damage would be about 18% of the total flight damage. Obviously, by either definition the ground-air-ground damage is a significant part of the total, and therefore special care should be taken to identify it properly for each flight.

SECTION IV

FATIGUE DAMAGE CALCULATION TECHNIQUE

Detailed fatigue damage calculations must be performed prior to formulating parametric charts. In order to perform these calculations, S-N diagrams for the required fatigue critical points must be available. In this study the following assumptions were made:

(1) The fatigue critical components have been identified by a full scale fatigue test.

(2) Constant amplitude S-N curves have been established for each critical component through component fatigue tests.

(3) The life of each component has been established in the full scale fatigue test and has been shown to be consistent with the S-N curves (of item 2) through the cumulative damage procedure employed for the analysis.

(4) 1-g time stress, incremental stress as a function of load factor, $\bar{A}$, and N_o values are available for the flight or ground conditions as required.

1. AIRBORNE SEGMENTS

All of the computerized analyses that were reviewed are of a general nature and can be used for any aircraft and almost any input spectra. The input spectra is limited on some to a discrete spectra of maneuver load factors and a gust spectra of

$$T\,N(y) = N_o\,T\left[P_1 e^{-\Delta y/b_1\bar{A}} + P_2 e^{-\Delta y/b_2\bar{A}}\right] \qquad (17)$$

Other programs allow a variety of input spectra forms. All of the programs perform the same task; that is, from the input data, calculate two values of stress or stress ratios so that the life cycles (N) at that load level can be determined. They also, from the spectra of the environment, determine the number of occurrences of that load level and then sum n/N to determine the total damage for that flight condition. The main difference in the various programs is how they calculate the mean and alternating stress (or the max and min stress) or whatever two parameters are needed to enter the S-N tables to look up the life cycles. Some programs use calibration factors which are simply stress/c.g. acceleration, to find the change in stress due to maneuver load factor and a factor wnich is stress per ft/sec gust velocity to find

the change in stress due to a gust. Changes in stress due to gust are then multiplied by a dynamic magnification factor. Other programs use a power spectral density approach for gust. Assuming that the calibration factors with dynamic magnification factors yield the same stresses as the PSD approach, the various programs should give the same damage. Some of the programs have the capability of combining gust and maneuver peaks simultaneously while others consider the gust and maneuver as separate occurrences. The use of this technique must be preceded by an analysis of the spectral data that is used for the gust and maneuver loads. If one had an input spectrum that was true vertical gust velocity and pure maneuver loads, then perhaps he should consider the probability of these occurring simultaneously. If one is using recorded data from a flight loads program he must know the ground rules used to separate the gust and maneuver loads. Each flight loads program in the past has had its own particular definition of gust and maneuver loads. In some programs, if a gust occurred during a maneuver the editor of the flight record would decide if the load should be considered a gust or a maneuver. In either case, only one value would be added into the statistical sample and therefore the maneuver spectrum may have gust contributions and the gust spectrum may have maneuver contributions. If this type of data is used, then one should not consider the probability of a gust and maneuver load occurring simultaneously, since this effect is already included in the spectra. These precautions also apply to the collection of data for usage in the Appendix. Also, some computer programs have the capability of combining the positive and negative maneuver load occurrences until all the negative ones are accounted for and then use the remaining positive cycles as only positive changes in stress. A computerized study was made for a critical control point on the B-58, using two methods of combining the positive and negative maneuver cycles. It was found that combining positive and negative cycles of equal magnitude into one cycle and then adding the residual positive cycles predicted 6 times more damage than by taking the positive and negative cycles independently. It has been observed in studying flight recordings that there is little likelihood other than on a random basis that positive cycles will immediately preceed or follow negative cycles. The conclusion is, therefore, that the maneuver damage should be calculated by taking the positive and negative maneuver loads independently.

All of the programs which were reviewed have the capability of inputting a flight condition, which specifies the 1-g trim stress, using the change in stress per unit gust or unit maneuver load factor, and then calculating the change in stress for the gust or maneuver spectrum. The trim stress and the response parameters should include thermal effects, and if necessary, the cabin pressurization effects. Some programs require more calculations to prepare the input data than others, and some require more runs to completely calculate a flight segment, but all can handle any flight profile

by inputting the flight conditions in small increments.

The asymmetrical loading conditions present a greater problem of correlating asymmetric and symmetric maneuvers. If damage is to be calculated for asymmetric loading conditions (asymmetric maneuver and asymmetric gust), the greatest effort will be in determining the mean stress level of the control point, proportioning the number of cycles of asymmetric loading which occur simultaneously with other loading conditions, and determining the corresponding stress increments as a function of control surface settings for the control point and flight condition involved. Lateral gust loading must be applied for certain control points such as aft fuselage and vertical surfaces.

A multiplicity of flight conditions exist for most mission segments. In a sense, the basis of the parametric study is to vary the parameters and determine the sensitivity of the damage of the control point and mission segment involved with regard to these variations. In a similar vein, it is important to find parameters which can be eliminated without incurring an appreciable error and as a result reduce the complexity of the analysis.

In calculating damage for fighter aircraft the approach will be considerably different and might best be determined by utilizing a counting accelerometer, and then specifying average flight conditions for certain mission segments.

2. GROUND SEGMENTS

Ground damage will most generally occur due to independent application of the various input spectra discussed in Section II, 1. Most ground cycles will start from a mean stress level dependent on control point, mass distribution, and ground reactions. For each choice of input spectra and the associated parameters which affect it, combined with the response and the parameters which affect it, the damage for various control points can be calculated. In other words, the response for each critical control point and attendant damage should be calculated for each ground environmental segment by fixing the aircraft dependent parameters and by varying the independent parameters discussed in Sections II and III in a controlled process.

3. GROUND-AIR-GROUND

Ground-air-ground damage calculations have been discussed in Section II, 2g and Section III, 2k. Computer programs have already been written which consider the two procedures of References 9 and 19. The major requirements of both procedures are:

(1) Designate a sufficient number of mission profiles to be representative of mission usage.

(2) Break down each mission profile into mission segments (i. e., climb, cruise, etc.). Further, break down the mission segments into divisions of Mach number and altitude and designate appropriate time increments according to gross weight variation.

(3) Apply the appropriate input spectra for a number of flights, say 1000. Calculate the number of occurrences of maximum cyclic stress at various flight stress levels in the 1000 flights for the control point involved. Calculate the number of minimum cyclic stress occurrences at the various ground stress levels in the 1000 flights for the same control point.

(4) A table of maximum stress levels vs. occurrences and minimum stress levels vs. occurrences for 1000 flights will provide the data necessary for ground-air-ground damage calculation. The use of this data will be different, depending on which of the two procedures is applied.

The major variables in either of the procedures are the mission profile and the initial gross weight.

SECTION V

PARAMETRIC DAMAGE CHARTS

1. GENERAL DISCUSSION

Due to the possible variation of both the input spectra and the response parameters from one flight to another for flights which have basically the same overall mission, it is believed that generally the flight should be divided into segments. These segments would be taxi, take-off, climb, cruise, in-flight refueling, low altitude penetration, weapon delivery or cargo drop, descent, landing, and the ground-air-ground cycle. Additional non flying segments would be ground handling and maintenance loadings and perhaps dry runs of store loadings.

One of the objectives of this study was to optimize the ease and convenience of using the parametric study for manual calculations of damage as well as to minimize the pilot log information without loss of accuracy. This section is presented as a summary of the optimum formats.

The following tables and charts are based on the parametric effects observed on the aircraft studied in this program. The various formats, assumptions, and calculations are not to be considered as the sole criteria for future parametric presentations, but rather as guidelines. Each model of aircraft will probably have unique characteristics inherent to its design such as (a) location of critical control points, (b) operational procedures and usage, and (c) aerodynamic design features, for instance, wing tip stall which will require additional parameters or breakdowns. In order to reduce the number of charts and/or tables, detailed studies must be made in a controlled manner before any potential parameter be classified as causing negligible damage for the control point involved. In the presentation of the charts and procedures, the following nomenclature is loosely used:

The heading and notes on each chart must contain all restrictions that apply to its usage.

Mission Segment and Type - includes not only the type of mission segment, such as ascent, cruise, etc., but also type of overall mission, i.e., training, operational, live combat zone, etc. It also includes operational procedures such as full power take-off, minimum internal take-off, etc.

Configuration - when this term is listed on a chart it designates that a specific external stores arrangement, wing sweep settings, cargo weight distribution exists.

Fuel Sequence - when this term is used it means that the fuel usage sequence is such that the fuel distribution for a given cargo weight is a function of the gross weight. The damage for various control points should be calculated using a predetermined fuel sequence procedure for that mission segment. If optional plans are provided each should be investigated and additional charts included whenever necessary. [For the situation where fuel sequencing cannot be pre-assigned, methods similar to that shown in Section III, 2 d must be used.]

Bending Moment - it is suggested in several places that bending moment be used instead of weight distribution. The bending moment referred to is the moment due to fuel or cargo distribution that causes the damage to be different than if a standard fuel sequence or cargo distribution were used. The bending moment would be for the 1-g condition.

Consideration as to the type of technical qualifications of the personnel required to perform the calculations was necessary in order to develop an optimum method of presenting the format. For a fleet-wide accounting of the fatigue damage for each flight by aircraft serial number, two methods are possible: (1) a central data processing center where the pilot log information would be used as input and a computer used to look up and sum the damage for each segment, and (2) Air Force personnel at each base would use the pilot log information with charts and look up the damage, then sum the damage for each segment. A second use of the parametric study would be for use of mission planners to estimate the effect of one mission profile relative to another.

The results of the format tests given to both fourth year engineering students and first year non-science students indicate that for large volumes of calculations, tabular formats are preferred to graphical formats. It was also found that correction factors cause additional errors unless the factor is simply a constant that relates the damage at one condition or configuration to another. Correction factors which are functions of velocity, altitude, or center of gravity position require excessive time to use, therefore additional charts for these combinations should be added. It was also determined that in the interest of speed and prevention of personnel fatigue, interpolation within tabular formats should not be required, but rather sufficient entries be made in the tables so that the nearest value could be used.

Because mission planners want to see the overall picture at a glance, it is preferred that graphic formats be made available to them.

Because computer solutions would be basically table look-up procedures, it is also preferred that the charts for manual solutions be tabular so that conversion to computers would be simpler. If computer solutions are used, the tables would not have to be as detailed or numerous because

interpolation and correction factors could be used without loss of accuracy or little increase in running time.

The cost of generating both graphic and tabular formats may dictate that only one be used for both the flight-by-flight calculations and mission planning. Therefore the following presentation shall apply to both.

2. BOMBER AIRCRAFT OR CARGO AIRCRAFT

The following charts and procedures apply to bomber and cargo aircraft.

a. Ascent

The format, either graphic or tabular, would be as follows:

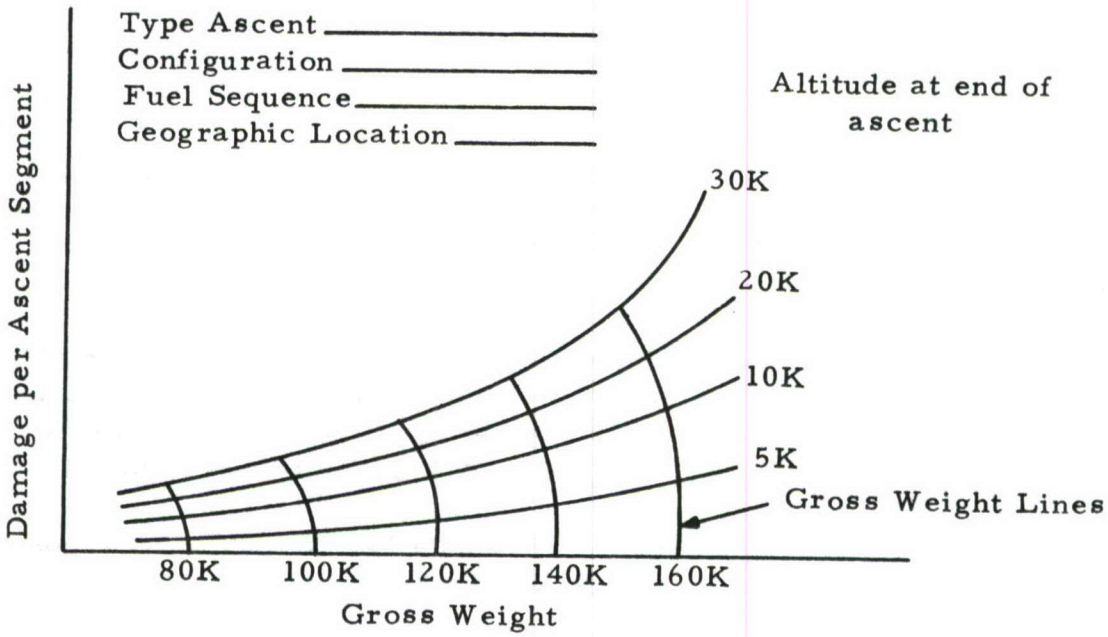

To construct this chart the following assumptions and calculations are required:

Assumptions:

(a) That the aircraft has a standard ascent profile which is a function of gross weight only. Therefore, altitude, velocity, gross weight time histories are known as a function of take-off gross weight.

Calculations:

(a) From flight test data or operational procedures determine altitude, velocity, gross weight time histories.

(b) Choose a number of altitude intervals, e.g., 0-1000, 1000-2000, 2000-5000, etc.

(c) Determine average altitude, velocity, gross weight for each altitude interval; determine incremental time for each altitude interval.

(d) At each average altitude, calculate the response parameters i.e., 1-g trim stress, Δ stress/Δ g, $\bar{A}$, N_o. (These are functions of altitude, velocity, gross weight.)

(e) Using the response parameters and the gust and maneuver spectrum for each average altitude, calculate a damage rate.

(f) For each average altitude, multiply damage rate by the appropriate time interval.

(g) Sum damage for each successive altitude, plot graph.

How to use format:

(a) For initial ascent.

Enter chart at takeoff gross weight; follow gross weight line up to altitude at end of ascent; read total damage for ascent mission segment.

(b) For changes in altitudes during mission.

Enter chart at lower altitude and at the gross weight for the beginning of the ascent. Follow gross weight line to higher altitude. The difference in the damage at the higher and lower altitude is the damage for a mid-mission segment.

NOTES: Calculations would have to be made for each control point and each aircraft configuration and fuel sequence.

After the charts are drawn, comparison of the charts for fuel sequence or configuration may show that some of them are proportional to others so that not all charts need be presented in the parametric study but only correction factors for certain configurations.

At the request of the Air Force, additional ascent profiles could be added, such as full power takeoff.

Pilot log information required:

(a) Takeoff gross weight.

(b) Fuel sequence.

(c) Cargo or weapon configuration.

(d) Initial and final altitude of ascent.

(e) Geographical location. This would be required if the spectrum of the environment is significantly different.

(f) Type of mission (pilot training, operational, etc.)

b. Cruise

The format, either graphic or tabular, will be as follows:

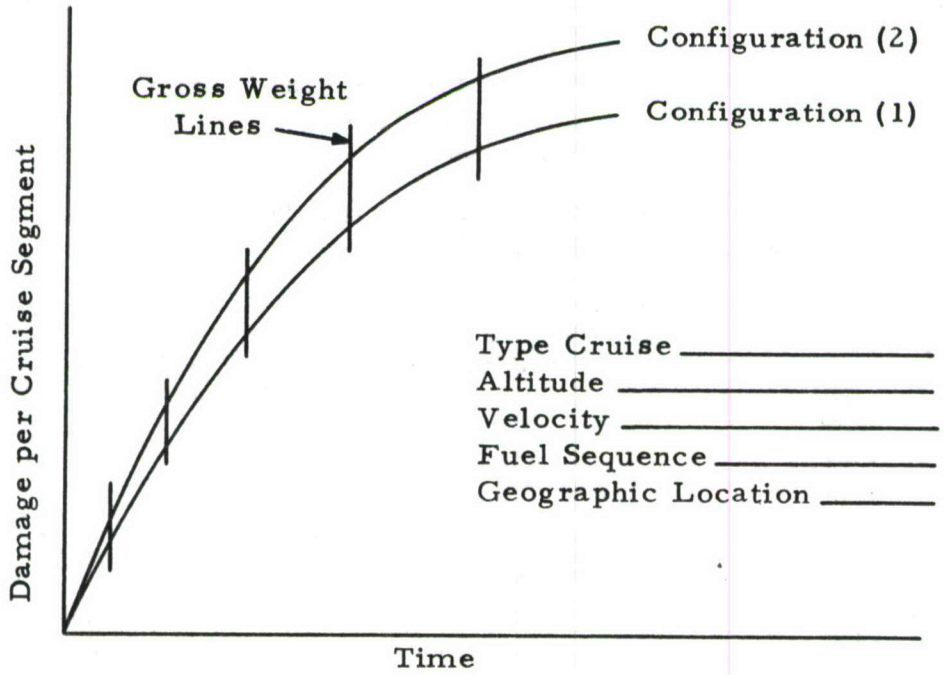

To construct this chart the following assumptions and calculations are required:

Assumptions:

(a) That the aircraft will cruise at constant altitude and velocity.

(b) That the fuel flow will be a predetermined function of the altitude, velocity, and instantaneous gross weight.

(c) That the c. g. variation either has an insignificant effect on damage or is a function only of gross weight for a given fuel sequence.

Calculations:

(a) From flight test data, determine fuel flow rates vs. gross weight for each configuration at the required altitudes and velocities.

(b) Starting with the maximum flying weight and going to the minimum flying weight for the given configuration divide the cruise into a number of small increments where the damage rate is assumed to be constant for each increment. Determine incremental time, ΔT.

(c) Determine the average gross weight and c.g. location for each increment.

(d) At each average gross weight and c.g. location, calculate the response parameters (1-g trim stress, Δ stress/Δg, $\bar{A}$, and N_o).

(e) Using the response parameters and the gust and maneuver spectrum for that altitude, gross weight, and c.g. location calculate the damage rate.

(f) For each increment, multiply the damage rate by ΔT to obtain the damage during each increment.

(g) Sum the damage for each successive increment and plot graph.

(h) See Section III, paragraph 2 d, for discussion of center of gravity effects.

How to use format:

(a) Enter graph at the gross weight at the beginning of the cruise segment. Read damage and time.
NOTE: The damage used is that which would have occurred had the cruise begun at the maximum gross weight.

(b) Add duration of cruise to time read in (a).

(c) At time equal to time from (b) read damage
NOTE: This is the damage which would have occurred had the cruise begun at maximum gross weight.

(d) Subtract damage (a) from damage (c); difference is the damage during this cruise.

NOTES: There would be one chart for each control point, fuel sequence, altitude velocity combination.

After the graphs are constructed it may be observed that some of them are proportional to each other so that only one graph need be presented in the parametric study and a correction factor used for the other conditions. For certain locations on cargo aircraft, one could use bending moment due to cargo and fuel weight distribution instead of configuration.

Pilot log information required:

(a) Gross weight at beginning of cruise.

(b) Velocity.

(c) Altitude.

(d) Duration of cruise at constant altitude and velocity.

(e) Configuration and fuel sequence.

(f) Geographic location if environment is different.

(g) Fuel distribution and/or c. g. location periodically during cruise. (only required if fuel distribution and c. g. location are unpredictable from the gross weight and if the damage varies significantly with these parameters)

c. Descent

The format, either graphic or tabular, would be as follows:

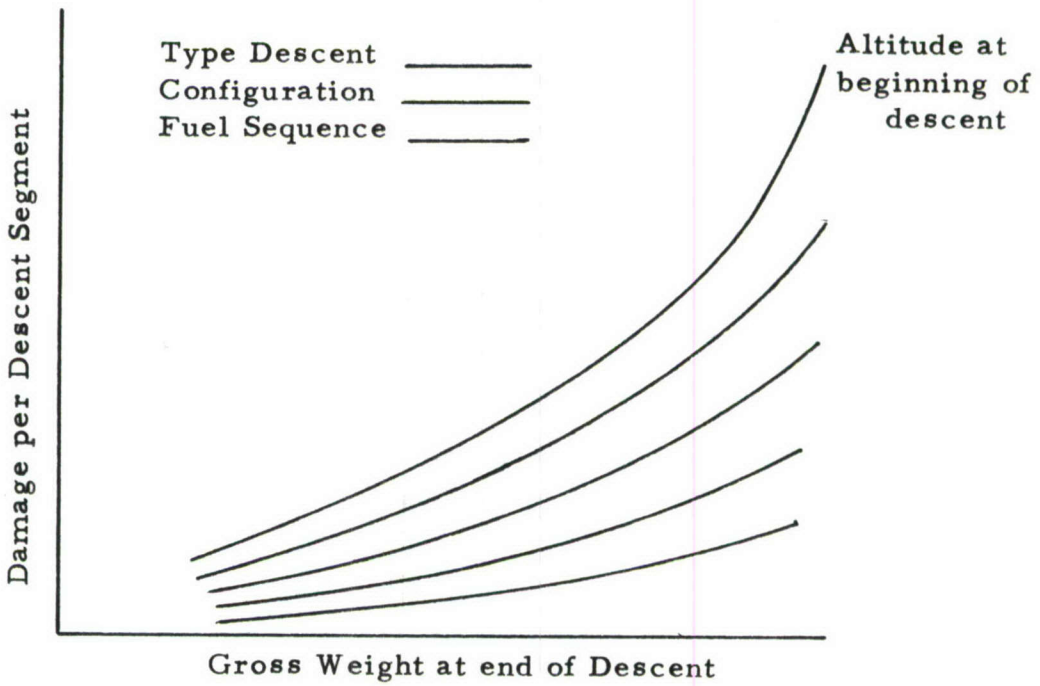

To construct this chart the following assumptions and calculations are required:

Assumptions:

(a) That the aircraft has a standard descent profile.

(b) That the fuel used during descent is insignificant.

Calculations:

(a) From flight test data or operational procedures, determine altitude and velocity vs. time curve.

(b) Select a number of altitude intervals, e.g., 0-1000, 1000-2000, 2000-5000, etc.

(c) Determine average altitude and velocity for each altitude interval. Determine time increment for each altitude interval.

(d) At each average altitude, calculate the response parameters for a selected number of gross weights.
NOTE: Gross weight would be constant for a given descent.

(e) Using the response parameters and the gust and maneuver spectrum, calculate the damage rate at each average altitude.

(f) For each altitude interval, multiply the damage rate by the ΔT.

(g) Sum the damage for each successive altitude from sea level to maximum altitude and plot graph.

How to use format:

(a) For descent to sea level.

Enter chart at gross weight at end of descent; follow a constant gross weight line to the altitude curve which corresponds to the altitude at the beginning of the descent; read damage for descent.

(b) For changes in altitudes during mission.

Use difference in damage between altitudes for gross weight at end of descent.

NOTE: Calculations would have to be made for each control point and aircraft configuration. It may or may not be necessary to consider fuel sequences.

Pilot log information required:

(a) Altitude at beginning of descent.

(b) Gross weight at end of descent.

(c) Aircraft configuration.

(d) Fuel sequence.

d. Landing Impact

The format would be a table of damage per landing vs. gross weight as follows:

Fuel Configuration _____

Aircraft Configuration _____

Touch Down Gross Weight	Control Point							
	1	2	3	4	5	6	7	8
80,000								
100,000								
120,000								
140,000								

To construct this chart the following assumptions and calculations are required:

Assumptions:

(a) That the aircraft lands on the main gear only.

(b) That the runway is flat and smooth at the point of touch down.

Calculations:

(a) From flight test data, determine a spectrum of sinking speeds.

(b) Determine the response of the aircraft. This could be c.g. load factor or load in main strut vs. sinking speed.

(c) Determine the dynamics of the aircraft, i.e., the number of cycles of response for each landing and their relative amplitude. Determine stress at each control point for the parameters of (b).

(d) Using the sinking speed spectrum and the response parameters, calculate the average damage per landing.

(e) Construct table.

How to use format:

Enter table at the touch-down gross weight read damage for control point of interest.

NOTE: There would be one chart for each aircraft configuration. It may be necessary to consider different fuel configurations.

When the aircraft sets down on the main gear, the various parts of the structure act like cantilever beams. Thus, it may be necessary to work in terms of bending moment at the control points rather than gross weight if the weight distribution can vary for a given gross weight.

Pilot log information required:

(a) Touch-down weight.

(b) Aircraft configuration.

(d) Perhaps weight distribution.

e. Taxi - Takeoff

The format would be a table of damage per taxi-takeoff vs. gross weight as follows:

Type Takeoff _____

Fuel Configuration _____

Aircraft Configuration _____

Air Base _____

Gross Weight At Ramp	Control Point							
	1	2	3	4	5	6	7	8
180,000								
160,000								
140,000								
120,000								

To construct the chart, the following assumptions and calculations are required:

Assumptions:

(a) That the taxi distance and speed and the number of left and right turns would be a constant for a given air base.

(b) That the takeoff-run speed versus distance and the takeoff distance are a function of gross weight only.

Calculations:

(a) Determine the spectrum of taxiway and runway roughness for

each airbase or determine an average spectrum of roughness for a number of air bases. Rough field would be classified by types and then considered just as other air bases.

(b) Determine aircraft response to roughness as functions of gross weight, configuration and velocity. The 1-g bending moment may be used in place of gross weight at some control points.

(c) Using response parameters and roughness spectrum, calculate damage.

(d) Construct table.

How to use format:

(a) Enter chart at ramp gross weight or 1-g bending moment, read damage for control point of interest. This damage would be the total damage for the taxi and the take-off run.

NOTES: There would be a separate chart for each configuration and each group of air bases where the spectrum or distance taxied varied significantly. There could also be a separate chart for minimum interval take-off.

Pilot log information required:

(a) Ramp weight.

(b) Air base.

(c) Aircraft configuration or weight distribution.

f. Landing - Rollout - Taxi

The format would be a table of damage per landing-rollout-taxi vs. gross weight as follows:

Air Base _____

Aircraft Configuration _____

Fuel Configuration _____

Touch Down Gross Weight	Control Point							
	1	2	3	4	5	6	7	8
80,000								
100,000								
120,000								
140,000								

To construct this chart the following assumptions and calculations are required:

Assumptions:

(a) That the roll out velocity versus distance is only a function of gross weight.

(b) That the first part of the landing would be a two wheel roll and then at a predetermined time it would become a three wheel roll.

(c) That the taxi distance, speed, and the number of left and right turns would be a constant for a given air base.

Calculations:

(a) Determine the spectrum of taxiway and runway roughness, braking and turning loads.

(b) Determine the aircraft response to roughness as a function of gross weight, configuration, and velocity. This should be done for both a two wheel and a three wheel roll. Also the primary and secondary cycles when the nose wheel is set down should be determined.

(c) Using the response parameters and the roughness, calculate damage.

(d) Construct table.

How to use format:

(a) Enter chart at touch-down gross weight and read damage.

NOTES: There would be a separate chart for each aircraft configuration and air base or group of air bases. Also, some control points may be better handled by the use of 1-g bending moment rather than gross weight. The 1-g bending moment listed in the table would be that due to the fuel and cargo only, since the moment due to the structural weight is a constant. If any form of arresting gear such as drag chutes are used, additional charts may be required.

Pilot log information required:

(a) Touch-down gross weight.

(b) Air base.

(c) Aircraft configuration or weight distribution.

g. In-Flight Refueling

The format, either graphic or tabular, would be as follows:

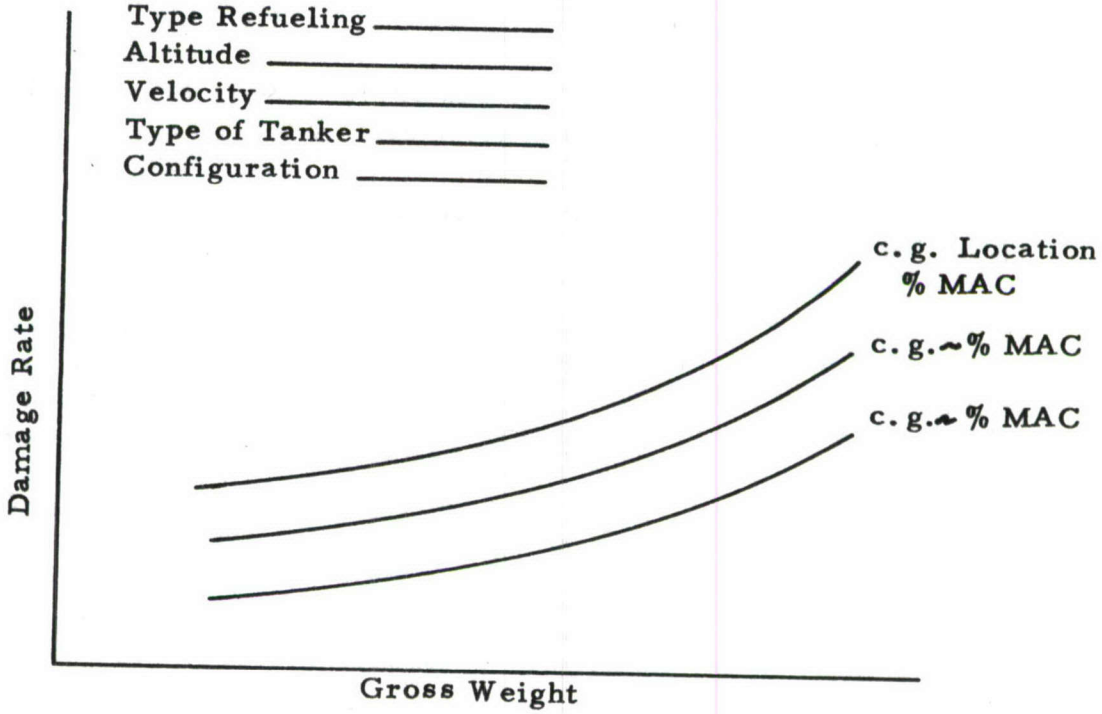

To construct the chart the following assumptions and calculations are required:

Assumptions:

(a) That refueling would occur at constant altitude and velocity.

(b) That fuel was being transferred at a constant rate during the hook up.

Calculations:

(a) From flight test data, determine the spectrum of gust and maneuver loading for refueling.

(b) Determine the response parameters, i.e., 1-g stress, Δ stress/Δg, $\bar{A}$ and N_o for each altitude, velocity, gross weight, aircraft configuration, and c.g. location.

(c) Using response and environmental parameters, calculate damage rates for a selected range of gross weight and c.g. locations.

(d) Plot curves.

How to use format:

(a) Enter chart at the gross weight before fuel transfer; go to proper c.g. curve; read damage rate.

(b) Enter chart at the gross weight after fuel transfer; go to the proper c.g. curve; read damage rate.

(c) Calculate average damage rate.

(d) Multiply average damage rate by duration of hook up.

(e) Answer in (d) is damage for refueling.

NOTE: There would be one chart for each control point, altitude velocity, type of tanker, and aircraft configuration.

If fuel was not transferred continuously during the hookup then the refueling should be divided into more than one segment. One segment would be for fuel being transferred, and the other segment would use the same procedure and charts but the change in gross weight would be that due to fuel usage.

Pilot log information required:

(a) Altitude.

(b) Velocity.

(c) Gross weight and cg location at beginning of refueling.

(d) Gross weight and cg location at end of refueling.

(e) Duration of refueling in minutes.

(f) Aircraft configuration (including flap position and autopilot).

h. Low Level Penetration Or Airdrop

The format, either graphic or tabular, would be as follows:

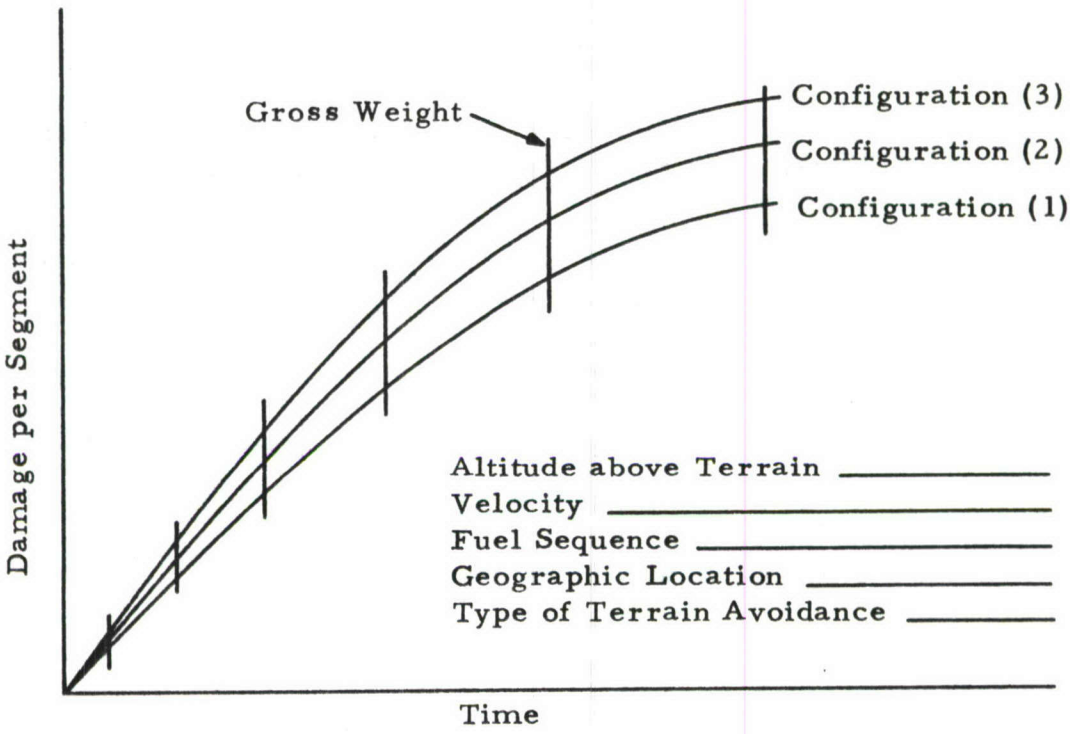

To construct the chart, the following assumptions and calculations are required:

Assumptions:

(a) That the aircraft will fly at constant altitude and velocity. For terrain following type avoidance, an average altitude would be used.

(b) That the fuel flow will be a predetermined function of altitude, velocity, and instantaneous gross weight.

(c) That the cg variation will be a function of fuel sequence and gross weight.

Calculations:

(a) From flight test data, determine fuel flow rate versus gross weight for each configuration at the required velocity and altitude.

(b) Also from flight test data, determine a gust and maneuver environmental spectrum. There would be an average spectrum for each geographic area. If data is available these spectra may also be related to the time of day.

(c) Starting with the maximum allowable weight and proceeding to the minimum weight for the given configuration, divide the low level segment into a number of small increments where the

damage rate is assumed to be a constant. Determine incremental time, ΔT.

(d) Determine the average gross weight and c.g. location for each increment.

(e) At each average gross weight and c.g. location, calculate the response parameters (1-g trim stress, Δ stress/Δg, $\bar{A}$, and N_o).

(f) Using the response parameters and the gust and maneuver spectrum for that altitude, gross weight and c.g. location, calculate the damage rate for each time increment.

(g) Multiply the damage rate for each increment by ΔT.

(h) Sum the damage for each successive segment and plot graph.

How to use format:

This is the same format as cruise.

(a) Enter graph at the gross weight at the beginning of the low-level run. Read damage and time.

(b) Add duration of run to time read in (a).

(c) At time equal to time from (b), read damage.

(d) Subtract damage (a) from damage (c), the difference is the damage for this segment.

NOTE: There would be one chart for each change in altitude-velocity combination, fuel sequence, geographic location, and type of terrain avoidance. For flights which had an off-load of cargo or a weapon drop, the damage would be obtained by using one configuration up to the time of the drop, and then use another configuration with the proper gross weight for the remainder of the segment. For certain control points on cargo type aircraft, bending moment may be more appropriate than aircraft configuration.

Pilot log information required:

(a) Gross weight at beginning of penetration.

(b) Velocity.

(c) Altitude above terrain.

(d) Type of terrain avoidance.

(e) Duration of flight at each configuration.

(f) Predrop and postdrop configuration.

(g) Fuel sequence.

(h) Geographic location.

i. Practice Landing

The format would be a table of damage per landing vs. gross weight as follows:

Type of Landing _____

Air Base _____

Configuration _____

Gross Weight at Lift Off	Control Point							
	1	2	3	4	5	6	7	8
80,000								
100,000								
120,000								
140,000								
160,000								

To construct this chart the following assumptions and calculations are required:

Assumptions:

(a) That practice landings will be either full stop or touch-and-go.

(b) That for the type of landing the flight pattern will be constant i.e., the altitude and velocity history of the go-around will be the same for each round trip. This may vary with air base.

(c) That the taxi-back distance and velocity will be a constant for a given air base.

Calculations:

(a) Determine the spectrum of runway and taxiway roughness, the gust and maneuver spectra for the go-around altitude.

(b) Determine the response parameters for both the ground and airborne segments.

(c) Define the time history of the total cycle, i.e., the velocity history for both the ground and in-flight phases and the altitude history of the go-around segment.

(d) Calculate a gross weight time history for a complete cycle for a number of lift-off gross weights.

(e) Divide the go-around segments into smaller segments during which the damage rate will be assumed constant.

(f) For each lift-off gross weight, calculate the damage for each of the following segments:
  (1) Take-off damage due to runway roughness during the take-off run.
  (2) Gust and maneuver damage during the go-around.
  (3) Landing impact damage.
  (4) Roll out damage up to the time where take-off power is applied.
  (5) A ground-air-ground cycle.

(g) Sum the damage for each segment in (f).

(h) Fill in table.

NOTES: The value in the table will be the total damage for a complete cycle of practice landing and therefore will be the sum of the ground and in-flight damage plus the ground-air-ground cycle.

The items listed in (f) are for a touch-and-go landing. For a full stop landing, item (4) would be extended to a full stop. A taxi back segment would be added for taxi from the down wind to the up wind end of the runway.

How to use format:

(a) Enter table at lift off gross weight and read damage.

NOTE: There would be one table for each aircraft configuration and air base where the pattern is significantly different. There would also be one table for full stop landings and one for touch-and-go landings.

Pilot log information required:

(a) Gross weight at lift off.

(b) Type of landing.

(c) Air base.

(d) Aircraft configuration, including fuel sequence and distribution.

j. Ground-Air-Ground

The format, either graphic or tabular, would be as shown in Figure 31. The assumptions, method of construction, and usage are presented in Section III.

k. Maintenance Cycles

The format for this damage would be a listing of events that could occur and the corresponding fatigue damage.

3. FIGHTER AIRCRAFT

The parametric formats for fighter aircraft would be different from those for bombers if a counting accelerometer is installed in each fighter aircraft. The format would be as shown in Figure 34 and described in Section III, 3 a. There would be a chart required for each mission segment that had a significant damage and also for each aircraft configuration. The mission segments would be defined by the probability of the Mach-altitude being consistent. For example, if the cruise segment is found to be damaging, then a chart for cruise would be presented for a number of Mach-altitude combinations. A different chart would be required for passes at the target and maneuvering in the target area, since the Mach-altitude conditions are different for these two segments.

If a counting accelerometer is not installed, formats for the ground damage, ascent, cruise, and descent would be the same as for bombers or cargo aircraft; however, the combat phase should be divided into two segments: (1) a maneuvering segment in the target area, and (2) a segment for weapon releases or passes at the target. The segment damage for maneuvering in the target area would be presented as a function of time similar to the low-level penetration or air drop format shown in paragraph 2 h of this section. The damages presented should be for a weighted Mach-altitude condition based on statistical data. In order to use the chart, at least two time increments would be required, one from the end of cruise out to the beginning of the passes at the target, and another from the end of passes at the target to the beginning of cruise back. Additional discussion of this segment is presented in Section III, 3 a. The segment damage for passes at the target should be a function of the number of passes or simply damage per pass vs. gross weight for each configuration.

If counting accelerometers are not used, the pilot's log would have to contain the time spent in each segment and the time of store release. A convenient means of automating this type of log could be an inexpensive tape recorder that ran only when the talk key was activated. The pilot could describe the flight as it progressed and after landing transcribe the tape

onto a log sheet.

Even if counting accelerometers with printing wheels were installed, the tape recorder could be used to identify the flight conditions and aircraft configuration at the time a printing was made.

SECTION VI

FORMAT FOR DAMAGE CHARTS

The results of a parametric fatigue analysis can be arranged in many different formats. From the studies conducted it was determined that the tabular format would be the most feasible for manual calculation of fatigue damage on a flight-by-flight basis. It was chosen because it proved easier, quicker, and less fatiguing to use. For flight planners, the graphical format would be best because it permits a readily seen relationship between the various parameters and fatigue damage. Nomograms have the disadvantage that generally a mathematic relationship would have to be developed between the variables, thus making construction difficult. Also, it is generally believed that excessive time would be required to use multivariable nomograms.

1. FORMAT ACCURACY

Tabular formats generated by computers will be as accurate as a detailed fatigue analysis when a sufficient number of entries are used. However, too many entries are impractical because of the large volume that would be introduced. In order to eliminate interpolation and maintain a consistent degree of accuracy, tabular formats could be constructed, using equal increments of damage. This can be accomplished by considering the damage as the independent variable; assigning values of damage in equal increments; then determining the corresponding values of the parameter(s) involved. An example is shown in Table XVII, where damage is expressed as a function of a single variable. The difference between using equal increments of the parameter (gross weight) and equal increments of the damage is shown as Methods 1 and 2 of Table XVII.

TABLE XVII

Comparison of Two Different Types of Typical Tabular Formats

METHOD 1		METHOD 2	
Gross Weight ($\times 10^3$ lbs.)	Damage ($\times 10^5$)	Gross Weight ($\times 10^3$ lbs.)	Damage ($\times 10^5$)
...-160.0	0	...-160.0	0
160.0-162.0	.010	160.0-164.3	.05
162.0-164.0	.055	164.3-167.1	.10
164.0-166.0	.085	167.1-168.6	.15
166.0-168.0	.125	168.6-169.6	.20
168.0-170.0	.190		

Using the fatigue damage format of Method 2 as compared to Method 1 would have the advantages of : (1) increased accuracy for a given number of entries, and (2) provides easier numbers to work with, i.e., less significant figures. However, this method is not compatible with the present computer programs.

The graphical format accuracy is dependent on: (a) the number of curves representing various values of the parameters, (b) the maximum and minimum independent and dependent variables, (c) the size of graph paper and border, (d) the size of grid, (e) the number of points used in construction, (f) the goodness of fit, and (g) the degree of curvature. Reasonable accuracy could be obtained with: (a) enough curves to minimize visual interpolation, (b) curves covering most of the page, (c) 8 1/2 x 11 graph paper, (d) 10 x 10 to the centimeter grid, and (e) appropriate number of points to draw a good curve. When more curves are needed to minimize visual interpolation, they could be approximated from the curves already drawn from the computer runs. If 10 x 10 to the centimeter grid is used, interpolation between two increments would be eliminated when possible by choosing the nearest line. This would speed up the time necessary to read the graphs without appreciable loss in accuracy. When 10 x 10 to the centimeter grid is used on 8 1/2 x 11 paper, using the nearest grid line would give better than 1% accuracy at the full scale value. Both the tabular and graphical formats can be made sufficiently accurate if the volume is large enough. Format volume is discussed below.

2. VOLUME AND COST OF GENERATING THE CHARTS

For a complete parametric study of bomber and cargo aircraft, it is estimated that the following number of computer runs would be required. The total runs for a mission segment is the product of the parameters.

		Total
Ascent		
Take-off Gross Weight	10	
Fuel Configuration	3	
Cargo or Weapon Configuration	3	90
Cruise		
Altitude	5	
Velocity	4	
Fuel Configuration	3	
Cargo or Weapon Configuration	3	180
Descent		
Landing Gross Weight	10	
Fuel Configuration	3	
Cargo or Weapon Configuration	3	90

		Total
Landing Impact		
Gross Weight	10	
Fuel Configuration	3	
Cargo or Weapon Configuration	3	90
Taxi and Take off		
Gross Weight	10	
Cargo or Weapon Configuration	3	30
Taxi Landing		
Gross Weight	10	
Fuel Configuration	3	
Cargo or Weapon Configuration	3	90
In-Flight Refueling		
Altitude	3	
Velocity	2	
Control Surface Position (flaps, etc.)	2	
Auto-Pilot On or Off	2	24
Low-Level Penetration or Air Drop		
Velocity	4	
Altitude Above Terrain	4	
Type of Terrain Avoidance	2	
Configuration	3	
Control Surface Position (flaps, etc.)	2	192
Practice Landing		
Type of Landing	2	
Gross Weight	10	20
Ground-Air-Ground		
Gross Weight	10	
Mission Type	6	60
Total Number of Computer Runs		866

These 866 computer runs represent the estimated total number of flight segments to be analyzed. Within each of these segments it would be necessary to calculate the damage rate as some of the parameters varied;

that is, for ascent one would have to vary the gross weight and altitude with time within the segment but this would be only one computer run. The above number of computer runs is for one control point; if one were to calculate the damage for 10 control points; then 8,660 runs would be required. Using the computer program provided in Reference 9 requires about 30 seconds to calculate the damage for one segment, using the IBM 7094. Therefore, for a complete analysis it would require about 72 hours of computer time. Using the reference run capability of the program, it is estimated that 1 hour would be required to prepare the input cards for each run, or a total of about 8,660 manhours.

When the damages are computed, the print out may be so designated that it would be in an appropriate form to use as a tabular format, or the print out may be rearranged and recopied into a more suitable form. If the print out is in too large of increments for accurate usage without interpolating the tables, some means of decreasing the block size must be devised. An interpolation process could be included in the program or a separate program could be written.

For the graphical format the gross weight, being a parameter, can be taken out of the above tables and the number of initial graphs would be reduced. It would then equal the sum of the products of the above segments, or 443 graphs, per control point. At 30 minutes construction time per graph 10 control points would require 2,215 manhours. Therefore the total cost of calculating the damages and plotting the initial graphs would be 72 hours of computer time and about 11,000 manhours. It should be pointed out that 26% of these 11,000 manhours is for the low-level penetration or air drop.

Since several of the conditions in the above listing could be plotted on one graph; since some of the conditions will be directly proportional to another conditions; and since some control points will have negligible damage for given segments; the number of pages actually presented in the parametric damage charts would be greatly reduced from the 4,430 initial graphs. The C-135 parametric study (Reference 19) has 110 pages for 7 control points, but it does not have any low-level penetration charts. If 10 control points had been used and low-level included (43% of the initial graphs would be for low-level), it is estimated that the total number of charts would then be $110 \times 10/7 \times 1.43 = 225$. However, half of the low-level conditions should be linear factors of the other conditions so that the estimated total number of charts would be 191 pages.

The volume required for the tabular format when eliminating interpolation is dependent upon: (a) the number of critical points, (b) the number of flight segments, (c) the number of parameters, and (d) the number of entries for each parameter. If one were to convert the C-135 parametric analysis, which is in graphical form, into tabular form using Method 2 with

with damage increments of 0.05×10^{-5} for critical points B1, H1, and V1, and increments of 0.1×10^{-5} for critical points W1, W2, W3, and W4, the resulting format would be large but not impractical. These increments would be sufficiently accurate when one considers that the damage for a typical 5-hour flight with a cruise altitude of 35,000 feet is of the order of 3×10^{-5} for critical points B1, H1, and V1, and 6×10^{-5} for points W1, W2, W3, and W4. Also, when one considers a fleet-wide application it may be justifiable to accumulate the damage for only three or four control points instead of seven, thus reducing the volume.

3. TESTS TO DETERMINE FORMAT PREFERENCE

A study was conducted using graphical and tabular formats. The study consisted of six tests given to various college students to determine the effect of background on the accuracy and time required to utilize the formats. Visual interpolation was required for the graphical format, while no interpolation was required for the tabular format. A summary of these tests is shown in Figure 43.

Nineteen juniors and seniors majoring in engineering took part in the first battery of tests which consisted of two tests using a graphical format and one test using a tabular format. The graphical format tests consisted of the necessary graphs (Figure 44) extracted from the C-135 parametric study (Reference 19), a pilot's log and a brief calculation sheet (Figure 45), and written instructions with examples included. The flight consisted of a 10 hour cargo mission with an ascent, cruise at 40,000 feet, descent, cruise at 30,000 feet, and a final descent. The damage for one critical point was calculated using gross weight, altitude, and fuel configuration from one graph, and a relative damage factor using c.g. location and speed from a second graph. When analyzing the first test results, it was found that the students made many mistakes and took an excessive amount of time (45-75 minutes). This was probably due to their lack of exposure to this type of problem. Weeks later, twelve of the nineteen students participated in a test using a tabular format, and on the same day the same students were tested again using a graphical format. The tabular format test was identical to the graphical format test. See Table XVIII for a typical page of the tabular format. It is believed that the students' results of this second graphical format test is the appropriate one to compare with the students' results of the tabular format.

The students completed the tabular format in 20 to 30 minutes and the graphical format in 20-35 minutes. Mistakes were slightly more numerous using the graphical format. There is a tendency to believe that there was a transfer of knowledge with the tabular and graphical tests given on the same day. This would have the effect of reducing the students' time to complete the graphical format test.

BATTERY 1

Order of Tests	TEST 1	TEST 2	TEST 3
Type Format	Graphical	Tabular	Graphical
Subjects Tested	19 Jr. & Sr. in Engr.	12 of 19 Jr. & Sr. in Engr.	12 of 19 Jr. & Sr. in Engr.
Type Mission	Cargo	Cargo	Cargo
Mission Profile	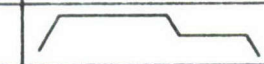		
Parameters	G. W., Alt., Conf. Mach No., C. G.	G. W., Alt., Conf. Mach No., C. G.	G. W., Alt., Conf. Mach No., C. G.
No. of Critical Points	1	1	1
Instruction Given	Verbal & Written Instruction, sample test	Verbal & Written Instruction	Verbal & Written Instruction
Instruction Time (includes sample test)	3 hrs. 15 min.	20 min.	30 min.
Calculation Aids	Brief Calculation Sheet	Brief Calculation Sheet	Brief Calculation Sheet
Subject Test Time	45-75 min.	20-30 min.	20-35 min.
Instructor Test Time	N/A	N/A	N/A

Figure 43 Description and Comparison of Six Format Tests

BATTERY 2

Order of Tests	TEST 1	TEST 2	TEST 3
Type Format	Graphical	Graphical	Tabular
Subjects Tested	11 Frosh: 8 Business, 3 Liberal Arts	7 of 11 Frosh	6 of 7 Frosh
Type Mission	Cargo	Cargo	Cargo
Mission Profile			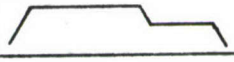
Parameters	G. W., Alt., Conf.	G. W., Alt., Conf.	G. W., Alt., Conf.
No. of Critical Points	7	7	7
Instruction Given	Verbal Instruction, Sample Test	Verbal Instruction	Verbal Instruction
Instruction Time (includes sample test)	4 hrs. 5 min.	1 hour	25 min.
Calculation Aids	Complete Worksheet	Complete Worksheet	Complete Worksheet
Subject Test Time	1 hr-1 hr. 25 min.	2 hr. 5 min-2 hr. 45 min.	50 min-1 hr. 5 min.
Instructor Test Time	55 min.	1 hr. 24 min.	50 min.

Figure 43 -- concluded

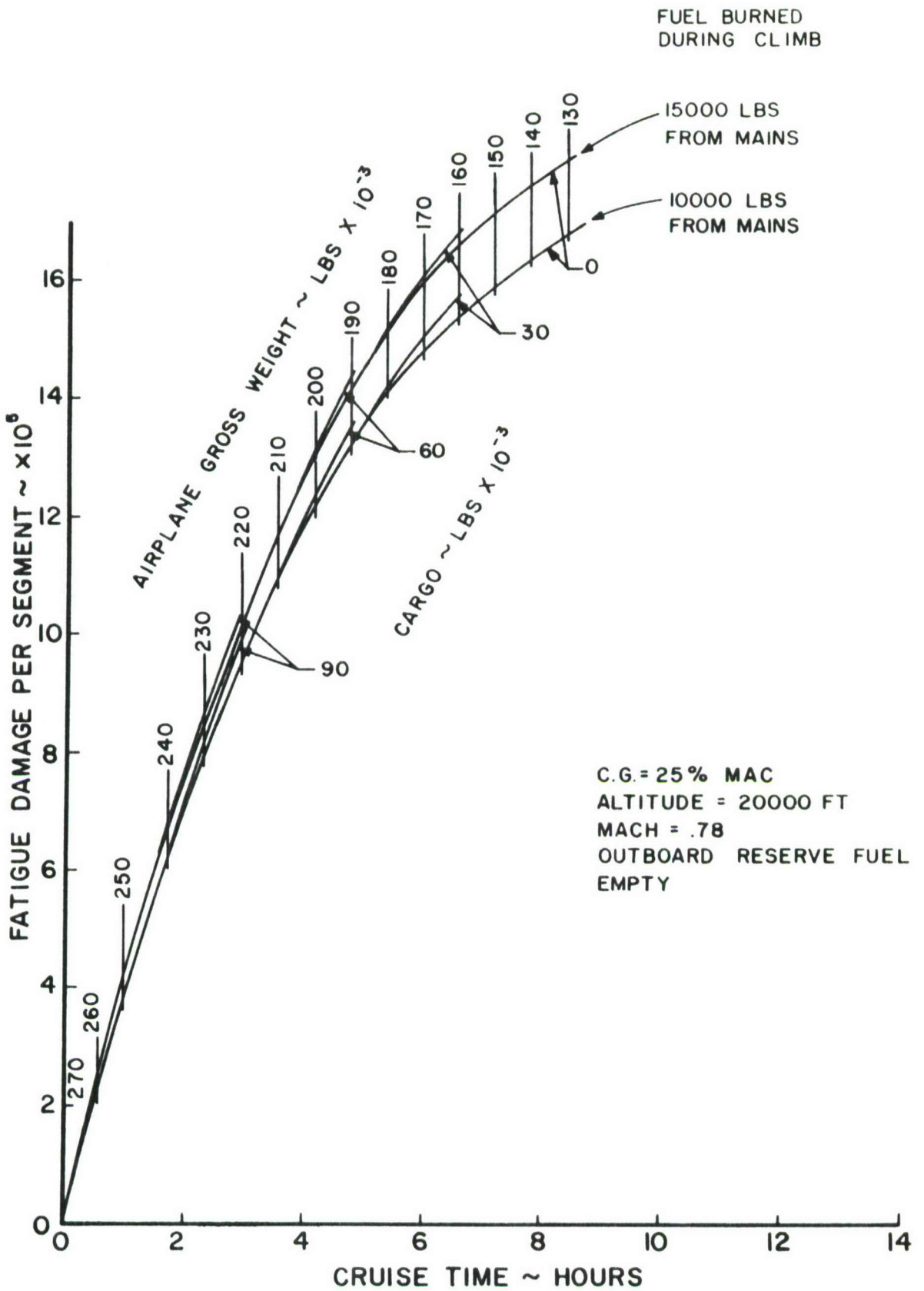

Figure 44 Typical Graph Used in Tests to Calculate Damage
(Actual Graph Was on 10 x 10 to the Centimeter Grid)

Flight Log

Aircraft No.	150
Date of Flight	3 Feb 1967
Pilot	
Take Off Base	Castle AFB
Landing Base	Walker AFB
Cargo Weight	15,000 lbs.
Moment Arm	300 in.
Aft Body Fuel	0

Flight Segment	Gross Weight (lbs)	Altitude (ft)	Time (hrs)	Reserve Tank	C. G. Location (% MAC)	Speed
Taxi (start)	280,000	0	0	Full		
Ascent (start)	270,000	0	0.05	Full	26.9	280 knots
Cruise (start)	258,000	40,000	0.64	Full	29.4	0.80 M
(end)		40,000	7.16	Full	29.4	0.80 M
Descent (end)	179,000	30,000	7.21	Full	29.4	0.74 M
Cruise (end)	149,000	30,000	9.73	Full	29.4	0.74 M
Descent (end)	146,600	0	10.0	Empty	32.7	280 knots
Landing		0				
Ground-Air-Ground Cycle						

Damage Calculation

Name _____

Date _____

Phone _____

Major _____

Year _____

Critical Point B1, Stiff. 7

Correction Factors			Uncorrected Damage ($\times 10^{-5}$)	Corrected Damage ($\times 10^{-5}$)
Reserve Tank	C. G. Location	Speed		
			Total Damage	

Cruise Calculation Aid

		1 Cruise	2 Cruise
1	Damage Corresponding to Initial G. W. of Cruise		
2	Plotted Time (time corresponding to initial G. W. of cruise)		
3	Time Spent in Cruise (from flight log)		
4	Sum of Plotted Time & Time Spent in Cruise 2 + 3		
5	Damage Corresponding to Final Time of Cruise		
6	Total Cruise Damage 5 + 1		

Taxi & Landing Calculation Aid

ΔM = -(Wt. of Cargo) (Moment Arm) - (Wt. of Aft Body Fuel) (Moment Arm)

Figure 45 Pilot's Log and Brief Calculation Sheet Used in First Battery of Tests

Table XVIII Typical Table Used in the First Battery of Tests To Calculate Damage

Body Item - B1
Cruise at 30,000 feet

C.G. = 25% M.A.C.
Speed = 0.78 Mach
O.R.F. = Full

Cargo = 0			Cargo = 15,000 lb			Cargo = 30,000 lb		
Time (hrs)	Gross Weight (x 10^3 lbs)	Damage (x 10^{-5})	Time (hrs)	Gross Weight (x 10^3 lbs)	Damage (x 10^{-5})	Time (hrs)	Gross Weight (x 10^3 lbs)	Damage (x 10^{-5})
0.0	270	0.00	0.0	270	0.00	0.0	270	0.00
0.4	264	0.05	0.4	264	0.05	0.4	264	0.05
0.7	260	0.10	0.8	259	0.10	0.9	258	0.10
1.1	255	0.15	1.3	253	0.15	1.7	247	0.15
1.5	250	0.20	1.9	244	0.20	3.0	230	0.20
2.1	241	0.25	2.9	232	0.25	5.0	207	0.25
2.9	232	0.30	4.1	217	0.30	6.6	188	0.30
3.8	221	0.35	6.1	193	0.35	7.9	173	0.35
5.3	203	0.40	8.5	168	0.40	9.1	161	0.40
10.5	147	0.45	10.1	150	0.45	10.1	150	0.45

It was believed that if one used an expanded and more useful calculation sheet or worksheet instead of the brief calculation sheet, the time needed to train people would be reduced considerably and there would be less likelihood of mistakes. Since it may not be feasible to use engineers' or officers' time to calculate the damage on a flight-by-flight basis, a second battery of tests were prepared in which non-technical oriented freshmen were tested using an expanded worksheet.

In the second battery of tests, eleven freshmen majoring in non-technical fields (Business and Liberal Arts) participated in calculating damages for seven critical points. In this battery of tests, the students used a pilot's log (Figure 46), a complete worksheet (Figure 47), an accumulated damage sheet (Figure 48), a 38-page booklet of graphs for the graphical format test (Figure 44) and a 17-page booklet of tables for the tabular format test (Table XIX). To conserve space in the tabular format, the tables were constructed so that when entering the tables with a number that lies between two numbers, the higher number is used, not the nearer. Parameters used were gross weight, altitude, and configuration; relative damage factors for speed and c.g. location were not used. To acquaint themselves with the test, the students were given verbal instructions and a sample test. After completing the sample test, which allowed much communication between instructor and student, the students were given the regular test. The 11 students completed this graphical test in a time span of 1 hour to 1 hour and 25 minutes. The mistakes were numerous and the accuracy was inadequate, so another graphical test was scheduled. On this second graphical test the students worked more accurately and made fewer mistakes. The time needed to complete the test was longer (2 hours 5 minutes to 2 hours 45 minutes) because two additional flight segments were included in the mission and also because of the time involved in the increased accuracy.

The time required to calculate the damage using the tabular format ranged from 50 minutes to 1 hour and five minutes. This is less than half the time required by the graphical format. The fact that the tabular format test was given to the students a few days after the graphical format tests suggests that a transfer of knowledge occurred. It is believed that this influenced the time required, but not to a great degree. It is also believed to have influenced the number of mistakes.

One student's results were eliminated from the final results because of the excess time taken to complete the test and also because of his large number of mistakes. It is believed that considering his test would distort the interpretation of the final results.

Using the graphical format, seven students made a total of 27 mistakes and 11 inaccurate readings. This is an average of almost 4 mistakes per student. The mistakes can be classified as follows:

Aircraft No.	169	Cargo Weight	30,000 lbs
Date of Flight	1/22/66	Moment Arm	325 in.
Pilot		Aft Body Fuel	0
Take-Off Base	Castle AFB	Moment Arm	350 in.
Landing Base	Walker AFB		

FLIGHT SEGMENT		GROSS WEIGHT (LBS)	ALTITUDE (FT)	TIME (HRS)	RESERVE TANK
TAXI	(START)	227,800	0	0	Full
	(END)	217,800	0	0.05	Full
ASCENT	(START)	217,800	0	0.05	Full
	(END)	207,000	40,000	0.68	Full
CRUISE	(START)	207,000	40,000	0.68	Full
	(END)	180,000	40,000	3.04	Full
DESCENT	(START)	180,000	40,000	3.04	Full
	(END)	178,900	20,000	3.14	Full
CRUISE	(START)	178,900	20,000	3.14	Empty
	(END)	160,600	20,000	4.84	Empty
DESCENT	(START)	160,600	20,000	4.84	Empty
	(END)	158,000	0	5.00	Empty
LANDING	(START)	158,000	0	5.00	Empty
	(END)				
GROUND-AIR-GROUND-CYCLE					

Figure 46 Pilot's Log Used in Second Battery of Tests

Abbr.	Word(s)	Units
G.W.	Gross Weight	10^3 lbs.
Alt.	Altitude	ft.
--	Damage	x10-5
Corr. Fact.	Correction Factor	--
ΔM	Bending Moment	in-lbs.
Cols.	Columns	--
O.R.	Outboard Reserve	--
Wt.	Weight	lbs.
--	Time	hours
Cr. Pt.	Critical Point	--

1 PL** Cargo Wt.	2 PL Moment arm of cargo	3 PL Aft Body Fuel wt.

4 PL Moment Arm of Aft Body Fuel	5 ΔM Cols. (1x2)+(3x4)

	Damage Use Col. 5
B1	

7 PL G.W. at Start of Ascent	8 PL Alt. at Start of Ascent	9 PL Alt. at End of Ascent	10 PL O.R. Fuel (full or empty)

	11 Damage Use Cols. 7,8	12 Damage Use Cols. 7,9	13 O.R. Fuel Corr.Fact. †	14 Damage Col.(12-11)	15 Corr. Damage Col.(13x14)
W1					
W2					
W3					
W4					

	16 Damage Use Cols. 7,8	17 Damage Use Cols. 7,9	18 Damage Col.(17-16)
B1			
H1			
V1			

* Taxi and landing damage for all control points other than B1 are listed in the table under ground damage. B1 is the only control point that requires a calculation.

** PL means that the value for the box below is obtained directly from the pilot's log.

† If O.R. fuel is full, Corr. Fact. = 1.0 If O.R. fuel is empty, Corr. Fact. = 1.4

Figure 47 Work Sheet Used In the Second Battery of Tests

19 PL	20 PL	21 PL	22 PL	23 PL	24 PL
G. W. at Start of Cruise	Cargo Wt.	Alt. at Start of Cruise	O. R. Fuel (Full or Empty)	G. W. at Start of Ascent	G. W. at End of Ascent

25	26 PL	27 PL	28	29	30
Fuel Burned From Mains Col.(23-24)	Time at Start of Cruise	Time at End of Cruise	Plotted Time ≠ Cols. 19, 21	Time spent In Cruise Col.(27-26)	Corrected Time Col.(28 + 29)

	31 Damage Use Cols. 19, 20, 21, 22, 25	32 Damage Use Cols. 20, 21, 22, 25, 30	33 Damage Col. (32-31)
W1			
W2			
W3			
W4			

	34 Damage Use Cols. 19, 20, 21, 22	35 Damage Use Cols. 20, 21, 22, 30	36 Damage Col.(35-34)
B1			
H1			
V1			

≠ Plotted time has a constant value for any given G. W. It can be determined by finding the graph with the appropriate altitude, entering the G. W., and determining the corresponding time on the horizontal scale. The plotted time is the same for all critical points.

Figure 47 --- continued

37 PL	38 PL	39 PL	40 PL
G.W. at End of Descent	Alt. at Start of Descent	Alt. at End of Descent	O.R. Fuel (Full or empty)

	41 Damage Use Cols. 37, 38	42 Damage Use Cols. 37, 39	43 O.R. Fuel Corr. Fact ‡	44 Damage Col. (41-42)	45 Corr. Damage Col. (43x44)
W1					
W2					
W3					
W4					

	46 Damage Use Cols. 37, 38	47 Damage Use Cols. 37, 39	48 Damage Col. (46-47)
B1			
H1			
V1			

‡ If O.R. Fuel is full, corr. fact. = 0.7

If O.R. Fuel is empty, corr. fact. = 1.0

49 PL	50 PL
Cargo Wt.	Moment Arm of Cargo

51 PL	52 PL
Aft Body Fuel Wt.	Moment Arm of aft Body Fuel

53 PL
ΔM Col. (49x50)+(51x52)

	54 Damage Use Col. 53
B1	

55 PL	56 PL
G.W. at Start of Taxi	Alt. at End of Ascent

	57 Damage Use Cols. 55, 56
W1	
W2	
W3	
W4	
B1	
H1	
V1	

Figure 47 -- concluded

FLIGHT SEGMENT	DAMAGE ($x10^{-5}$)						
	W1	W2	W3	W4	B1	H1	V1
TAXI							
ASCENT							
CRUISE							
DESCENT							
LANDING							
G-A-G							
TOTAL DAMAGE							

Figure 48 Accumulated Damage Chart Used in the Second Battery of Tests

Table XIX Typical Table Used in the Second Battery of Tests to Calculate Damage

Cruise at 20,000 feet, Outboard Reserve Fuel Empty

WING ITEM - W2

10,000 lbs. from mains, cargo=30,000 or 90,000			(cont.)			10,000 lbs. from mains, cargo = 30,000		
Time (hrs)	Gross Weight (10^3lbs)	Damage ($x10^{-5}$)	Time (hrs)	Gross Weight (10^3lbs)	Damage ($x10^{-5}$)	Time (hrs)	Gross Weight (10^3lbs)	Damage ($x10^{-5}$)
0.00	270	0	0.90	253.7	3.6	2.03	236.5	7.1
0.02	269.5	.1	0.91	253.5	3.7	2.06	236.0	7.2
0.05	269	.2	0.97	253.2	3.8	2.09	235.5	7.3
0.07	268.5	.3	1.00	253.0	3.9	2.12	235.0	7.4
0.10	268	.4	1.02	252.5	4.0	2.15	234.0	7.5
0.12	267.5	.5	1.05	252	4.1	2.18	233.0	7.6
0.15	267	.6	1.08	251.5	4.2	2.21	232.5	7.7
0.17	266.5	.7	1.10	251	4.3	2.24	232.0	7.8
0.20	266	.8	1.12	250.5	4.4	2.28	231.0	7.9
0.22	265.5	.9	1.15	250	4.5	2.32	230.0	8.0
0.25	265	1.0	1.20	249.5	4.6	2.35	229.0	8.1
0.27	264.5	1.1	1.22	249	4.7	2.38	228.0	8.2
0.30	264	1.2	1.27	248.5	4.8	2.41	227.5	8.3
0.32	263.5	1.3	1.30	248	4.9	2.45	227.0	8.4
0.35	263	1.4	1.35	247.5	5.0	2.50	226.0	8.5
0.37	262.5	1.5	1.37	247	5.1	2.53	225.0	8.6
0.40	262	1.6	1.39	246.5	5.2	2.58	224.0	8.7
0.42	261.5	1.7	1.42	246	5.3	2.61	223.0	8.8
0.45	261	1.8	1.47	245.5	5.4	2.64	222.0	8.9
0.47	260.5	1.9	1.53	245	5.5	2.67	221.0	9.0
0.50	260	2.0	1.56	244.5	5.6	2.70	220.0	9.1
0.52	259.5	2.1	1.59	244	5.7	2.73	219.0	9.2
0.55	259	2.2	1.61	243.5	5.8	2.77	218.0	9.3
0.57	258.5	2.3	1.66	243	5.9	2.81	216.0	9.4
0.60	258	2.4	1.69	242.5	6.0	2.86	214.0	9.5
0.62	257.5	2.5	1.73	242	6.1	2.90	213.0	9.6
0.65	257	2.6	1.79	241.5	6.2	2.95	212.0	9.7
0.67	256.5	2.7	1.81	241	6.3	3.00	211.0	9.8
0.70	256	2.8	1.84	240.5	6.4	3.05	210.0	9.9
0.72	255.5	2.9	1.88	240	6.5	3.10	209.0	10.0
0.75	255	3.0	1.90	239.5	6.6	3.15	208.5	10.1
0.78	254.5	3.1	1.92	239	6.7	3.20	208.0	10.2
0.81	254	3.2	1.94	238.1	6.8	3.25	207.5	10.3
0.93	254.2	3.3	1.97	237.5	6.9	3.30	207.0	10.4
0.86	254.1	3.4	2.00	237.0	7.0	3.35	206.5	10.5
0.89	254.0	3.5				3.40	206.0	10.6

Explanation of Mistakes	Number of Mistakes
1) Misread scale on graph	6
2) Used wrong graph	6
3) Used wrong line on graph	2
4) Decimal point mistake	1
5) Miscalculation of plotted time on cruise segment	1
6) Included an additional flight segment	1
7) Addition or subtraction	1
8) Copied number incorrectly when transferring to accumulated damage page	1
9) Unknown	8
Total	27

Using the tabular format the six students made a total of 17 mistakes which is an average of almost 3 mistakes per student. However, seven of these mistakes were made because the numbers were arranged in blocks with only the higher number given. This was done to reduce the volume of the tables, but probably would not be used in the future. The mistakes can be classified as follows:

Explanation of Mistakes	Number of Mistakes
1) Failed to use higher number when entering table	7
2) Addition or subtraction	3
3) Failed to use taxi damage	1
4) Copied number incorrectly when transferring to accumulated damage page	2
5) Unknown	4
Total	17

Although the number of mistakes seem quite large, it is believed that with more practice most of these mistakes can be eliminated. It is also believed that selected airmen can learn to use either format; however, they would probably prefer the tabular format because it eliminates scale reading difficulties, requires less time, and is less fatiguing to use.

4. COST OF UTILIZATION

It is believed that the times needed to complete Test 2 (graphical format) and Test 3 (tabular format) of the second battery of tests are the appropriate times to compare because the conditions under which these tests were taken are similar to the conditions anticipated in actual practice, i.e., more than one critical point being monitored and non-technical personnel performing the calculations. The instructor's time to complete Test 2 (graphical) and Test 3 (tabular) was 1 hour 24 minutes and 50 minutes, respectively. It is concluded that the graphical format may require 50% more time than the tabular format. It is believed that after the students accumulate experience, the time required for them to complete the format tests will be approximately the same as that of the instructor.

In reviewing the second battery of tests, the major factors which affected the students' time were: seven critical points; gross weight, altitude, and configuration as parameters; predetermined value for c.g. location; predetermined value for speed (separate pages might be introduced for speed variations); six segments -- ascent, cruise, in flight descent, cruise, descent, and ground damage (ground damage was constant for all critical points except one). Under these conditions, one could say that the above man-hours were sufficiently accurate on a per flight basis independent of the length of the flight.

SECTION VII

PILOT'S LOG

1. BOMBER AND CARGO AIRCRAFT

The pilot's log must contain all the information required for the calculation of the damage from the parametric damage charts. After a review of the data required for bomber and cargo aircraft it was decided that of the existing forms, AFTO-70, February 1964 (Figure 49) and SAC-198, September 1962 (Figure 50) contain the required data. The AFTO-70 form contains all of the mission profile data required and with changes in the weapon type and locations (which are presently specified for the B-58) would be satisfactory for most bombers. The SAC-198 form contains the remaining required data, such as more accurate gross weight, fuel distribution and center of gravity location. For cargo aircraft, the same type of form could be used with data block 6 changed to read "Cargo Weight Distribution" and the headings NONE, MB-1C, TCP UPPER, TCP COMPLETE, FORWARD, AFT changed to read "Fuselage Compartment H, I, J, K, L, etc.". The entries in data block 6 would then be the weight of cargo in that fuselage compartment. For flights which had a cargo drop, the time of the drop and the weight dropped could be entered in data block 16 on AFTO form 70. The weight of cargo dropped would also be obtainable from the SAC-198 form from the DRY WEIGHT entry. For aircraft that do no t require any knowledge of the center of gravity location or fuel distribution, the AFTO-70 form would be sufficient by itself; however, for aircraft that require this knowledge, both forms would be required. For those aircraft which have different parametric charts for types of mission (i.e., test flight, pilot check-out, live combat, etc.) the type of mission could be entered in data block 16.

2. FIGHTER AIRCRAFT

For fighter aircraft, it is suggested that the counting accelerometer with a printer be installed on each aircraft as the optimum system. Some pilot information would be required to interpret the printout. This information could be obtained after the flight if only a few printings were taken; however, for a flight which had several printings, it would be desirable to have the pilot's log completed each time a printing was taken. It is therefore suggested that the pilot also be provided with a small magnetic tape recorder and a log sheet. Part of the log sheet would be completed before takeoff. This part would contain the gross weight before takeoff, the weight of fuel, and the weapon configuration; that is, the type and number of weapons on each pylon. Then the pilot would describe the flight as it progressed and record it on the tape recorder. He would record the takeoff time; cruise altitude and

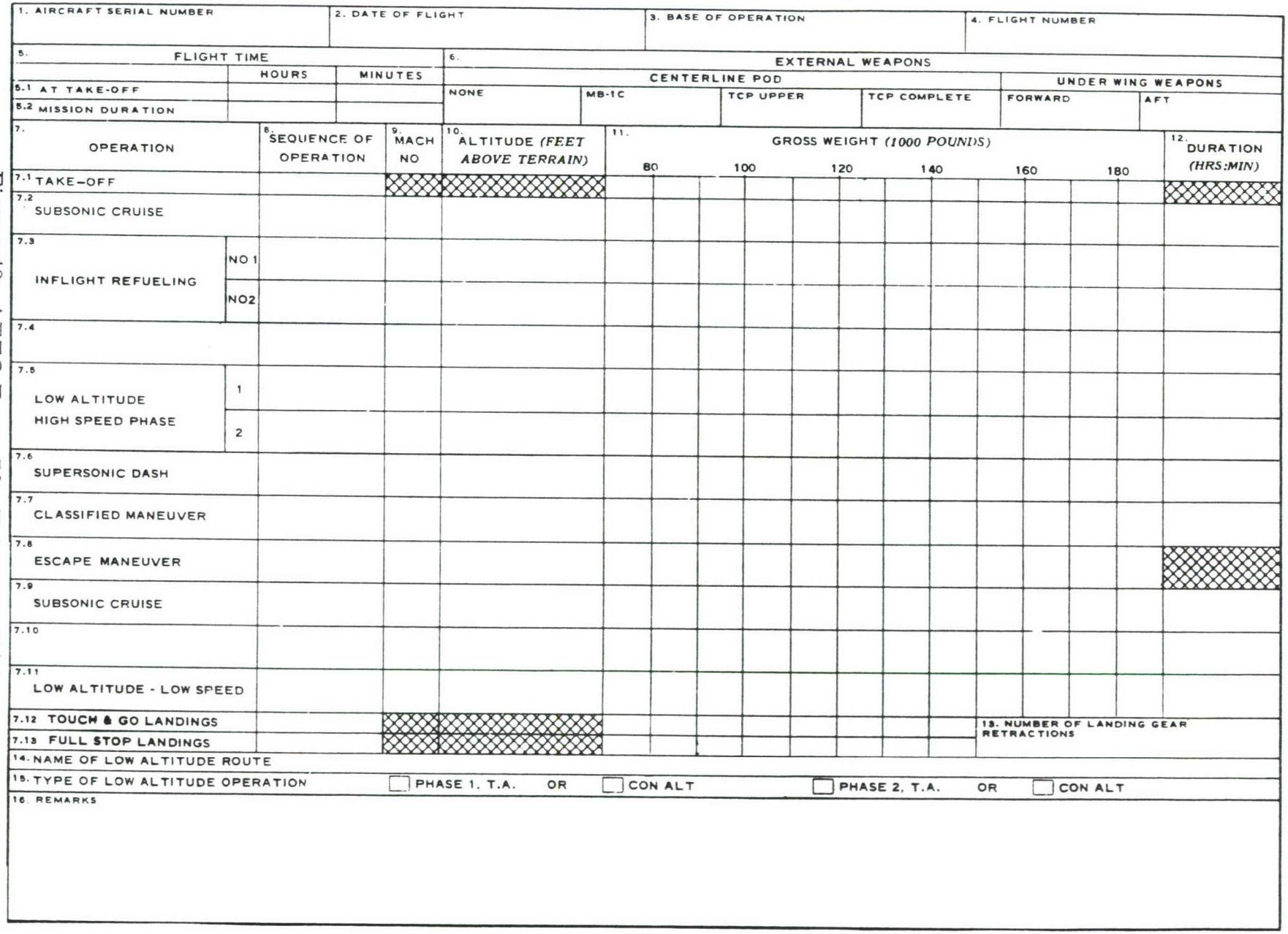

1. AIRCRAFT SERIAL NUMBER | 2. DATE OF FLIGHT | 3. BASE OF OPERATION | 4. FLIGHT NUMBER

5. FLIGHT TIME

	HOURS	MINUTES
5.1 AT TAKE-OFF		
5.2 MISSION DURATION		

6. EXTERNAL WEAPONS

CENTERLINE POD				UNDER WING WEAPONS	
NONE	MB-1C	TCP UPPER	TCP COMPLETE	FORWARD	AFT

7. OPERATION		8. SEQUENCE OF OPERATION	9. MACH NO	10. ALTITUDE *(FEET ABOVE TERRAIN)*	11. GROSS WEIGHT *(1000 POUNDS)* 80 100 120 140 160 180	12. DURATION *(HRS:MIN)*
7.1 TAKE-OFF						
7.2 SUBSONIC CRUISE						
7.3 INFLIGHT REFUELING	NO 1					
	NO2					
7.4						
7.5 LOW ALTITUDE HIGH SPEED PHASE	1					
	2					
7.6 SUPERSONIC DASH						
7.7 CLASSIFIED MANEUVER						
7.8 ESCAPE MANEUVER						
7.9 SUBSONIC CRUISE						
7.10						
7.11 LOW ALTITUDE - LOW SPEED						
7.12 TOUCH & GO LANDINGS						13. NUMBER OF LANDING GEAR RETRACTIONS
7.13 FULL STOP LANDINGS						

14. NAME OF LOW ALTITUDE ROUTE

15. TYPE OF LOW ALTITUDE OPERATION ☐ PHASE 1, T.A. OR ☐ CON ALT ☐ PHASE 2, T.A. OR ☐ CON ALT

16. REMARKS

Figure 49 AFTO Form 70, February 1964

T/O DATA	TEMP	PA	WIND	S_1 SPD	S_2 SPD	TIME	PAGE OF PAGES

TIME																			
CONDITION																			
ALTITUDE																			
MACH KIAS																			
RAT FF																			
ELEV.POS.AVAIL																			
IND C.G.																			
TOTALIZER																			
HYD QTY	UTIL																		
	PRIM																		
FUEL READING	FWD																		
	RES																		
	AFT																		
	BAL																		
	FWD. P.																		
	AFT. P.																		
TOTAL FUEL																			
DRY WT.																			
GROSS WT.																			
COMP. C.G.																			
TIME																			
CONDITION																			
ALTITUDE																			
MACH KIAS																			
RAT FF																			
ELEV.POS.AVAIL																			
IND C.G.																			
TOTALIZER																			
HYD QTY	UTIL																		
	PRIM																		
FUEL READING	FWD																		
	RES																		
	AFT																		
	BAL																		
	FWD. P.																		
	AFT. P.																		
TOTAL FUEL																			
DRY WT.																			
GROSS WT.																			
COMP. C.G.																			

Figure 50 Pertinent Section of SAC Form 198, September 1962

Mach number of initial cruise; time at end of cruise; time of a refueling and weight of fuel transferred; the weapon passes describing what stores were released and at what time; the time when he began the return cruise; altitude and Mach number of the return cruise; and time he began the descent for landing. After landing the pilot would play back the tape and complete the log sheet, adding in the time of landing and the final gross weight. After landing, he would fill in the log sheet or the comments on the printout of the accelerometer registers. For bookkeeping purposes it is believed it would be better if the pilot transcribed the tape and the accelerometer printout onto a log sheet himself so that from then on, there would be only one sheet of paper required to make the damage calculations. It is estimated that the cost of adding a small voice recorder to the accelerometer package should not make the total package cost more than $3000.00.

Alternate devices and methods were considered for recording the required parameters at the beginning and end of each mission segment. Two procedures are:

(1) Take a sequence of pictures of the appropriate instrument dial faces.

(2) Record transducer readings of the required parameters.

Since transition into new mission segments will most generally require the use of the throttle or the stick, the actuating mechanism could be a trigger switch located on the throttle or the stick. The switch could also be used to print out the accelerometer registers, thus correlating spectra with mission segment. The transducer data could also be transcribed on the same sheet used for the accelerometer register if sufficient instrumentation is provided.

The number of parameters to be recorded can be held to Mach number or velocity, altitude, and time. Since the accelerometer register had already included a time recording, adding a fuel totalizer reading would assist to better identify the gross weight history, especially if a refueling segment occurs in a flight.

The advantages of using these alternate methods and devices are:

(1) Minimum pilot effort in recording.

(2) Correlation exists between the mission segments, initial and final segment environment, and the accelerometer counts.

(3) An adoit pilot could provide a complete history of the flight environment by taking intermediate recordings.

The disadvantages of these alternate methods are:

(1) Cost of installation and maintenance could be prohibitive.

(2) Film development might create problems, such as process time and equipment needed at the field. Transducer data would have to be converted from analog to digital form in order to record data.

(3) The benefit of this Mach-altitude-gross weight data may not be sufficient to advocate the installation of the equipment needed. The Mach number and altitude printouts would be instantaneous values and may not be representative of the conditions that existed during the period of time when the accelerometer counts were being accumulated. This would be particularly true of the non-weapon-drop combat segments.

SECTION VIII

UPDATING CHARTS AND DAMAGE

Parametric damage charts may become obsolete due to:

(1) Availability of more accurate input spectra, response parameters, S-N data, etc. from testing and/or fleet operation.

(2) Changes or additions to the original anticipated operating procedures.

For the Type 1 change, the accumulated damage by tail number for the critical control point is in error and a method must be devised to update the damage. Some examples which would apply to Type 1 are: (1) updating of input spectra (e.g., the input spectrum used for the original parametric charts is found to be in error); (2) the environmental flight conditions assumed for certain mission segments are found to be incorrect due to a study of actual flight histories; (3) new fatigue test data for the control point shows a change in S-N data. In all of these cases the actual stress history of the control point has not changed for a duplicated mission, but due to improper assumptions and/or inputs in formulating the original parametric curves, the previous damage calculations are in error. The question is, what to do about updating the damage accumulation?

The damage curve changes classified as Type 2 will not require alteration of prior damage calculations for the critical control point involved. In a sense, the original parametric charts involved do not become obsolete, but rather their use will be restricted only to situations which are similar to the original assumptions. Examples of Type 2 changes would be (1) new configuration conditions or fuel usage programs; (2) addition of new tactical mission segments; (3) new input spectra (examples of this are pilot training, simulated or actual wartime conditions, or special defensive maneuvers). The most difficult problem with Type 2 changes is to recognize the changes and ascertain when they should be applied. Both Type 1 and Type 2 changes will be discussed in greater detail in the following paragraphs.

1. ERRONEOUS CHARTS (TYPE 1)

Type 1 changes will be initiated upon the discovery that assumptions or decisions made in formulating the original parametric charts are sufficiently in error to warrant replacement of these charts or graphs. Some insight as to the effect of these changes may be arrived at by comparing the two parametric charts or graphs in question. The method used in formu-

lating the new parametric charts will be the same as the original analysis with the appropriate changes in input spectra, response, or S-N data. Upon receipt of any new parametric damage charts involving Type 1 changes, it will be necessary to update the damage accrued for each critical control point by tail number. Suppose that an aircraft has been in operation for a year and a Type 1 change is found necessary. To retrace the aircraft history by going into the pilot's log for each aircraft and flight would be a laborious, time consuming task; however, if the change is of sufficient complexity, this way may be the only solution.

An alternate approach would be to anticipate the need for recalculation of damage by keeping parametric tabular data on each flight as it is flown. This would reduce the need for maintaining a huge portfolio for each aircraft by tail number with the attendant damage calculations and/or pilot logs. This approach would involve representing each mission segment of each flight by a coded number, where each digit represents a value of a parameter which affects fatigue damage. Thus, for example, given a number A B C D, the letter A designates the mission segment, B an altitude range, C a gross weight range, and D a configuration, cargo weight, etc. The number of digits and their definition would depend on the aircraft type and the mission segment, and the number could be more or less than the four digits shown. This code number would be associated with the aircraft tail number and the flight number in a set of books kept by a base personnel. As an example of how the system would be used to correct for a Type 1 change, consider changes that might be made in the ascent mission segment. For ascent, the code number would be of the form 1BCDE, where 1 refers to the ascent mission segment, B is the altitude at the beginning of ascent, C is the initial gross weight block, D is the configuration, and E is the altitude at the end of ascent. Typical values for these categories are shown in Table XX.

Table XX

Key for Flight Segment Classification (Ascent)

B or E	Altitude Blocks	C	Gross Weight Blocks	D	Configuration	
0		1	80K - 90K	1	Cargo A	Fuel Sequence A
1	1K - 5K	2	90K - 100K	2	Cargo B	
2	5K - 10K	3	100K - 110K	3	Cargo C	
3	10K - 20K	4	110K - 120K	4	Cargo D	
4	20K - 25K	5	120K - 130K	5	Cargo A	Fuel Sequence B
5	25K - 30K	6	130K - 140K	6	Cargo B	
6	30K - 35K	7	140K - 150K	7	Cargo C	
7	>35K	8	150K - 160K	8	Cargo D	

Assume that two ascent segments experienced in a given flight could be represented as:

Tail No.	Flight No.	A	B	C	D	E
0001	112	1	0	7	3	5
0001	112	1	5	6	3	7

The first segment is the initial climb, and the second is a climb enroute. The block number values under the letter columns shown above will describe any ascent segment. The classification of block values shown in Table XX is intended only as an example, therefore additional letter columns (parameters), smaller or larger block increments, etc., may be used. A problem does exist in using the data for updating if the breakdown is too refined or if too many letter columns are used. For example, the ascent segment shown by Table XX would have 4096 possible combinations. It is possible to reduce this number at a later date by combining adjacent blocks if the difference in damage is minor.

After a period of time, the log book would contain a large number of entries containing various combinations of the coded number. By parametric fatigue computations, the damage change associated with each coded number could be determined as the damage difference before the Type 1 change and after the change.

The accumulation of climb segments for a given aircraft serial number will undoubtedly show groupings of identical block combinations for ABCDE. The method for accumulating the identical block groupings will be as follows:

(1) Punch one card for each coded number in the log book using the notation as shown in the table above.

(2) Using a card sorter, collect cards into the eight configuration blocks (column D); next using the largest stacks collected by configuration blocks sort them into gross weight blocks (column C); the final step is to sort the cards into altitude blocks (column B and column E).

(3) This sorting process would provide a rapid means of determining the number of each different ascent segment.

The general procedure discussed above for collecting common ascent segments may be performed by combining cards for the total fleet. The final operation would be to extract the cards according to serial number. Once the cards have been sorted by the designated blocking procedure for an aircraft tail number, the updating can be performed for the ascent segment in the following manner:

(1) For each block designation and for a given control point, calculate the difference in damage between new and old chart (Δ damage = damage new - damage old).

(2) Multiply this Δ damage by the number of cards collected in the block designation. After all the block cards for a given tail number have been considered, the Δ damage is summed.

(3) The accumulated damage from all the old charts is added to the $\sum \Delta$ damage.

The correction due to the change in the ascent parametric chart would be completed. A process similar to this would be performed on other mission segments which had a change in their parametric charts. The updating procedure (card punching, sorting, etc.) would most probably be performed at a central location where computer facilities are available. The responsibility of signature designation (i.e., appropriate number blocking) would be assigned to the person performing the original damage calculations from the pilot's log.

A similar approach would have to be formulated for the other flight segments. Only column A designations must be maintained. The other columns (number, designation) and the block breakdown may be altered according to the parameters that constitute the damage format for that segment. The parameters for each mission segment would be broken down to account for any anticipated change.

The above approach is intended to show a general record keeping system in anticipation of future changes of Type 1. For a specific situation it is possible that updating may not require the details as put forth; however, this can only be determined after the fact. There are many instances where simple adjustments or calculations may be made to update the damage. Thus if S-N data changes are represented by a shift in the curves parallel to the N axis, or if input spectra changes are due to percentage increase or decrease in intensity at all load levels, then a common multiplying factor times the old damage accumulation would show the new damage. Other simplifications can be made concerning the number of blocks required (e.g., the majority of climb segments will be at the high end of the gross weight block for the configuration involved; the majority of descent segments will be at the low end of the gross weight blocks for the configuration involved; a high percentage of the cruise segments will be in one

altitude-Mach number block). Actual data shows that for subsonic cruise segments of the B-58, 86% of the cruise time is spent between Mach .85 and .97 and 70% of the time between 20,000 and 35,000 feet. Similarly, for the C-135, 81% of the cruise time is between 250 and 300 KEAS with 71% between the 30,000 and 40,000 foot altitude band and 10% between 20,000 and 30,000 feet. There are other situations where a ratio of damage from the new chart to the old multiplied by old damage accumulation might be used as an updating procedure for certain mission segments. However, a more detailed study should be made before implementing this feature. In order to be protected for all situations, a procedure as outlined above for the ascent mission segment would be beneficial.

The categorization of the mission segments may also be of value in showing the usage of the various aircraft and may point out certain salient features.

2. NEW CHARTS (TYPE 2)

Type 2 changes will not affect the previous damage calculations for the aircraft except for a time lag in the implementation. Some Type 2 changes will be by design (i.e., a new operational procedure is added to the aircraft, a new fuel sequencing procedure is used, aircraft are used for pilot training, etc.). There are, however, changes which cannot be accounted for, due to insufficient information. One of the prime examples is a change in input spectra. For instance, suppose new V-G-H data for the maneuver input spectrum of a given mission segment is significantly different from that used in the past. In order to properly control the damage calculations, the following requirements must be met:

(1) The initial or original input spectrum must include sufficient data to be stabilized. The breakdown of this spectrum used is sufficiently restricted as to stores configuration, comparable pilot training, tactical methods, etc.

(2) The new data should be checked for sufficient amount of data, introduction of additional parameters or change in parameters, such as target terrain, enemy defenses (small arms fire and/or anti-aircraft shells, etc.)

Only when reasons can be found for the change in spectrum can the damage by tail number be reasonably assessed. If the change is purely a statistical addition (such as the birth of quintuplets), then it must be accepted and will temporarily affect the spectrum on the extreme end (i.e., the high n_z levels). A method by which the authenticity of new data may be checked (i.e., whether it is a bona fide member of the parent distribution) is the (χ^2) Chi Squared Test of Goodness of Fit.

Pilot comments are an important item in determining whether new input spectra and new damage charts should be made. A good mathematical tool for testing the effect of parameters on the spectra, provided all parameters are included, is the χ^2 test of independence which involves use of contigency tables. If new parametric charts are found necessary, the results will be the addition of new decision junctions and parametric charts with an attendant increase in accuracy of the damage calculations.

SECTION IX

CONCLUSIONS

The use of parametric fatigue charts will substantially improve the prediction of fatigue damage on a tail number basis over the use of flight-hour criteria. These charts could be used manually to calculate the damage on a flight-by-flight basis if the calculations are made at the home base of the aircraft. If the calculations can be made at a central data processing center, then a computer solution would be preferred.

The tabular formats are preferred for manual solution of large volumes of flights but graphical formats are preferred for mission planning and analysis.

To gain the advantage of using a mission segment approach, a separate environmental spectra should be used for each segment. It was also noted that, to completely cover the expected range of the various parameters, input-response transfer factors would have to be determined for more and finer divisions of Mach-altitude regions than is the current practice.

The formats presented as the optimum configuration are based on the analysis of present day aircraft and the limited number of transfer factors available. Changes in future design and operating procedures may require a different arrangement of the parameters.

The pilot log input is a very important factor in determining the damage from parametric charts and therefore the log sheets must be clear and complete. Two standard forms now in use were found to contain all the information required for bomber and cargo aircraft.

It was concluded that fighter aircraft in live combat do not experience a representative spectra of maneuver loads and therefore the vertical acceleration should be recorded by a counting accelerometer similar to the one proposed herein.

APPENDIX

METHOD OF DERIVING TURBULENCE ENVIRONMENT BY SEASONAL, GEOGRAPHIC, TERRAIN PARAMETERS

The derived equivalent vertical gust velocity (U_{de}) approach has been used for many years as the basis for establishing a description of experienced atmospheric turbulence environment. In recent years inspection of V-G-H data has shown in the U_{de} approach that considerable differences exist in the gust spectrum due to flights in various geographical locations. Breakdown of U_{de} data by parameters such as season and terrain also pointed out significant differences in the spectrum. Current efforts have been directed towards utilizing the power spectral density approach in establishing the description of the atmospheric turbulence environment. The following paragraphs discuss the application of power spectral density techniques in establishing a description of the atmospheric turbulence environment in terms of the previously mentioned parameters.

1. OUTPUT POWER SPECTRAL DENSITY

In the application of the power spectral approach for a linear system, the relation between the disturbance (input) power spectral density function $\Phi_w(\Omega)$ and the response (output) power spectral density function $\Phi_y(\Omega)$ is:

$$\Phi_y(\Omega) = |T_y(\Omega)|^2 \Phi_w(\Omega) \qquad (17)$$

where $|T_y(\Omega)| = |T_y(\omega)|$ is the frequency response function due to a unit sinusoidal gust velocity. The value for $T_y(\Omega)$ may be found by theory or experimental methods.

a. Theoretically Determined Frequency - Response Functions

Since each aircraft manufacturer uses different methods and/or combinations of procedures for calculating the frequency response functions, only a general discussion will be given to show what parameters affect this $T_y(\Omega)$ value. The analysis should include effects of all components of airplane motion — rigid body and structural deformation. The analysis should also consider longitudinal and lateral motions separately where a unit sinusoidal velocity (usually one dimensional - i.e., uniform spanwise distribution) is applied to the surfaces involved. Longitudinal motion includes wing and horizontal tail surface loading, whereas lateral motion includes wing and vertical-tail surface loading. Various methods are used to simulate the airload distribution, such as strip theory, quasi-steady or non-steady lifting-line or surface theory. Generally, the equations of motion are formulated either by a modal approach or by a lumped-parameter method using Lagrange's dynamical

equation. The lumped-parameter method generally involves a relatively large number of degrees of freedom compared with the modal approach.

b. Experimentally Determined Response Functions

The major reason for experimental determination of response functions is to compare them with calculated values and/or to assess the degree of complexity required to simulate analytically the dynamics of the airplane. To determine the experimental value it is necessary to determine the power spectrum of the input, e.g., $\Phi_w(\omega)$ and the cross spectrum $\Phi_{wy}(\omega)$ or the output spectrum $\Phi_y(\omega)$ using the methods of Reference 4. The response function may then be expressed

$$|T_y(\omega)|^2 = \frac{\Phi_y(\omega)}{\Phi_w(\omega)} \qquad (18)$$

or

$$T_y(\omega) = \frac{\Phi_{wy}(\omega)}{\Phi_w(\omega)} \quad . \qquad (19)$$

The frequency response functions, whether determined by experimental or theoretical methods, may be for various response parameters (y) (i.e., y may be the c.g. acceleration, a control point stress, or bending moment, etc.). The frequency response functions will also be a function of the aircraft Mach number, gross weight, altitude and mass distribution.

The input power spectral density function used and the choice of the scale of turbulence L will have a considerable effect on the response. The functional forms for the spectra that are most commonly used are

$$\Phi_w(\Omega) = \frac{\sigma_w^2 L}{\pi} \quad \frac{1 + 3L^2\Omega^2}{(1 + \Omega^2 L^2)^2} \qquad (20)$$

or

$$\Phi_w(\Omega) = \frac{\sigma_w^2 L}{\pi} \quad \frac{1 + 8/3\,(1.339\,L\,\Omega)^2}{[1 + (1.339\,L\,\Omega)^2]^{11/6}} \qquad (21)$$

which are the Dryden and Von Karman functions, respectively. By substituting into Equation 19, the appropriate frequency response function $T_y(\Omega)$, the chosen input power spectral density function $\Phi_w(\Omega)$ and scale factor value L (Equations 20 or 21), the response output power spectral density function $\Phi_y(\Omega)$ can be determined.

2. RESPONSE FACTOR AND PEAK COUNT

The rms deviation of response is thus

$$\sigma_y = \left[\int_0^\infty \Phi_y (\Omega) \, d\Omega \right]^{\frac{1}{2}} . \tag{22}$$

It is convenient to introduce a factor $\bar{A}$ such that

$$\bar{A} = \frac{\sigma_y}{\sigma_w} \tag{23}$$

where the value for the rms of the input response σ_w, is

$$\sigma_w = \left[\int_0^\infty \Phi_w (\Omega) \, d\Omega \right]^{\frac{1}{2}} . \tag{24}$$

Since a linear system is assumed, the airplane response functions may be determined for a unit rms gust $\sigma_w = 1$ or as

$$\bar{A} = \frac{1}{\sigma_w} \left[\int_0^\infty \Phi_y (\Omega) \, d\Omega \right]^{\frac{1}{2}} . \tag{25}$$

$\bar{A}$ is the type of a gust response factor which depends on such airplane parameters as weight, wing area, speed, air density, and also reflects the number of degrees of freedom that are taking part in the response.

The approximate number of peaks per unit distance of the response is

$$N(y) = N_o e^{-\left(\frac{y^2}{2\sigma_y^2} \right)} \tag{26}$$

where N_o is the average number of times per unit distance that the analog response function y crosses the reference value with positive slope. Thus,

$$N_o = \frac{1}{2\pi} \left[\frac{\int_0^\infty \Omega^2 \left| T_y(\Omega) \right|^2 \Phi_w(\Omega) \, d\Omega}{\int_0^\infty \left| T_y (\Omega) \right|^2 \Phi_w (\Omega) \, d\Omega} \right]^{\frac{1}{2}} . \tag{27}$$

NOTE: The demoninator of Equation A. 11 is equal to σ_y. For a unit rms gust velocity ($\sigma_w = 1$) this value is equal to $\bar{A}$.

By using a similar approach to that used in Section II, 1a, the composite discrete turbulence patch model for response using Equation 26 would be expressed as

$$N(y) = \frac{1}{d}\left[d_1 N_o e^{-\left(\frac{y^2}{2\sigma_1^2 \bar{A}^2}\right)} + \ldots + d_n N_o e^{-\left(\frac{y^2}{2\sigma_n^2 \bar{A}^2}\right)} \right]$$

or

$$N(y) = N_o \left[p_1 e^{-\left(\frac{y^2}{2\sigma_1^2 \bar{A}^2}\right)} + \ldots + p_n e^{-\left(\frac{y^2}{2\sigma_n^2 \bar{A}^2}\right)} \right]. \quad (28)$$

NOTE: σ_n is the rms deviation of the gust velocity for the nth discrete patch and $\sigma_n \bar{A} = \sigma_y$ from Equation 24

For a continuous variation in σ_n, Equation 28 would be represented by:

$$N(y) = N_o \int_0^\infty p(\sigma) e^{-\left(\frac{y^2}{2\sigma^2 \bar{A}^2}\right)} d\sigma \quad . \quad (29)$$

Equations 7 and 29 are very similar, in fact $p(\sigma)$ is also the probability density distribution of σ_w for a given altitude and may be expressed as

$$p(\sigma) = \frac{1}{b}\sqrt{\frac{2}{\pi}} e^{-\left(\frac{\sigma^2}{2b^2}\right)} \quad (30)$$

where b is the composite rms gust velocity of all the patches. It can also be shown that by substituting Equation 30 into Equation 29 and integrating that

$$N(y) = N_o e^{-\left(\frac{y}{\bar{A} b}\right)} \quad . \quad (31)$$

It should be mentioned again that all turbulence patches of Equation 28 are obtained from a given altitude or altitude band and for a fixed aircraft speed and weight. Some of the reasons for this are that (1) the $T_y(\Omega)$ and consequently $\bar{A}$ and N_o values are also dependent on these parameters; (2) the composite rms gust velocity b and at times scale (L values) are also dependent on altitude bands; (3) it is possible to convert N_o which represents number of crossings of y = 0 with positive slope per unit distance to N_o' crossings per unit time, i.e., $N_o' = V_T N_o$.

By accumulating patches of vertical gust data for various altitudes or altitude bands it is possible to assign descriptive terminology to each component of the turbulence model. Methods used in the past divide the turbulence model into non-storm and storm environment for each altitude band. The probability density distribution of σ for a given altitude is expressed by

$$p(\sigma) = P_1 p_1(\sigma) + P_2 p_2(\sigma) \tag{32}$$

where

$$p_1(\sigma) = \sqrt{\frac{2}{\pi}} \frac{1}{b_1} e^{-\left(\frac{\sigma^2}{2b_1^2}\right)} \tag{33}$$

$$p_2(\sigma) = \sqrt{\frac{2}{\pi}} \frac{1}{b_2} e^{-\left(\frac{\sigma^2}{2b_2^2}\right)} \tag{34}$$

The values for P_1 and P_2 have been used to represent, respectively, the portion of time or distance spent in non-storm and storm type turbulence for the altitude band involved, and the values for b_1 and b_2 represent, respectively, the composite rms gust velocity for non-storm and storm turbulence for a given altitude band. By substituting Equations 32 through 34 into Equation 29 and integrating, we have

$$N(y) = N_o \left[P_1 e^{-\left(\frac{y}{\bar{A} b_1}\right)} + P_2 e^{-\left(\frac{y}{\bar{A} b_2}\right)} \right] \tag{35}$$

Equation 35 represents an expression which will give an exceedance rate N(y) of response level (y) for a designated altitude band and vehicle gross weight and speed. The independent parameter y may represent c.g. acceleration, a fatigue point stress or a fatigue point bending moment. The table on the following page shows the functional relationships of the symbols in Equation 35.

	N_o	P_1	P_2	b_1	b_2	$\bar{A}$	N(y)
Altitude	yes	yes	yes	yes	yes	yes	yes
Mach Number	yes	no	no	no	no	yes	yes
Gross Weight	yes	no	no	no	no	yes	yes
External Configuration	yes	no	no	no	no	yes	yes
y parameter	yes	no	no	no	no	yes	yes
Storm Probability	no	no	yes	no	yes	no	yes
Non-Storm Probability	no	yes	no	yes	no	no	yes

One can see that the b and P values are only functions of altitude and the probability of existence of storm or non-storm conditions. Values of b and P have been determined for various altitude bands in References 6 and 7. The values for $\bar{A}$ and N_o are functions of Mach number, altitude, gross weight, external configuration, and the y parameter for the particular aircraft. The aircraft manufacturer must determine $\bar{A}$ and N_o values for an adequate number of flight conditions for each aircraft configuration and/or critical point so that for any anticipated flight conditions, $\bar{A}$ and N_o values may be determined by using interpolation procedures. N(y) is thus a function of all the parameters and represents the number of exceedances per unit distance for positive or for negative values of y.

Equation 35 can be rewritten as

$$\frac{N(y)}{N_o} = P_1 e^{-\left(\frac{y}{\bar{A}b_1}\right)} + P_2 e^{-\left(\frac{y}{\bar{A}b_2}\right)} \tag{36}$$

or

$$N(y)/N_o = f\left(\frac{y}{\bar{A}}, h\right) \tag{37}$$

3. CONVERSION OF V-G-H DATA TO TURBULENCE ENVIRONMENT

Equation 37 suggests the form and manner for analyzing gust-response data collected during routine airplane operations to obtain generalized curves for prediction purposes. A response quantity that has been widely collected in routine operations is the center-of-gravity load factor (i.e., $y = n_z$). Such data can be processed to yield the number of exceedances N(y) of given load factor levels, and should be separated according to altitude brackets and flight conditions. The values of $\bar{A}$ and N_o for a vehicle can be defined for various flight conditions (i.e., speed, altitude, gross weight blocks). Thus, according to equation 37, these data may

be plotted as $N(y)/N_o$ vs. $y/\bar{A}$ for various altitude bands.

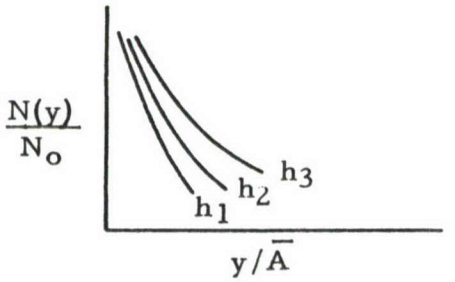

Figure 51. Generalized Curve for Gust Loads

It is quite significant that the generalized curves of Figure 51, although derived from a response quantity that is convenient to record (e.g., c.g. load factor), apply to other responses as well. In other words the curves of Figure 51 would be duplicated for any response parameter (such as stress for a control point) under the same environmental conditions provided accurate $\bar{A}$ and N_o values are known and an analog recording of (y = stress) is properly processed. Thus for a coordinate point on a curve of Figure 51 $\left[y/\bar{A}\,,\ \frac{N(y)}{N_o}\right]$, the stress y and the corresponding number of exceedances of that stress per unit distance or time N(y) may be obtained by multiplying by the appropriate $\bar{A}$ and N_o values, provided the same restrictions are imposed. The value $y/\bar{A}$ is in the dimensional form of velocity and has been called true gust velocity by some authors. $N(y)/N_o$ represents the cumulative probability of the occurrence of this $y/\bar{A}$ value under the same conditions.

If the terms on the right-hand side of Equation 36 are plotted one at a time, the result will be straight lines when plotted on semi-log graph paper. In view of this feature, the following conclusions can be made concerning Figure 51:

(1) Select any group of observed data points having common parameters affecting turbulence (i.e., altitude, season, geographic location, terrain, etc.) and plot them on semi-log paper as shown in Figure 52.

(2) Draw a tangent (line 1) to the tail of the observed distribution. The ordinate intercept value of line 1 equals P_i. The value for b_i can be found as

$$b_i = \frac{\Delta(y/\bar{A})_1 \log e}{\log P_i - \log\left(\frac{N(y)}{N_o}\right)_1} = \frac{\Delta(y/\bar{A})_1\,(.4343)}{\log P_i - \log\left(\frac{N(y)}{N_o}\right)_1}$$

NOTE: $(y/\bar{A})_1$ may be any value desired along the abscissa; however, $\left(\frac{N(y)}{N_o}\right)_1$ must be the corresponding ordinate value.

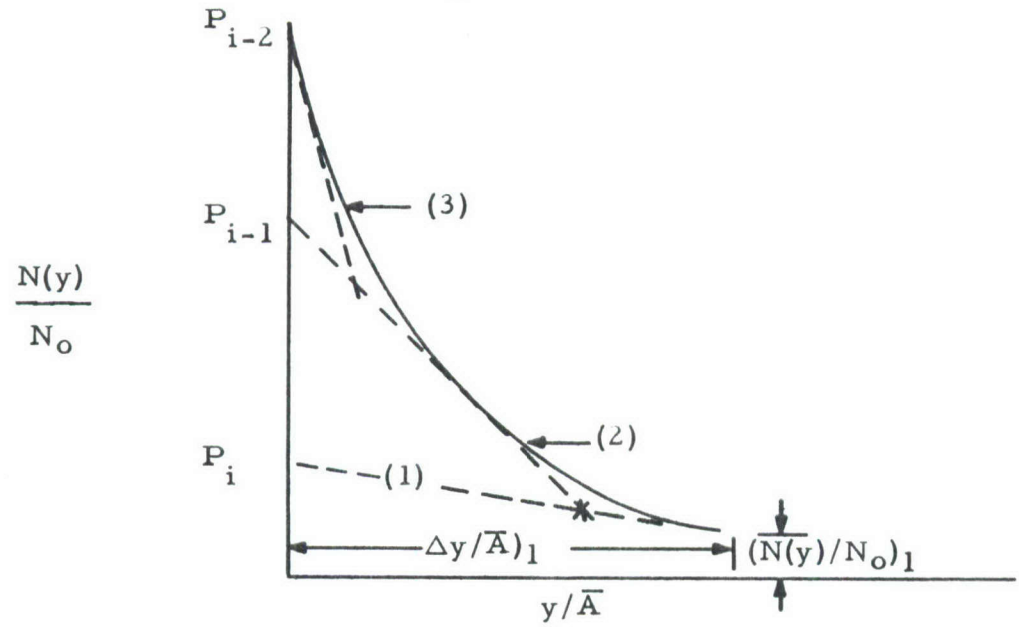

Figure 52. Graphic Procedure for P and b Determination

(3) Line 2 is then taken from the point on line 1 which underestimates the observed distribution by one-half and is drawn tangent to the upper part of this observed distribution curve. The value for P_{i-1} is the ordinate intercept of line 2 and the value for b_{i-1} is:

$$b_{i-1} = \frac{.4343\Delta(\frac{y}{A})_2}{\log P_{i-1} - \log\left(\frac{N(y)}{N_o}\right)_2}$$

(4) The third line, if required, is then obtained from line 2 in the same manner that line two was obtained from line 1. If we call the ordinate intercept of the plotted curve P_0, then

$$P_{i-2} = P_0 - P_i - P_{i-1}$$

Several features may be observed from this procedure: (a) at the intersection point of line 1 and line 2 the accuracy is assured by the construction procedure, i.e., the ordinate of line 1 plus the ordinate of line 2 is equal to the observed value. (b) in most cases i = 2 will be sufficient to yield a good approximation of the observed distribution. The resulting

equation which represents the observed distribution is

$$\frac{N(y)}{N_o} = P_{i-2}\, e^{-\frac{y}{\bar{A}\, b_{i-2}}} + P_{i-1}\, e^{-\frac{y}{\bar{A}\, b_{i-1}}} + P_i e^{-\frac{y}{\bar{A}\, b_i}} \qquad (38)$$

where the P_{i-2} and b_{i-2} terms will seldom be necessary.

The representation in Equation 37 no longer refers to storm and non-storm turbulence but rather to the statistically controlled method of accumulating the observed data. For example, clear air turbulence can at times be quite severe; thus large $y/\bar{A}$ values need not be attributed entirely to storm conditions. Certain parameters which have not been investigated in the past because of insufficient data are

(1) Surface conditions (i.e., land, water, smooth or rugged terrain),
(2) Seasons of the year,
(3) Route of operation,
(4) Geographic location.

One of the questions to answer is, do these parameters affect the variations in turbulence frequency and magnitude? According to U_{de} data collected from C-135 (Reference 23) and B-52 flights (Reference 24) the answer is in the affirmative. The U_{de} data of Figures 53 through 63 show some of the exceedance curves to differ by an order of magnitude for the same altitude bands. Figures 53 through 56 show the variation in turbulence due to terrain for various altitude bands. Figures 57 through 63 show the variation in turbulence due to seasons and geographic location for low level penetration flights.

Therefore, cg gust load factor data may be collected for an aircraft and sorted by any combination of the above parameters. This data can then be divided into altitude bands and Mach number gross weight blocks so that appropriate combinations of $N(y)/N_o$ vs. $y/\bar{A}$ can be collected to formulate generalized curves. From any grouping of data by this process, appropriate b and P values can be determined. These b and P values may now be applied under the same parametric conditions for other aircraft and for various critical control points as well as for the center of gravity load factors.

4. SUMMARY

In review, the following steps are advocated to include the effects of any parameter or combination of parameters on gust damage by power spectral techniques.

(1) Center of gravity load factor data due to gust may be extracted from V-G-H data by altitude bands and by season, geographical location, time of day, or by terrain. Care must be taken in removing maneuver data.

(2) Experimental or theoretically determined frequency response functions for the center of gravity load factor must be used in calculating the $\bar{A}$ and N_o values required for the study. Care must be taken to choose the proper input power spectral density function and the appropriate scale of turbulence value L (see Equations 20 and 21).

(3) In addition to the previous breakdowns of the data, the flight segments must be allocated to various gross weight and speed blocks in order to construct the $N(y)/N_o$ vs $y/\bar{A}$ generalized curves according to the parameter or parameters chosen.

(4) Values for b and P for each altitude band can be determined by graphic procedure or by the method of least squares using Equation 38.

Once the b and P values have been determined according to the parameter or combination of parameters chosen, a table may be constructed for the various altitude bands with the appropriate b and P terms. Equation 38 can now be applied to determine the number of exceedances at various response levels (y) for any aircraft or control point by using the following steps: (a) define the combination of parameters desired and the altitude band involved; (b) extract b and P values from the appropriate table; (c) collect $\bar{A}$ and N_o values for the flight condition and control point for the aircraft involved; (d) designate the proper time increment and/or distance in this flight segment. As mentioned before, y may be the stress or bending moment of a control point, or the cg load factor. The major requirement is that the application be under the same seasonal, geographic, etc., restrictions that were imposed in the development of the generalized curves. Another restriction which should be imposed is to assign ground rules for storm and clear air turbulence avoidance procedures. This ground rule should be equally applied to flights which provide data for the generalized curves and to flights for which damage is being calculated.

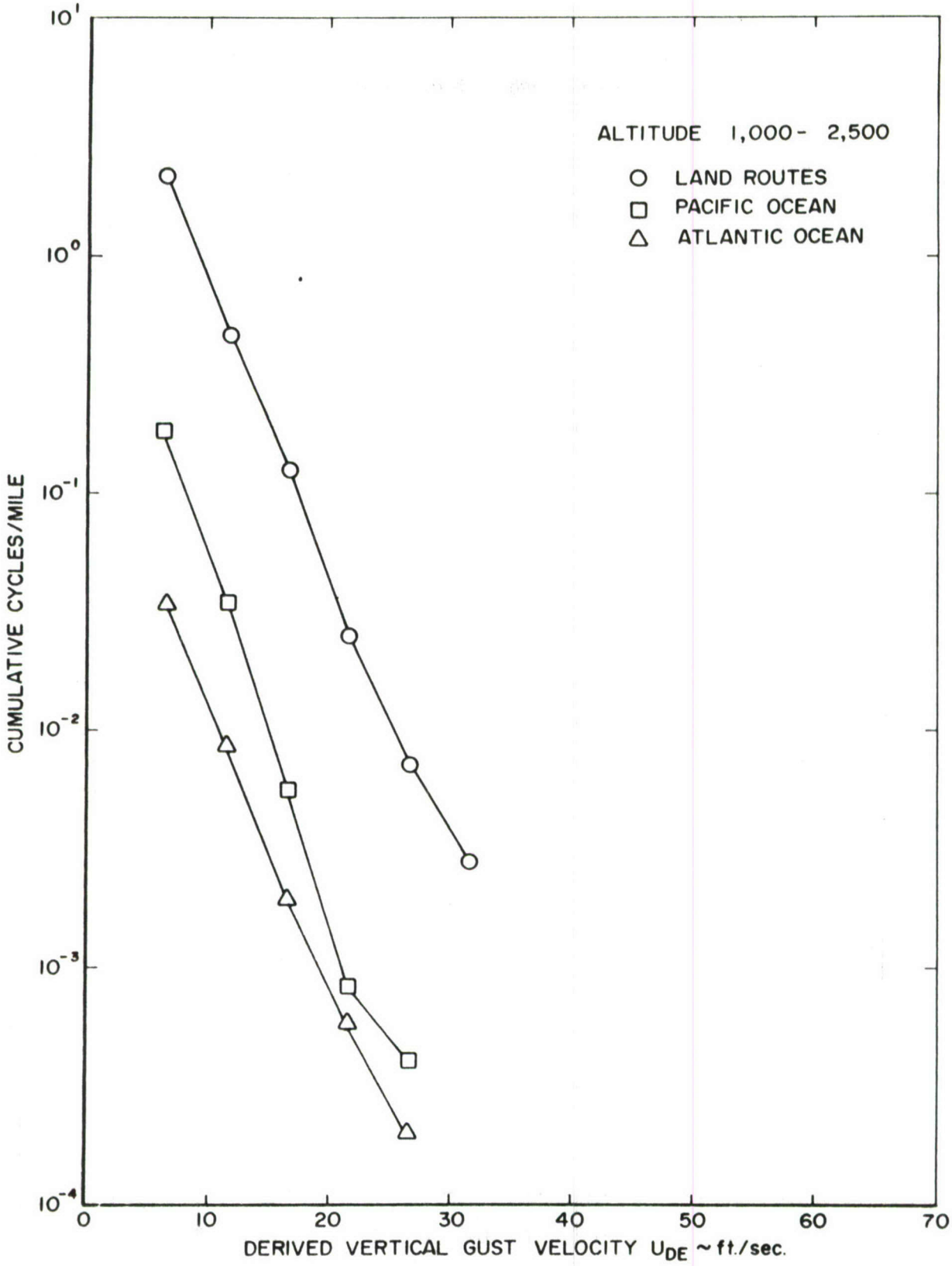

Figure 53 Cumulative Cycles per Mile vs. Derived Vertical Gust Velocity for Various Terrains for C-135 A-B, 1000 Feet to 2500 Feet

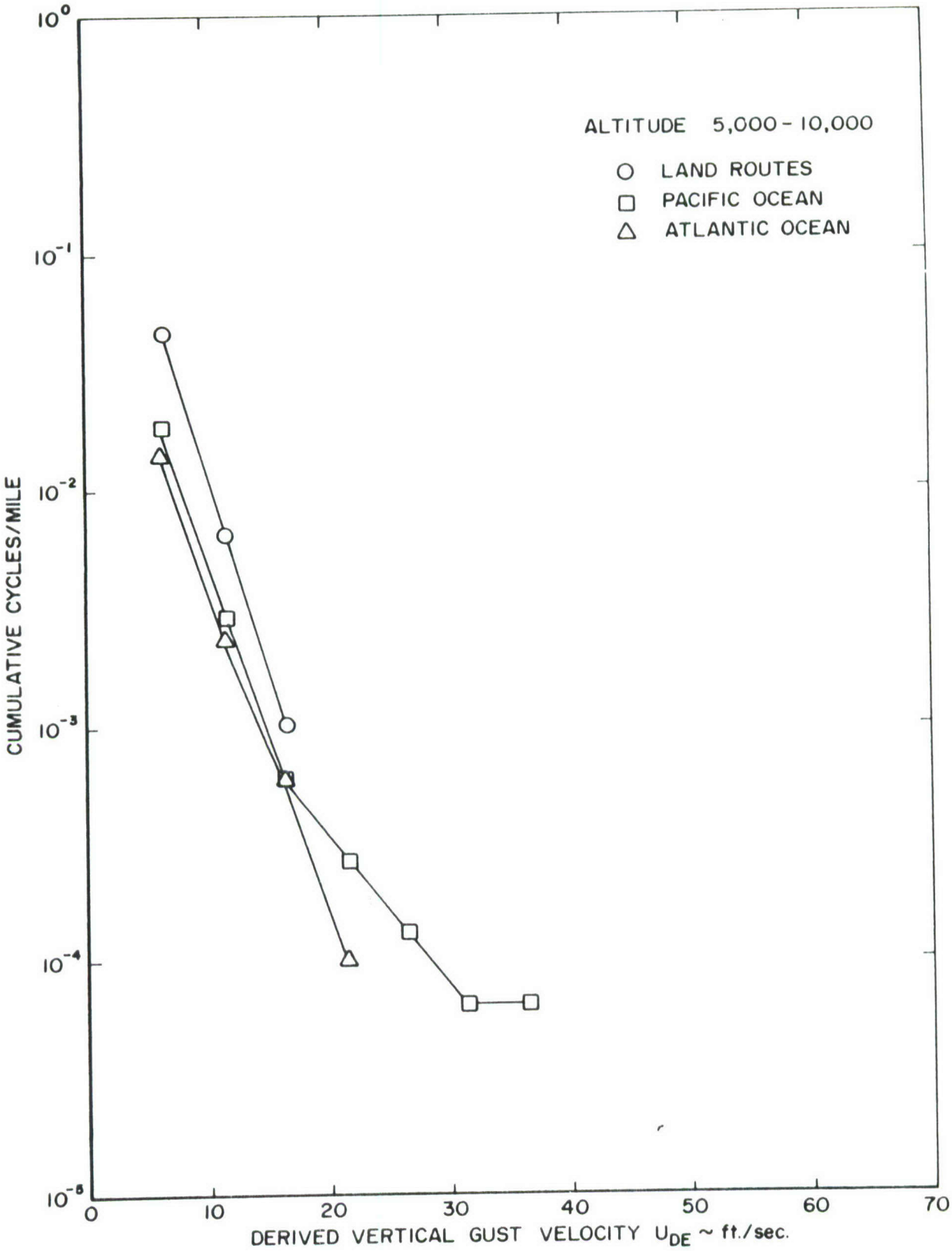

Figure 54 Cumulative Cycles per Mile vs. Derived Vertical Gust Velocity for Various Terrains for C-135 A -B, 5000 Feet to 10,000 Feet

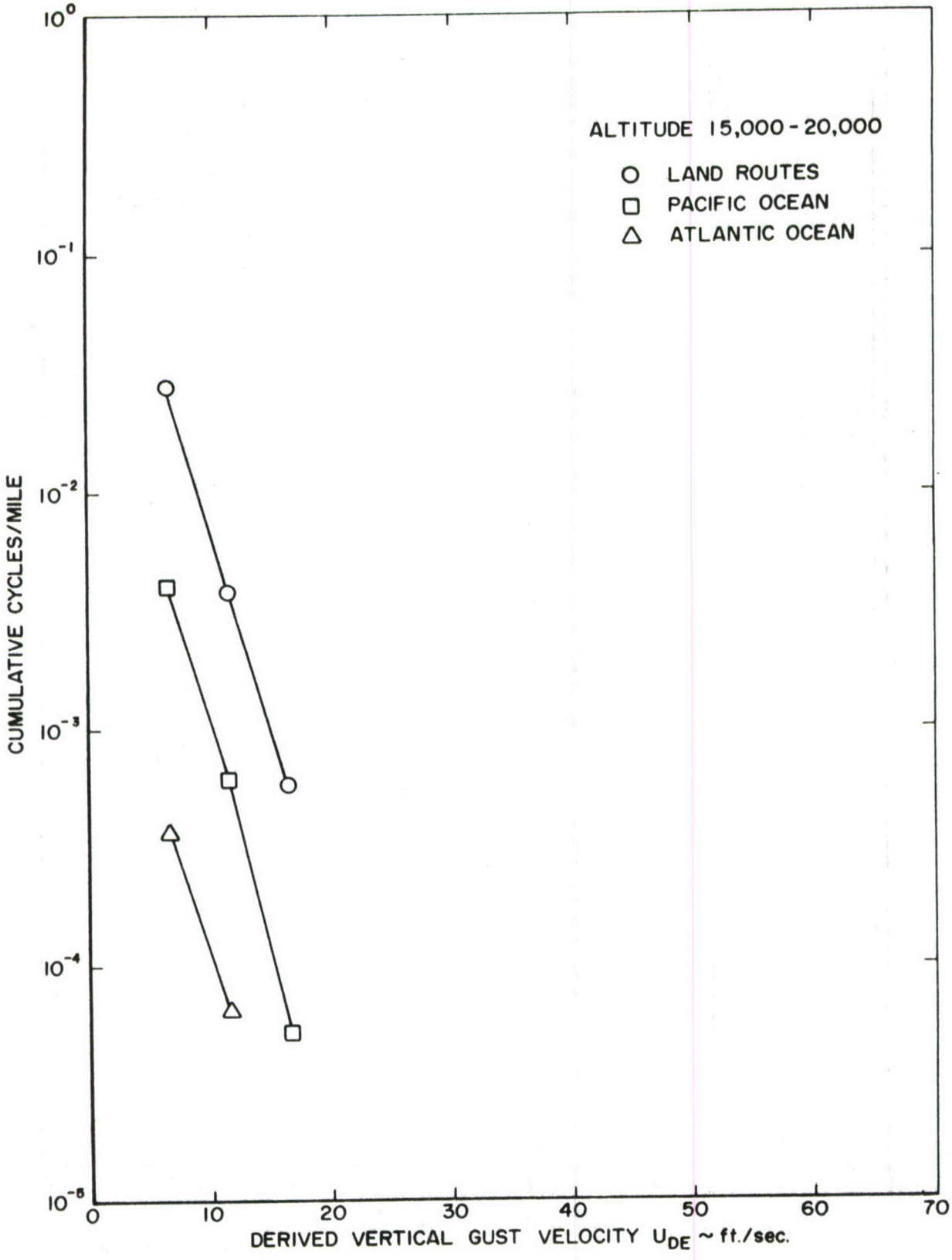

Figure 55 Cumulative Cycles per Mile vs. Derived Vertical Gust Velocity for Various Terrains for C-135 A-B, 15,000 Feet to 20,000 Feet

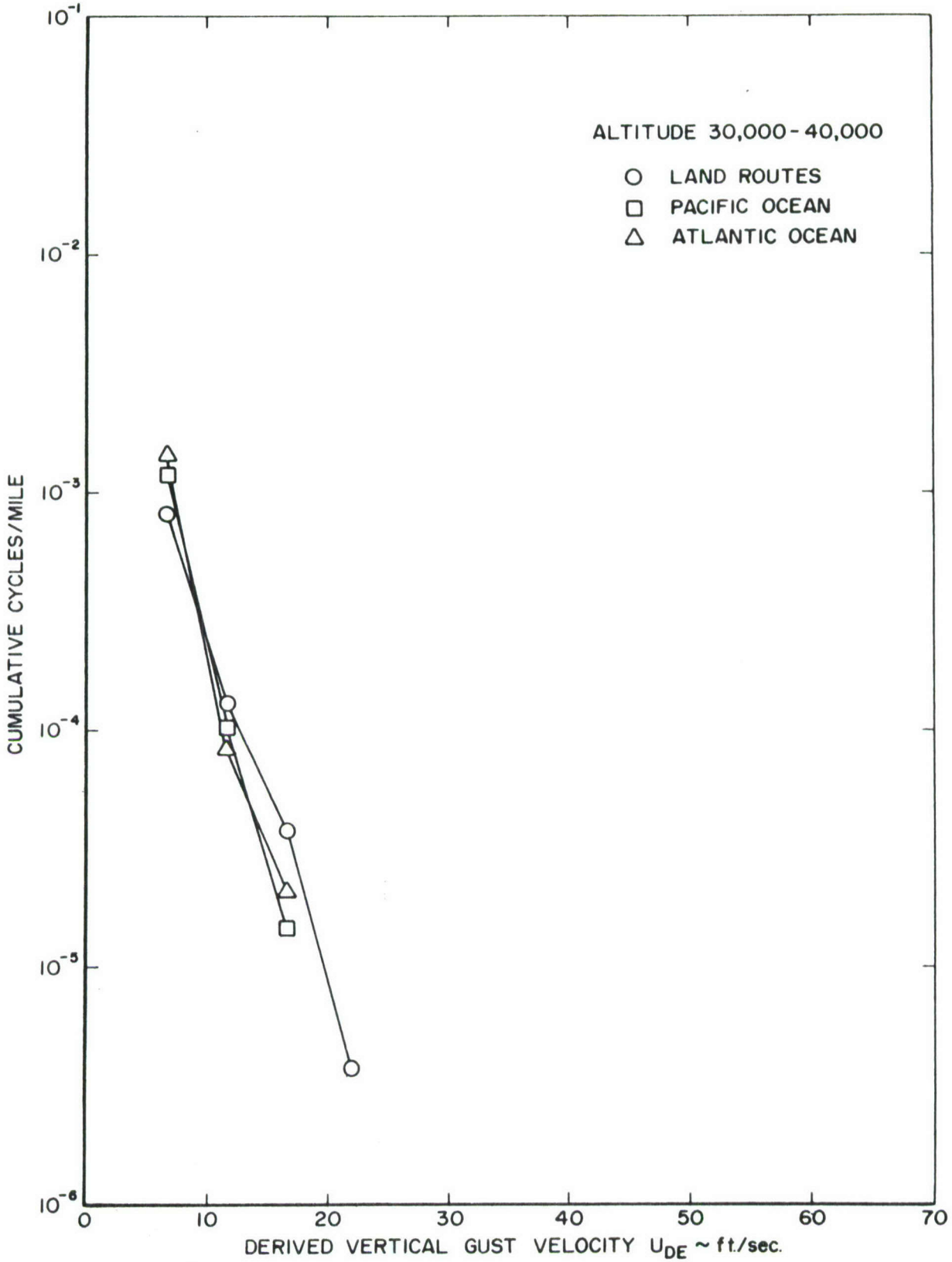

Figure 56 Cumulative Cycles per Mile vs. Derived Vertical Gust Velocity for Various Terrains for C-135 A -B, 30,000 Feet to 40,000 Feet

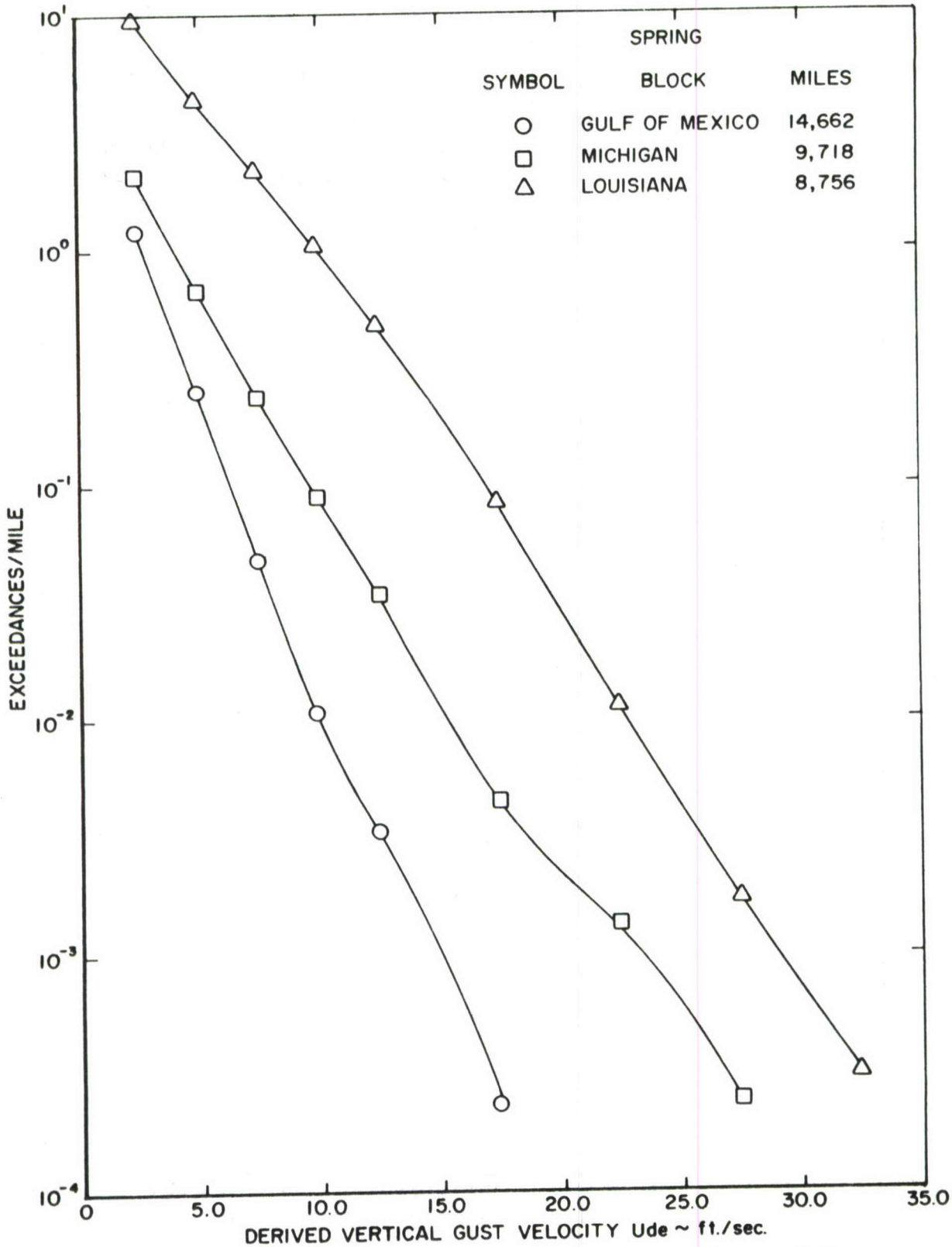

Figure 57 Cumulative Cycles per Mile vs. Derived Vertical Gust Velocity by Geographic Location for the Spring Season for B-52 B-F Low Level Penetration

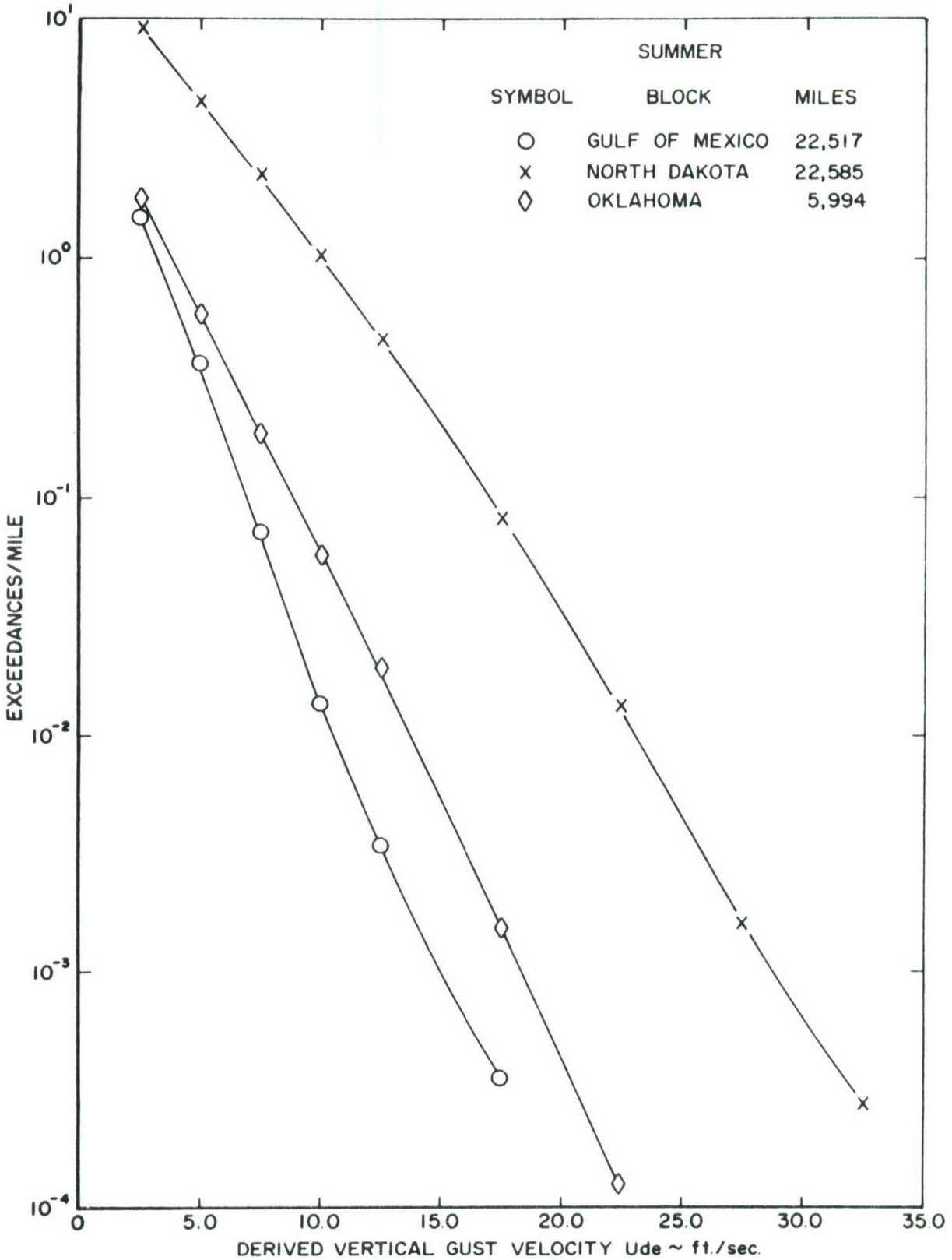

Figure 58 Cumulative Cycles per Mile vs. Derived Vertical Gust Velocity by Geographic Location for the Summer Season for B-52 B-F Low Level Penetration

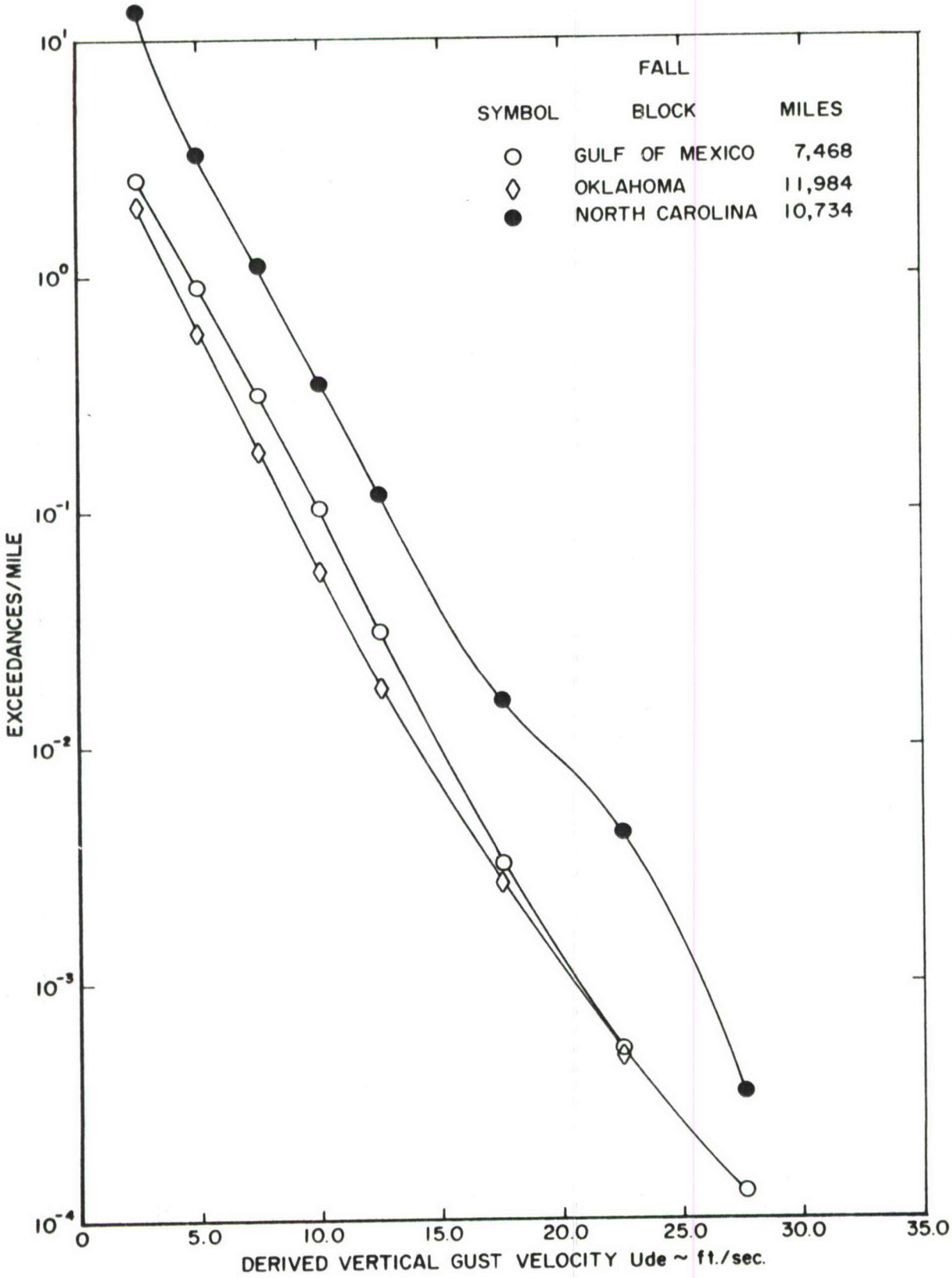

Figure 59 Cumulative Cycles per Mile vs. Derived Vertial Gust Velocity by Geographic Location for the Fall Season for B-52 B-F Low Level Penetration

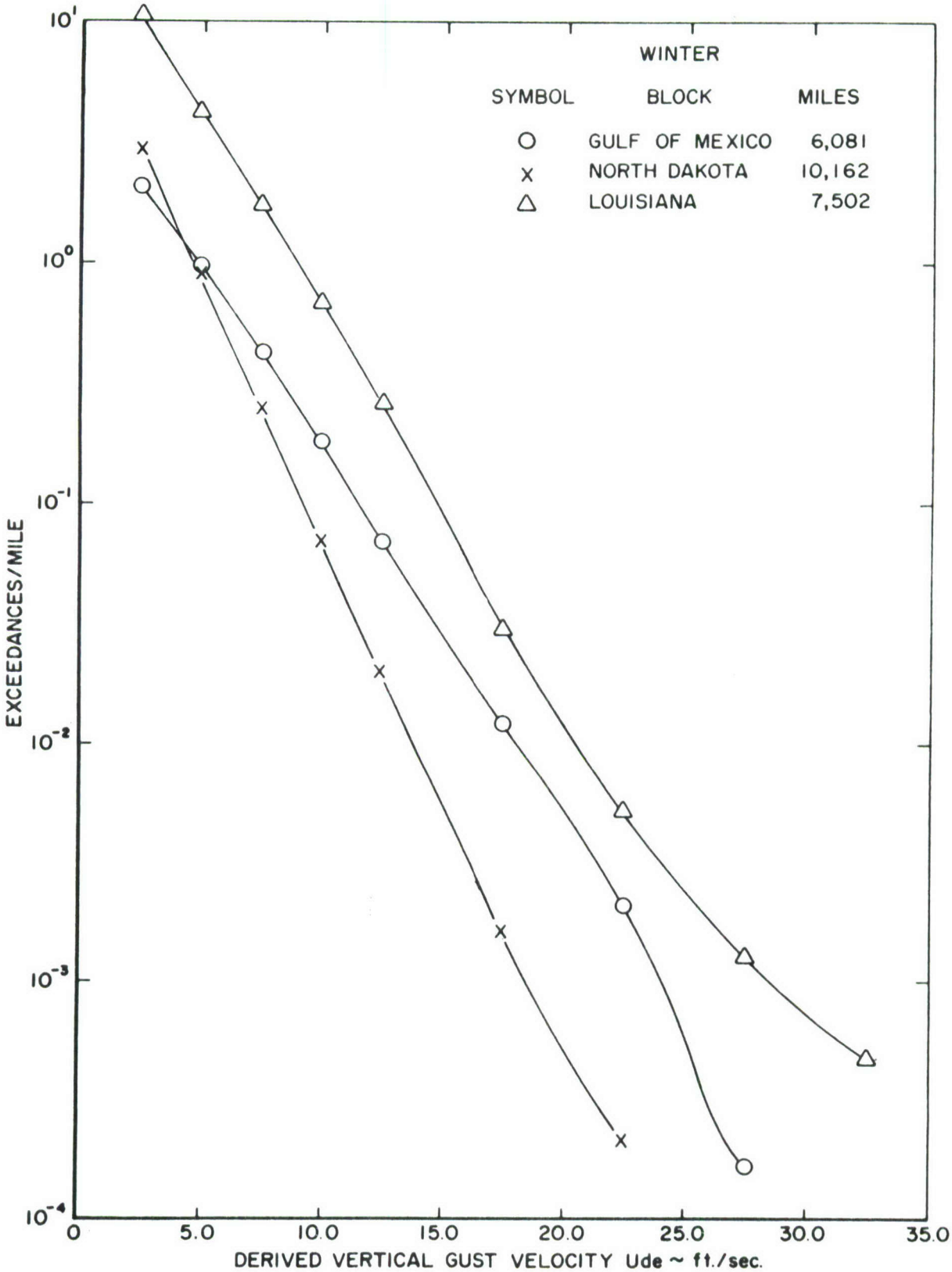

Figure 60 Cumulative Cycles per Mile vs. Derived Vertical Gust Velocity by Geographic Location for the Winter Season for B-52 B -F Low Level Penetrat

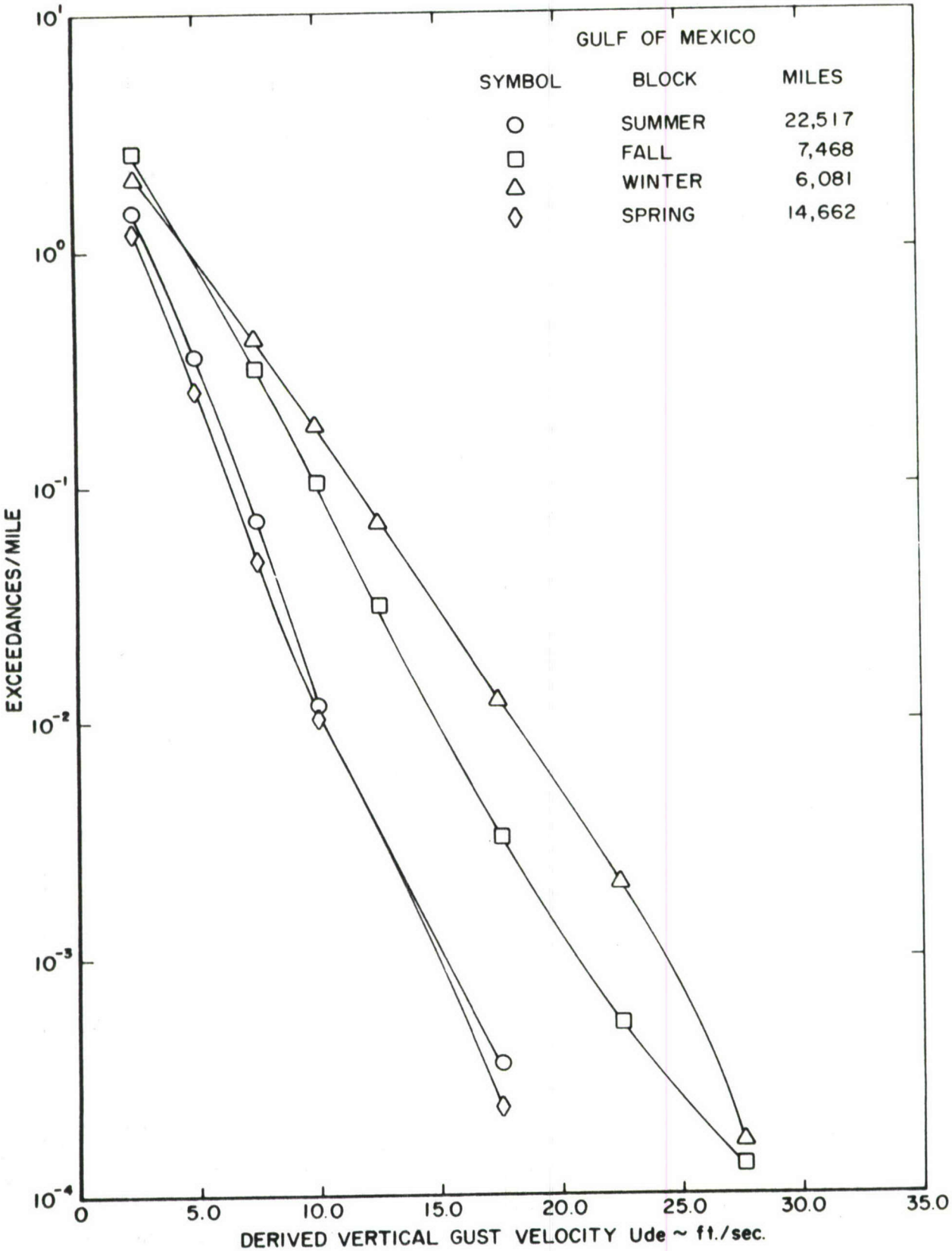

Figure 61 Cumulative Cycles per Mile vs. Derived Vertical Gust Velocity by Season for Flights Over Gulf of Mexico for B-52 B-F Low Level Penetration

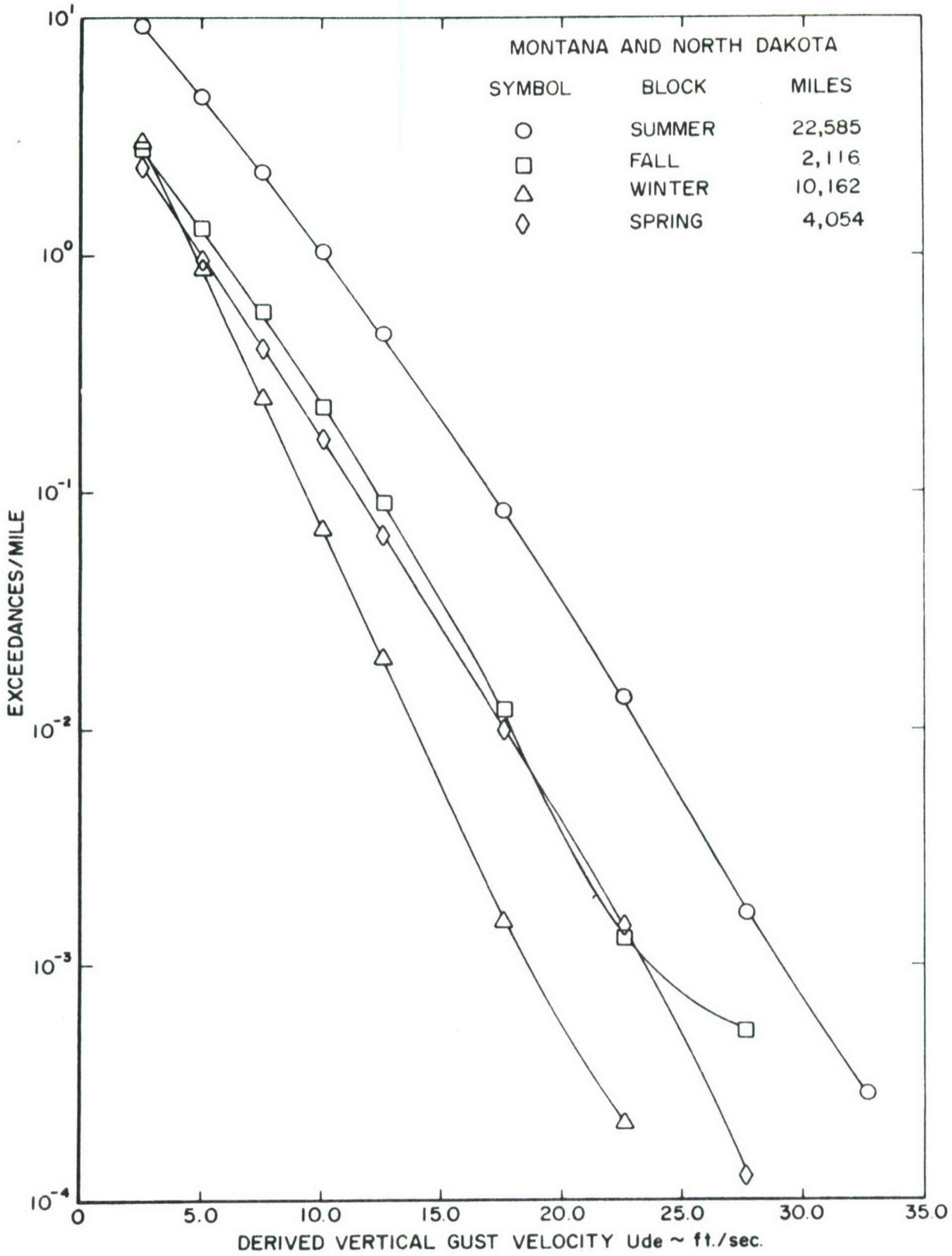

Figure 62 Cumulative Cycles per Mile vs. Derived Vertical Gust Velocity by Season for Flights Over Montana and North Dakota for B-52 B-F Low Level Penetration

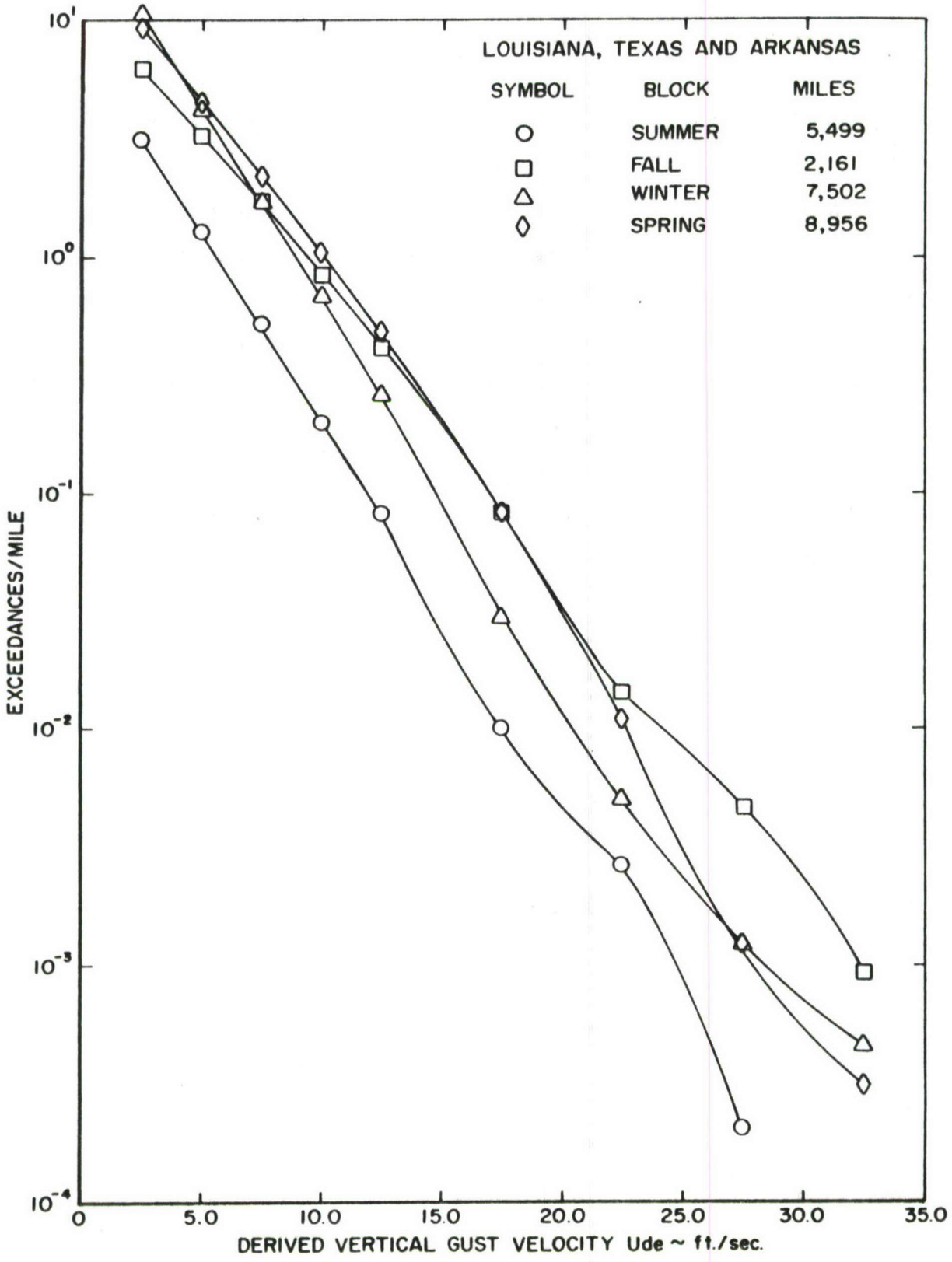

Figure 63 Cumulative Cycles per Mile vs. Derived Vertical Gust Velocity by Season for Flights Over Louisiana, Texas, and Arkansasfor B-52 B-F Low Level Penetration

To Convert From:	To:	Multiply by:
Feet	Meters	0.3048
Feet/Minute	Meters/Second	0.00508
Feet/Second	Meters/Second	0.3048
Hours	Seconds	3600
Inches	Meters	0.0254
Knots	Meters/Second	0.514444
Miles	Meters	1609.344
Pounds	Kilograms	0.4535
Minutes	Seconds	60.0
Pounds per Square Inch (psi)	Newton/Meter^2	6894.7572

Figure 64 Conversion Factors to the International System of Units

REFERENCES

1. Y. C. Fung, An Introduction to the Theory of Aeroelasticity John Wiley & Sons Inc., 1955.

2. G. S. Neuls, et al., Optimum Fatigue Spectra ASD TR-61-235 April 1962.

3. John C. Houbolt and Eldon E. Kordes, Structural Response to Discrete and Continuous Gusts of an Airplane Having Wing-Bending Flexibility and a Correction of Calculated and Flight Results NACA Rep. 1181 1954.

4. John C. Houbolt, et al., Dynamic Response of Airplanes to Atmospheric Turbulence Including Flight Data on Input and Response NASA TR R-199 June 1964.

5. Harry Press, et al., A Reevaluation of Data on Atmospheric Turbulence and Airplane Gust Loads for Application in Spectral Calculations NACA Rep. 1272 1956.

6. Harry Press and Roy Steiner, An Approach to the Problem of Estimating Severe and Repeated Gust Loads for Missile Operations NACA TN 4332 1958.

7. Airplane Strength and Rigidity - Reliability Requirements, Repeated Loads, and Fatigue MIL-A-8866 (ASG) May 18, 1960.

8. W. Wallace Morton, Jr. and Cyril G. Peckham, Structural Flight Loads Data from F-5A Aircraft SEG-TR-66-51 November 1966.

9. P. R. Abelkis, Fatigue Design Criteria and Life Prediction Computer Program for Aircraft Structures FDL-TDR-64-56 February 1965.

10. Mitchell Lopatoff, et al., F-105D Statistical Flight Loads Program SEG TR-66-16 June 1966.

11. Edward E. Hahn, Design Criteria For Ground-Induced Dynamic Loads RTD-TDR-63-4139-Vol. I November 1963.

12. G. S. Neuls, Optimum Fatigue Spectra WADD TR 60-298 March 1962.

13. J. G. Thiesen, Methods for Analyzing Flight Vehicles During the Taxi Condition ASD-TR-61-177 January 1962.

14. Airplane Strength and Rigidity - Landplane Landing and Ground Handling Loads MIL-A-8862 (ASG) May 18, 1960.

15. Airplane Strength and Rigidity - Additional Loads for Carrier-Based Landplanes MIL-A-8863 (ASG) May 18, 1960.

16. A. J. McCulloch, et al., Investigation of the Representation of Aircraft Service Loadings in Fatigue Tests ASD-TR-61-435 January 1962.

17. P. R. Abelkis, Fatigue Design Criteria and Life Prediction Computer Program for Aircraft Structures FDL-TDR-65-56, February 1965.

18. R. K. Newman, B-58 Lead the Force Flight Loads Program, Volume I UDRI-TM-66-104 February 1966.

19. A. F. Laier and C. E. Harris, Fatigue Analysis of Models KC-135 and C-135A and B Aircraft Boeing Company D6-7328 January 1964.

20. R. S. Wilson, F-106 Fatigue Program, Preliminary Fatigue Analysis, Cumulative Damage Analysis Convair Report ZS-855, Part 2 June 1962.

21. T. Tsucalas, F-105D Fatigue Analysis Based on VGH Data Volume 2 ESAR-105-100 May 31, 1966.

22. T. Ishimini, F-105 A/B Service Life Estimates Analysis, Vol. III Northrop Corp., Norair Division NOR 63-35 March 1966.

23. Robert B. Schwartz, C-135A/B Aircraft Flight Loads Program UDRI TR 66-105, June 1966.

24. Unpublished Data. B-52 B-F Service Load Recording Program ECP 1019 University of Dayton Research Institute, Dayton, Ohio.

UNCLASSIFIED

Security Classification

DOCUMENT CONTROL DATA - R&D

(Security classification of title, body of abstract and indexing annotation must be entered when the overall report is classified)

1. ORIGINATING ACTIVITY (Corporate author) University of Dayton Research Institute 300 College Park Dayton, Ohio 45409	2a. REPORT SECURITY CLASSIFICATION Unclassified 2b. GROUP

3. REPORT TITLE

Parametric Fatigue Analysis of USAF Aircraft

4. DESCRIPTIVE NOTES (Type of report and inclusive dates)

Final (1 May 1966 through 1 May 1967

5. AUTHOR(S) (Last name, first name, initial)

Roth, George J.;
Ryan, John P.;
Sliemers, James C.

6. REPORT DATE	7a. TOTAL NO. OF PAGES	7b. NO. OF REFS
June 1967	194	24

8a. CONTRACT OR GRANT NO. AF 33(615)-3812 b. PROJECT NO. c. Task No. 146704 d.	9a. ORIGINATOR'S REPORT NUMBER(S) 9b. OTHER REPORT NO(S) (Any other numbers that may be assigned this report) AFFDL-TR-67-89

10. AVAILABILITY/LIMITATION NOTICES This document is subject to special export controls and each transmittal to foreign governments or foreign nationals may be made only with prior approval of the Air Force Flight Dynamics Laboratory (AFSC), Wright-Patterson Air Force Base, Ohio 45433, ATTN: FDTR

11. SUPPLEMENTARY NOTES	12. SPONSORING MILITARY ACTIVITY
	Air Force Flight Dynamics Laboratory Directorate of Laboratories Air Force Systems Command Wright-Patterson Air Force Base, Ohio

13. ABSTRACT

This report contains the results of an effort to optimize the format and procedures for conducting a parametric fatigue analysis of Air Force aircraft on a flight-by-flight basis. Parameters which affect the environmental loads and those which affect the resulting stresses are discussed. It is suggested that flights be divided into mission segments of taxi, ascent, cruise, descent, landing, etc., to take advantage of the standard operational procedures of the Air Force. Methods of calculating and presenting the parametric damage charts for each segment are presented for both heavy bomber and cargo aircraft and for fighter aircraft. It is suggested, to obtain a reasonable accuracy, that a statistical counting accelerometer with a pilot controlled print-out be installed in all fighter aircraft. Results indicate that tabular formats are preferred to graphical formats for manual solution of large volumes of flights. It is concluded that a parametric analysis can be used to calculate the fatigue damage on a flight-by-flight basis and that the required pilot log information is now available. This abstract is subject to special export controls and each transmittal to foreign governments or foreign nationals may be made only with prior approval of the Air Force Flight Dynamics Laboratory (AFSC), Wright-Patterson Air Force Base, Ohio 45433, ATTN: FDTR.

DD FORM 1 JAN 64 1473

UNCLASSIFIED

Security Classification

14. KEY WORDS	LINK A		LINK B		LINK C	
	ROLE	WT	ROLE	WT	ROLE	WT
Fatigue Analysis						
Gust Loads Analysis						
Maneuver Loads Analysis						
Parametric Presentation						

INSTRUCTIONS

1. ORIGINATING ACTIVITY: Enter the name and address of the contractor, subcontractor, grantee, Department of Defense activity or other organization *(corporate author)* issuing the report.

2a. REPORT SECURITY CLASSIFICATION: Enter the overall security classification of the report. Indicate whether "Restricted Data" is included. Marking is to be in accordance with appropriate security regulations.

2b. GROUP: Automatic downgrading is specified in DoD Directive 5200.10 and Armed Forces Industrial Manual. Enter the group number. Also, when applicable, show that optional markings have been used for Group 3 and Group 4 as authorized.

3. REPORT TITLE: Enter the complete report title in all capital letters. Titles in all cases should be unclassified. If a meaningful title cannot be selected without classification, show title classification in all capitals in parenthesis immediately following the title.

4. DESCRIPTIVE NOTES: If appropriate, enter the type of report, e.g., interim, progress, summary, annual, or final. Give the inclusive dates when a specific reporting period is covered.

5. AUTHOR(S): Enter the name(s) of author(s) as shown on or in the report. Enter last name, first name, middle initial. If military, show rank and branch of service. The name of the principal author is an absolute minimum requirement.

6. REPORT DATE: Enter the date of the report as day, month, year; or month, year. If more than one date appears on the report, use date of publication.

7a. TOTAL NUMBER OF PAGES: The total page count should follow normal pagination procedures, i.e., enter the number of pages containing information.

7b. NUMBER OF REFERENCES: Enter the total number of references cited in the report.

8a. CONTRACT OR GRANT NUMBER: If appropriate, enter the applicable number of the contract or grant under which the report was written.

8b, 8c, & 8d. PROJECT NUMBER: Enter the appropriate military department identification, such as project number, subproject number, system numbers, task number, etc.

9a. ORIGINATOR'S REPORT NUMBER(S): Enter the official report number by which the document will be identified and controlled by the originating activity. This number must be unique to this report.

9b. OTHER REPORT NUMBER(S): If the report has been assigned any other report numbers *(either by the originator or by the sponsor)*, also enter this number(s).

10. AVAILABILITY/LIMITATION NOTICES: Enter any limitations on further dissemination of the report, other than those imposed by security classification, using standard statements such as:

(1) "Qualified requesters may obtain copies of this report from DDC."

(2) "Foreign announcement and dissemination of this report by DDC is not authorized."

(3) "U. S. Government agencies may obtain copies of this report directly from DDC. Other qualified DDC users shall request through _____."

(4) "U. S. military agencies may obtain copies of this report directly from DDC. Other qualified users shall request through _____."

(5) "All distribution of this report is controlled. Qualified DDC users shall request through _____."

If the report has been furnished to the Office of Technical Services, Department of Commerce, for sale to the public, indicate this fact and enter the price, if known.

11. SUPPLEMENTARY NOTES: Use for additional explanatory notes.

12. SPONSORING MILITARY ACTIVITY: Enter the name of the departmental project office or laboratory sponsoring *(paying for)* the research and development. Include address.

13. ABSTRACT: Enter an abstract giving a brief and factual summary of the document indicative of the report, even though it may also appear elsewhere in the body of the technical report. If additional space is required, a continuation sheet shall be attached.

It is highly desirable that the abstract of classified reports be unclassified. Each paragraph of the abstract shall end with an indication of the military security classification of the information in the paragraph, represented as *(TS), (S), (C), or (U)*.

There is no limitation on the length of the abstract. However, the suggested length is from 150 to 225 words.

14. KEY WORDS: Key words are technically meaningful terms or short phrases that characterize a report and may be used as index entries for cataloging the report. Key words must be selected so that no security classification is required. Identifiers, such as equipment model designation, trade name, military project code name, geographic location, may be used as key words but will be followed by an indication of technical context. The assignment of links, rules, and weights is optional.